ZEB1 in Colorectal Cancer.

A thesis submitted for the degree of Doctor of Medicine to the University of Leicester.

Mr Chris Briggs MB ChB MRCS(Ed)

Cancer Biomarkers and Prevention Group, Department of Cancer Studies and Molecular Medicine, Biocentre, University of Leicester, University Road, Leicester.

ZEB1 in Colorectal Cancer Mr Chris Briggs MB ChB MRCS(Ed)

Abstract:

Colorectal cancer (CRC) is one of the commonest malignancies in the United Kingdom and tumour cell invasion and metastasis is the main cause of death. The transcriptional repressor ZEB1 has been shown to be expressed in several epithelial malignancies and embryonic epithelial-mesenchymal transitions (EMT). The understanding of cellular signalling cascades should allow the discovery of novel targets for potential future therapeutic manipulation in the treatment of colorectal cancer and other malignancies.

Here, in order to further investigate the role of ZEB1 in CRC, *in vitro* investigations and immunohistochemical analysis of 101 colorectal cancers and their matched lymph node and liver metastases are performed. The Wnt-Inducible Signalling Proteins and Plakophilin-3 are also investigated for their relationship with ZEB1 signalling.

ZEB1 is expressed in tumour cell lines with mesenchymal characteristics and over-expression in an epithelial-phenotype cancer cell line causes down-regulation of epithelial markers such as E-cadherin and Plakophilin-3. Knockdown of ZEB1 in mesenchymal cell lines caused up-regulation of PKP-3 expression. *In vitro* attempts at manipulation of WISP expression were unsuccessful. In CRC tumours ZEB1 was noted to be up-regulated at the tumour invasive front, with concomitant loss of Plakophilin-3 expression. However expression of these markers did not correlate with disease stage or survival on multivariable analysis. Increased WISP-1 nuclear and cytoplasmic expression were noted at the tumour invasive front and correlated with disease stage and several pathological factors on univariable analysis. Increased nuclear WISP-1 expression at the invasive front correlated with survival on uni- and multivariable analysis.

This study demonstrates that ZEB1, Plakophilin-3 and WISP-1 are expressed in CRC and may be involved in tumour cell invasion and dissemination at the invasive front. Expression of nuclear WISP-1 is an independent predictor of poor survival and is worthy of further investigation as a target of future therapeutic intervention.

Acknowledgements:

The compilation of this thesis has taken many a long day in the laboratory in addition to many even longer days sat at my desk composing the longest prose I have ever attempted. From a scientific point of view I must give thanks to the many colleagues and friends who have offered knowledgeable support, both at the Biocentre and from other groups at the University of Leicester. A special mention is required for Drs Mann and Neal who provided vital intellectual support and made me feel a part of life in Leicester.

No project can proceed without good supervision, and I was fortunate to receive this in abundance from Professor Margaret Manson and Mr David Berry. I am extremely grateful for all their support in my attempt to complete this MD.

Finally I must mention my wife Rebecca. I cannot begin to imagine the rollercoaster of emotions that she has experienced through my trials and tribulations in completing this thesis. Firstly in my move away for 2 years, secondly through the diagnosis of chronic illness which she has suffered without a hint of pressure on me and without my being on hand to support her. And lastly through endless hours sat at my desk, sometimes on the verge of giving up she has been a constantly supportive presence. I am totally convinced that I would never have succeeded without her.

Contents

Abstract: 2

Acknowledgements: 3

List of figures 10

List of tables 13

List of Abbreviations 15

Chapter 1: Introduction 18

1.1 Colorectal Cancer: 18

1.2 CRC - Clinical overview 19

1.3 Epithelial-mesenchymal transition (EMT) 21

1.4 Cellular adhesion 22

1.4.1 Tight junctions (zonula occludens) 22

1.4.2 Gap junctions 22

1.4.3 Desmosomes 23

1.4.4 Adherens junctions 23

1.5 Control of E-cadherin expression 25

1.5.1 Gene mutation 25

1.5.2 Epigenetic factors 25

1.5.3 Transcriptional repressors of E-cadherin 28

1.6 ZEB1 (also known as TCF8, δEF1, nil-2-a, bzp, areb6, zfhx1a, zfhep) 29

1.6.1 ZEB1 in development and normal tissues 32

1.6.2 ZEB1 in carcinogenesis 34

1.6.3 ZEB1 and micro-RNA 42
1.6.4 ZEB1 and cancer therapeutics 44
1.6.5 ZEB1 isoforms 46
1.7 ZEB1, WISPs and Plakophilin-3 47
1.7.1 Wnt-Induced Signalling Proteins (WISPs) 47
1.7.2 Plakophilin-3 (PKP-3) 58
1.8 Summary 61
1.9 Hypothesis, aims and objectives 61
Aims: 61
Hypothesis: 62
Objectives: 62
Chapter 2: Materials and methods 75
2.1 Materials 75
2.1.1 Chemicals 75
2.1.2 Antibodies against the following proteins 76
2.1.3 Plasmids 76
2.1.4 Immunohistochemistry materials 76
2.2 Solutions and buffers 77
2.2.1 Immunohistochemistry 77
2.2.2 Western blotting 78
2.2.3 Plasmid preparation 79
2.3 Cell lines 80

2.4 Methods 81
2.4.1 Maintenance of cell lines 81
2.4.2 Cell passage 81
2.5 Preparation of cellS 82
2.5.1 Whole cell lysates 82
2.5.2 Bio-rad protein assay and standard curve 82
2.6 Western blotting 83
2.7 Preparation and transfection of plasmid DNA and siRNA 85
2.7.1 Transformation of competent bacteria 85
2.7.2 Preparation of plasmid DNA 86
2.7.3 Restriction digest of plasmid DNA 88
2.7.4 Transient transfection of plasmid DNA and siRNA into cells 89
2.8 Immunocytochemistry 91
2.9 Immunohistochemistry 92
2.9.1 Tissue specimens 92
2.9.2 Preparation of cell pellets as controls for immunohistochemistry 94
2.9.3 Envision detection system 94
2.9.4 Haematoxylin and Eosin (H&E) staining 97
2.9.5 Scoring of immunohistochemistry 98
2.10 Statistics 100
Chapter 3: Results – The relationship between ZEB1 and E-cadherin 101
Introduction 101

3.1 Expression of ZEB1 and E-cadherin in a panel of colorectal lines 101

3.2 Cloning of ZEB1 expression construct 103

3.3 Optimisation of chemical transfection in HCT116 and SW620 cells 108

3.4 Effect of ZEB1 expression in HCT116 cells 109

3.5 Cloning and transfection of E-cadherin expression construct 111

3.6 ZEB1 and E-cadherin expression *in vivo* 116

3.6.1 Selection of positive control tissue for ZEB1 116

3.6.2 ZEB1 in colorectal cancer specimens 118

Chapter 4: Results – The relationship between ZEB1 and Wnt-Inducible Signalling Proteins (WISPs). 122

Introduction 122

4.1 WISP expression in cell lines 123

4.2 Effect of ZEB1 on WISP expression 125

4.3 Manipulation of WISP protein expression 127

4.3.1 WISP-3 127

4.3.2 WISP-1 132

4.3.3 WISP-2 133

4.4 WISP expression *in vivo* 140

4.4.1 Selection of Positive controls 140

Chapter 5: Results - Plakophilin-3. 152

Introduction 152

5.1 Expression of PKP-3 in a panel of colorectal and breast cell lines 153

5.2 Knockdown of PKP-3 in HCT116 cells 154

5.3 Effect of ZEB1 knockdown on PKP-3 expression 157

5.4 Effect of E-cadherin expression on PKP-3 159

5.5 Effect of ZEB1 expression on PKP-3 161

5.6 Analysis of protein expression at the cellular level 163

5.7 PKP-3 expression *in vivo* 166

5.7.1 Selection of positive control tissue 166

5.7.2 PKP-3 in colorectal cancer 168

Chapter 6: Results – The relationship between ZEB1, WISP-1, Plakophilin-3 and clinicopathological data. 172

Introduction 172

6.1 Patient and tumour characteristics 174

6.2 Immunohistochemistry scoring correlations 175

6.3 Expression patterns and relationship between ZEB1, WISP-1 and PKP-3 ... 176

6.3.1 ZEB1, WISP-1 and PKP-3 expression patterns 176

6.3.2 Statistical relationship between ZEB1, WISP-1 and PKP-3 at the invasive front 176

6.4 The relationship between ZEB1, WISP-1, PKP-3 and Clinicopathological variables. 180

6.4.1 ZEB1 180

6.4.2 Nuclear WISP-1 181

6.4.3 Cytoplasmic WISP-1 182

6.4.4 PKP-3 183

6.5 The relationship between clinicopathological variables, the development of liver metastases and survival. 184

6.5.1 Liver Metastases 186

6.5.2 Survival 186

6.6 The relationship between ZEB1, WISP-1, PKP-3 and survival in Colorectal Cancer. 186

6.7 Multivariable analysis of factors predictive of the development of liver metastases, overall and disease-specific survival. 189

Chapter 7: Discussion, summary and future directions. 192

7.1 Discussion 192

7.1.1 Expression of markers *in vitro* – ZEB1 and E-cadherin 192

7.1.2 Expression of markers *in vitro* – ZEB1, WISP-1, WISP-2 and WISP-3 194

7.1.3 Expression of markers *in vitro* – ZEB1 and PKP-3 197

7.1.4 Expression of markers *in vivo* – ZEB1, WISP-1 and PKP-3. 199

7.2 Summary 200

7.3 Future directions 201

References 203

List of figures

Figure 1.1. Cancer mortality in the United Kingdom 2005 (% all malignant mortality). 18

Figure 1.2. Structure of adherens and desmosomal adhesion complexes. 24

Figure 1.3. Schematic representation of ZEB1. 30

Figure 1.4. Current evidence of signalling pathways demonstrated to be involved in the upstream control and downstream targets of ZEB1. 31

Figure 1.5. Schematic of WISP protein structure. 48

Figure 2.1. Diagram of the Envision immunohistochemistry reaction system. 95

Figure 3.1. Expression of ZEB1 and E-cadherin in cell lines. 102

Figure 3.2. Analysis of pZEB1 construct by agarose gel electrophoresis. 104

Figure 3.3. Transfection of HeLa cells with pZEB1 construct. 105

Figure 3.4. Effect of transfection of colon cells lines with pZEB1 construct 107

Figure 3.5. Optimisation of colon cell line DNA transfection. 108

Figure 3.6. Effect of pZEB1 transfection on ZEB1 and E-cadherin expression in HCT116 cells 110

Figure 3.7. Analysis of pE-cadherin vector by agarose gel electrophoresis. 112

Figure 3.8. Transfection of HeLa cells with pE-cadherin construct. 113

Figure 3.9. Effect of transfection with the pE-cadherin construct on ZEB1 and E-cadherin expression in SW480 cells. 115

Figure 3.10. Optimisation of ZEB1 antibody in endometrial tissue. 117

Figure 3.11. Optimisation of ZEB1 in A431-ZEB1 cells. 118

Figure 3.12. Immunohistochemical detection of ZEB1 in colonic specimens. 119

Figure 3.13. Immunohistochemical detection of ZEB1 in lymph node and liver specimens. 120

Figure 4.1. WISP-1, WISP-2 and WISP-3 expression in a panel of colorectal and breast cell lines. 124

Figure 4.2. Effect of ZEB1 expression on WISP proteins in A431 cells..... 126

Figure 4.3. Initial test of 4 siRNAs to knockdown WISP-3 in HCT116 cells. 128

Figure 4.4. Transfection of WISP-3 siRNA into HCT116 cells using 3 different chemical agents. 129

Figure 4.5. Transfection of WISP-3 siRNA into HCT116 and SW620 cells using Amaxa technique. 131

Figure 4.6. Transfection of WISP-1 siRNA into HCT116 cells using Lipofectamine 2000. 132

Figure 4.7. Effect of varying concentration of siRNA on knockdown of WISP-1..... 133

Figure 4.8. Schematic of the original pSilencer 1.0-U6 sh/siRNA expression vector (A) and analysis of cloned pshWISP2 and pshControl vectors by agarose gel electrophoresis (B). 135

Figure 4.9. Attempted knockdown of WISP-2. 137

Figure 4.10. Effect of blocking WISP-2 antibody with recombinant protein. 139

Figure 4.11. Optimisation of WISP-1 antibody in normal colon sections..... 142

Figure 4.12. Immunohistochemical detection of WISP-1 in colonic specimens. 144

Figure 4.13. Immunohistochemical detection of WISP-1 in lymph node and liver specimens. 145

Figure 4.14. Optimisation of WISP-2 antibody in femoral head sections. 147

Figure 4.15. WISP-2 in normal colonic epithelium and colorectal cancers. 149

Figure 4.16. Optimisation of WISP-3 antibody in femoral head sections. 151

Figure 5.1. Expression of PKP-3 relative to other proteins of interest in a panel of cell lines. 153

Figure 5.2. Knockdown of PKP-3 in HCT116 cells. 155

Figure 5.3. Effect of knockdown of PKP-3 in HCT116 cells. 156

Figure 5.4. Effect of ZEB1 knockdown on PKP-3 expression in SW480 and MDA-MB-231 cells. 158

Figure 5.5. Effect of E-cadherin on PKP-3 expression in SW480 cells. 160

Figure 5.6. Effect of ZEB1 knockdown on PKP-3 expression in SW480 cells..... 164

Figure 5.7. Effect of ZEB1 knockdown on E-cadherin expression in SW480 cells.... 165

Figure 5.8. Optimisation of PKP-3 antibody in normal skin. 167

Figure 5.9. Immunohistochemical detection of PKP-3 in colonic specimens. 169

Figure 5.10. Immunohistochemical detection of PKP-3 in lymph node and liver specimens. 170

Figure 6.1. Kaplan Meier survival curves for increased nuclear WISP-1 at the invasive front. 188

Figure 7.1. Possible signalling interaction between ZEB1 and WISP-3. 195

List of tables

Table 1.1. 5 year survival rates in colorectal cancer according to Duke's and TNM stage. 20

Table 1.2. *In vivo* studies examining ZEB1 expression in normal tissues and development. 63

Table 1.3. *In vivo* studies examining ZEB1 expression in carcinogenesis. 65

Table 1.4. *In vivo* studies examining WISP-1 expression in normal tissues and development. 67

Table 1.5. *In vivo* studies examining WISP-1 expression in carcinogenesis. 68

Table 1.6. *In vivo* studies examining WISP-2 expression in normal tissues and development. 70

Table 1.7. *In vivo* studies examining WISP-2 expression in carcinogenesis. 71

Table 1.8. *In vivo* studies examining WISP-3 expression in normal tissues and development. 72

Table 1.9. *In vivo* studies examining WISP-3 expression in carcinogenesis. 73

Table 1.10. *In vivo* studies examining Plakophilin-3 expression in development and disease. 74

Table 2.1 Recipes for denaturing running gels. 79

Table 2.2. Bradford assay standard curve dilutions. 83

Table 2.3. Conditions for use of primary antibodies and expected molecular weight of proteins on western blots. 84

Table 2.4. Identification of plasmids by restriction digests. 89

Table 2.5. Inclusion and exclusion critieria for the selection of tumour tissues for immunohistochemistry. 93

Table 2.6. Conditions of primary antibodies for immunohistochemistry. 96

Table 2.7. Published studies using immunohistochemistry to assess ZEB1, WISP-1 and PKP-3 expression, the type of scoring system used and statistical analysis undertaken. 99

Table 3.1. Estimated transfection efficiency in HCT116 cells as quantified by percentage of cells with GFP expression. 109

Table 6.1. Demographics and tumour related variables of patients included in study. 175

Table 6.2. Intraclass correlation coefficient agreement between immunohistochemistry scores. 176

Table 6.3. Univariable analysis of correlations between ZEB1, WISP-1 and PKP-3 scores in varying tumour locations. 178

Table 6.4. Univariable analysis of ZEB1 scores and clinicopathological variables. ... 180

Table 6.5. Univariable analysis of nuclear WISP-1 scores and clinicopathological variables. 181

Table 6.6. Univariable analysis of cytoplasmic WISP-1 scores and clinicopathological variables. 182

Table 6.7. Univariable analysis of PKP-3 scores and clinicopathological variables. .. 183

Table 6.9. Univariable analysis of immunohistochemical markers (H score) according to overall and disease-specific survival. 187

Table 6.10. Multivariable analysis of clincopathological and immunohistochemical factors predictive of the formation of liver metastases, overall and disease-specific survival..... 190

List of Abbreviations

BD	-	Bile Duct
BMP	-	Bone Morphogenic Protein
BSA	-	Bovine Serum Albumin
Ca	-	Carcinoma
CCN	-	Cysteine-rich 61, Connective Tissue Growth Factor, Nephroblastoma Overexpressed
ChIP	-	Chromatin Immuno-Precipitation
COPD	-	Chronic Obstructive Pulmonary Disease
COX	-	Cyclooxygenase
CRC	-	Colorectal Cancer
DAB	-	Diaminobenzidine
DIM	-	Di-indolylmethane
DME	-	Dulbecco Modified Eagle's (medium)
DNA	-	Deoxyribonucleic Acid
ECL	-	Enhanced Chemiluminescence
EGFR	-	Epidermal Growth Factor Receptor
EMT	-	Epithelial Mesenchymal Transition
FACS	-	Fluorescence-Activated Cell Sorting
FCS	-	Fetal Calf Serum
FECD	-	Fuchs Endothelial Corneal Dystrophy
GFP	-	Green Fluorescent Protein
HA	-	Hepatic Artery
HCC	-	Hepatocellular Carcinoma
HD	-	Homeodomain
H&E	-	Haematoxylin and Eosin
HRP	-	Horseradish Peroxidase
IHC	-	Immunohistochemistry
IJA	-	Idiopathic Juvenile Arthritis
ILK	-	Integrin Linked Kinase
IMS	-	Industrial Methylated Spirit
JAMS	-	Junctional Adhesion Molecule

LB	-	Lysogeny Broth (medium)
LRI	-	Leicester Royal Infirmary
MET	-	Mesenchymal Epithelial Transition
MI	-	Myocardial Infarction
miRNA	-	Micro Ribonucleic Acid
MMMT	-	Malignant Mixed Mullerian Tumour
MMP	-	Matrix Metalloproteinase
MSI	-	Micro Satellite Instability
MVA	-	Multivariable Analysis
N/A	-	Not Applicable
NS	-	Not Significant
NSCLC	-	Non-Small Cell Lung Cancer
OA	-	Osteo-Arthritis
Panc Adeno	-	Pancreatic Adenocarcinoma
PBS	-	Phosphate Buffered Saline
PBST	-	Phosphate Buffered Saline with Tween-20
PIC	-	Protease Inhibitor Cocktail
PKP	-	Plakophilin
PPCD	-	Posterior Polymorphous Corneal Dystrophy
PPD	-	Progressive Pseudorheumatoid Dysplasia
PV	-	Portal Vein
Prost Adeno	-	Prostatic Adenocarcinoma
RA	-	Rheumatoid Arthritis
RNA	-	Ribonucleic Acid
RPM	-	Revolutions Per Minute
RPMI	-	Roswell Park Memorial Institute (medium)
RT-PCR	-	Real-Time Polymerase Chain Reaction
SCC	-	Squamous Cell Carcinoma
SDS	-	Sodium Dodecyl Sulphate
SEM	-	Standard Error of the Mean
shRNA	-	Short Hairpin Ribonucleic Acid
siRNA	-	Short Interfering Ribonucleic Acid
TBS	-	Tris Buffered Saline
TNM	-	Tumour, Nodes, Metastases

UK	-	United Kingdom
UPSC	-	Uterine Papillary Serous Carcinoma
USA	-	United States of America
UV	-	Ultra-Violet
UVA	-	Univariable Analysis
VDR	-	Vitamin D Receptor
WB	-	Western Blot
WISP	-	Wnt-Induced Signalling Protein
Wnt	-	Wingless Pathway in Drosophilia
Wt	-	Wild type

Chapter 1: Introduction

1.1 COLORECTAL CANCER:

Colorectal cancer (CRC) remains the second commonest malignancy in women and third most common in men in the United Kingdom (UK). Of over 500,000 registered deaths in the UK in 2004, 150,000 were related to malignancies and of these 10% were due to colorectal cancer (figure 1.1)[1]. The majority of these deaths were not due to the primary malignancy, but to the distant metastases. Approximately 25% of patients with CRC will present with synchronous liver or lung metastases and a further 8-25% will develop metachronous disease post primary resection[2, 3]. In this group with metastatic deposits less than a third are amenable to further surgical intervention due to the extent of disease dissemination[4]. Recent advances in chemotherapy have opened the door to "down-staging" therapy for locally advanced liver metastases, and this has been shown to convert potentially fatal disease into a resectable and possibly curative state[5]

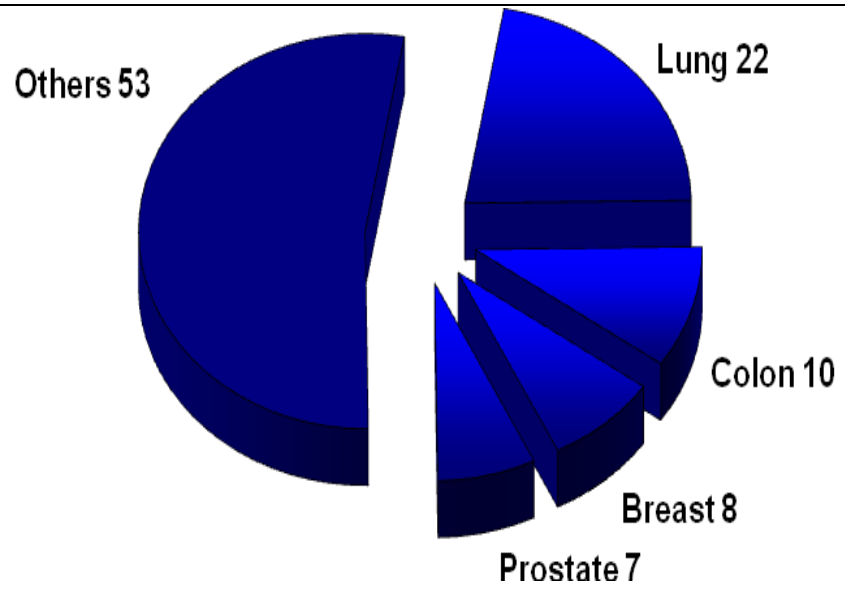

Figure 1.1. Cancer mortality in the United Kingdom 2005 (% all malignant mortality). Adapted from Cancer research UK figures, 2005.

1.2 CRC - CLINICAL OVERVIEW

Patients presenting with CRC fall into two categories – those with bowel obstruction who present as an emergency and require urgent treatment to prevent life threatening complications and those with other symptoms of the disease which can be vague and non-specific. These include abdominal pain, a change in bowel habit (diarrhoea or constipation), rectal bleeding, tenesmus (the feeling of incomplete evacuation) and iron deficient anaemia. However, all these non-emergent symptoms are common in other gastrointestinal conditions and for this reason the diagnosis can only be confirmed after further assessment.

Investigation of patients' symptoms centres on two common methods of imaging the colon, endoscopic examination (colon / sigmoid-oscopy) or double-contrast barium enema. More recently computed tomographic colonography has been introduced, although there is controversy about the sensitivity of the test in comparison to colonoscopy and its availability is currently limited by local radiology facilities and expertise[6]. Once a diagnosis of colonic carcinoma is established (ideally by endoscopic biopsy and histological confirmation) then a full chest, abdominal and pelvic computed tomography scan is undertaken to stage the disease.

Treatment must take into account multiple factors including the patients' age, co-morbidity, stage of the disease and their choice of treatment. The complexity of these issues accounts for the move toward a "Multi-Disciplinary Team" approach to the decision making process. The overall aim is usually curative therapy, although this will largely depend on the patient's fitness and the stage of the disease at presentation. Overall survival has been shown to correlate with stage at presentation, although with newer "down-staging" treatments, this picture may be changing (table 1.1).

Table 1.1. 5 year survival rates in colorectal cancer according to Duke's and TNM stage.

Modified Duke's Stage	Equivalent TNM Stage	Pathological description	5 Year Survival (%)
A	I	Localised to mucosa / sub mucosa	93
B	IIA and IIB	Invading into muscle, no lymph node metastasis	72-85
C	IIIA-C	Lymph node involvement	44-83
D	IV	Distant Metastasis	8-35

Adapted from the colon cancer survival rates according to the American Joint Committee on cancer sixth edition staging[7].

One (or a combination) of surgical resection, chemo or radiotherapy may be offered as treatment options. Surgical resection of the primary tumour and any metastatic disease remains the only treatment offering hope of a cure. However, only approximately 11% of patients will present with early (Duke's A) disease[8], meaning that surgical resection alone provides a relatively low chance of long term survival. Even after resection of the primary tumour in early cancers, a significant proportion of patients present with recurrent disease, suggesting that microscopic disease which could not be identified for surgical excision may have been left behind, or that tumour cell dissemination in the blood stream or lymph system had already occurred. Despite advances in surgical technique, such as the introduction of total mesorectal excision in order to clear local disease, the only hope of a cure in patients with tumour cell dissemination is to target neoplastic progression at the molecular level[9, 10]. In patients with moderate or advanced disease, particularly those with rectal cancer and initially unresectable liver metastases, adjuvant or neo-adjuvant chemo-radiotherapy has been found to dramatically improve survival[5, 11, 12].

For this reason attention is now focused on the understanding of pathways leading to tumour metastasis and the development of agents which can complement the current chemotherapeutic armoury. Recent advances in treatment strategies include targeting de-regulated signalling pathways, in order to induce tumour cell cycle arrest or apoptosis[13]. It is envisaged that alongside these new agents molecular markers will be identified which will predict responsiveness and prognosis on an individual basis, enabling the design of treatment according to scoring systems which target therapies not just according to the histology, but truly at the molecular level.

1.3 EPITHELIAL-MESENCHYMAL TRANSITION (EMT)

CRC is an epithelial malignancy, arising from changes in the behaviour of the normal colonic epithelial cells which line the lumen of the bowel. These normal epithelial cells form layers that are closely joined together by specialised cellular junctions, such as desmosomes, gap junctions, tight junctions and adherens junctions. Epithelial cells line other cavities and surfaces of the body, as well as being present throughout the colon. Under normal conditions these adherence mechanisms control cellular motility and maintain normal tissue architecture. During tumour formation it is apparent that there is significant architectural disturbance with cellular motility and invasiveness increasing. These changes in cellular adhesion which occur during carcinogenesis are similar to an embryonic process during development termed epithelial-mesenchymal transition[14].

During development mesenchymal cells are motile and can settle at sites of mesenchymal-epithelial interaction, or differentiate into new structures and solid organs. Unlike epithelial cells, mesenchymal cells have the ability to migrate and move to distant sites as individual cells. This enables mesechymal stem cells to move within the embryo and settle at sites where they will be needed for the formation of various tissues and organs. During embryonic EMT, epithelial cells are able to modulate their

phenotype and acquire morphology appropriate for migration in an extracellular environment and settle in areas where organs will develop. This phenomenon is very similar to that which has been observed in carcinoma cells, which attain the ability to metastasise and invade into other tissues, and has been proposed as a potential mechanism for carcinoma progression[15-18]. One of the main mechanisms thought to account for EMT is the disruption of intercellular adhesion, and a major hallmark of EMT is the loss of E-cadherin expression.

1.4 CELLULAR ADHESION

As previously mentioned, epithelia consist of layers of cells with adhesional bonds between them. These bonds link the intra-cellular cytoskeletal mesh-works of cytoplasmic filament bundles of each individual cell to its neighbour. This is achieved through four known types of filament-binding adhesion complexes; adherens junctions, desmosomes, gap and tight junctions.

1.4.1 Tight junctions (zonula occludens)

Tight junctions are areas of extremely close cell membrane contact and act as a barrier to the passage of molecules between epithelial cells. They are formed by integral membrane proteins such as occludin, claudins and junctional adhesion molecules (JAMS). For a review see Schneeberger and Lynch [19].

1.4.2 Gap junctions

Gap junctions are areas where the cellular membranes of two cells have fused, connexins being the major building block in this type of junction. These channels allow direct communication between the cytoplasmic domains of the two cells via ionic exchange and serve less of a role in adhesional strength than tight junctions, desmosomes and adherens junctions [20].

1.4.3 Desmosomes

Desmosomes are found in epithelial and cardiac muscle cells. They confer strong cell-cell adhesion properties, but their constituent proteins are also thought to interact with several intracellular messaging cascades which influence multiple cellular characteristics such as mobility, invasiveness, and cell survival[21]. They are made up of the membrane-spanning desmosomal cadherins (desmocollins 1 to 3 and desmogleins 1 to 4), armadillo proteins (plakoglobin and plakophilins 1 to 3) and plakin proteins such as desmoplakin (figure 1.2). These molecules interact and bind with the keratin intermediate filaments of the cellular cytoskeleton to form cell-cell adhesions[22].

1.4.4 Adherens junctions

Adherens junctions are responsible for the initiation of cell-cell adhesion and the subsequent formation of tight junctions. Adherens junction formation also has consequences for multiple cell-signalling cascades. This is due to the fact that the constituent proteins in the adhesion complex also participate in several molecular signalling pathways. The trans-membrane classical cadherin protein E-cadherin is the major building block for this type of junction, and interacts with members of the catenin family (α- and β– catenin, and p120-catenin) to form complexes which bind to the actin cytoskeleton and stabilise cell-cell interactions (figure 1.2)[23]. Decreased E-cadherin expression has been shown in several epithelial malignancies and has been associated with metastasis formation and poor survival[24-27]. It is postulated that this loss of E-cadherin is a marker of decreased adherens junction formation and thus decreased cellular adhesion and increased mobility. The control of E-cadherin expression is therefore central to the formation of cellular adhesion and the changes in cellular characteristics associated with EMT.

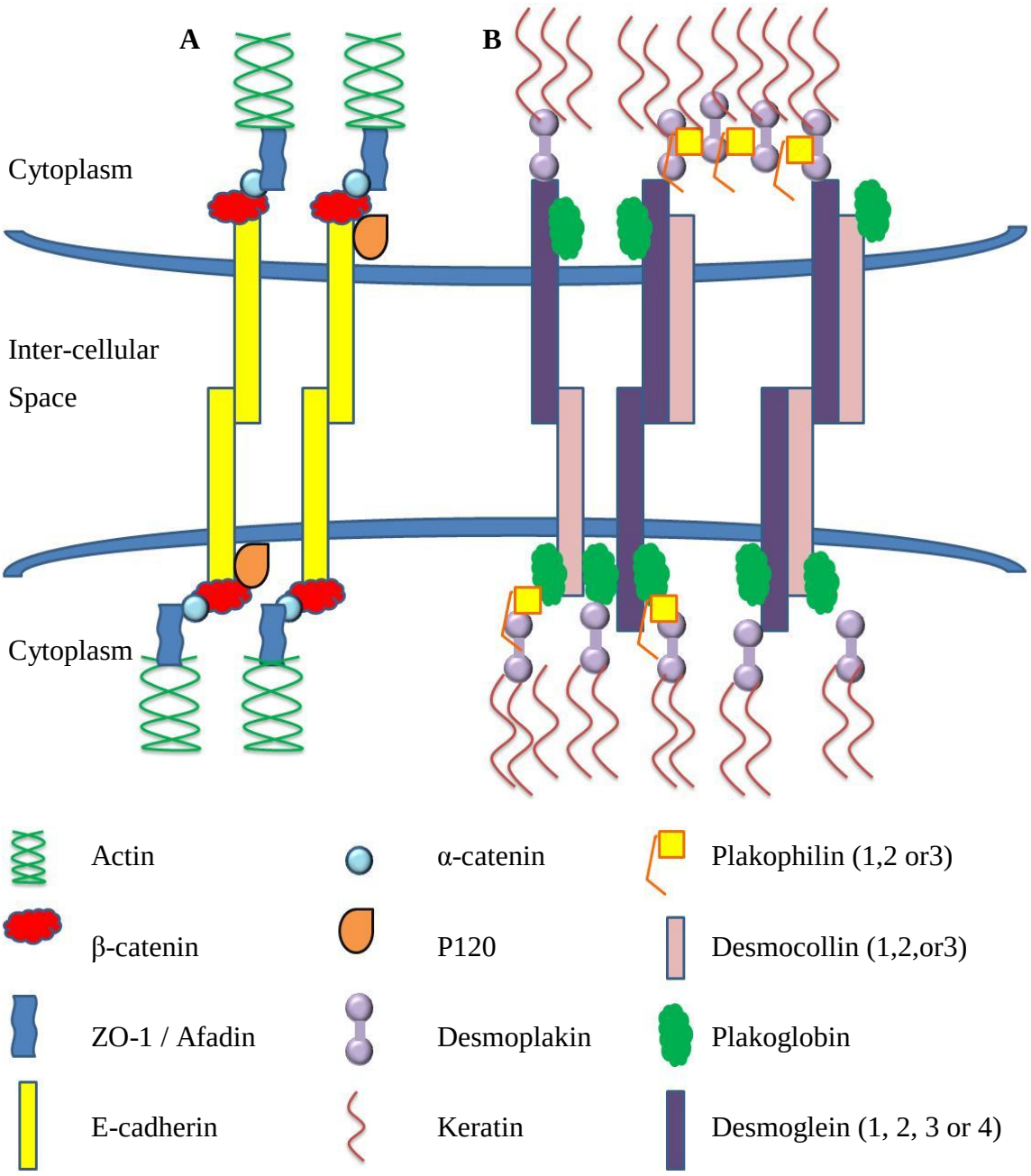

Figure 1.2. Structure of adherens and desmosomal adhesion complexes. Adherens junctions (**A**) form through homophilic E-cadherin extracellular binding to cadherins on neighbouring cells. The intracellular portion of E-cadherin associates with β-catenin / α-catenin complexes which in turn bind to the actin micro-filaments of the cytoskeleton either directly, or through other catenin binding proteins such as ZO-1 or afadin. Desmosomes (**B**) consist of the trans-membrane desmosomal cadherins, desmoglein and desmocollin, which bind to their counterparts on neighbouring cells in a calcium-dependent fashion. The cytoplasmic portion of these molecules combines with armadillo family proteins, such as plakoglobin and plakophilin, and desmoplakin to form the desmosomal plaque. This plaque links the desmosomal cadherins to the keratin intermediate-length filaments of the cellular cytoskeleton.

1.5 CONTROL OF E-CADHERIN EXPRESSION

E-cadherin expression appears to be under the control of three major mechanisms: Gene mutation, so-called “epigenetic” factors and transcriptional repression[28]. The relative importance of each is discussed below.

1.5.1 Gene mutation

Inactivating mutations of the *CDH1* gene sequence encoding E-cadherin have been described in several carcinoma tissues – breast[29-31], gastric[31-33], endometrial[34], oesophageal[35], colorectal[36], ovary[34] and thyroid[37]. However, inactivating mutations are relatively rare *in vivo*, only occurring frequently in two carcinoma subtypes – diffuse gastric carcinoma and infiltrative lobular breast carcinoma[29-31, 33]. This evidence suggests that the loss of E-cadherin expression witnessed in carcinomas of epithelial origin is rarely due to gene mutations alone, and must be caused by other regulatory mechanisms.

1.5.2 Epigenetic factors

Epigenetic silencing refers to non-mutational gene inactivation which may be propagated from one cell to its daughter clones, and therefore may be inherited without a change in DNA sequence. Factors which may induce this silencing are histone modification and DNA methylation. There is significant evidence that these factors may play a major role in carcinogenesis[38].

1.5.2.1 Histone modification

Histones were discovered in 1884 by the German Nobel prize-winning medic Albrecht Kossel. They are proteins around which 147 base pairs of DNA are wound in order to form a nucleosome. These are then grouped together to form chromatin. The structural state of chromatin has been shown to determine the functional state of the genes within

it[39]. This structural state is dependent upon the histone proteins and several post-translation covalent modifications which they can undergo. These modifications include:

- Acetylation of lysine residues on histone tails
- Methylation of lysine and arginine residues on histone tails
- Serine and threonine phosphorylation
- Glutamic acid ADP-ribosylation
- Lysine ubiquitination and sumoylation

The combination of these modifications result in different "packaging" of chromatin and this then determines the access of transcriptional promoter proteins to the DNA they contain. The array of different structural states of chromatin became known as the "histone code" and was proposed to account for the variable expression of many genes[40]. However, this theory is constantly evolving and although it is accepted for some molecules, other explanations have been proposed to explain variable gene transcription which may be more complex.

1.5.2.2 DNA methylation

DNA methylation is the only commonly occurring modification of human DNA. It results from the addition of a methyl group to cytosine residues at CpG dinucleotides by a family of DNA methyltransferase enzymes. CpG dinucleotides are relatively sparse in the human genome. However, there are short stretches of DNA where they are clustered together, known as CpG islands. Outside these islands, CpG dinucleotides are on the whole highly methylated. In normal adult tissues the majority of CpG islands remain methylation-free, but after extensive investigation in several human cancer types, it is apparent that in almost all of these cancers there is loss of the normal control of DNA

methylation. It appears that there is a resultant decrease in the genome wide methylation status, accompanied by a local hypermethylation of CpG islands in certain areas[38, 41].

In some known tumour suppressor genes, hypermethylation of CpG islands within promoter regions has been associated in many studies with transcriptional repression of the gene product[42]. Precisely how this hypermethylation interferes with transcription is not known, but two proposed mechanisms are as follows:

1. Methylation directly impedes binding of transcriptional proteins.

2. Methyl-CpG-binding domain proteins not related to the transcription process bind to DNA due to methylation and this causes recruitment of proteins which are able to modify histones (see histone modification) such as histone deacetylases.

This second theory links hypermethylation with histone modification as a dual causality for silencing of transcription.

In the context of the E-cadherin promoter, hypermethylation was first reported in a number of human carcinoma cell lines by Yoshiura and colleagues[43]. They demonstrated that hypermethylation was associated with inactivation of expression of E-cadherin and conversely that reversal of methylation caused re-activation of transcription. As previously stated, the majority of epithelial cancers show loss of E-cadherin expression, and many investigators have shown a correlation between loss of expression and hypermethylation of the promoter in epithelial-derived cancers[28].

At this stage it should be noted that although this positive correlation suggests a definitive role for hypermethylation in the control of E-cadherin expression, it is not

known whether the hypermethylation itself is responsible for lack of expression, or whether it is a surrogate marker of another mechanism of transcriptional inactivation. It has been proposed that the binding of a transcriptional repressor to the promoter may itself cause hypermethylation as a secondary effect, and that it is the repressor which is responsible for inactivation of expression[28].

1.5.3 Transcriptional repressors of E-cadherin

Transcriptional repressors are proteins which are able to bind to promoter regions on DNA and prevent protein transcription. In recent years several repressors have been implicated in the control of E-cadherin expression, including the zinc-finger and basic helix-loop-helix transcriptional repressor families. The E-cadherin promoter has been studied in various mammals, and its analysis in mice and humans revealed a conserved modular structure of two E2 boxes (CATCCTG) in the proximal sequence of the promoter which may have a potential repressor function[44, 45]. More recently investigators have found that binding of the zinc-finger repressors to these E-boxes causes down-regulation of E-cadherin expression both *in vitro* and *in vivo*[46-48]. As discussed, regulation of E-cadherin expression is not completely explained by mutation or epigenetic factors. Therefore there is considerable interest in the regulatory role of these repressors.

Transcriptional repressors are known to work through several different mechanisms of action, but can broadly be divided into two groups – passive and active repressors[49]. Passive repressors compete with transcriptional activators for DNA binding by forming inactive protein heterodimers with the activators, rendering them incapable of DNA binding. Alternatively they bind co-activators which are required by the transcriptional activators for the initiation of transcription. These passive mechanisms are thought to be less important than active repression in E-cadherin silencing.

Active repression is transcriptional activator-independent and functions by targeting the structure of chromatin and modifying the histone code which was previously discussed. When an active repressor binds at the promoter region, histone deacetylases are recruited by the repressor and remove the acetyl group from the ε–amino group of lysine residues in the core histones. This allows ionic interactions between the negatively charged DNA and positively charged amino terminal resulting in compaction of chromatin. In turn this inhibits access of transcription factors to DNA[50].

1.6 ZEB1 (also known as TCF8, ΔEF1, NIL-2-A, BZP, AREB6, ZFHX1A, ZFHEP)

Several proteins have been proposed as transcriptional repressors of E-cadherin and the list is constantly growing. Those identified to date include SNAIL, SLUG, ZEB1, SIP1, TWIST, E12/47, CBF-A, FOXC2, HOXB7 and kruppel-like Factor 8 (KLF-8)[51-58]. The investigations detailed here concentrate on the role of ZEB1 (for an overview of studies involving the other repressors refer to Peinado 2007 and Vanderwalle 2009)[52, 59].

ZEB1 was first identified in the early 1990's as a nuclear factor which specifically binds and represses the lens-specific delta1-crystallin enhancer in chicken[60]. Subsequent investigation identified a zinc-finger cluster at the N- and C-terminal ends of the molecule capable of binding to E-boxes (CACCT(G)) found in the promoter regions of certain genes, such as E-cadherin[61]. These zinc fingers are separated by a central homeodomain which does not bind DNA, but may be involved in interactions with other proteins important in repressive / activator functions (figure 1.3)[62]. Interest in ZEB1 has increased as its role in the regulation of E-cadherin expression has been

established in various developmental processes and epithelial malignancies (figure 1.4, and tables 1.2 and 1.3).

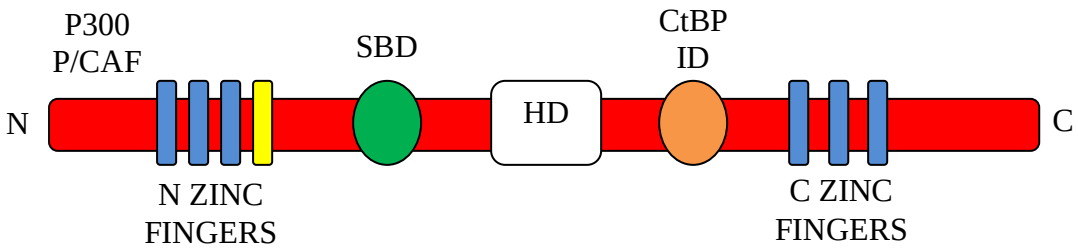

Figure 1.3. Schematic representation of ZEB1. The molecule consists of a central Homeodomain (HD), two zinc finger clusters, one at the C and one at the N terminal. A Smad Binding domain (SBD) and CtBP interacting portion have been identified (CtBP ID) in addition to the finding that the N terminal may associate with the transcriptional activators p300 and P/CAF.

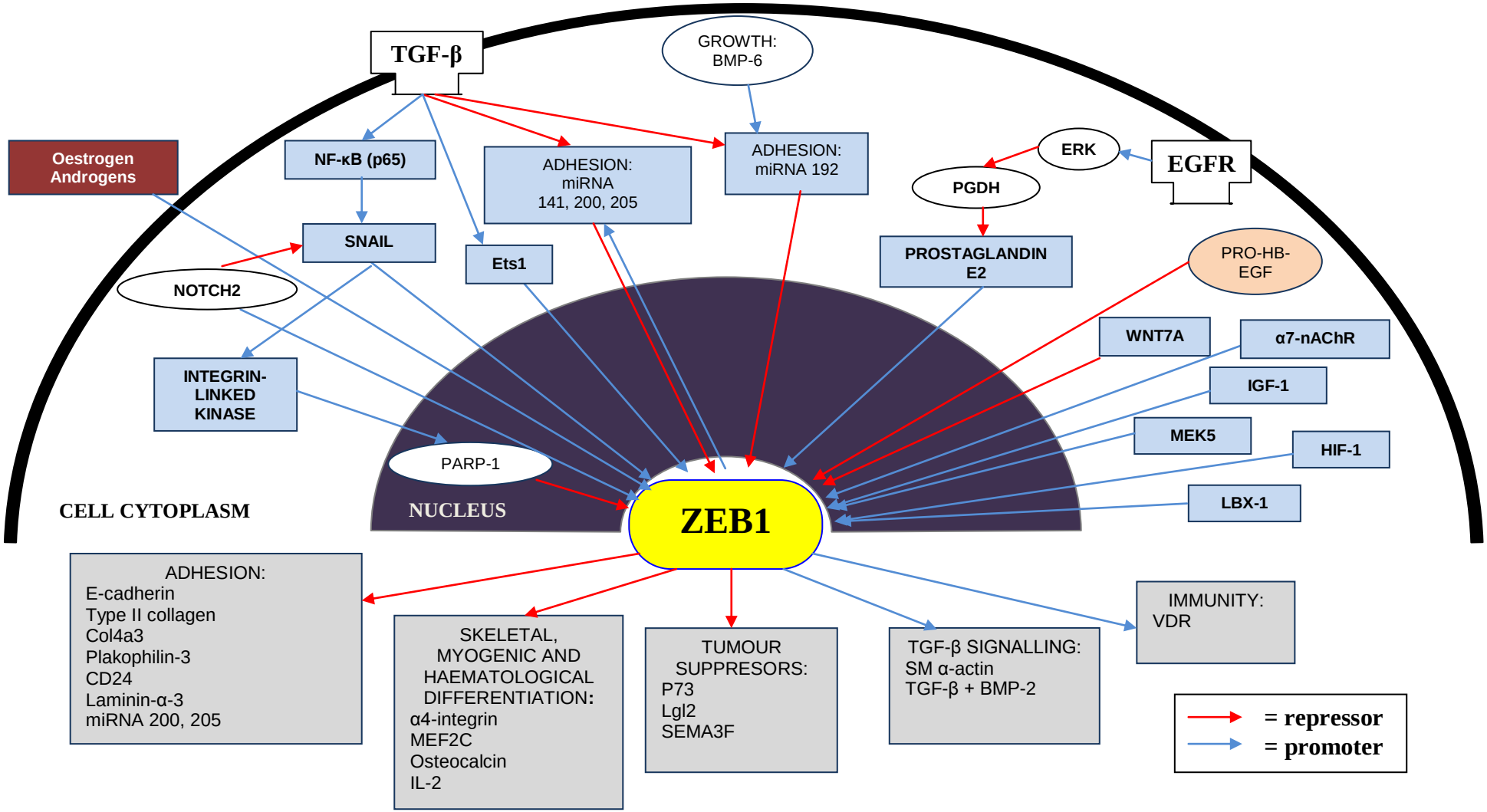

Figure 1.4. Current evidence of signalling pathways demonstrated to be involved in the upstream control and downstream targets of ZEB1.

1.6.1 ZEB1 in development and normal tissues

In the developing chick embryo Funahashi and colleagues found dynamic ZEB1 expression in mesodermal tissues in the notochord, somites and nephrotomes, indicating a role in muscle and skeletal development, findings later confirmed in the mouse embryo by other groups[60, 63-65]. Further evidence for this role has been found in the later stages of the developing mouse and chick skeleton, where ZEB1 expression has been noted in cells adjacent to sites of chondrogenesis and tenogenesis[66, 67]. Confirmation of the importance of ZEB1 in skeletal development has been demonstrated in ZEB1 null mice by several investigators. These ZEB1 knockout mice show craniofacial, palatal and limb defects, rib fusion, sternal defects, hypoplasia of intervertebral discs and die perinatally due to respiratory failure[68-71].

In non-carcinomatous cell lines evidence from several *in vitro* studies confirm the role of ZEB1 in the control of skeletal tissue formation and remodelling. Sooy and colleagues found ZEB1 associates with the osteocalcin gene, repressing transcription and increasing bone formation[72]. Several genes related to collagen formation have also been studied with regard to ZEB1 and investigators have found evidence supporting the role of ZEB1 in their transcriptional regulation. In chick mesenchymal and chondrocyte cells (Murray and colleagues) and in mouse mesangial cells (Kato and colleagues) ZEB1 binds the COL1a2 gene and represses transcription, causing decreased type II collagen formation[73, 74]. ZEB1 expression also plays a role in smooth muscle cell differentiation. In their examination of A404 smooth muscle cells, ZEB1 knockout mice and adult rats, Nishimura and colleagues found ZEB1 bound to and trans-activated smooth muscle α-actin exerting a controlling influence over differentiation, and was expressed in smooth muscle cells of arteries and cardiomyocytes[75].

Posterior Polymorphous Corneal Dystrophy (PPCD) is an autosomal dominant corneal disorder that may cause problems ranging from asymptomatic corneal vesicles, to congenital corneal oedema and childhood glaucoma. Studies of families with this genetic disorder have identified mutations in the ZEB1 gene in the majority of patients, and implicate a lack of ZEB1 expression as a causative factor[76-79]. The corneal abnormalities are thought to relate to changes in collagen synthesis, as demonstrated by increased COL4a3 expression in the corneal epithelia of ZEB1 null mice[76, 80]. In addition, several patients with PPCD have been found to have associated abdominal herniae and skeletal abnormalities, suggesting defects in collagen and connective tissue formation[76, 78, 79].

Little expression of ZEB1 has been found in embryonic endo or ecto-dermal tissues in the species examined, other than in the central nervous system[60, 64, 71, 81, 82]. Here, along with SIP1, ZEB1 appears to play a central role in the differentiation of developing neuronal cells. However, ZEB1 null mouse embryos show little evidence of neurological deficit and it is postulated that compensatory SIP1 expression may perform the role of ZEB1 in this scenario[68, 69, 83, 84]. In contrast to these findings in the embryo, normal human adult endothelial tissues display varying ZEB1 expression characteristics. Hurt and colleagues found high ZEB1 RNA expression in bladder, uterus, skeletal muscle, aorta and thymus, with much lower or absent signal in liver and pancreas specimens[85]. Spoelstra and colleagues found similar expression of ZEB1 in uterine tissues, but noted dynamic modulation according to the menstrual cycle, raising the possibility of hormone-responsive ZEB1 expression[86]. The reasons behind this response remain unclear, though other investigators have noted similar findings in mouse and chicken model systems[87, 88]

Taken together this evidence suggests a prominent role for dynamic ZEB1 expression during the developmental EMTs which occur in the maturing skeleton, muscle and neurological systems. The embryonic formation of neural crest cells is one of the best characterised EMT processes which occur during development[59]. The discovery that ZEB1 plays a significant role in this EMT generated interest in the effect of ZEB1 in carcinogenesis. As previously discussed several investigators have proposed that some epithelial malignant transformations display characteristics similar to those seen in embryonic EMT[89].

1.6.2 ZEB1 in carcinogenesis

1.6.2.1 ZEB1 in cancer cell signalling

Several studies have investigated the role of ZEB1 in cancer cell lines and tissues (figure 1.4 and table 1.3). A number of groups have observed a reciprocal relationship between ZEB1 and E-cadherin expression both at mRNA and protein levels in many different types of tissue[89-99]. This indirect evidence of the role of ZEB1 in the transcriptional repression of E-cadherin has been more closely examined by chromatin immuno-precipitation (ChIP) and promoter-specific reporter assays. In breast, colorectal and several other cell line systems ZEB1 has been shown to specifically bind the E-cadherin promoter at E-box sites and repress its expression[83, 89, 100]. Over-expression of ZEB1 has been engineered in several cell lines. The MCF10A cell line shows myoepithelial characteristics in culture, but upon over-expression of ZEB1 by retroviral transduction, Chua and colleagues observed an EMT in these cells, with a decrease in epithelial markers such as E-cadherin and an increase in mesenchymal phenotype characteristics such as disorganised culture in matrigel 3-dimensional assays[101]. *In vitro* studies in other cell lines have revealed similar results[99]. Taken

together this *in vitro* evidence strongly supports the role of ZEB1 in the control of E-cadherin and its involvement in carcinogenic EMT.

The hormone sensitivity of ZEB1 transcription described earlier in developmental processes has been further demonstrated in various carcinoma cell line systems. Anose and colleagues noted an increase in ZEB1 expression in response to androgen exposure in prostate carcinoma cell lines[102]. Breast carcinoma has been associated with hormone dependency and evidence from *in vitro* studies suggests that ZEB1 may be induced by oestrogens, potentially causing a carcinogenic EMT and increasing the likelihood of metastasis[89]. As previously discussed and supporting this theory, Dillner and colleagues found ZEB1 to be induced by oestrogen treatment of chick embryos[88]. Eger and colleagues investigated this potential link further in a mouse mammary cell line which acts as a model of EMT. When treated with oestrogen these cells undergo an EMT, and on gene micro-array analysis a significant 12-fold up-regulation of the ZEB1 gene was seen, likely acting as a major inducer / maintaining factor in the EMT[89]. However, in contrast to these studies, in ovarian and endometrial cancer cell lines Hurt and colleagues found an increase in ZEB1 expression in response to oestrogen treatment in only 1 of 10 cell lines examined. In normal adult endometrial and ovarian tissue biopsies a clear association was found between ZEB1 expression and oestrogen levels. However, in 5 endometrial carcinomas examined there was no correlation between ZEB1 and oestrogen expression[85]. It should be noted though that this study was performed at the mRNA level, and only 5 tumours from a particular subgroup of endometrial carcinomas were examined. Questions therefore still remain as to the role of oestrogen and ZEB1 in these gynaecological carcinomas, although the overall weight of evidence suggests hormones may induce ZEB1 expression in breast, gynaecological

and prostatic tumours, possibly leading to EMT / poor differentiation and subsequently poor prognosis.

1.6.2.2 ZEB1 in breast cancer

In breast cancer cell lines which are known to have an aggressive phenotype and mesenchymal features such as increased mobility, metastatic and invasive tendencies (e.g. MDA-MB-231) ZEB1 has been shown to be over-expressed when compared to the less invasive, epithelial-like cell lines such as MCF-7[103]. This association suggests a propensity for ZEB1 expression in invasive, aggressive tumours and Aigner and colleagues found ZEB1 expression inversely correlated with differentiation in the 8 ductal and 5 lobular breast carcinomas they examined by Immunohistochemistry (IHC)[104]. Chua and colleagues demonstrated that NF-κB expression directly induced ZEB1 expression in MCF-7 cells, indicating that this transcription factor may be involved in the induction of EMT[101]. In a later study, Hugo and colleagues examined the pattern of transcriptional repressor up-regulation and found NF-κB initially induced expression of SNAIL and SLUG, but by 72 hours ZEB1 was the only repressor to remain over-expressed. SNAIL in itself induced integrin-linked kinase (ILK) expression which directly up-regulated ZEB1 expression[105]. Mcphee and colleagues also observed ILK to induce EMT through ZEB1 induction in their experiments in prostatic carcinoma cells, confirming Hugo's findings[106]. These data indicate that EMT may be induced by SNAIL / SLUG, but is maintained in the longer term by ZEB1 over-expression. Several studies from Michigan in the United States of America have indicated a significant role for WISP-3 (CCN6) in ZEB1 expression[94, 107-109]. Knockdown of WISP-3 in breast cell lines causes an increase in motility, invasiveness and anchorage-independent growth, hallmarks of EMT[109]. Further examination of this effect demonstrated an up-regulation of ZEB1 on WISP-3 knockdown[108]. Low

WISP-3 expression in breast tumours was also found to be associated with an up-regulation of SNAIL and ZEB1 expression, and decreased E-cadherin, along with an increase in lymph node metastases[108]. The role of WISPs in relation to cancer and ZEB1 is discussed later in this chapter (see section 1.7.1).

Contrary to the histological associations noted by Aigner and colleagues, the only study to examine survival related to ZEB1 expression in breast tumours found a highly significant correlation between low expression and decreased disease-free and overall survival (table 1.3)[105]. The conflicting results seen here may be due to the differing methodologies used to examine ZEB1 expression (Aigner = immunohistochemistry, Hugo = gene micro-array), although it is likely that the small sample size (13 tumours) examined by Aigner and colleagues confounds definitive conclusions being drawn from their work.

1.6.2.3 ZEB1 in gynaecological cancer

In 2006 Spoelstra and colleagues recorded their observations in 66 endometrial tumours of high ZEB1 expression in the tumour-associated stroma and tumours themselves compared to normal controls[86]. In their series of 88 endometrial carcinomas, Singh and colleagues also found ZEB1 over-expressed in tumours in comparison to normal matched controls (P=<0.001)[99]. In agreement with these findings, Hurt and colleagues demonstrated a correlation between increasing ZEB1 mRNA levels and tumour grade in their examination of 10 endometrial and ovarian tumours[85]. The agreement between these studies in endometrial and ovarian carcinomas suggests a significant role for ZEB1 in molecular signalling in these tumours, although the nature of its impact on survival remains to be examined.

1.6.2.4 ZEB1 in lung cancer

In non-small cell lung carcinoma (NSCLC) the reciprocal relationship between ZEB1 and E-cadherin expression has also been confirmed in cell lines[93, 97, 110, 111]. In addition, ZEB1 may play a role in other adhesion mechanisms in NSCLC cells. Veena and colleagues found ZEB1 expression correlated with expression of coxsackie-adenovirus receptor expression, a member of the immunoglobulin super family which may act as an adhesion protein[112]. ZEB1 has also been shown to directly bind the *SEMA3F* tumour suppressor gene promoter (ChIP assay), repressing expression of the semaphorin-3F protein. Semaphorin-3F has been shown to act as a tumour suppressor in lung cancer cell lines, and its loss in lung cancer tissues is associated with poor pathological features. In this study, expression of ZEB1 in H358 lung carcinoma cells was also found to cause increased angiogenesis, possibly through down-regulation of semaphorin-3F which has anti-angiogenic actions *in vitro*[110]. Fontemaggi and colleagues demonstrated in their study that ZEB1 binds the tumour suppressor P73 promoter and can repress its expression in NSCLC cells[113]. The full implications of this finding and whether or not this relationship is present *in vivo* remain to be established.

1.6.2.5 ZEB1 in colorectal cancer

In CRC cell lines several investigators have investigated ZEB1 expression and correlated it with other proteins, along with cellular behaviour and characteristics. Spaderna and colleagues investigated ZEB1 expression in relation to E-cadherin in SW480, SW620 and HCT116 cells, demonstrating high levels of ZEB1 in SW480 cells and a reciprocal relationship with E-cadherin expression as previously discussed in other cell lines[114]. Transient knockdown of ZEB1 expression in SW480 dramatically changed the cellular phenotype, with increased cellular adhesion and expression of E-

cadherin, typical of a mesenchymal to epithelial transition (MET)[115]. The same group also found ZEB1 is able to bind the Lama3 promoter (a gene encoding the basement membrane protein Laminin) and repress its expression in SW480 cells[115]. Guaita and colleagues found that expression of the transcriptional repressor SNAIL in HT29 cells up-regulated ZEB1 expression, also demonstrating that SNAIL directly induced ZEB1 expression through binding to its promoter[96]. Wang and colleagues found that disruption of the actin skeleton in SW480 cells by expression of the G-actin binding peptide thymosin β4 caused an EMT[116]. The same group subsequently demonstrated that this EMT is driven by ZEB1 expression, possibly implicating ZEB1 as a mediator of thymosin β4 action[117].

Metabolites of vitamin D_3 have been shown to have tumour suppressor properties. In their study using SW480 cells, Alvares-Diaz and colleagues demonstrated that Vitamin D_3 metabolites induce cystatin D expression, accompanied by a decrease in ZEB1 and increased E-cadherin expression[118]. The implication here is that cystatin D may play a role in the control of ZEB1 expression, although the exact mechanism of this relationship remains to be examined. Loss of the Vitamin D receptor and subsequent loss of Vitamin D_3 responsiveness has been demonstrated in CRC and is thought to be a pivotal point in the progression of tumourigenesis[119]. Larriba and colleagues postulated that ZEB1 expression may play a role in VDR loss, but in their examination of SW480 cells forced to over-express ZEB1 no effect was seen on VDR status[120]. Another known tumour suppressor, Rb, was recently examined in the DLD-1 cell line by Arima and colleagues. Knockdown of Rb in these cells was associated with increased ZEB1 expression and loss of E-cadherin, indicating potential ZEB1 interactions in Rb tumour suppressor function[121]. Cigarette smoking has been shown to be associated with an increased incidence of colorectal and other cancers. Wei and

colleagues demonstrated that treatment of the HT29 and DLD-1 cell lines with a nicotine derivative (α7-nAChR) caused increased ZEB1 expression and decreased E-cadherin, leading to increased migratory and invasive properties in cellular assays[122].

Examination of CRC tissue specimens has been attempted by several groups, using a variety of different methods and analyses (table 1.3). Dominguez and colleagues found over-expression of ZEB1 RNA in 40% of the 81 CRC specimens they examined. However, there was no correlation with pathological factors in the univariable analysis[123]. Aigner and colleagues examined 10 CRC specimens by IHC and RT-PCR for ZEB1 expression and noted little or absent ZEB1 in normal epithelial cells, but observed high expression in tumour-associated stromal cells at points of invasion. They conjectured that these stromal cells may represent epithelial-derived tumour cells which have undergone a ZEB1-dependent EMT and have invaded the stromal compartment. This study also examined the desmosomal adhesion protein plakophilin-3 (PKP-3) and noted an inverse relationship between PKP-3 and ZEB1 expression at the invasive tumour fronts in 8 out of 10 of the tumours examined[124]. In a further report, the same group noted loss of E-cadherin at these points of invasion associated with high stromal cell ZEB1 expression[104]. The relationship between plakophilins and ZEB1 is discussed in more detail later in this chapter (section 1.7.2). Spaderna and colleagues also examined expression of ZEB1 at the invasive front of the primary tumours in their studies, observing significant loss of the basement membrane components laminin α3 and cytokeratin 18 in conjunction with increased ZEB1 at these points[115]. These data suggest an important role for ZEB1 at the invasive front of the primary tumour in CRC, perhaps key in the carcinogenic EMT which allows the epithelial-derived tumour cell to invade the stroma and metastasise via lymphatic or vascular structures.

In a xenograft model, HCT116 cells with ZEB1 knocked down were injected into mice and the resulting tumours compared to those in mice inoculated with control cells. The knockdown clones showed significantly fewer metastases indicating a decreased propensity for tumour spread, though the primary tumours were of a similar size[114]. However, HCT116 cells display a relatively low level of inherent ZEB1 expression and the implications of further knockdown in these cells are not clear. Contrary to these data, Pena and colleagues examined E-cadherin expression by IHC in 114 tumours, and found no difference in expression between central areas and invasive fronts (ZEB1 was not examined by IHC). They further examined 10 tumours for ZEB1 and E-cadherin RNA by RT-PCR at invasive fronts and in central tumour areas, but found no over-expression of ZEB1 in either area. Again contrary to other reports, there was also no indication of a negative correlation between ZEB1 and E-cadherin expression at the RNA level in the 114 tumours. Interestingly, there was a significant correlation between low ZEB1 expression and polyp formation[98]. In a further examination of these specimens, Pena and colleagues reported a trend towards significance in the negative correlation of ZEB1 and E-cadherin expression RNA when the co-factors CtBP and p300 were analysed. They postulated that CtBP and p300 were important co-regulators necessary for ZEB1 function, although this relationship remains to be fully examined[90].

The overriding impression in these studies indicates an important role for ZEB1 in CRC, particularly in relation to the control of cellular adhesion molecules and at the tumour invasive front.

1.6.2.6 ZEB1 in other cancers

Several other cancer types have been investigated to some extent in relation to ZEB1. In pancreatic carcinoma cell lines two studies have implicated ZEB1 in the process of

tumourigenesis. Pro-HB-EGF, a protein involved in EGF signalling and associated with tumour progression, appears to have some role in influencing ZEB1 expression. Although Wang and colleagues did not directly examine the mechanism, they found a positive correlation between pro-HB-EGF expression and ZEB1 in PANC-1 cells[125]. Notch signalling has been shown to be of importance in pancreatic cancer. In a gemcitabine-resistant pancreatic cancer cell line, knockdown of Notch-2 caused a ZEB1 dependent MET through decreased NF- κB. As discussed previously NF-κB appears to induce ZEB1 expression in breast cell lines, therefore reductions in NF-κB will lead to decreased levels of ZEB1[101]. Notch-2 may therefore exert influence over ZEB1 expression via NF-κB modulation[126]. As in the earlier study of pancreatic carcinoma , the mechanism of ZEB1 control in these cells remains to be fully established through promoter reporter or ChIP assays. In the A431 squamous cell carcinoma cell line from head and neck cancer, Taki and colleagues investigated the relationship between ZEB1 and the Wnt pathway. They found ZEB1 inversely correlated with Wnt-4 and positively correlated with Wnt-5a expression, and SNAIL over-expression in these cells caused up-regulation of ZEB1 and Wnt-5a, with reduced Wnt-4 expression[127]. The influence of SNAIL on ZEB1 expression in this cell line is consistent with the previous study in HT29 CRC cells by Guaita and colleagues[96]. Further to this in 2006, Takkunen and colleagues showed SNAIL transfection in primary squamous cell carcinoma (SCC) cells caused an increase in ZEB1 expression and EMT. Interestingly an examination of cells cultured from the primary SCC showed a lack of ZEB1 expression, but the recurrent tumour demonstrated significant ZEB1 expression[128].

1.6.3 ZEB1 and micro-RNA

Micro-RNAs (miRNA) are short RNA molecules which may bind target messenger RNA transcripts, controlling protein expression at the post-transcriptional level. This is

achieved by degradation of the target mRNA and/or inhibition of the translation process through pairing with the micro-RNA molecule[129]. Interest in their role as biological signalling regulators took off in the early 21st century after investigators reported their potential role in negative regulation of protein expression (for a review see Bartel 2009[130]). Several groups have found correlations between ZEB1 expression and micro-RNAs, and it appears that the miRNA-200 group plays a significant role in ZEB1 regulation[131]. Initial studies in lung and breast cell lines indicated an inverse correlation between miR-200c and miR-200b expression and ZEB1[132, 133]. Further studies have confirmed the importance of the miR-200 family in relation to ZEB1 expression and EMT in a variety of cell lines and also implicated miR-205, miR-141 and miR-192 in this process[134-139]. Forced expression of these micro-RNAs in mesenchymal cell line systems causes a morphological change akin to MET, with loss of ZEB1 expression and increased E-cadherin[135, 137]. More recently, regulatory feedback loops have begun to emerge, operating within this framework to communicate between the molecules orchestrating EMT. Burk and colleagues noted miR-200c and miR-141 family members to be down-regulated at the transcriptional level by over-expression of ZEB1[140]. Bracken and colleagues further investigated this, indicating in some cell lines that a double-negative feedback loop exists, with decreased ZEB1 expression and over-expression of miR-200 family members, but also a decrease in these micro-RNAs on forced over-expression of ZEB1[141]. The up-regulation of TGF-β expression has also been demonstrated to repress micro-RNAs important in EMT, as well as causing increased NF-κB expression and subsequent ZEB1 induction[137, 142]. In the last year Saydam and colleagues have reported that over-expression of miR-200a causes a similar decrease in ZEB1 expression in meningioma cell lines. In addition, miR-200a appears to target β-catenin and cause decreased expression of this important

protein in the Wnt signalling cascade, a further example of the complexity of the crosstalk between these signalling networks[139]. The interplay which exists between these molecules remains incompletely explored and possibly explains some of the inconsistent results found between studies. It appears that these micro-RNAs may be the bridge between several cellular signalling systems and will form the focal point of scrutiny in many EMT signalling studies in the near future[131].

1.6.4 ZEB1 and cancer therapeutics

Expression of ZEB1 also appears to play a role in chemo-sensitivity, or lack thereof, in various cell lines. In 2005 Thomson and colleagues demonstrated that the expression of EMT markers, such as ZEB1 and loss of E-cadherin, correlated with EGFR inhibitor resistance in NSCLC cells, a finding later confirmed by Witta and colleagues in these cell lines[143, 144]. Haddad and colleagues also found a similar association in their panel of head and neck cell lines, demonstrating that ZEB1 knockdown increased Erlotinib sensitivity *in vitro*[100]. Li and colleagues found increased resistance to gemcitabine treatment in pancreatic carcinoma cell lines over-expressing ZEB1 and other EMT markers such as vimentin[145].

In colorectal and breast carcinoma cell lines, Buck and colleagues confirmed that expression of ZEB1 correlated with increasing resistance to the EGFR inhibitor Erlinotib, and conversely increasing E-cadherin expression was associated with increased sensitivity[91]. Given the newly discovered role of micro-RNAs in the control of ZEB1 expression, Cochrane and colleagues over-expressed miR-200c in two breast cell lines to examine the effect on chemo-sensitivity. An MET was observed and in Hec-50 cells over-expression of miR-200c increased sensitivity to cisplatin and paclitaxel treatment, but this did not hold true in MDA-MB-231 cells, the reasons for which remain unclear[92]. Adam and colleagues performed a similar analysis in bladder

cell lines, finding over-expression of miR-200c to reverse EGFR-inhibitor resistance[138]. These studies suggest promising lines of investigation for the use of micro-RNA based therapy in the future.

The combination of oxaliplatin and 5-flurouracil is a commonly encountered chemotherapy regime in CRC and has been proven to increase long term survival[146]. Tang and colleagues established a CRC cell line which was resistant to this drug combination and examined the differences in gene expression compared to control cells by micro-array. ZEB1 was found to be down-regulated in the resistant line, perhaps suggesting cells in the process of invasion / metastasis (high ZEB1 mesenchymal-type cells) are more sensitive than established metastatic deposits. However no knock-down experiments were performed and the translational application of this finding is yet to be fully examined[147].

No investigators have attempted to measure ZEB1 levels in living patients. However Reckamp and colleagues failed to find any association between serum E-cadherin levels and chemo-sensitivity in their phase 1 study of 22 patients[148]. Despite this preliminary finding, the *in vitro* studies suggest there may be an interesting role for ZEB1 as a biomarker in chemo-sensitivity / treatment selection.

In the setting of ZEB1 being a major metastasis initiator / propagating factor it would be desirable to investigate therapy aimed at decreasing or blocking its expression in tumour cells, perhaps decreasing the ability of cells to undergo an EMT and metastasise. Few investigators have examined the effect of any treatment agents on ZEB1 expression. As described above, Dohadwala and colleagues found that treatment of NSCLC cells with the cyclooxygenase-2 (COX-2) inhibitor celecoxib caused an increase in E-cadherin expression alongside a decrease in ZEB1, indicating a potential link between COX-2

expression and ZEB1 control[111]. The anti-cancer properties of cyclooxygenase-inhibiting drugs have been well established, with a decreased incidence of CRC in patients taking low-dose aspirin being clearly documented in epidemiological studies(for a review see de Souza Pereira[149]). It may be that the decrease in ZEB1 expression is a factor in this effect. In 2009, Moody and colleagues demonstrated that treatment of NSCLC cells with sodium diclofenac (a non-steroidal anti-inflammatory drug) caused inhibition of prostaglandin E2, and a subsequent decrease in ZEB1 expression and cellular proliferation[150]. This confirmed Dohadwala and colleagues' previous observations using celecoxib. In pancreatic carcinoma cells Li and colleagues investigated the effects of treatment with a dietary indole, diindolylmethane (DIM), and observed a decrease in ZEB1, increased E-cadherin and miR-200s and an increase in gemcitabine sensitivity[145]. These studies open potentially rewarding avenues for further investigations regarding modulation of ZEB1 expression in the treatment of various cancers.

1.6.5 ZEB1 isoforms

Two separate studies by Cabanillas and Costantino and colleagues found ZEB1 present in two differing isoforms in the cell lines examined by nuclear extraction and western blot, suggesting that ZEB1 is post-translationally modified, possibly by phosphorylation. No studies have examined the function of the different isoforms in cell lines, but one isoform lacks the PCAF/p300 interaction domain necessary for binding the p300 co-activator. Binding of p300, PCAF and Smad to this domain has been shown to displace the CtBP co-repressor from the central homeo-domain of ZEB1, possibly converting the protein into a transcriptional activator in some circumstances[151, 152]. This could be a factor accounting for the different repressive / enhancing effects of ZEB1 in various cell lines and the conflicting results in some reports[153, 154]. In

addition, a recent investigation in the Jurkat T lymphocyte cell line revealed a z-box in the ZEB1 promoter region which may itself be bound by ZEB1, indicating that ZEB1 may be able to auto-regulate its expression in some cell lines[155].

1.7 ZEB1, WISPS AND PLAKOPHILIN-3

The repressive effect of ZEB1 on E-cadherin expression was one of the first significant interactions demonstrated in ZEB1 signalling. However, the E-boxes in the E-cadherin promoter region bound by ZEB1 are not unique, and are found in many other protein encoding regions of the genome. Several potential targets of ZEB1 have been identified by genomic blast searching, and a number of these interactions have been investigated *in vitro* and *in vivo*. Known ZEB1 interactions are illustrated in figure 1.4 and many have been discussed above. Considered below in more detail are some specific molecules which are potentially affected by interaction with ZEB1 and which were identified as being worthy of further investigation.

1.7.1 Wnt-Induced Signalling Proteins (WISPs)

As has already been outlined, ZEB1 interacts with several signalling pathways both in its up-stream regulation of expression and downstream effects on other molecules. The Wnt (Wingless pathway in Drosophila) signalling pathway is aberrantly activated in a number of human cancers, and in particular over 90% of CRCs have a Wnt-activating mutation[156, 157]. This pathway therefore appears to be a key factor in CRC progression, and links between EMT and the Wnt pathway may well explain the processes underlying conversion of normal epithelia to invasive, metastasising tumours. It has been proposed that the elucidation of Wnt signalling molecules may lead to the identification of targets for future inhibitory therapies aimed at this pathway[158-160]. One group of proteins participating in the Wnt signalling cascade are the Wnt-induced Signalling Proteins (WISPs). These molecules belong to the wider **C**ysteine-rich

protein-61, **C**onnective-tissue growth factor and **N**ephroblastoma over-expressed gene (CCN) family of multifunctional proteins, consisting of 9 known members (CCN1-9). All of the CCN molecules exhibit closely-related structures and share similar molecular make-up. Each protein contains an N-terminal secretory peptide and four functional domains (figure 1.5)[161]. However, the links between these domains are susceptible to proteolysis, and therefore multiple truncated molecules may be derived from the original, conferring a multitude of possible biological activities to each CCN protein[162, 163].

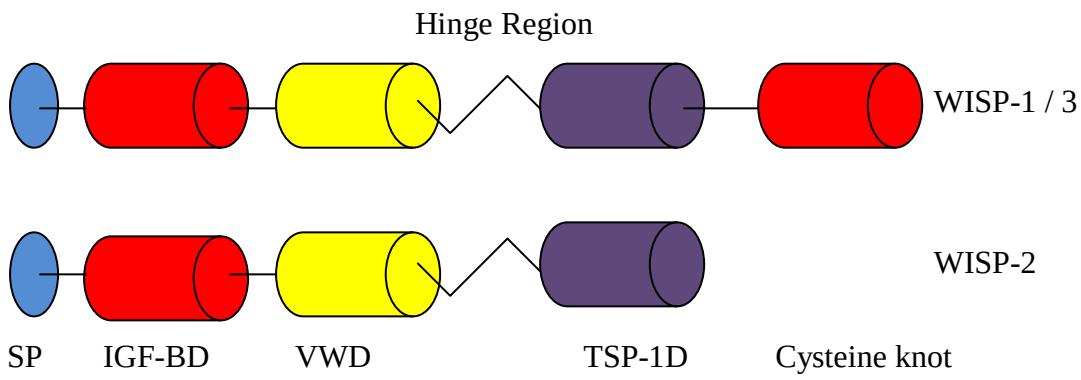

Figure 1.5. Schematic of WISP protein structure. The three WISP proteins have similar molecular structure, each having a secretory signal peptide (SP), an insulin-like growth factor-binding domain (IGF-BD), a von-Willebrand type C domain (VWD) and thrombospondin-1 domain (TSP-1D). WISP-1 and 3 also have a cysteine knot region, which is absent from the WISP-2 molecule. Each domain is connected to the next by a hinge module which is susceptible to proteolysis.

1.7.1.1 WISP-1

Several investigators have identified WISP-1 as an important factor during the development of bone and related tissues (table 1.4). French and colleagues found expression of WISP-1 in mesenchymal tissues during osteoblast and bone progenitor cell development in mice, and expression is also seen in the developing mouse tibia[164, 165]. Case and colleagues found mechanical stress can induce WISP-1

expression in mouse osteoblasts[166]. In a study of human bone marrow cells, Inkson and colleagues found treatment with recombinant WISP-1 protein increased proliferation and differentiation in these cells, and in a later study showed WISP-1 to be important in osteogenic differentiation, confirming French's observations in murine tissues[167, 168]. Djouad and colleagues have also observed increased WISP-1 levels after chondrogenic differentiation of mesenchymal stem cells[169]. Parisi and colleagues attempted to identify factors which may regulate WISP-1 expression during osteoblast differentiation in a mouse model, and found changes in TGF-β, BMP-2 and cortisol to affect WISP-1 expression[170].

Further supporting the role of WISP-1 in bone cell maintenance and differentiation is the observation of up-regulation of WISP-1 expression in disease states such as rheumatoid arthritis. Mori and colleagues found increased expression of WISP-1 in synoviocytes from rheumatoid arthritis joints compared to osteoarthritis controls on gene microarray and RNA analysis, although Tanaka and colleagues could not confirm this *in vivo*[171, 172]. However, in more recent studies WISP-1 was shown to be up-regulated in osteoarthritis synovial cells and cartilage on mRNA PCR and IHC[173, 174]. WISP-1 also appears to play a role in other types of fibrotic and inflammatory disease. In a murine model of colitis and in colonic cell lines treated with nitric oxide (an inflammatory mediator), WISP-1 was over-expressed in comparison to controls and this was confirmed in human colonic biopsies from colitis patients[175]. Treatment of AT11 cells (lung fibrosis model cells) with WISP-1 protein caused an increase in cell migration and proliferation, consistent with an EMT. Knockdown of WISP-1 had the reverse effect in this cell line, indicating that WISP-1 may have a role in EMT signalling. Treatment of mice with bleomycin-induced lung fibrosis using an anti-WISP-1 antibody caused a decrease in the degree of lung fibrosis and increased

survival[176]. This study demonstrates the use of WISP-1 as a potential therapeutic target in these inflammatory diseases in the future.

Two other studies have examined WISP-1 expression in relation to the development of the pancreas and liver. Preliminary findings identified variations in WISP-1 expression as possible directors of pancreatic and hepatic cell differentiation[177, 178].

Investigation of cell signalling pathways have shown WISP-1 is transcribed in response to Wnt-1 or β-Catenin expression and leads to increased cellular proliferation[179, 180]. In 2002, Su and colleagues found activation of Akt kinase and GSK3β following WISP-1 treatment of NRK-49F rat kidney cells, leading to stabilisation of β-catenin and its translocation to the nucleus. This led to an increase in cell proliferation and decreased cell death due to increased Bcl-XL. This cascade was thought to inhibit p53-mediated cell death and promote tumourigenesis[181]. In the same year You and colleagues found similar anti-apoptotic properties and cell survival in Rat-1 cells in response to WISP-1 induction. However, this pro-survival signal was independent of Akt, suppressing the release of caspase-9 and cytochrome C, proteins involved in cellular apoptosis[182]. Further support for the role of WISP-1 in the Akt signalling pathway emerged in 2007 when WISP-1 was demonstrated to activate Akt in rat cardiomyocytes in culture, with a subsequent increase in proliferation[183]. Taken together, these studies indicate a pro-oncogenic role for WISP-1, inducing increased cell proliferation and survival.

In support of this theory initial investigation of the role of WISP-1 in cancer demonstrated that WISP-1 mRNA was up-regulated in various tumour cell lines compared to normal controls[184]. In human chondrosarcoma cells WISP-1 was also over-expressed in comparison to other non-carcinomatous derived cell lines[165]. In

lung cancer cell lines initial studies over-expressing WISP-1 appeared to decrease invasion and motility, and to decrease the expression of matrix metallo-proteinase 1 (MMP-1), a pro-enzyme thought to participate in the invasion and metastasis of tumour cells, indicating that WISP-1 may be a tumour suppressor in this context[185]. In a murine model the H460 lung carcinoma cell line over-expressing WISP-1 gave rise to fewer pulmonary metastases compared to control cells, confirming the previous observations in cell lines[185]. However, Margalit and colleagues found a 2.5-fold increase in WISP-1 expression in mouse pulmonary metastases[186]. Indeed, further study of NSCLC tissues did not reveal any association between WISP-1 expression and survival, although expression was up-regulated in the vast majority of the tumours examined and was associated with the histological subtype of the tumour[187]. This study examined only WISP-1 mRNA levels and it may be that there was insufficient power to detect a significant survival difference. A larger cohort of specimens may confirm or refute this and should be subjected to further investigation in the future.

In addition to lung carcinomas, WISP-1 expression has been investigated in several other types of cancer tissue, using a variety of methods (table 1.5). In CRC six studies have examined WISP-1 expression and all found it to be up-regulated in a significant proportion of the tumours examined[184, 188-192]. Tian and colleagues correlated WISP-1 expression with lymph node stage, differentiation and tumour stage, and Davies and colleagues have recently confirmed these findings in a similar series of tumours[191, 192]. Contrary to these studies, Khor and colleagues found high WISP-1 scores to correlate with low tumour grades[188]. The reasons behind this discrepancy are currently unclear. No investigators have examined the relationship between WISP-1 and survival in CRC.

In breast cancers the reports from *in vivo* studies provide conflicting data. Davies and colleagues examined 120 breast carcinomas and found low WISP-1 expression in tumours compared to normal tissues, and this correlated with lymph node metastasis, high Nottingham Prognostic Index and poor survival[193]. However, Xie and colleagues found WISP-1 mRNA was higher in tumours compared to normal controls and high expression correlated with several poor pathological factors[194]. These reports both examined WISP-1 at the mRNA level, although Davies and colleagues also employed immunohistochemistry (IHC) to examine protein expression. The reasons behind the discrepancies in their results are therefore unclear and demand examination in further studies.

It has recently become clear that each of the WISP proteins may exist in different isoforms, due to alternate splicing of mRNAs or post-translational modification[195]. As early as 2001 Tanaka and colleagues reported that WISP-1v, a variant lacking the Von Willebrand Factor type C repeat module, was expressed in certain upper gastrointestinal malignancies and increased cell migration and chemotaxis in culture[196, 197]. Yamashita and colleagues also found significant over-expression of WISP-1v in their examination of 60 cholangiocarcinomas, and found it to be an independent poor prognostic factor for survival[198]. These differing isoforms of WISP proteins may go some way towards explaining the varying findings in the studies outlined above. Dependent upon the type of antibody used, if the domain of the WISP protein which it targets is missing in the variant, then WISP expression would obviously not be detected.

In other tumour types the association of WISP-1 with tumourigenesis is less clear. In desmoid tumours and uterine leiomyosarcomas WISP-1 appears to be up-regulated compared to normal control tissues[199-201]. In chondrosarcomas, prostatic and

ovarian adenocarcinomas the reverse appears to be the case[202-204]. However, only single studies exist examining these cancers and the low number of tissues included prohibit firm conclusions being drawn.

The weight of evidence to date supports the role for WISP-1 as an oncogenic protein, participating in the signalling cascades relating to EMT and invasion and metastasis. No reports have examined the relationship between WISP-1 and ZEB1 expression.

1.7.1.2 WISP-2

In comparison to WISP-1, little is known of the role of WISP-2 in development (table 1.6). *In vitro* studies indicate that WISP-2 may play a role in mesenchymal stem cell differentiation into hepatic or osteoblastic progenitor cells, but as yet this remains poorly understood[169, 170, 178, 205]. Jones and colleagues noted WISP-2 expression was virtually absent at the basal crypts and increased in the upper layers of foetal colonic epithelium, suggesting a dynamic role during cell maturation[206]. Other investigators have found little effect of WISP-2 expression on cell differentiation[207]. Similar to the expression pattern of WISP-1, WISP-2 is up-regulated in the fibrotic areas of rheumatoid synovium, but is especially prominent in fibroblasts[171, 172].

In contrast to WISP-1, high WISP-2 expression seems to be associated with the epithelial phenotype in breast cancer cell lines[193, 208, 209]. Knockdown of WISP-2 expression causes increased migration, invasion and anchorage-independent growth, along with a loss of E-cadherin expression; factors associated with EMT[210, 211]. Worthy of note in one of these studies is the observation that WISP-2 knockdown was accompanied by up-regulation of the E-cadherin transcriptional repressor SNAIL, though ZEB1 and the other transcriptional repressors of E-cadherin were not examined[212]. However, contrary to this role as a mesenchymal suppressor, WISP-2

has also been shown to participate in signalling related to increased mesenchymal characteristics and cellular proliferation in certain breast cell lines. Banerjee and colleagues found knockdown of WISP-2 to decrease proliferation of MCF-7 cells. Indeed expression of EGF in these cells induced WISP-2 expression, with subsequent increased cellular proliferation[210, 213]. Dhar and colleagues observed that knockdown of WISP-2 expression in MCF-7 cells caused loss of IGF-1 mediated proliferation and this knockdown has also been shown to negate the effect of phorbol ester treatment of these cells (a tumourigenic substance known to increase proliferation)[214, 215]. In addition WISP-2 can induce increased motility and invasion in response to hypoxia[216]. These roles appear to be conflicting and the nature of the signalling networks involved remains to be fully established.

In breast cancer tissues WISP-2 expression studies have also demonstrated heterogeneous results (table 1.7). Banerjee and colleagues negatively correlated WISP-2 expression with differentiation[212]. However, other groups have found high WISP-2 expression in tumours, with little correlation with pathological factors, but associated with increased survival[193].

As previously discussed, oestrogens appear to play an important role in breast cancer, and have been found to influence the control of WISP-2 expression in breast cancer cell lines. Several investigators have found induction of WISP-2 in response to oestrogen treatment of cell lines, indicating possible links with hormone responsive gene targets[213, 217-219]. Indeed high WISP-2 expression has been shown to correlate with tumour oestrogen receptor-α status[213]. In addition WISP-2 expression in uterine tissues appears to be hormone responsive[220]. WISP-2 may also play a role in tumour angiogenesis. Lake and colleagues noted increased vascular smooth muscle cell proliferation, migration, motility and invasion on WISP-2 knockdown[221, 222].

Hawizy and colleagues reported their observation that WISP-2 expression is associated with an epithelial phenotype in prostatic cell lines. Over-expression of WISP-2 exerts anti-proliferative effects in prostatic carcinoma cell lines and its expression is decreased in prostatic tumours[204]. Gery and colleagues noted decreased WISP-2 expression in their examination of 59 ovarian adenocarcinomas, but there was no correlation with pathological variables or survival[203]. In agreement with these other tumour types, WISP-2 expression is decreased in scirrhous gastric tumours[196]. However, in salivary gland cell lines WISP-2 appears to be over-expressed in tumour-derived lines compared to control cells, but in tissues the reverse is true[223]. The reasons behind the contradictory data in salivary gland tumour cell lines are unclear, though the weight of evidence suggests that WISP-2 expression is down-regulated during tumourigenesis in these cancers.

There have been only two studies of WISP-2 expression in CRC. The first in 1998 by Pennica and colleagues was conducted using DNA copy number and mRNA analysis, and found decreased WISP-2 expression in 79% of tumour samples[184]. More recently Davies and colleagues have examined expression at the protein level and found decreased WISP-2 expression correlated with increased Dukes stage, TNM stage, poor differentiation and lymph node metastasis[191]. Neither group examined survival related to WISP-2 expression.

The overall body of evidence to date suggests WISP-2 is a tumour-suppressor protein, capable of participating in proliferation cell signalling pathways and may be involved in EMT, possibly through a SNAIL-dependent mechanism. However, there is clearly a large cohort of conflicting data in the literature and the reasons for this remain elusive. Therefore further studies may more clearly define the role of WISP-2 in malignancy.

1.7.1.3 WISP-3

In-keeping with the roles of WISP-1 and 2 in skeletal development and disease, WISP-3 also appears important in this area (table 1.8). WISP-3 is highly expressed in human primary mesenchymal stroma cells, but is decreased during chondrocytic differentiation[169, 205]. It may also be expressed by chondrocytes, both in cell culture and *in vivo*, and over-expression causes increases in type II collagen and aggrecan expression, both important in the maintenance of normal cartilage[224, 225]. This protective effect of WISP-3 expression on cartilage was also observed by Miller and colleagues, noting that WISP-3 treatment decreased the number of reactive oxygen species which may cause cartilage damage[226]. In addition WISP-3 has been found at high levels in the synovial lining of joints of rheumatoid arthritis sufferers and is able to act as a chemo-attractant to mesenchymal stroma cells, perhaps indicating attempts at damage repair[171, 172, 227, 228].

Further support for the role of WISP-3 in this context comes from the observation of patients with Progressive Pseudorheumatoid Dysplasia (PPD) and idiopathic juvenile arthritis. These patients develop arthritis in childhood due to damage to articular cartilage. A number of mutations in the WISP-3 gene have been identified in patients with these conditions[229-235]. Despite the clear associations between WISP-3 gene mutation and PPD, attempts to create a transgenic murine model of the disease have failed, with mutant WISP-3 mice having no obvious phenotypic abnormalities[236, 237]. This raises the possibility that murine models and cell lines used to examine WISP-3 functions may be inherently flawed, as this protein may not be essential to the normal phenotype in this animal. Parisi and colleagues failed to demonstrate any WISP-3 expression in their examination of murine osteoblasts, perhaps supporting this theory[170].

The majority of studies relating to WISP-3 expression in cancer have been performed in breast cell lines and tissues (table 1.9). Kleer and Huang and colleagues have both reported decreased WISP-3 expression in mesenchymal-type carcinoma cell lines[94, 107]. Forced knockdown of WISP-3 in breast cell lines has been shown to cause an EMT, with increased proliferation, growth, migration and invasion[109, 238]. Further examination of this EMT by Huang and colleagues demonstrated an up-regulation of both SNAIL and ZEB1 in the cell lines, and that decreased WISP-3 expression in tumours was associated with down-regulation of E-cadherin and an increased incidence of lymph node metastases. However, neither SNAIL nor ZEB1 were examined *in vivo* in this study[94]. Despite the possible problems in murine models described above, Kleer and colleagues found SUM149 cells over-expressing WISP-3 formed smaller and better differentiated tumours in nude mice compared to control cells, and the mice survived longer[239]. However, in the largest study of WISP expression in breast cancer, Davies and colleagues found no significant associations of WISP-3 expression with pathological variables in their study of 120 carcinomas[193].

The very few studies that have been conducted in other cancer tissues or cell lines in relation to WISP-3 expression provide conflicting data. In lung cancer cell lines, expression of motility-related protein-1 has been shown to decrease WISP-3 expression, with a subsequent decrease in cellular motility (the contrary situation to that observed in breast cell lines on WISP-3 knockdown)[240]. In ovarian carcinomas WISP-3 expression was found to be up-regulated, but did not correlate with any clinico-pathological variables[203]. In gastric and prostate carcinomas WISP-3 expression did not vary within the tumour population or compared to normal control tissues[196, 241].

As is the case for WISP-2, only the studies by Pennica and Davies and colleagues have examined WISP-3 in CRC tissues at the RNA or protein level. WISP-3 was over-

expressed in 63% of CRCs at the RNA level in Pennica's analysis, but Davies and colleagues could not confirm this in their more recent study and found no association between WISP-3 expression and clinico-pathological variables[184, 191].

Subsequent to the discovery of WISP-3 mutation in relation to PPD and juvenile arthritis, several groups have analysed cancer tissues for WISP-3 mutation. A frame shift mutation was found in 18.5% of metaplastic breast cancers, 11% of gastric carcinomas, and 28-31% of right sided CRCs with micro-satellite instability[242-245]. However, none of these studies has demonstrated a correlation with pathological factors or survival in relation to these mutations, perhaps indicating that this mechanism of WISP-3 silencing in isolation does not influence disease progression. Rather the combination of WISP-3 loss associated with changes in other cell signalling pathways is the key to a more aggressive tumour phenotype.

The evidence relating to the role of WISP-3 in carcinogenesis remains difficult to interpret. *In vitro* studies would suggest that WISP-3 may participate in the EMT signalling pathway, and is lost in conjunction with E-cadherin on SNAIL / ZEB1 induction. However, in some tumour tissues WISP-3 appears to be over-expressed. Further studies in several epithelial malignancies are required to clarify these findings.

1.7.2 Plakophilin-3 (PKP-3)

Plakophilins (PKPs) are members of the armadillo family of intercellular junction molecules which participate in the formation of desmosomes (see figure 1.2). As such they participate in the formation of inter-cellular adhesion complexes, localising to the cytoplasmic-face of desmosomes and linking the intermediate filament cytoskeleton to the junctional plaque. Recent studies indicate that in addition to this role in cellular adhesion, PKPs may also participate in several intra-cellular signalling pathways when

not bound in the desmosomal adhesion complex (for a review see Hatzfeld, 2007)[246]. The body of research relating to PKPs 1 and 2 has increased significantly in recent years, however little is known of the expression patterns and functions of PKP-3 (table 1.10).

In contrast to PKP-1 and PKP-2 which show varied tissue distribution, PKP-3 appears equally distributed among all the epidermal layers in normal skin sections and is found in most simple and stratified epithelia, except hepatocytes[247, 248]. Initial work examining PKP expression suggested that their role was confined to peripheral cellular adhesion complexes[249]. However, more recent localisation studies have demonstrated PKPs are involved in nuclear and cytoplasmic complexes, suggesting significant signalling roles[246]. Certainly the cellular localisation of PKP-2 has been widely studied and it appears to be involved in the regulation of gene transcription, co-localising with β-catenin to the nucleus and potentiating TCF-mediated transcriptional activity[250]. PKPs 1 and 2 also appear important in junctional cross-talk between desmosomes and adherens junctions due to their ability to co-localise to both types of adhesion complex[251]. Mutation in the PKP-1 gene causes a rare autosomal recessive skin fragility syndrome, demonstrating the importance of desmosomes in epidermal adhesion[252]. Interestingly mouse knockout models of PKP-3 demonstrated hair follicle abnormalities and inflammatory skin changes, perhaps indicating fragility in cutaneous cellular adhesion[253].

Stress granules are localisations of RNA-binding proteins, such as PABPC1, FXR1 and G3BP, within the cell cytoplasm which occur when the cell is exposed to adverse environmental conditions (e.g. heat, oxidation). PKP-3 expression has been found in these granules, and nuclear expression has been reported in some cell lines, although there are conflicting reports in this area[247, 254, 255]. The exact nature of PKP-3

activity in these regions remains to be established, though its presence may indicate a role in transcriptional activation / inhibition[254]. In the context of ZEB1 signalling, a recent study by Aigner and colleagues reported knockdown of ZEB1 in the MDA-MB-231 breast carcinoma cell line caused up-regulation of PKP-3 expression, along with E-cadherin. Further investigation with a gene reporter assay demonstrated that ZEB1 is able to bind and repress the PKP-3 promoter in this cell line. Examination of 10 CRC blocks by this group revealed loss of PKP-3 at the invasive fronts in 8 of the 10 tumours[124].

Consistent with these data, Kundu and colleagues found knockdown of PKP-3 in HCT116 cells caused an increase in cell migration and decreased cellular adhesion. When the knockdown PKP-3 HCT116 clones were injected into the flanks of nude mice a significant increase in the number of lung metastases and size of primary tumours were also observed[256]. Recently, Valladares-Ayerbes and colleagues have isolated PKP-3 mRNA from the serum of patients with GI tract tumours, and found a significant increase in expression compared to non-matched control samples, perhaps indicating a release of PKP-3 into the general circulation which may act as a potential biomarker[257]. In oral SCC decreased PKP-3 expression was associated with higher grade tumours and poor survival, findings later confirmed by Schwarz and colleagues[258, 259]. By contrast, PKP-3 was over-expressed in all NSCLC cell lines compared to normal epithelial lung cell lines. Knockdown of PKP-3 caused a decrease in cell viability, and over-expression in COS-7 cells increased growth and cellular invasion. In a micro-array of 279 NSCLC tissues, PKP-3 expression was associated with positive lymph node metastases in adenocarcinomas, and shorter overall survival[260].

These apparently contradictory reports of high PKP-3 expression in lung carcinomas, and decreased PKP-3 expression in other cancer types may indicate a tissue-specific role for PKP-3. However, the lack of studies in this area, and different methods used to examine PKP expression confounds an overall analysis of the role of PKP-3 in cancer. The single study by Aigner and colleagues connecting PKP-3 to ZEB1 signalling in CRC suggests ZEB1 may act as a master regulator of cellular adhesion not just through E-cadherin repression in adherens junctions, but also through the control of desmosomal adhesion.

1.8 SUMMARY

ZEB1 appears to play complex roles in developmental signalling and is important in regulating mesenchymal-epithelial transitions during the formation of the embryo, as demonstrated in several animal model systems. In later life there is now a large body of evidence suggesting that ZEB1 is a crucial EMT mediator in cancer progression. It is involved in several signalling cascades in various epithelial tumours and may be an excellent target for therapeutic modulation through micro-RNA therapy. Further understanding of the role of ZEB1 in cancer progression is essential to the development of these future therapies.

1.9 HYPOTHESIS, AIMS AND OBJECTIVES

AIMS:

This study was initiated with the overall goal to identify molecular targets for new cancer therapies in order to prevent, or slow down, the development of invasion and metastasis in colorectal cancer. Increased understanding of cellular adhesion and mobility may identify such targets. To this end knowledge of the effects of ZEB1 signalling on adhesion-related molecules, such as E-cadherin and Plakophilin-3, and in

important up-regulated signalling pathways in colorectal cancer, such as the Wnt pathway, is necessary. This study aimed to examine *in vitro* and *in vivo* relationships between ZEB1 and these molecules.

HYPOTHESIS:

It is postulated that the transcriptional repressor ZEB1 is an important facilitator of EMT in colorectal cancer through repressive effects on E-cadherin and Plakophilin-3 expression and that cross-talk with Wnt signalling molecules, such as the WISPs, occurs in order to promote cellular proliferation and growth. These combined effects have a direct impact on cancer cell metastasis and patient survival in CRC.

OBJECTIVES:

1. To examine expression of ZEB1, E-cadherin, Plakophilin-3 and WISPs *in vitro* using a panel of colorectal cell lines.
2. To determine the effect of over-expression or of expression blockade on these proteins *in vitro* using transfection of siRNA and constructs.
3. To determine the expression of these molecules *in vivo* using immunohistochemical methods on 101 resected primary colorectal carcinomas and their matched lymph nodes and liver metastases.
4. To define the relationship between expression of these molecules and clinical parameters such as tumour grade and stage, disease-free survival, overall survival and development of metastases. This may lead to the identification of independent prognostic biomarkers in colorectal cancer.

Table 1.2. *In vivo* studies examining ZEB1 expression in normal tissues and development.

Study	Year	Animal / Human tissue	n=	Method	Findings
Nguyen *et al[79]*	2009	PPCD	5	Gene sequencing	Novel mutation identified in ZEB1 gene in this PPCD family, patients also had associated extra-ocular features (hernia, hydrocele and skeletal abnormalities).
Aldave *et al[78]*	2007	PPCD	192	Gene micro-array	25% of screened PPCD sufferers had ZEB1 gene mutation. Mutation found to be associated with abdominal herniae (P=<0.001) and hydrocele's when compared to non ZEB1 gene mutation PPCD families (P=0.014).
Liskova *et al[77]*	2007	PPCD	24	Gene sequencing	37.5% of screened PPCD patients had ZEB1 gene mutation. No association found with extra-ocular features described elsewhere (Aldave *et al*, Krafchak *et al*).
Krafchak *et al[76]*	2005	PPCD	11	Gene mutation analysis	45% of PPCD families screened carry ZEB1 gene mutation. 11 of 14 males with mutation had extra-ocular manifestations (hydrocele or hernia) and several individuals reported skeletal abnormalities (bone spurs, extra vertebrae). ZEB1 gene mutation associated with COL4A3 gene over-expression in the one patient examined.
Dillner and Sanders [88]	2002	Chicks	-	RT-PCR	Δef1 (mouse / chick ZEB1) expressed in response to Oestradiol treatment binds Ovalbumin promoter and activates transcription.
Chamberlain and Sanders [87]	1999	Chick embryo	-	RT-PCR WB	ZEB1 gene transcripts, RNA and protein up-regulated in Chick embryos treated with Oestradiol. ZEB1 identified as a positive regulator of Ovalbumin gene.
Funahashi *et al[60]*	1993	Chick embryos	-	IHC	First report of δef1expression and assessment of embryological expression. Initial expression in post-gastrulation period in mesodermal tissues in the notochord, somites and nephrotomes. Expression noted to be dynamic and correlated with cell differentiation. Little expression in ecto- or endodermal tissues other than in the nervous system.
Bui *et al[261]*	2009	Mouse ZEB-/- Rat neurones	-	*In situ* immune-fluorescence RT-PCR WB	Mouse ZEB1 knockouts half the size of wt mice. ZEB1-/- mice show decreased resistance to ischaemic brain injury. Induction of ZEB1 by p63 is protective of neurones through inhibition of p73 protein (pro-apoptotic).
Liu *et al[71]*	2008	ZEB1 -/-, -/+ and wt mice	-	*In situ* hybridisation	ZEB1 null mice demonstrate palatal, nasal, neural tube and cartilage abnormalities. Loss of ZEB1 expression associated with decreased Vimentin expression and increased E-cadherin compared to wild type mice.
Liu *et al[80]*	2008	ZEB1 -/-, -/+ and wt mice	-	IHC	ZEB1 gene mutant mice examined as model of PPCD. Increased expression of epithelial markers (E-cadherin, Cytokeratin and COL4A3) found in endothelial cell layers of ZEB1 -/- and -/+ mice and associated with increased corneal endothelial cell proliferation compared to wild type mice.
Miyoshi *et al[69]*	2006	ZEB1 -/- and wt Mouse embryo	-	*In situ* hybridisation	Detailed analysis of ZEB1 expression at all stages of mouse development, particularly important for palatal, neuronal and skeletogenesis. Also investigated relationship to SIP1 expression and found that SIP1 overexpression may replace the functions of absent ZEB1.
Moribe *et al[70]*	2000	ZEB1 -/- and wt mice	-	*In situ* hybridisation	ZEB1 dynamically expressed during mouse limb development and important for digit number.

Takagi *et al[68]*	1998	ZEB1 -/- mice	-	*In situ* hybridisation	ZEB1 null mice die pre-natally and show defects in skeletal development: craniofacial, palate and limb defects, rib fusion, sternal defects, hypoplasia of intervertebral discs and severe T cell deficiency of thymus.
Higashi *et al[65]*	1997	ZEB1 -/- mice	-	IHC RT-PCR FACS	ZEB1 expression seen in similar pattern to chick embryos in normal mice embryos. δEF1 knockout led to significant reduction in size of Thymus and production of abnormal T-cells. Only 20% of mice survived to adulthood.
Darling *et al[64]*	2003	Mouse embryo	-	IHC RT-PCR WB	ZEB1 expression dynamic in developing palate, essential for palatal development and expressed in mesenchymal but not epithelial cells. High levels seen in developing striated muscle, forebrain ventricular zone cells, trigeminal nuclei and grey and white matter of the spinal cord.
Tylzanowski *et al[66]*	2003	Mouse and chick embryos	-	*In situ* hybridisation	ZEB1 expressed in cell populations adjacent to developing cartilage and tendons in mouse and chick limbs.
Davies *et al[67]*	2002	Mouse adult	-	IHC	Δef1 (mouse ZEB1) expressed in nuclei of chondrocytes in growth plates, menisci and cartilage of mouse tibia, -ve correlation with Type II collagen and cartilage-derived retinoic-acid-sensitive-protein (CD-RAP) expression.
Furusawa *et al[63]*	1999	Mouse embryo	-	*in situ* hybridisation	Co-repressors CtBP1 and CtBP2 expressed in similar pattern to ZEB1 expression.
Genetta and Kadesch [262]	1996	Mouse brain DNA	-	Gene sequencing	Mouse δEF1 gene shows 99% homology with human, hamster and chicken ZEB1 genes.
Hurt *et al[85]*	2008	Normal human adult and foetus	43 7	*In situ* RNA hybridisation	ZEB1 expressed at high levels in foetal lung. In adults ZEB1 RNA expression very low in liver and pancreas, high in bladder, uterus, aorta, thymus and skeletal muscle.
Mehta *et al[263]*	2008	FECD	74	Gene sequencing	ZEB1 gene mutation found in only 1 patient, therefore not thought to be important in FECD.
Spoelstra *et al[86]*	2006	Endometrium	8	IHC	ZEB1 expressed in stromal myometrial cells, no expression in normal endometrial epithelium. Expression noted in secretory>proliferative endometrial phase (Oestrogen responsive?).
Van Grunsven *et al[84]*	2006	Xenopus embryo	-	*In situ* hybridisation	ZEB1 expressed in migratory cranial neural crest, the retina and neural tube of early tail-bud Xenopus.
Wacker *et al[81]*	2003	C. Elegans nematodes	-	*In situ* hybridisation	Nematodes ortholog of ZEB1 (zag-1) identified and found to be expressed in head and tail ganglia and ventral cord motor neurones in early embryos. Zag-1 mutant animals show pharyngeal defects and exhibit axonal outgrowth defects, indicating zag-1 may be important in axonal navigation and differentiation.
Darling *et al[264]*	1998	Rat adult	-	RT-PCR	Zfhep (rat ZEB1) RNA expressed at high levels in heart, brain and oesophagus. Little in liver or spleen.
Yen *et al[82]*	2001	Rat embryo brain	-	*In situ* hybridisation	ZEB1 expressed in proliferating cells within the ventricular zone during early development, but decreased during and after differentiation of neural cells.

IHC, immunohistochemistry; RT-PCR, RNA real-time polymerase chain reaction; WB, western blot; -, number not stated; MI, myocardial infarction; PPCD, posterior polymorphous corneal dystrophy; FECD, Fuchs endothelial corneal dystrophy; wt, wild type.

Table 1.3. *In vivo* studies examining ZEB1 expression in carcinogenesis.

Study	Year	Animal / Human tissue	Patients (n)	Method	Clinico-pathological analysis?	Findings
Spaderna *et al[114]*	2008	CRC Breast Ca Mouse tumour model	-	IHC	UVA	ZEB1 expressed at invasive fronts associated with decreased Lgl2 expression and correlated with tumour differentiation. ZEB1 Knockdown breast and colorectal cell lines injected into flanks and tail veins of nude mice show significant decrease in metastasis formation, although primary tumours unchanged in size.
Aigner *et al[124]*	2007	CRC	10	IHC	No	ZEB1 rarely expressed in normal colonic epithelial stromal cells, bur high expression in stromal cells at points of tumour invasion. Inverse correlation noted with PKP-3 expression 8 out of 10 tumours.
Aigner *et al [104]*	2007	CRC Breast Ca	10 13	IHC	No	For CRC as per Aigner 2007. In Breast tumours ZEB1 expression was associated with decreased differentiation of tumour cells. High ZEB1 expression seen in invasive lobular Ca.
Dominguez *et al[123]*	2006	CRC	81	RT-PCR Gene RT-PCR	UVA MVA	Over-expression of ZEB1 in 40.7% of tumours compared to normal tissues. No correlation with pathological factors. ZEB1 known to be factor in regulation of p73 oncogenic variants, p73 variant expression independently correlated with worsening stage.
Pena *et al[90]*	2006	CRC*	101	RT-PCR	UVA	Tumours examined for expression of ZEB1 co-factors CtBP and p300. Trends toward significant inverse association between ZEB1 and E-cadherin RNA expression when CtBP levels high (P=0.053), positive association between ZEB1 and Vitamin D Receptor expression when p300 high (P=0.070).
Spaderna *et al[115]*	2006	CRC	125	IHC	UVA MVA	Basement membrane components Lama3 and Cytokeratin 18 lost at the invasive front of primary tumours and associated with ZEB1 expression. Basement membrane re-expressed in metastases.
Pena *et al[98]*	2005	CRC	114	RT-PCR	UVA	Trend of High ZEB1 RNA with decreased E-cadherin only in tumours with low SNAIL RNA expression (P=0.070). No differences in E-cadherin expression between invasive front and central tumour seen on IHC, ZEB1 IHC not performed. Low ZEB1 RNA associated with colonic polyps in the surgical specimen (P=0.041).
Hugo *et al[105]*	2009	Breast Ca	242	Gene micro-array data	UVA	Low ZEB1 gene expression associated with decreased disease-free survival (P=0.026) and overall survival (P=0.004).
Yang *et al[134]*	2009	Breast Ca	28	RT-PCR	-	ZEB1 expression negatively correlated with BMP-6 and miR-192 expression in 19 of 28 samples examined.

Yang *et al[95]*	2007	Breast Ca	16	RT-PCR	-	ZEB1 expression negatively correlated with BMP-6 and E-cadherin expression.
Singh *et al[99]*	2008	Endometrial Ca	88	IHC	UVA	Significant over-expression of ZEB1 in stromal cells in cancers compared to normal / hyperplastic tissues (P=<0.001).
Hurt *et al[85]*	2008	Endometrial Ca Ovarian Ca	10 10	RT-PCR	UVA	High ZEB1 mRNA correlated with high grade endometrial tumours (P=<0.0001), and high levels also seen in high grade ovarian tumours. No correlation with oestrogen status in either group.
Spoelstra *et al[86]*	2006	Endometrial tumours: Leiomyosarcoma – Adenocarcinoma – UPSC – MMMT -	 10 15 12 29	IHC	-	ZEB1 over-expressed in all tumour-associated stroma and myometrial cells compared to normal tissues. In high grade tumours ZEB1 expression seen in tumour-derived epithelial cells.
Dohadwala *et al[111]*	2006	NSCLC	25	IHC	No	Inverse correlation between E-cadherin and ZEB1 expression. Similar expression pattern of ZEB1 and COX-2 and increasing staining intensity consistent with increasing tumour grade.
Sayan *et al[93]*	2009	Bladder Ca	134	IHC	UVA MVA	ZEB1 expressed in 7% of tumours and inversely correlated with E-cadherin expression (P=<0.0001), but no correlation with survival or pathological factors.
Graham *et al[265]*	2008	Prost Adeno	90	IHC	UVA	Weak / absent ZEB1 staining in normal tissues. Over-expression in high grade tumours, expression correlated with Gleason grade (P=<0.001)
Hidaka *et al[266]*	2008	T-cell lymphoma, ZEB1-/- or -/+ mice	34	Gene RT-PCR	No	ZEB1 gene mutation common and leads to decreased ZEB1 expression. Decreased ZEB1 expression in mice (-/+ or -/-) associated with formation of T-cell lymphoma or thymic tumours.
Inuzuka T *et al[267]*	2009	δEF1 +/- mice	10	IHC	No	ZEB1 +/- mice injected subcutaneously with melanoma cells showed increased size and weight of tumours, and increased formation of lung metastases in heterozygous ZEB1 knockouts vs wt controls.
Vermeer *et al[268]*	2008	Sezary syndrome (T-cell lymphoma)	20	Gene Micro-array	-	ZEB1 gene deletion detected in 9/20 patients examined and postulated to lead to increased Interleukin-2 signalling with subsequent cutaneous T-cell lymphoma formation.
Adachi *et al[269]*	2009	Gallbladder Ca	30	IHC	No	Weak / absent ZEB1 expression in normal epithelium. High ZEB1 expression at invasive front in 76.7% of tumours. Inverse relationship with T-cadherin expression.

IHC, immunohistochemistry; RT-PCR, RNA real-time polymerase chain reaction; -, number not stated; NS, not significant; UVA, univariable analysis; MVA, multivariable analysis; N/A, not applicable; Ca, carcinoma; NSCLC, non-small cell lung cancer; CRC, colorectal cancer; UPSC, uterine papillary serous carcinoma; MMMT, malignant mixed mullerian tumour; Prost Adeno, prostatic adenocarcinoma;BMP-6, Bone Morphogenic Protein-6; wt, wild type; *, analysis on subset of tumours from Pena 2005 study.

Table 1.4. *In vivo* studies examining WISP-1 expression in normal tissues and development.

Study	Year	Animal / Human tissue	Patients (n)	Method	Findings
Blom *et al*	2009	Mouse OA, Human synovium	10	IHC RT-PCR	WISP-1 mRNA up-regulated 37-fold in mouse model of OA compared to normal controls. IHC confirmed over-expression at protein level in mice and human samples.
Yanagita *et al*	2007	Mouse cartilage	-	IHC	WISP-1 expressed in chondrocytes in cartilage.
Geyer *et al*	2009	Cartilage in OA	5	Micro-array IHC RT-PCR	WISP-1 gene up-regulated and mRNA increased in OA compared to normal controls. On IHC WISP-1 expressed in chondrocyte nuclei in OA.
Urano *et al*	2007	Spinal OA	304	Genotyping	Single nucleotide WISP-1 polymorphism correlated with end plate sclerosis score, but not other measures of OA.
Tanaka *et al*	2005	Synovium in OA	10	IHC RT-PCR	No obvious pattern to WISP-1 expression.
Konigshoff *et al*	2009	Lung fibrosis, pneumonia, COPD Mouse model of lung fibrosis	30	IHC WB RT-PCR	In human biopsy specimens WISP-1 significantly up-regulated (mRNA and protein) in interstitial fibrosis compared to normal, pneumonia and COPD controls. Treatment of mice with induced lung fibrosis with anti-WISP-1 monoclonal antibody improved lung function and increased survival.
Luo *et al*	2006	Myometrium	27	IHC RT-PCR	mRNA and cytoplasmic WISP-1 expression higher in secretory than proliferative Myometrium.
Wang *et al*	2009	Colitis biopsies Mouse model of colitis	-	IHC RT-PCR	In mouse model and human biopsy samples WISP-1 up-regulated in colitis samples at RNA and protein level compared to normal controls. Expression in cytoplasm of epithelial cells.
Colston *et al*	2007	Mouse model of MI	4	RT-PCR WB	WISP-1 mRNA and protein increased in tissues around zone of infarction.

IHC, immunohistochemistry; RT-PCR, RNA real-time polymerase chain reaction; WB, western blot; -, number not stated; MI, myocardial infarction; OA, osteoarthritis; COPD, chronic obstructive pulmonary disease; mRNA, messenger RNA.

Table 1.5. *In vivo* studies examining WISP-1 expression in carcinogenesis.

Study	Year	Animal / Human tissue	Patients (n)	Method	Clinico-pathological analysis?	Findings
Davies *et al*	2010	CRC	94	IHC RT-PCR	UVA	WISP-1 mRNA and protein over-expressed in tumours compared to normal controls. High expression associated with increased Duke's stage and TNM classification (P=0.017, 0.037) poor differentiation (P=0.0035), lymph node metastasis (P=0.011).
Tian *et al*	2007	CRC	86	IHC RT-PCR	UVA	WISP-1 mRNA over-expressed in 65% of rectal cancers and confirmed by IHC. Cytoplasmic epithelial cell expression in tumours, weak expression in normal controls. WISP-1 over-expression correlated with lymph node metastases (P=0.004), stage (P=0.011) and tumour differentiation (P=0.039).
Khor *et al*	2005	CRC	47	IHC	UVA	WISP-1 weak cytoplasmic staining in 12.5% of normal colons, high expression in 31.9% of tumours. High WISP-1 score associated with low tumour grade (P=0.029).
Fischer *et al*	2001	CRC	37	RT-PCR	No	WISP-1 mRNA significantly higher in tumours compared to normal tissues.
Desnoyers *et al*	2001	CRC	-	*In situ* Immuno-fluorescence	No	Immunoflourescent staining of CRC specimens revealed WISP-1 expression in stromal cells, but not in tumour or normal epithelium.
Pennica *et al*	1998	CRC	25	Gene RT-PCR	No	WISP-1 gene copy number increased in 60% of tumours compared to non-matched normal control tissue. WISP-1 mRNA increased in 84% of tumours compared to matched controls.
Kim *et al*	2008	Mouse Breast Ca model	5	IHC RT-PCR	N/A	WISP-1 expression induced in tumour-associated stromal cells in Wnt-1 transgenic mice.
Davies *et al*	2007	Breast Ca	120	IHC RT-PCR	UVA	WISP-1 mRNA lower in tumours compared to normal tissues (P=NS). On IHC low WISP-1 expression confirmed in tumours and found to correlate with lymph node mets (P=<0.05), high Nottingham Prognostic Index (P=<0.05) and poor survival (P=<0.05).
Xie *et al*	2001	Breast Ca	44	RT-PCR	UVA	WISP-1 mRNA over-expressed in 46% of breast tumours compared to normal controls and associated with increased stage (P=0.001), lymph node metastases (P=0.020), increased tumour size (P=0.003) and HER2 status (P=0.040).
Tanaka *et al*	2001	Gastric Ca	110	RT-PCR	No	WISP-1v splice variant mRNA expressed in 89% scirrhous tumours compared with only 15% in other tumour types. None found in normal tissues.
Chen *et al*	2007	NSCLC	60	IHC RT-PCR	UVA	WISP-1 mRNA up-regulated in 83% of tumours and confirmed on IHC at protein level (P=<0.001). WISP-1 mRNA expression assoc with histological subtype (P=0.017) and younger age (P=0.047), but no correlation with overall survival (P=0.214).
Soon *et al*	2003	Mouse lung Ca model	-	IHC	N/A	H460-WISP-1 clones and control cells injected into nude mice. WISP-1 clones produced fewer and smaller metastases.

Margalit *et al*	2003	Mouse lung Ca model	10	Micro-array RT-PCR	N/A	WISP-1 gene up-regulated in pulmonary metastases compared to primary tumours 3.7 and 4.5 fold in lung tumour and melanoma models respectively. RT-PCR confirmed similar finding at mRNA level.
Xu *et al*	2000	Mouse kidney tumour model	13	NB	N/A	Mice injected with NRK-WISP-1 cells showed tumour formation (10/10 mice), whereas normal controls (NRK cells) did not (0/3).
Yamashita *et al*	2006	Cholangio-Ca	60	IHC	UVA MVA	WISP-1v over expressed in tumours and poor prognostic factor on MVA (P value not given)
Tanaka *et al*	2003	Cholangio-Ca	39	RT-PCR	UVA	WISP-1v expressed in 49% of all tumours, and 89% of scirrhous type. WISP-1v expression associated with lymph node metastases (P=<0.05) and poor overall survival (P=<0.01). Expression of WISP-1v localised to stroma and not epithelial cells.
Yu *et al*	2003	Chondrosarcomas	15	IHC RT-PCR	UVA	Trend for low WISP-1expression in high grade tumours (P=NS)
Bacac *et al*	2006	Desmoid tumours	33	Micro-array	No	WISP-1 gene up-regulated in tumours compared to normal tissues.
Skubitz *et al*	2004	Desmoid tumours	12	Micro-array	No	WISP-1 gene highly up-regulated compared to normal control tissues (n=448).
Hawizy *et al*	2005	Prost Adeno	-	RT-PCR	No	WISP-1 mRNA low in tumour compared to normal tissues.
Cho *et al*	2005	Uterine Leiomyosarcomas	11	Micro array	No	WISP-1 gene upregulated in 40% of sarcomas compared to benign controls
Gery *et al*	2005	Ovarian Ca	59	RT-PCR	UVA	WISP-1 mRNA decreased in tumours compared to normal tissues. No correlation with pathological factors or survival.

IHC, immunohistochemistry; RT-PCR, RNA real-time polymerase chain reaction; NB, northern blot; -, number not stated; NS, not significant; UVA, univariable analysis; MVA, multivariable analysis; N/A, not applicable; Ca, carcinoma; NSCLC, non-small cell lung cancer; CRC, colorectal cancer; Prost Adeno, prostatic adenocarcinoma; mRNA, messenger RNA.

Table 1.6. *In vivo* studies examining WISP-2 expression in normal tissues and development.

Study	Year	Animal / Human tissue	Patients (n)	Method	Findings
Mori *et al*	2006	OA and RA	12	IHC	WISP-2 over-expressed in areas of fibrosis of RA synovium when compared to OA synovium.
Tanaka *et al*	2005	OA and RA	10	IHC RT-PCR	WISP-2 over-expressed at RNA level in RA synovium, localised to fibroblasts in areas of inflammation on IHC of RA tissues. Little seen in OA.
Bourdeau *et al*	2004	Adrenal cortical hyperplasia	58	Micro-array RT-PCR	WISP-2 gene and mRNA expression up-regulated compared to normal tissues. WISP-2 proliferation enhancing?
Gardner *et al*	2006	Systemic sclerosis	9	Micro-array	WISP-2 gene down-regulated compared to normal controls.
Jones *et al*	2007	Mouse and human embryo	-	IHC	WISP-2 absent in basal crypts of colonic epithelium, but expressed at epithelial surface.
Gray *et al*	2007	Rat and Mouse normal tissues	-	IHC	WISP-2 expression in hepatocyte cytoplasm, but nuclear expression in gastric pit, duodenal villi, kidney, ovarian and thymus cells.
Mason *et al*	2004	Rat uterus	-	IHC RT-PCR WB	mRNA and Cytoplasmic WISP-2 expression seen mainly in endometrial cells during high oestrogen phases of menstrual cycle. Treatment with Oestrogen induced WISP-2 expression.
Mason *et al*	2004	Human uterus	-	RT-PCR	Low WISP-2 mRNA expression in uterine fibroids compared to normal endometrium.

IHC, immunohistochemistry; RT-PCR, RNA real-time polymerase chain reaction; -, number not stated; RA, rheumatoid arthritis; OA, osteoarthritis; mRNA, messenger RNA.

Table 1.7. *In vivo* studies examining WISP-2 expression in carcinogenesis.

Study	Year	Animal / Human tissue	Patients (n)	Method	Clinico-pathological analysis?	Findings
Banerjee *et al*	2008	Breast Ca	112	IHC RT-PCR	UVA	WISP-2 mRNA and protein expression inversely correlated with tumour grade (P=NS) and lymph node metastases (P=NS).
Dhar G	2008	Breast Ca	20	*in situ* hybridisation	UVA	WISP-2 mRNA inversely correlated with mutant p53 expression (P=0.001).
Fritah *et al*	2008	Breast Ca	48	RT-PCR	No	WISP-2 mRNA expression correlated with the transcriptional regulator ID2 (P=0.002)
Davies *et al*	2007	Breast Ca	120	IHC RT-PCR	UVA	WISP-2 mRNA low in tumours compared to normal tissues. On IHC WISP-2 high in tumours compared to normal tissues. High mRNA level associated with lymph node metastases (P=0.0043), poor Nottingham Prognostic Index score (P=<0.05), high grade tumours (P=<0.05) and the development of metastases (P=<0.05), but not overall survival.
Banerjee *et al*	2003	Breast Ca	108	IHC RT-PCR	UVA	High WISP-2 mRNA expression in tumours compared to normal tissues. On IHC WISP-2 expressed in tumour cell cytoplasm and associated with ER positivity (P=0.0174), but no other pathological factors.
Hawizy *et al*	2005	Prost Adeno	-	IHC RT-PCR	No	Low WISP-2 expression in tumours compared to normal controls.
Kouzu *et al*	2006	Salivary gland tumours	34	IHC RT-PCR	No	WISP-2 mRNA expression lower in tumours than normal controls (P=0.009). Confirmed by IHC.
Gery *et al*	2005	Ovarian Ca	59	RT-PCR	UVA	Low WISP-2 mRNA expression in tumours compared to normal controls. No correlation with clinico-pathological variables.
Davies *et al*	2010	CRC	94	IHC RT-PCR	UVA	Low WISP-2 mRNA and protein expression in tumours compared to normal tissues (P=0.082). Significant decrease in WISP-2 expression in Dukes C (P=0.044), poorly differentiated (P=0.019), TNM stage 3 (P=0.020) and node positive (P=0.048) tumours.
Pennica *et al*	1998	CRC	25	Gene RT-PCR	No	WISP-2 gene copy number increased in 92% of tumours compared to non-matched normal controls. However, at mRNA level 72% of tumours under-expressed WISP-2 compared to matched controls.
Tanaka *et al*	2001	Gastric Ca	110	RT-PCR	No	Low WISP-2 mRNA expression in tumours compared to normal controls.

IHC, immunohistochemistry; RT-PCR, RNA real-time polymerase chain reaction; -, number not stated; NS, not significant; UVA, univariable analysis; MVA, multivariable analysis; Ca, carcinoma; CRC, colorectal cancer; Prost Adeno, prostatic adenocarcinoma; mRNA, messenger RNA; TNM, tumour/nodes/metastasis.

Table 1.8. *In vivo* studies examining WISP-3 expression in normal tissues and development.

Study	Year	Animal / Human tissue	Patients (n)	Method	Findings
Cheon *et al*	2004	RA and OA synovium	-	IHC RT-PCR	High WISP-3 expression at synovial lining, mainly in fibroblasts in RA, lower expression in OA.
Kleer *et al*	2004	Breast	10	IHC	Low WISP-3 expression in all epithelial cells, but also observed into duct secretions.
Mori *et al*	2006	RA and OA synovium	12	Micro-array IHC RT-PCR	WISP-3 over-expressed in areas of fibrosis and inflammation in RA synovium compared to OA.
Tanaka *et al*	2005	RA and OA synovium	10	RT-PCR	WISP-3 mRNA expressed at low levels in 1/5 of RA and OA synovial tissues, absent in 4/5.
Yue *et al*	2009	PPD	2	Gene RT-PCR	Two WISP-3 mutations identified.
Zhou *et al*	2007	PPD	1	RT-PCR	WISP-3 gene deletion identified.
Delague *et al*	2005	PPD	16	Gene RT-PCR	Serum samples analysed all had at least one of 3 different WISP-3 gene mutations.
Ehl *et al*	2004	PPD	1	Gene RT-PCR	WISP-3 gene mutation present.
Hurvitz *et al*	1999	PPD	13	Gene RT-PCR	Nine different types of WISP-3 gene mutation identified and all patients had at least one mutation.
Lamb *et al*	2005	IJA	101	Gene RT-PCR	WISP-3 84AA polymorphism associated with IJA.
Nakamura *et al*	2009	Transgenic and knockout Zebra fish	-	-	WISP-3 over-expression inhibited BMP and Wnt- signalling. WISP-3 knockouts showed skeletal defects.
Nakamura *et al*	2009	Transgenic mouse model	-	-	WISP-3 over-expression no difference in phenotype.
Kutz *et al*	2005	Transgenic and knockout mice	-	-	No phenotypic abnormalities seen in any tissues.
Sen *et al*	2004	Cartilage	-	IHC RT-PCR	WISP-3 expression in chondrocytes in mid-zone of cartilage.

IHC, immunohistochemistry; RT-PCR, RNA real-time polymerase chain reaction; -, number not stated; RA, rheumatoid arthritis; OA, osteoarthritis; PPD, progressive pseudorheumatoid dysplasia; IJA, idiopathic juvenile arthritis.

Table 1.9. *In vivo* studies examining WISP-3 expression in carcinogenesis.

Study	Year	Animal / Human tissue	Patients (n)	Method	Clinico-pathological analysis?	Findings
Davies *et al*	2010	CRC	94	IHC RT-PCR	UVA	No significant variation in WISP-3 expression compared to controls.
Thorstensen *et al*	2005	All CRC with MSI	38	Gene RT-PCR	UVA	WISP-3 frame shift mutation found in 28% of tumours with MSI, but no correlation with clinico-pathological factors.
Thorstensen *et al*	2001	Right Colon CRC with MSI	36	Gene RT-PCR	No	WISP-3 mutation in 31% of tumours with MSI.
Pennica *et al*	1998	CRC	25	RT-PCR	No	High WISP-3 mRNA expression in 63% of tumours compared to matched controls. DNA copy number unchanged in tumours.
Hayes *et al*	2008	Metaplastic Breast Ca	27	Gene RT-PCR	No	WISP-3 frame shift inactivating mutation found in 18.5% of tumours.
Huang *et al*	2008	Breast Ca	116	IHC	UVA	Low cytoplasmic and occasional nuclear WISP-3 expression in 60.7% of tumours associated with low E-cadherin expression (P=0.02) and lymph node metastases (P=0.04)
Davies *et al*	2007	Breast Ca	120	IHC RT-PCR	UVA	High WISP-3 mRNA expression in tumours compared to normal controls. However, low expression of WISP-3 seen in all tissues on IHC, and no significant correlation with clinico-pathological factors.
Kleer *et al*	2002	Mouse Breast Ca model	31	IHC RT-PCR	UVA	Mice injected with SUM149-WISP-3 clones. Compared to control SUM149 cells tumours were slower to develop (P=0.05), showed lower tumour volume (0.05) and mice survived longer (P=<0.001).
Hawizy *et al*	2005	Prost Adeno	-	IHC RT-PCR	No	WISP-3 expression unchanged in tumours compared with controls.
Gery *et al*	2006	Ovarian Ca	59	RT-PCR	UVA	High WISP-3 mRNA expression in tumours compared to normal tissues. No Correlation with clinico-pathological factors.
Tanaka *et al*	2001	Gastric Ca	110	RT-PCR	No	No WISP-3 mRNA expression in any tumours.
Thorstensen *et al*	2003	Gastric and Endometrial Ca with MSI	27 and 7	Gene RT-PCR	No	WISP-3 mutation in 11% of gastric tumours, but none of the endometrial carcinomas.

IHC, immunohistochemistry; RT-PCR, RNA real-time polymerase chain reaction; -, number not stated; NS, not significant; UVA, univariable analysis; MVA, multivariable analysis; Ca, carcinoma; CRC, colorectal cancer; Prost Adeno, prostatic adenocarcinoma; MSI, micro-satellite instability; mRNA, messenger RNA.

Table 1.10. *In vivo* studies examining Plakophilin-3 expression in development and disease.

Study	Year	Animal / Human tissue	Patients (n)	Method	Clinico-pathological analysis?	Findings
Kundu *et al*	2008	Mouse tumour model	20	IHC	N/A	Mice injected with HCT116 PKP-3 knockdown clones showed significantly larger primary tumours and increased incidence of lung metastases compared to HCT116 injected controls.
Aigner *et al*	2007	CRC	10	IHC	No	High cytoplasmic PKP-3 expression in central tumour, but decreased / absent at invasive front.
Sklyarova *et al*	2007	Mouse PKP-/-	-	IHC	N/A	Decrease in hair growth and number of desmosomes in basal epidermis. Transient increase in epidermal cell proliferation, but not in other epithelia, in young mice (P7). Susceptibility to dermatitis.
Schwarz *et al*	2006	Oral SCC CRC Panc Adeno Prost Adeno HCC	40 9 10 12 8	IHC	No	High PKP-3 expression in low/mod grade oral SCCs. High grade tumours show <PKP-3 expression. High PKP-3 expression in CRC, Pancreatic and Prostatic adenocarcinomas. No PKP-3 expression in normal liver or HCC tumour cells. Biliary epithelium weak PKP-3 staining.
Furukawa *et al*	2005	NSCLC	279	IHC + Gene expression microarray (n=37)	Yes (UVA)	PKP-3 gene expression 5-fold > in tumours compared to normal tissues. IHC = -ve PKP-3 in normal lung. >94% tumours +ve PKP-3 expression. In adenocarcinomas high PKP-3 expression associated with increased nodal metastases (P=0.0017) and poor disease-specific survival (P=0.009).
Schmidt *et al*	2005	Normal oesophagus	1	IHC	No	Cytoplasmic PKP-3 stain in basal cell layers, but membranous expression observed in surface epithelial cells. No nuclear expression.
Papageraki s *et al*	2003	Oral SCC	37	IHC	Yes (UVA)	Weak PKP-3 expression in normal epithelium. PKP-3 expression inversely correlated with tumour grade (P=<0.02) and survival (P=<0.01)
Bonne *et al*	2003	Normal Skin Normal colon	1 1	IHC	No	Moderate PKP-3 cytoplasmic and membranous expression in epidermis, but absent in dermis and stratum corneum. Weak expression in normal colonic epithelium
Schmidt *et al*	1999	Human skin, liver, pancreas duodenum Bovine muzzle Amphibian skin	1 1 1 1 1	Immuno-fluorescent microscopy	No	Diffuse weak cytoplasmic staining observed in all human epithelia except liver. Bovine and amphibian tissues displayed similar reactivity to human.

PKP, Plakophilin; IHC, immunohistochemistry; UVA, univariable analysis; N/A, not applicable; SCC, squamous cell carcinoma; CRC, colorectal cancer; Panc Adeno, pancreatic adenocarcinoma; Prost Adeno, prostatic adenocarcinoma; HCC, hepatocellular carcinoma; NSCLC, non-small cell lung cancer.

Chapter 2: Materials and methods

2.1 MATERIALS

2.1.1 Chemicals

Unless otherwise stated, all chemicals were purchased from Sigma-Aldrich Company Limited, Poole, Dorset, UK. Solvents were provided by Fisher Scientific, Loughborough, Leicestershire, UK.

Acrylamide (30%)	Anachem (Beds, UK)
Agarose (high melting point)	Gibco BRL (Paisley, UK)
BioRad protein assay reagent	Bio-Rad (Herts, UK)
DH5-α competent cells (library efficiency)	Invitrogen (Paisley, UK)
DNA molecular weight markers	New England Biolabs (Herts, UK)
ECL detection kit	GE Healthcare (Bucks, UK)
ECL-hyperfilm	GE Healthcare
Plasmid Maxi kit	Qiagen (West Sussex, UK)
Fetal calf serum	Autogen Bioclear (Wiltshire, UK)
Codebreaker	Promega (Southampton, UK)
Neo Fx	Ambion (Warrington, UK)
Lipofectamine 2000	Invitrogen
Protran nitrocellulose	Geneflow (Fradley, Staffordshire, UK)
Luciferase reporter assay kit	Promega
Marvel (dried milk powder)	Premier brands (St Albans, UK)
Protein molecular weight markers	Fermentas (MD, USA)
Odyssey blocking solution	Li-COR (Cambridge, UK)

2.1.2 Antibodies against the following proteins

ZEB1	Santa Cruz Biotechnology (Heidelberg, Germany)
WISP-1	Abcam (Cambridge, UK) and Santa Cruz Biotechnology
WISP-2	Santa Cruz Biotechnology [sc25442] and Abnova (Heidelberg, Germany) [H00008839-M09]
WISP-3	Santa Cruz Biotechnology
E-cadherin	BD Biosciences (Oxford, UK)
α-Tubulin	Santa Cruz Biotechnology
β-Actin	Santa Cruz Biotechnology
Plakophilin-3	Invitrogen

2.1.3 Plasmids

pCS3mDeltaEF1FL (ZEB1) - Gift from Dr. E. Tulchinsky, Department of Cancer Studies and Molecular Medicine, University of Leicester, Leicester, UK.

P-silencer 1.0 U6 WISP2shRNA - Gift from Dr. S. Banerjee, Cancer Research Unit, VA Medical Centre, Kansas City, USA.

P-silencer 1.0 U6 control - Gift from Dr. S. Banerjee.

pmaxGFP - Amaxa biosystems (Walkersville, USA)

pCMV-E-cadGFP - Gift from Dr. E. Tulchinsky

pRetro-shZEB1 - Gift from Prof. T. Brabletz, Department of Surgery, University of Freiburg, Germany.

pRetro-shGFP - Gift from Prof. T. Brabletz

2.1.4 Immunohistochemistry materials

Superfrost Plus microscope slides by Menzel-Glaser were purchased from Fisher Scientific (Surrey, UK). Cover slips were from Chance Propper (West Midlands, UK).

Primary antibodies were as for western blotting. Envision detection kits were purchased from DakoCytomation (CA, USA) along with appropriate control antibody immunoglobulin fractions against rabbit and mouse. Haematoxylin counter stain was from Vector Laboratories (CA, USA).

2.2 SOLUTIONS AND BUFFERS

2.2.1 Immunohistochemistry

Tris-buffered saline (x10 stock solution) for washing slides (TBS)

0.5M Tris-base, 1.5M NaCl, pH 7.6; 60.5g Tris base, 87.6g NaCl dissolved in 1L distilled water and pH adjusted to 7.6, stored at room temperature and diluted 1 in 10 prior to use.

Tris-EDTA solution for antigen retrieval

10mM Tris-base, 1mM EDTA, pH9; 0.555g EDTA, 1.818g Tris base dissolved in 1.5L distilled water. 1.5ml Tween 20 was added once the salts were dissolved.

Tris-HCl buffer for dilution of the primary antibodies

0.05M Tris-HCl, pH 7.2-7.6; 0.785g Tris-HCl added to 100ml distilled water. This solution was stored at room temperature and 1% BSA was added immediately prior to use.

Envision detection system

Peroxidase blocking solution; 0.03% hydrogen peroxide

Secondary antibody; Peroxidase-labelled polymer conjugated to goat anti-rabbit or anti-mouse immunoglobulins, in Tris-HCl buffer.

Detection; 1 drop of 3,3-diaminobenzidine (DAB) chromagen was added to 1ml substrate buffer, containing hydrogen peroxide, before use on tissue samples.

2.2.2 Western blotting

10X Cell Lysis buffer

200mM Tris-HCl, 10% triton X-100, 1.5M NaCl, 25mM sodium pyrophosphate, 10mM EDTA, 10mM β-glycerophosphate, 10mM sodium orthovanadate

The above solution was made up to 500ml with distilled water, and stored at 4C. Prior to use, it was diluted 1 in 10 in distilled water, and 1% protease cocktail inhibitors (Sigma) were added.

3x Sample buffer

187.5mM Tris-HCl (pH 6.8), 6% w/v SDS, 30% glycerol, 0.03% w/v bromophenol blue, 150mM DTT

This solution was aliquoted, stored at -20°C, and thawed immediately prior to use.

Polyacrylamide denaturing stacking gel (10ml)

6.8ml distilled water, 1.7ml 30% acrylamide, 1.25ml 1M tris (pH 6.8), 100µl 10% SDS, 100µl 10% ammonium persulphate

Polymerisation was initiated immediately prior to pouring by adding 10µl TEMED.

Polyacrylamide denaturing running gel (10ml)

A standard solution of 2.5ml 1.5M Tris (pH 8.8), 100µl 10% ammonium persulphate and 100µl 10% SDS was made. Varying amounts of distilled water and 30% acrylamide were added to create different percentage gels as in table 2.1.

Table 2.1 Recipes for denaturing running gels.

Percentage Gel	8%	10%	12%	15%
Distilled water (ml)	4.6	4	3.3	2.3
30% acrylamide (ml)	2.7	3.3	4	5

Polymerisation was initiated immediately prior to pouring by adding 10µl TEMED.

Stock solutions of running and transfer electrophoresis buffers (10X) were purchased from Geneflow (Staffordshire, UK).

Running Buffer - Each 100ml of buffer was diluted in 900ml distilled water to make 0.025M Tris / 0.192M glycine / 0.1% SDS

Transfer Buffer - Each 100ml of buffer was diluted in 700ml distilled water and 200ml methanol to make 0.025M Tris / 0.192M glycine

PBST (10X stock) - 0.1M phosphate buffer containing 0.027M KCl, 1.37M NaCl and 1% Tween 20. Diluted 1 in 10 in distilled water prior to use.

2.2.3 Plasmid preparation

Tris / Borate / EDTA buffer (5X stock)

445mM Tris Boric acid, 10mM EDTA (pH 8.0)

Made up to 1L in distilled water and diluted 1 in 5 to a 1X working solution prior to use.

6X DNA loading buffer

0.25% Bromophenol blue, 0.25% xylene cyanol FF, 40% sucrose

2.3 CELL LINES

The HCT116, SW480, SW620, HT29, MCF-7 and MDA-MB-231 cell lines were purchased from the American Type Culture Collection (Middlesex, UK). HCEC was a kind gift from Dr Andrea Pfeiffer (Nestlé Research Center, PO Box 44, CH-1000 Lausanne 26). The DLD-1-SIP1 and A431-ZEB1 cell lines were a kind gift from Dr. E. Tulchinsky (Cancer Studies and Molecular Medicine, University of Leicester, UK).

HCT116: derived from a primary colonic carcinoma in a male.

SW480 and SW620: derived from the primary colonic adenocarcinoma and a lymph node metastasis from a 51 year old male Caucasian.

HT29: derived from a primary colonic adenocarcinoma in a 44 year old Caucasian female.

HCEC: a non-carcinomatous colon cell line derived from a 69 year old female undergoing surgery for diverticular disease.

MCF-7: isolated from a pleural effusion from a 69 year old patient with metastatic breast adenocarcinoma.

MDA-MB-231: isolated from the pleural effusion of a 51 year old Caucasian female with metastatic breast adenocarcinoma.

A431-ZEB1: derived from an 85 year old female with epidermal squamous cell carcinoma, and transformed by Dr E. Tulchinsky to express ZEB1 when treated with doxycycline (unpublished data).

All cell culture was performed in a class II laminar flow cabinet with strict aseptic technique.

2.4 METHODS

2.4.1 Maintenance of cell lines

Cell lines were cultured in a Sanyo incubator at 37°C, with 5% CO_2 and 100% humidity in the following media:

High Glucose Dulbecco's Modified Eagle's (DME) Medium : A431-ZEB1, HCT116, HT29, SW480, SW620 and HCEC cell lines

With 4500mg/L glucose, 10% fetal calf serum warmed to 37°C and added before use.

Low Glucose Dulbecco's Modified Eagle's (DME) Medium : MCF-7 cell line

With 1000mg/L glucose, 10% fetal calf serum warmed to 37°C and added before use.

Roswell Park Memorial Institute (RPMI) Medium : MDA-MB-231 cell line

With 0.3g/L L-glutamine, 10% fetal calf serum warmed to 37°C and added before use.

All media were stored at 4°C and warmed to 37°C prior to use.

2.4.2 Cell passage

All cells were split once they had reached approximately 70% confluence. Adherent cells were washed twice in PBS to remove all medium, and an appropriate amount of trypsin added to the flask (3ml large, 2ml medium, 1 ml small). Cells were returned to the incubator until they had detached. The TE was then neutralised by the addition of 5ml of appropriate medium containing 10% FCS and the solution was centrifuged at 200xg for 3-5 minutes to pellet the cells. The supernatant was discarded and the cells re-suspended in 10ml of medium containing 10% FCS. An appropriate amount of the cell suspension (generally 0.75-1ml) was added to a new flask containing fresh medium with 10% FCS.

2.5 PREPARATION OF CELLS

2.5.1 Whole cell lysates

Cultured plates were removed from the incubator and placed on ice. The medium was removed and centrifuged at 200xg to collect any floating cells. Plates were washed with PBS 3 times, this was collected and centrifuged with the previous cells. All residual liquid was removed from the plate and an appropriate amount of 1x lysis buffer with PIC was added to the plates and the collected cells (this was approximately 300µl for a 10cm plate). These were incubated on ice for 15 minutes. The plates were scraped and the contents removed to small centrifuge tubes along with any lysates from floating cells. The lysate was then cleared by centrifugation at 13000xg for 5 minutes and stored at -20°C.

2.5.2 Bio-rad protein assay and standard curve

The protein concentration of cell lysates was determined prior to use in order that equal amounts of protein could be loaded for each set of experiments (generally 30µg).

A standard protein solution (2mg/ml) containing bovine serum albumin was used to create serial dilutions as detailed in table 2.2. Biorad reagent (200µl) was added to each, mixed and incubated for 5 minutes. The absorbance at 595nm was determined using a Perkin Elmer λ2 UV/VIS spectrophotometer. A standard curve of protein concentration against optical density was then created using Microsoft Excel software.

Table 2.2. Bradford assay standard curve dilutions.

Final Protein Concentration (µg/ml)	Amount of (0.2 mg/ml) BSA (µl)	Amount of Water (µl)
0	0	800
0.5	2.5	797.5
1	5	795
2	10	790
4	20	780
6	30	770
8	40	760
10	50	750

To determine the protein concentration of lysates, 5µl of sample was added to 795µl of distilled water along with 200µl of Biorad reagent. This solution was mixed, transferred to a cuvette, incubated for 5 minutes at room temperature and the absorbance determined as above. The protein concentration of each sample was determined by reference to the standard curve. All samples were assayed in duplicate and an average reading used to determine concentrations. The volume of sample required for 30µg of protein was then determined.

2.6 WESTERN BLOTTING

This was based on the method described by Shapiro and Maizel in 1969. Polyacrylamide, denaturing running gels were prepared according to the molecular weight of the protein of interest, as detailed in table 2.3. A 2cm layer of 5% denaturing stacking gel was placed on top of this and a well-forming comb inserted. The samples were combined with 3x sample buffer to give a final concentration of 1x SDS. The samples were mixed and boiled in a heat block for 5 minutes. Once set, the comb was removed from the gel and samples of known protein concentration loaded into the wells. The samples were then subjected to a 100V current in 1x running buffer for approximately 1 hour until sufficient separation had occurred. The mini protean or

Dodeca kit (Bio-Rad, CA, USA) was utilised as determined by the number of gels being run together.

Table 2.3. Conditions for use of primary antibodies and expected molecular weight of proteins on western blots.

Primary Antibody	Dilution	Expected Molecular Weight (KDa)	Running Gel (%)
ZEB1	1:1000	170	8
E-cadherin	1:2000	135	8
WISP-1	1:1000	44	10
WISP-2	1:500	51	10
WISP-3	1:200	39	10
Plakophilin 3	1:1000	87	10

The proteins were then transferred onto Protran nitrocellulose at 0.7A for 1.5 hours in the transfer buffer, using a Bio-Rad wet blotting system. The membrane was then washed in phosphate buffered saline tween-20 (PBST) 3 times and blocked for 1 hour with either Odyssey blocking solution (diluted 1:1 with PBS), or 5% non-fat milk according to the analysis method to be used. The membrane was then immersed in fresh blocking solution (Odyssey or 5% milk) to which the primary antibody was added at the dilutions detailed in table 2.3, and incubated overnight at 4°C.

The following day the antibody solutions were removed and stored at 4°C for future use (once more only) and the membrane washed through 5 cycles of PBST. The secondary antibody, diluted in the appropriate blocking solution, was added and incubated for 1 hour at room temperature (in the dark if a fluorescent-tagged antibody was used). The membrane was washed a further 5 times with PBST and analysis performed:

ECL Detection

Proteins can be visualised by chemi-luminescence using ECL reagent. After final washing, the nitrocellulose membrane was covered in ECL reagent and left for 1

minute. Any excess liquid was drained and the membrane wrapped in saran film. It was then placed into an autoradiographic cassette, protein side up, and a sheet of ECL-hyperfilm placed on top in the dark. After appropriate exposure, the film was removed and developed using an X-ograph automated developer.

Odyssey Detection

The Odyssey infra-red detection system (LICOR) allows proteins to be visualized and quantified by detection of direct fluorescence emitted by special fluorescently-labeled secondary antibodies. The imager has two channels for detection and therefore allows simultaneous detection of two proteins of interest as long as they are of differing molecular weights and are tagged with primary antibodies from different species. After incubation with primary antibodies the nitrocellulose membrane was washed as before and secondary infra-red labeled antibodies to rabbit or mouse (LICOR, 1:10,000 concentration) applied for 1 hour at room temperature. Membranes were washed 5 times in PBST and placed on the Odyssey imager protein side down. The blots were scanned and the protein band of interest quantified using Odyssey software according to the manufacturer's instructions.

2.7 PREPARATION AND TRANSFECTION OF PLASMID DNA AND siRNA

2.7.1 Transformation of competent bacteria

(Based on the methods described in Molecular Cloning, Edition 3, Sambrook and Russell, 2001)

A 50µl aliquot of library efficiency® DH5α competent cells (Invitrogen) was thawed on ice, 0.5µg of plasmid DNA was added and incubated on ice for a further 30 minutes.

The cells were heat shocked in a water bath at 42°C for 30 seconds and returned to ice for 2 minutes. Pre-warmed S.O.C medium (900µl) (Invitrogen) was added and the cells allowed to recover in a shaking incubator at 37°C for 1 hour at 225r.p.m. Agar plates were prepared, as detailed below, with appropriate antibiotics and 10µl and 50µl aliquots of the mix spread across the plates with 50µl of S.O.C medium. The plates were incubated overnight at 37°C.

Selective agar plates for bacterial cell transformation were prepared by the addition of 50µg/ml of either ampicillin or kanomycin to liquid L-agar, and approximately 10ml applied to sterile petri dishes. Once set the dishes were inverted and allowed to dry at room temperature for 1 hour.

All constructs used for transient transfection contained either an ampicillin or kanomycin resistance gene, conferring survival upon transformed cells when cultured in the presence of the appropriate antibiotic. Bacterial colonies which contained the recombinant plasmids were easily identifiable by the formation of white colonies on the plate.

2.7.2 Preparation of plasmid DNA

From each transformation, one single colony was picked under sterile conditions and inoculated into a starter culture containing 500µl LB medium with appropriate antibiotic at 50µg/ml. This mixture was shaken at 225 r.p.m at 37°C for 6 - 8 hours. The resultant mix was added to a sterile flask containing 100-200ml of LB medium with 50µg/ml of appropriate antibiotic. The flask was transferred back to the shaker at 225 r.p.m and 37°C overnight.

The following day purification of plasmid DNA was undertaken using the Qiagen Qiafilter Plasmid Maxi Kit, according to the manufacturer's instructions, and / or

caesium chloride selection. In brief, bacterial cells were pelleted at 6000xg for 15 minutes at 4°C and resuspended in 10ml resuspension buffer (P1). Ten ml of lysis buffer (P2) was added and the solutions mixed by vigorously inverting 4 – 6 times. Once incubated for 5 minutes at room temperature, 10ml of chilled neutralisation buffer (P3) was added and either the Maxi kit protocol followed, or caesium chloride preparation performed.

2.7.2.1 Qiagen Qiafilter Plasmid Maxi Kit:

The mixture was poured into a QIAfilter cartridge. This cartridge removes chromosomal DNA, salt, detergent and protein complexes. The solution was allowed to incubate and settle for 10 minutes at room temperature in the cartridge. Meanwhile, a QIAGEN-tip was equilibrated with 10ml of the QBT buffer. The cleared lysate resulting from passage through the QIAfilter cartridge was allowed to enter the QIAGEN-tip resin by gravity flow. Thirty mls of wash buffer (QC) was twice passed through the tip and discarded before the DNA was eluted into a suitable glass tube with 15ml high salt elution buffer (QF). DNA was precipitated with 10.5ml isopropanol at room temperature and centrifuged at 15000xg for 30 minutes at 4°C. The supernatant was carefully decanted, the pellet of DNA washed with 5ml 70% ethanol and centrifuged again at 15000xg for 10 minutes at 4°C. The ethanol was decanted and the pellet of DNA allowed to air dry for 5 minutes before being suspended in a suitable volume of Tris-EDTA (TE) buffer.

2.7.2.2 Caesium chloride preparation:

The mixture was centrifuged at 9000xg for 15 minutes at 4°C and the supernatant removed into a clean centrifuge tube containing 50ml ice-cold isopropanol. This was mixed and centrifuged at 9000xg again for 15 minutes. The resulting pellet was resuspended in 6ml TE buffer, transferred to a 15ml centrifuge tube and 6g of caesium

chloride added. Once dissolved, 550µl ethidium bromide (5mg/ml) was added, mixed and centrifuged for 5 minutes at 4000xg, 4°C. The supernatant was removed to an ultra-centrifuge tube which was sealed and placed in the centrifuge at 80000xg for 16-24hours, at 20°C. The following day a dark red band was visible containing the ethidium bromide. This was removed by piercing the tube with a 21 gauge needle and aspirating until nearly all the band had disappeared. The ethidium bromide was then extracted by mixing several times with equal quantities of water-saturated isobutanol, until the solution became colourless. Two volumes of water were added, and the DNA precipitated with 2 further volumes of ethanol. The mixture was centrifuged at 9000xg for 15 minutes and the resulting pellet of DNA washed with 70% ethanol and the centrifugation repeated. The pellet was then air-dried and resuspended in a suitable volume of TE buffer.

The DNA concentration of the solutions was ascertained by measurement of absorbance at 260 nm by UV spectrophotometry. The purity of the samples was ascertained by calculation of the absorbance ratio 260/280 nm. Pure DNA should give a ratio between 1.8 and 2.0.

2.7.3 Restriction digest of plasmid DNA

The DNA produced from the preparation was further analysed either by excision of the DNA insert or linearisation of the plasmid with the appropriate restriction enzyme(s). Restriction reactions were prepared with 0.5 – 1.0µg of plasmid DNA, 1µl of restriction enzyme, 5µl of BSA (10X), 5µl of enzyme buffer solution and made up to 50µl total volume with distilled water. Uncut DNA was prepared alongside these samples, with only the restriction enzyme omitted. Following incubation at 37°C for 3 hours, the samples were run on a 0.8% or 1% agarose gel (depending on the expected molecular weight) containing 1µg/ml of ethidium bromide. Two µl of 6X DNA loading buffer was

mixed with 5µl of sample and 5µl of distilled water prior to running on the agarose gel at 80V for 1-2 hours. DNA bands were then visualised and photographed using a SYNGENE CHEMI GENIUS^2® transilluminator and bio imaging system.

Table 2.4. Identification of plasmids by restriction digests.

Plasmid	Restriction Enzymes	Expected Fragments
pCS3mDeltaEF1FL (ZEB1)	HindIII	1847bp, 1847bp, 4041bp
P-silencer 1.0 U6 WISP2shRNA	Sma1	Linearised at 3292bp
P-silencer 1.0 U6 control	Sma1	Linearised at 3292bp
pCMV-E-cadGFP	Nhe1 / Xba1	793bp, 6394bp

2.7.4 Transient transfection of plasmid DNA and siRNA into cells

Plasmids and siRNA were transiently transfected into cells using either Amaxa nucleofection® or lipid-based chemical transfection.

2.7.4.1 Nucleofection of HCT116 and SW620 cells

Cells were cultured to 70% confluency, washed in PBS and trypsinised to detach, before centrifugation at 200xg and resuspension in PBS. After estimation of cell count using a haemocytometer, the required number of cells (~2x10^5 for a 6-well plate) was pelleted and resuspended in pre-warmed nucleofector solution. Appropriate siRNA was added, the suspension mixed by gentle tapping and the cells transferred to Amaxa certified cuvettes. The Amaxa nucleofector device was used to carry out nucleofection on programme D-017 (SW620) or D032 (HCT116). Pre-warmed medium (500µl) was added and the cell suspension titurated 20 times to mix thoroughly with the provided Amaxa plastic pipettes. The cells were then transferred to plates with appropriate amounts of medium containing 10% FCS and cultured at 37°C.

2.7.4.2 Chemical transfection of HCT116, SW480 and SW620 cells

Plasmids containing sequences for Green Fluorescent Protein (GFP), ZEB1, E-cadherin and shRNA to WISP-2 and ZEB1 or appropriate siRNA to the protein of interest were transiently transfected into HCT116, SW480 and SW620 cells using the lipid-cased transfection reagents Lipofectamine 2000 (Invitrogen), siPORT NeoFx (Ambion) and Codebreaker (Promega) according to the manufacturer's instructions.

Lipofectamine:

Briefly, cells were cultured to 50% (siRNA) or 70% (DNA) confluency in medium supplemented with 10% FCS. For a 6-well plate, 5µl of Lipofectamine 2000 and 100pmol of siRNA were mixed with 250µl of serum-free medium in separate micro-centrifuge tubes. These were left for 15 minutes at room temperature and then combined. Complexes were allowed to form for 20 minutes at room temperature and then the mix was added into the appropriate well containing cells and medium. For DNA transfection the same protocol was followed, but with varying Lipofectamine 2000: DNA ratios (2:1 to 4:1) according to the results of optimisation experiments. Cells were cultured at 37°C for 24, 48 and 72 hour time points as necessary.

siPORT NeoFx:

Cells were cultured as above. For a 6 well plate, 5µl of siPORT NeoFx reagent was mixed with 100µl of serum-free medium. At the same time 12.5µl of 1µM siRNA was mixed with 100µl of serum-free medium. After 5 minutes at room temperature the siRNA and siPORT NeoFx were combined and incubated for a further 10 minutes. This mix was then spotted into the well containing cells and 2.3ml of complete medium. Cells were maintained at 37°C for 24, 48 and 72 hour time points as necessary.

Codebreaker:

Cells were cultured as for Lipofectamine transfection. For a 6 well plate, 5µl of Codebreaker reagent was mixed with 525µl of serum-free medium. At the same time 12.5µl of 1µM siRNA was mixed with 100µl of serum-free medium. After 15 minutes at room temperature the siRNA and Codebreaker were combined and incubated for a further 15 minutes. This mix was then spotted into the well containing cells and 2.5ml complete medium. Cells were maintained at 37°C for 24, 48 and 72 hour time points as necessary.

2.8 IMMUNOCYTOCHEMISTRY

SW480 and MDA-MB-231 cells were seeded on cover slips in 6-well plates ($1X10^5$ cells per well) and incubated for 24 hours. The following day cells were transfected with pshZEB1 or pshControl plasmids with Lipofectamine 2000 according to the previously described protocol. Cells were cultured for a further 48 hours and then washed 3 times with PBS. Fixation was performed in 4% paraformaldehyde for 10 minutes and cells washed 3 times in PBS. 0.1% Triton X-100 was then added for 5 minutes to permeabilise the cells and a further 3 washes of PBS performed. Non-specific binding was blocked with the addition of 3% BSA for 1 hour, and then the primary antibody (Plakophilin-3 1:200, ZEB1 1:100 or E-cadherin 1:150) added for 3 hours at room temperature. The cells were then washed 3 times in PBS and secondary antibodies (anti rabbit 1:100 and anti mouse 1:250) added and incubated in the dark for 1 hour at room temperature. The cells were then washed three times in PBS, once in distilled water and turned on the cover slips onto slides (superfrost, Menzel Glazer) with 1 drop of Prolong mounting solution. Slides were left to cure overnight and viewed on a Nikon Eclipse fluorescence microscope.

2.9 IMMUNOHISTOCHEMISTRY

2.9.1 Tissue specimens

Archival primary tumour specimens from patients who had undergone surgical resection of a colorectal tumour were collected from the Pathology Department of Leicester University Hospitals NHS Trust, along with any matched lymph node, normal colon and liver metastases specimens. All tissues were formalin fixed and embedded in paraffin, the standard method of storage and preservation of pathology specimens in the Leicester Hospitals NHS Trust. Ethical committee approval was received for cell signalling research to be performed on these tissues without seeking specific patient consent (REC reference 7176).

Patient tissues included in the study were from those treated with primary CRC between 1998 and 2000 at the Leicester General Hospital. Patient lists were generated from Leicester Colorectal Multidisciplinary Team records. Case notes were reviewed to confirm suitability for inclusion. Inclusion and exclusion criteria for the study are summarised on the next page (Table 2.5).

Table 2.5. Inclusion and exclusion critieria for the selection of tumour tissues for immunohistochemistry.

Inclusion Criteria
Radically resected colorectal carcinoma with curative intent
Availability of adequate demographic and follow up data
Exclusion Criteria
Histological tumour type other than adenocarcinoma (eg. Lymphoma)
History of Familial Polyposis Coli or Hereditary Non-Polyposis Colon Cancer Syndrome, or strong family history (1st degree relative with CRC at less than 45 years of age)
Pre-existing colonic condition (eg. Ulcerative Colitis)
History of previous neoplasia at other site
History of metachronous or synchronous colonic tumour
Pre-operative radiotherapy
Peri-operative mortality

From information obtained from the medical notes, a database was compiled detailing patient demographics and clinico-pathological factors including:

- Age and gender
- Site of disease (colon or rectum)
- Dukes' and TNM tumour stage
- Histopathological factors including vascular and perineural invasion
- Presence of synchronous metastases
- Clearance at resection margin(s)
- Use of adjuvant chemotherapy
- Survival data (overall survival, cancer-specific survival, disease-free survival, hepatic disease-free survival)
- Subsequent treatment if recurrence developed

The processing of tissue blocks onto slides was performed with the kind assistance of Karen Kulbicki in the Department of Cancer Studies and Molecular Medicine, University of Leicester. A Leica (Wetzlar, Germany) Microtome was used to cut 4µm

sections from the tissue blocks onto the slides. After staining, slides were examined on an Axioskop 2 plus microscope, manufactured by Carl Zeiss Ltd (Hertfordshire, UK).

2.9.2 Preparation of cell pellets as controls for immunohistochemistry

In cases where a validated positive control tissue was not identified from the literature, cells known to express the protein of interest were pelletted and processed in the same way as tissues for use as control sections. The Shandon (Pittsburgh, USA) Cytoblock cell block preparation system was used and the protocol followed according to the manufacturer's instructions.

2.9.3 Envision detection system

The Dako Envision system has been used with success in our laboratory for several years, and has been validated against other staining methods in the literature. It contains secondary reagents designed to be highly sensitive to the primary antibody which has bound to the antigen of interest on the tissue section. Once primary antibody incubation is complete, the peroxidase-labelled polymer is used to amplify antigen signal. The polymer contains a dextran backbone attached to a large number of horseradish peroxidase (HRP) and secondary antibody molecules which react strongly with the primary antibody species and allow a large number of binding sites for subsequent chromagen reaction (figure 2.1). The HRP reacts with its substrate, hydrogen peroxide, in the presence of an electron-donating chromagen (in this case 3,3 DAB) which produces a brown coloured molecule at the site of antigen binding easily visible by light microscopy.

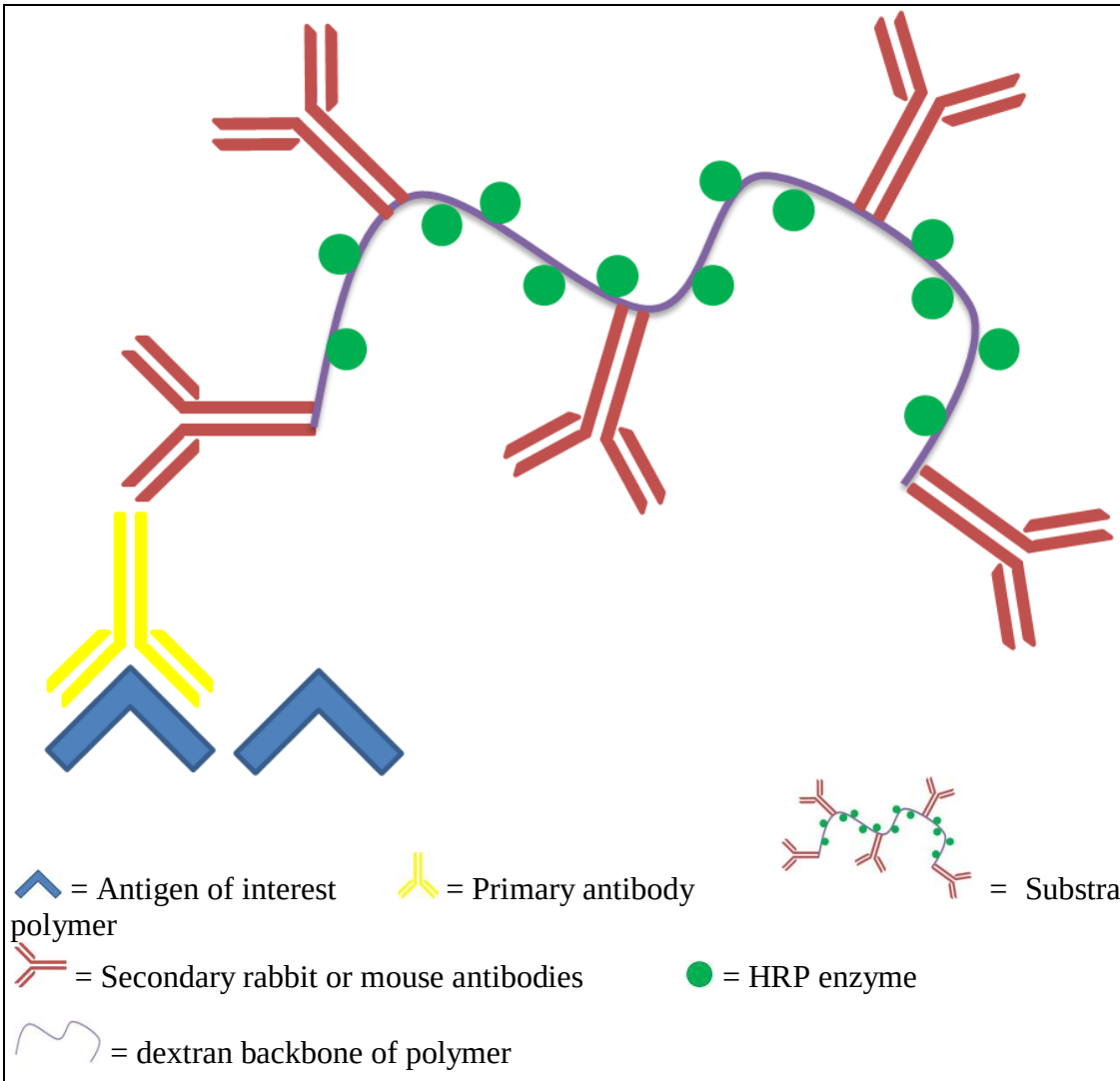

Figure 2.1. Diagram of the Envision immunohistochemistry reaction system.

De-paraffinisation

The slide mounted sections were de-waxed through two changes of xylene (5 minutes each). Rehydration was achieved by 5 minute washes in 99% industrial methylated spirit (IMS), 99% IMS and 95% IMS. Further exchanges through tap water and distilled water were then performed for 5 minutes each.

Antigen retrieval

The slides were placed in pre-heated TRIS-EDTA buffer and heated in a 900W microwave for 11 minutes at high power, and 21 minutes at 40% power. They were then

left to cool in the buffer bath until they had returned to room temperature (approximately 30 minutes). Washes of tap water and TBS were then performed for 5 minutes each.

Peroxidase Blocking

Endogenous peroxidase activity was blocked after wiping excess liquid from around the sections. Slides were placed in a humidified chamber and incubated with blocking solution for 10 minutes. The solution was rinsed off with TBS, and then the slides were cycled through two further washes of TBS (5 minutes each).

Primary Antibody

Excess liquid from around the sections was again removed by wiping with tissue and the primary antibodies applied. Antibodies were diluted to the concentrations listed in table 2.6 in 0.05M Tris-HCl buffer, to which 1% BSA was added just before use. The slides were transferred to a humidified chamber and incubated overnight at 4°C. As a positive control, sections of tissue or cells known to express the protein of interest were incubated with the primary antibody or, as a negative control, with an immunoglobulin fraction from the same species as the primary antibody.

Table 2.6. Conditions of primary antibodies for immunohistochemistry.

Primary Antibody	Dilution
ZEB1	1:500
WISP-1	1:500
WISP-2	1:500
WISP-3	1:250
Plakophilin 3	1:3000

Peroxidase Labelled Polymer

The following day slides were rinsed with TBS and then cycled through two washes of TBS (5 minutes each). Tissue was used to remove excess liquid around sections and peroxidase labeled polymer applied, followed by incubation in a humidified chamber at room temperature for 40 minutes. Slides were then rinsed in TBS, and washed in TBS twice for 5 minutes each.

Substrate-chromagen

Excess liquid was removed from the slides and liquid DAB+ substrate chromagen added and incubated for a further 10 minutes at room temperature. Slides were then rinsed and washed two times in distilled water.

Counter staining

The sections were rinsed in tap water and incubated with vector haematoxylin QS for 5 seconds. The slides were rinsed in tap water again and then graded back through 1 change of 95% IMS, 2 of 99% IMS and 2 of Xylene (3 minutes each). Cover slips were then mounted with DPX mounting solution.

2.9.4 Haematoxylin and Eosin (H&E) staining

From each tissue block one section was stained with H&E to confirm quality and histological appearance.

Technique:

Tissue sections were de-paraffinised and rehydrated as per the protocol for the Envision system. Following removal of excess liquid around sections, 3 drops of haematoxylin QS solution were added and incubated for 10 seconds. The slides were then washed

briefly under the running tap and rinsed in 95% IMS. Sections were then counterstained with Eosin Y 0.5% solution for 30 seconds and quickly rinsed under a running tap. Rehydration and application of cover slips was then performed as above.

2.9.5 Scoring of immunohistochemistry

Each tumour section was examined by a single histopathologist and fully reported using a standardised proforma. This included size of primary tumour (mm), Duke's stage, T stage, presence / absence of vascular invasion, lymph node status, number of lymph nodes involved, and tumour differentiation (poor / moderate / well / mucinous).

In previously published analyses of ZEB1, WISP-1 and PKP-3 two main scoring systems have been in use for the quantification of protein expression; the average percentage of cells stained per high power field or a variation of the H score (table 7.1). The percentage system is generally performed by counting the total number of cells within one or more high power fields and then the number of cells positively stained for the protein of interest. A percentage score is then gained by dividing the latter by the former and multiplying by 100. The molecular marker of interest is then assigned either a percentage score, or subdivided into groups using an arbitrary system - either into thirds, quartiles, standard deviations or range values. It does not involve an estimation of the intensity of staining and therefore has been considered by some to be of limited value in terms of quantification of protein expression (ie. The protein is either there or not there), but it is simple to use and open to less subjectivity by the observer than the H score[270].

By contrast the H score similarly uses an estimation of the percentage of cells stained in the same manner, but also incorporates an estimation of staining intensity as quantified by the observer on a scale from 0 (no stain) to 3 (intense black staining of nuclei or

cytoplasm). These results are then multiplied together to reach a final score between 0 and 300. Each run of immunohistochemistry is compared by examination of the positive control slides within that experiment so as to allow for inter-experimental error and attempt to decrease the subjectivity of observer assessment[271].

Table 2.7. Published studies using immunohistochemistry to assess ZEB1, WISP-1 and PKP-3 expression, the type of scoring system used and statistical analysis undertaken.

Marker	Author / year	Number of observers	Score type			Statistical Analysis		
			H Score	Percentage Only	Intensity System	Uni variable	Multi variable	Survival
ZEB1	Dohadwala 2006	2	Yes	Yes	0-3	No	No	No
	Sayan 2009	2	Yes	No	NR	Fisher	Cox regression	Log rank
	Graham 2008	1	No	No	0-3	Fisher	No	No
	Spoelstra 2006	NR	Yes	No	0-4	No	No	No
	Tian 2007	IA	IA	IA	IA	X^2	No	No
WISP-1	Khor 2006	2	Yes	No	0-3	Mann-Whitney	No	No
	Davies 2007	IA	IA	IA	IA	Mann-Whitney	No	No
	Chen 2007	3	No	Yes	-	T-test	No	No
PKP-3	Schwarz 2006	NR	Yes	No	0-3	No	No	No
	Furukawa 2005	3	Yes	No	0-3	Fisher	No	Yes
	Papagerakis 2003	2	Yes	No	0-3	X^2	No	No

NR, not recorded; IA, image analysis by optical density

There is considerable debate, but little agreement, in the literature as to which scoring system allows the most accurate estimation of protein expression[272, 273]. More recent studies have considered the use of automated staining and computerised image analysis scoring systems which allow quantification by light absorption[274]. However, these systems are at present extremely costly, require considerable user expertise and are only available in high volume centres.

Given that the vast majority of previous studies examining ZEB1, WISP-1 and PKP-3 expression with immunohistochemistry used semi-quantitative scoring systems, with either an intensity measurement by image analysis or H score, it appeared desirable to perform the analysis here in the same manner so as to enable comparison with these prior investigations.

Two investigators (The author and Dr C D Mann, Department of Cancer Studies and Molecular Medicine, University of Leicester, UK), who were blinded to the pathologists assessment of the tumour, independently assessed immunohistochemistry marker staining according to the H score. Each section was examined in normal colon (where available), central tumour and at the invasive front. ZEB1 and PKP-3 were scored according to nuclear and cytoplasmic expression respectively, WISP-1 being scored for both.

2.10 STATISTICS

All statistical analysis was undertaken using the statistical software package SPSS v16.0 (Lead technologies, USA). Data were assessed for significance using ANOVA, Chi-square test or logistic regression as appropriate. Log rank and Kaplein Meier tests were used to assess survival statistics. The agreement between immunohistochemistry scores was assessed by the intra-class correlation coefficient (one-way random). Results were deemed significant when a P value of <0.05 was reached.

Chapter 3: Results – The relationship between ZEB1 and E-cadherin.

Introduction

Evidence in the literature demonstrates an inverse correlation between E-cadherin and ZEB1 expression in several cell lines and human tissues. *In vitro* studies suggest a multi-faceted role for ZEB1 in cellular signalling during development and in carcinogenesis[59]. Investigators have implicated ZEB1 in several signalling pathways, the majority of which have been studied in breast cell lines and tumours. The role of ZEB1 in Wnt, TGF-β and EGFR signalling and non-adherens junction adhesion remains to be established in other epithelial malignancies.

Direct evidence of the role of ZEB1 in colorectal cancer is relatively sparse. Only five publications to date examined expression *in vivo*, and none of these correlated clinic-pathological factors with ZEB1 expression[98, 104, 114, 115, 123]. Spaderna and colleagues did however demonstrate up-regulation of ZEB1 at the invasive front of primary tumours, accompanied by a loss of basement membrane constituents, such as lamin[115]. The role of ZEB1 in CRC metastases has not been examined to date, so here its interaction with E-cadherin in CRC cell lines and tumours, including metastases is investigated.

3.1 EXPRESSION OF ZEB1 AND E-CADHERIN IN A PANEL OF COLORECTAL LINES

Western blots examining ZEB1 and E-cadherin protein expression in a panel of colon lines were performed using whole cell lysates from untreated cells cultured to

approximately 70% confluency. Two breast cell lines with known expression patterns were included as positive controls.

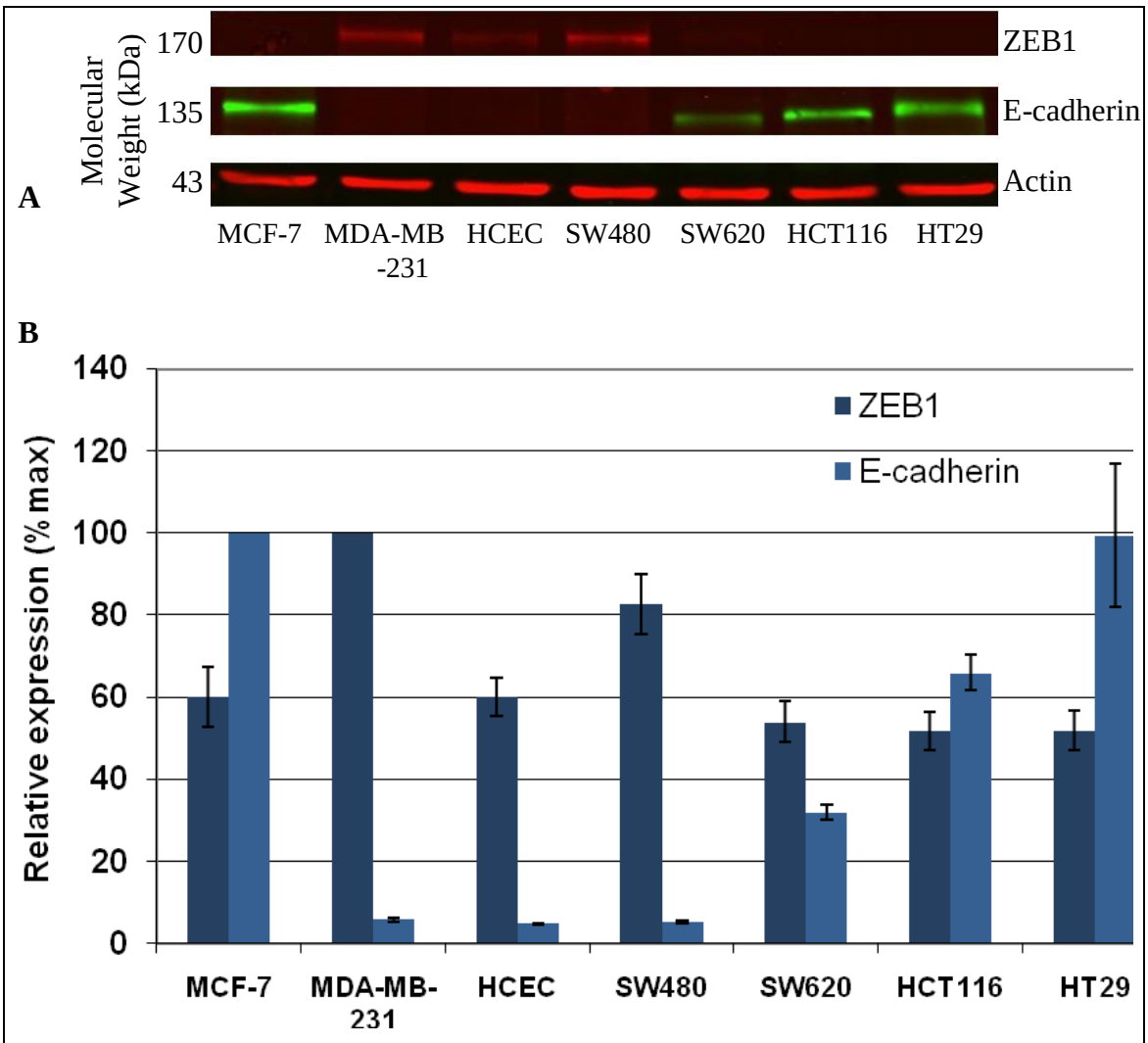

Figure 3.1. Expression of ZEB1 and E-cadherin in cell lines. (**A**) Typical western blot and (**B**) histogram of relative ZEB1 and E-cadherin protein expression levels as a percentage of the maximum level in any cell line, quantified from western blots using actin as a loading control and Odyssey imager software. (n=3, error bars +/-SEM.)

This initial experiment confirmed a similar inverse correlation between ZEB1 and E-cadherin expression in colon cell lines to that seen in previous studies in other cell types. This would support the hypothesis that ZEB1 is a repressor of E-cadherin, as demonstrated by several investigators[89, 100]. Worthy of note are the expression patterns in the SW480 and SW620 cell lines. In the primary tumour-derived, aggressive and invasive SW480 line E-cadherin expression is almost undetectable, and there is

high ZEB1 expression. In the metastasis-derived SW620 line E-cadherin is expressed at moderate levels and, although ZEB1 is still present, it is at a lower level than that seen in the SW480 cell line. It was postulated that this could represent a dynamic expression of ZEB1 in cells with metastatic potential, suggesting a role for ZEB1 in EMT-MET switching, ZEB1 being expressed at high levels in the primary tumour with metastatic potential, and decreased in the secondary tumour metastasis which re-expresses epithelial characteristics at the new tumour location.

3.2 CLONING OF ZEB1 EXPRESSION CONSTRUCT

To examine the effect of changes in ZEB1 expression *in vitro*, an expression construct (kind gift from DR E. Tulchinsky, Cancer Studies and Molecular Medicine, University of Leicester) was acquired.

The pZEB1 expression construct was used to transform competent *E. coli* and cloned as described in the Methods. The resulting DNA was examined, after appropriate restriction enzyme digest, by agarose gel electrophoresis and confirmed to be of the correct size (figure3.2).

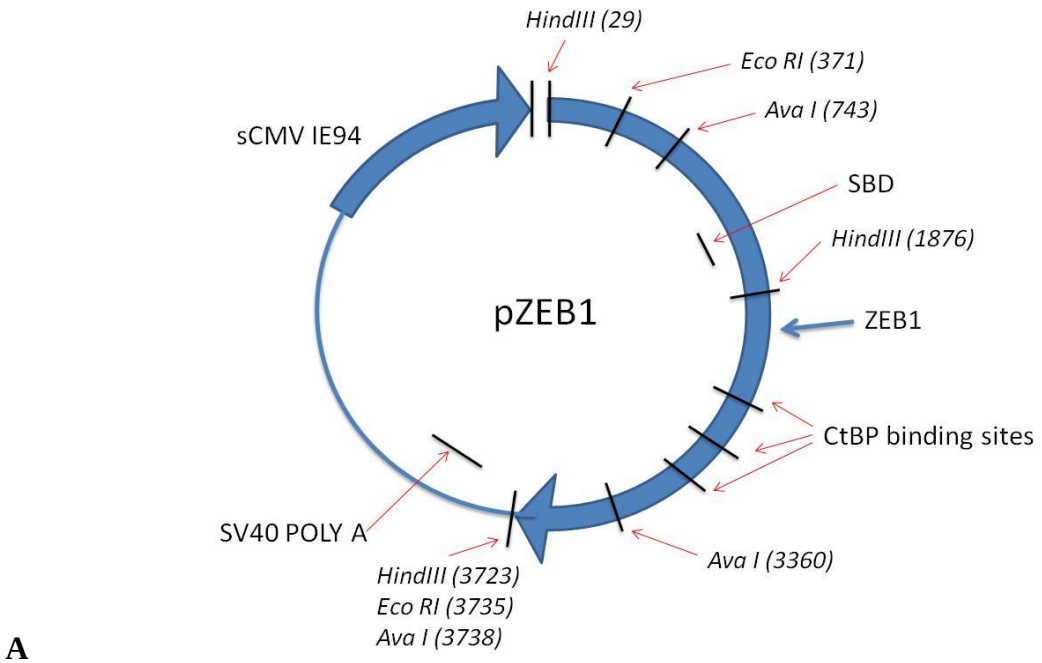

A

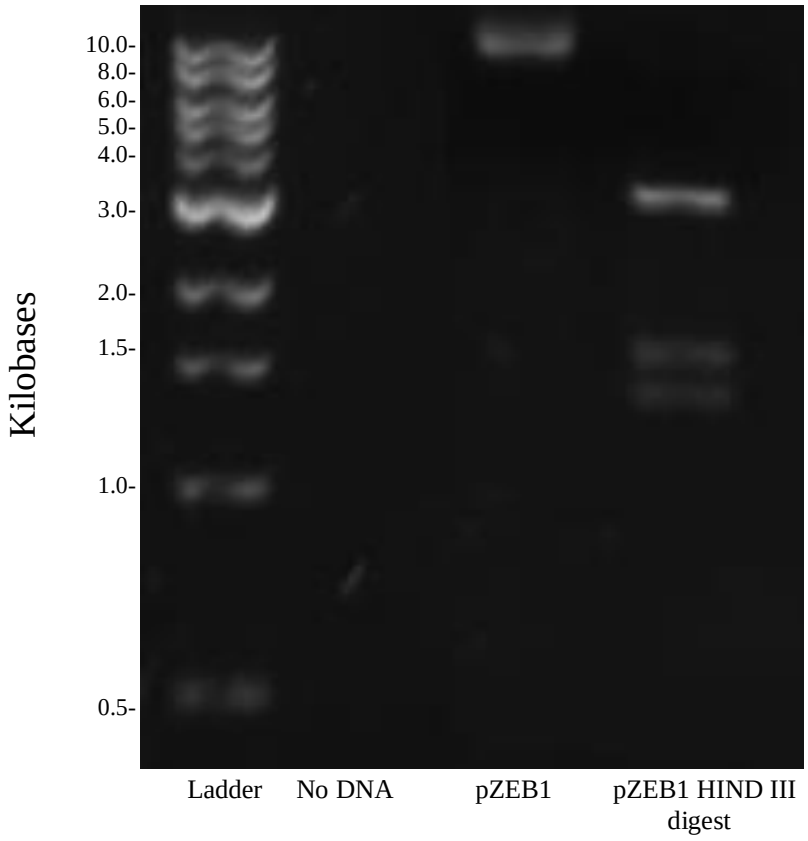

B

Figure 3.2. Analysis of pZEB1 construct by agarose gel electrophoresis. The cloned pZEB1 vector was digested by HindIII and subjected to electrophoresis on a 0.8% agarose gel. (**A**) pZEB1 vector map (**B**) agarose gel. The full length construct is 7735 Kb. The predicted fragment sizes were 1857, 1847 and 4041Kb.

In order to test the pZEB1 expression construct an initial transfection experiment was performed in HeLa cells, which had previously been optimised for transfection in our laboratory and had been shown to accept DNA expression constructs with relative ease. Transfections were performed in 6-well plates, utilizing 1µg of plasmid DNA and 2µl of Lipofectamine 2000 reagent. A pGFP expression construct was also used as a control for transfection efficiency. Whole cell lysates were prepared after 48 hours and western blotting performed to confirm expression of ZEB1 (figure 3.3).

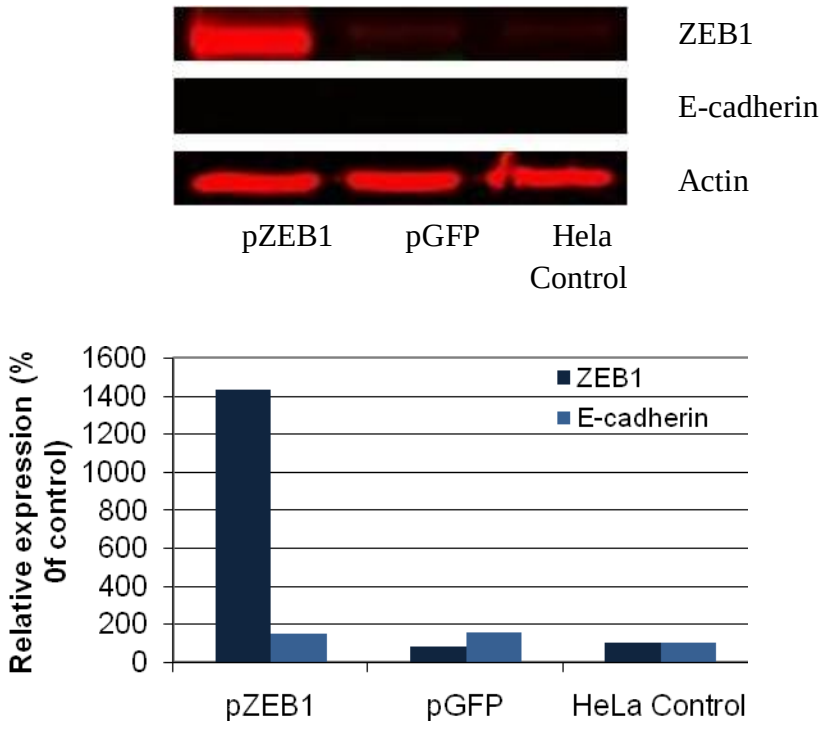

Figure 3.3. Transfection of HeLa cells with pZEB1 construct. HeLa cells were transfected using Lipofectamine 2000 with the pZEB1 or pGFP constructs and cultured for 48 hours. The resulting western blot (**A**) and histogram (**B**) of quantitative analysis on Odyssey imager are shown. (n=1)

Unlike the reciprocal expression pattern noted in colorectal lines no correlation between ZEB1 and E-cadherin expression was observed in HeLa cells. Transfection of the pZEB1

construct caused a 14-fold increase in ZEB1 expression, but no change in E-cadherin was observed. This experiment confirmed successful over-expression of ZEB1 and detection of the construct-derived protein at the same molecular weight as endogenous ZEB1.

Following successful transfection into HeLa cells, transfection of colorectal cell lines was attempted. HCT116, SW480 and SW620 were selected for their varying profiles of ZEB1 and E-cadherin expression (see figure 3.1). In this initial transfection experiment both high and low ZEB1 expressing cells were used to examine any effects of overexpression in these cells. Transfections were again performed in 6-well plates, using Lipofectamine 2000 as described in methods. Cells were harvested after 48 hours, whole cell lysates prepared and protein expression analysed by western blot. The results are shown in figure 3.4.

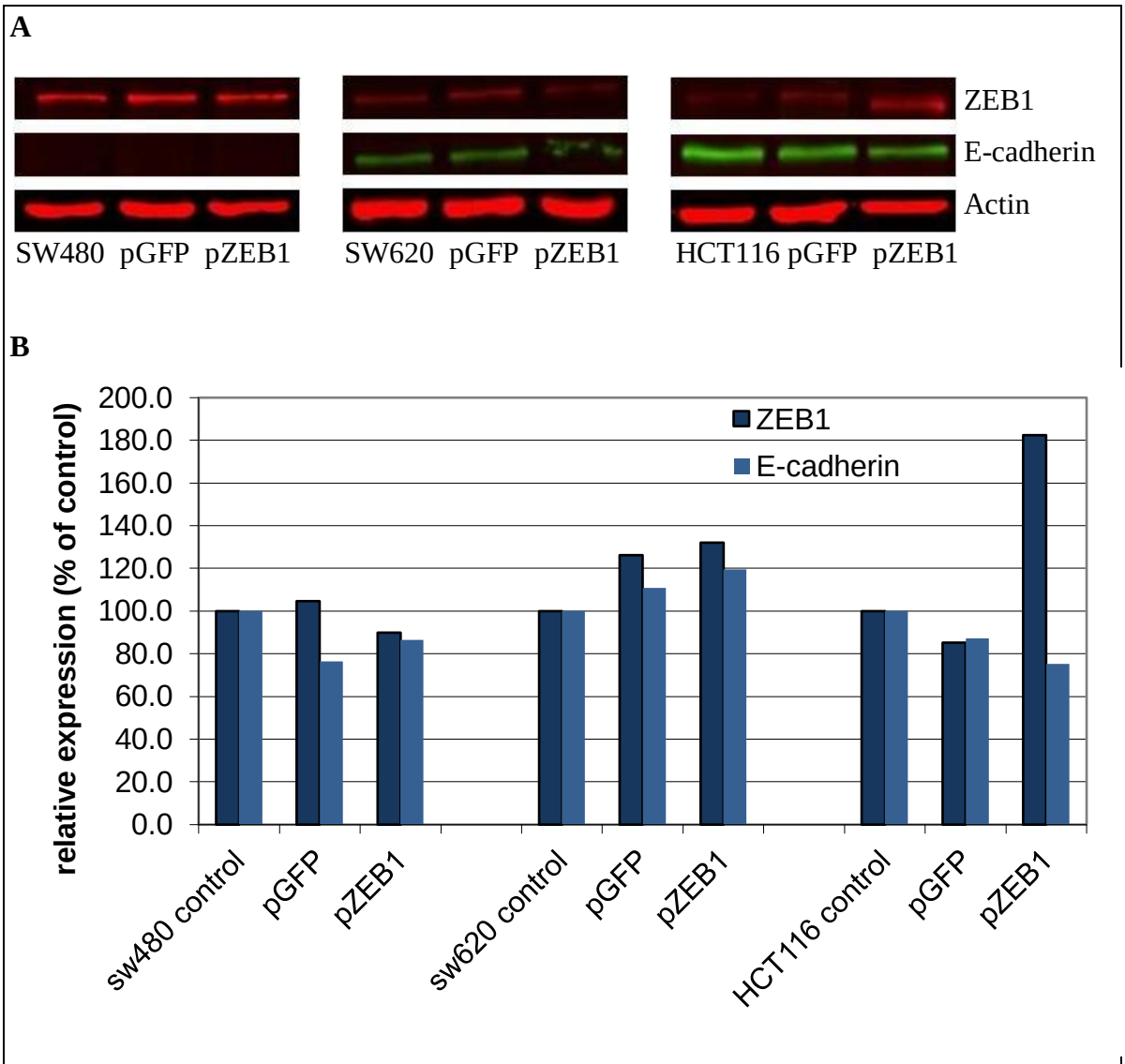

Figure 3.4. Effect of transfection of colon cells lines with pZEB1 construct. SW480, SW620 and HCT116 cells were transfected with pZEB1 or pGFP as a control, using Lipofectamine 2000. After 48 hours whole cell lysates were prepared. Representative western blot (**A**) and Histogram of quantitative analysis (**B**) are shown. (n=1)

No change in the expression of ZEB1 was seen in either SW480 or SW620 cells, but a 2-fold increase was observed in HCT116 cells compared to pGFP transfected or untreated cells. Expression of plasmid DNA in SW480 cells had previously been attempted in our laboratory by various methods with limited success suggesting these cells are difficult to

transfect. Therefore the SW620 and HCT116 cell lines were chosen for further investigation of ZEB1.

3.3 OPTIMISATION OF CHEMICAL TRANSFECTION IN HCT116 AND SW620 CELLS

An attempt was made to optimise transfection efficiency in HCT116 and investigate the transfection difficulties in SW620. Both cell lines were seeded into 6-well plates the day before transfection. The pGFP construct was used to allow quantification of transfection efficiency. Varying ratios of DNA to Lipofectamine 2000 reagent were used from 1:1 up to 1:12 in the 6 plates. Cells were cultured for 48 hours and then examined under a fluorescent microscope. The number of fluorescing cells was estimated as a percentage of the total cells in the microscope bright field. Three fields of view were examined for each plate and an average taken. Figure 3.5 shows a typical successful transfection of HCT116 with pGFP, and the results of the various ratios of DNA to Lipofectamine 2000 are detailed in table 3.1.

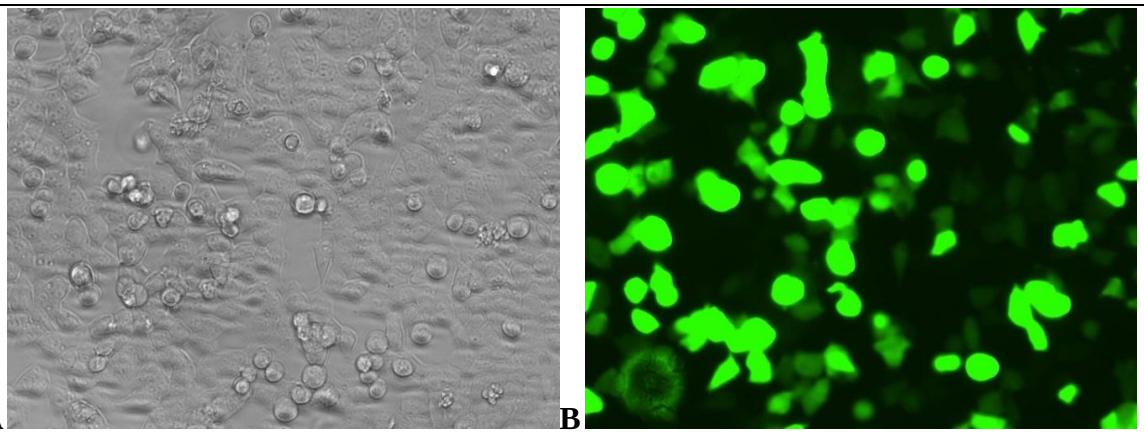

Figure 3.5. Optimisation of colon cell line DNA transfection. HCT116 cells were transfected with pGFP construct using Lipofectamine 2000 and cultured for 48 hours. Views of the same field under (**A**) bright field and (**B**) ultra-violet light microscope were used to quantify transfection efficiency.

Table 3.1. Estimated transfection efficiency in HCT116 cells as quantified by percentage of cells with GFP expression.

Lipofectamine 2000(µl) to DNA (µg) ratio	Estimated transfection efficiency at 48 hours
1:1	50%
2:1	60%
4:1	50%
6:1	40%
9:1	40%
12:1	25%

Transfection of SW620 cells revealed very few fluorescent cells (<10%) and it was clear that transfection had been relatively unsuccessful. Therefore HCT116 cells were selected for further transfection experiments with the pZEB1 construct, using the optimised Lipofectamine:DNA ratio of 2:1.

3.4 EFFECT OF ZEB1 EXPRESSION IN HCT116 CELLS

HCT116 cells were transfected with the pZEB1 expression construct, whole cell lysates prepared and western blots performed to ascertain expression levels of ZEB1 and E-cadherin (figure 3.6).

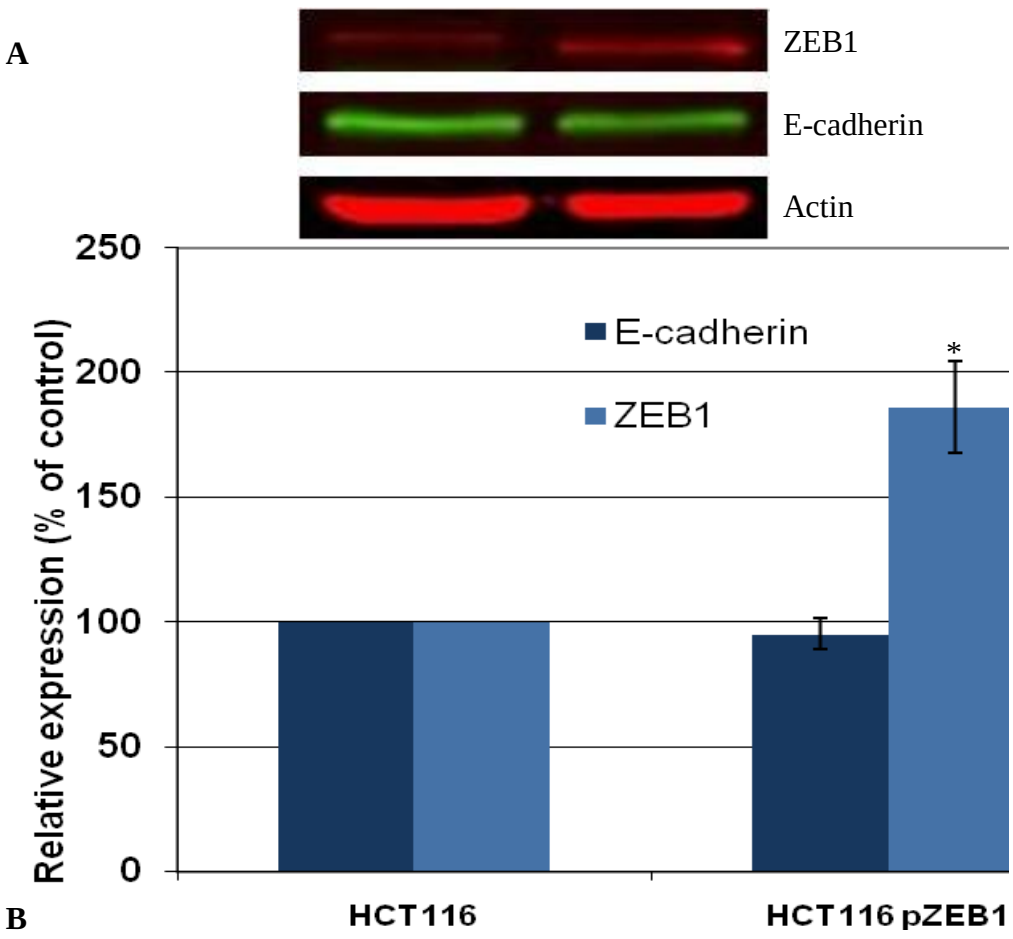

Figure 3.6. Effect of pZEB1 transfection on ZEB1 and E-cadherin expression in HCT116 cells. Representative western blot (**A**) and histogram showing quantitative analysis (**B**) of ZEB1 and E-cadherin expression in cells cultured for 48 hours following transfection. A significant change in ZEB1 expression was observed in the transfected cells (* indicates P=0.010; One-way ANOVA), however no significant change in E-cadherin expression was found (P=0.478; One-way ANOVA, n=3, error bars= ±SEM)

In the HCT116 cells only a minor effect was seen on E-cadherin expression when ZEB1 was over-expressed. Experience in cell lines from other epithelial malignancies clearly demonstrates the repressive effect of ZEB1 through the binding of E-boxes in the E-cadherin promoter region[93, 96]. The reasons for the absence of changes in E-cadherin expression here may be multi-factorial. For example the half life of endogenous E-cadherin

may be sufficient to maintain expression at the 48 hour time-point examined here, although this appears to be an unlikely explanation given results from previous studies indicating that it is between 6-8 hours[275]. The half-life is itself affected by several cellular signalling mechanisms such as p120 availability[276]. In addition, ZEB1 has been shown to require co-repressors such as CtBP and p300 in order to exert its repressive effects in certain cellular systems[90, 277]. The lack of full DNA sequencing of the construct raises the possibility of a non-functioning protein being produced, though conformation of the correct molecular weight on agarose gel electrophoresis and the band on western blot suggests this is less likely to be the cause for lack of E-cadherin repression. In addition this construct has been used by other investigators within our group to successfully repress E-cadherin in non-colorectal cell lines (unpublished data).

3.5 CLONING AND TRANSFECTION OF E-CADHERIN EXPRESSION CONSTRUCT

In order to investigate the effect of changes in E-cadherin expression in colon cell lines an expression construct was acquired (kind gift from Dr E. Tulchinsky) and used to transform competent *E. coli*. The resulting DNA was examined, after appropriate enzyme restriction digests, by agarose gel electrophoresis and confirmed to be of the correct size (figure 3.7).

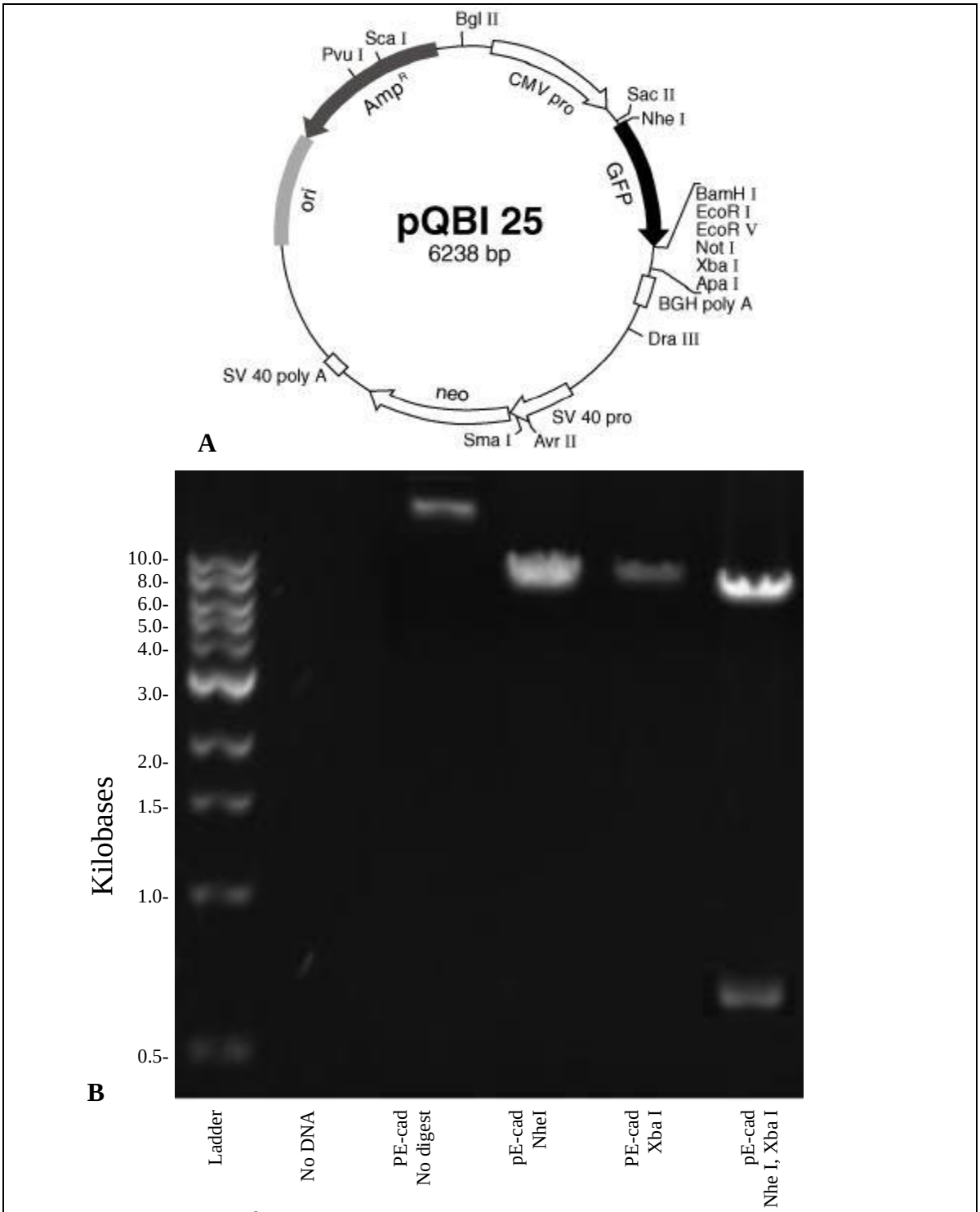

Figure 3.7. Analysis of pE-cadherin vector by agarose gel electrophoresis. The cloned pE-cadherin vector was digested by Nhe I and Xba I and subjected to electrophoresis on a 0.8% agarose gel. (**A**) DNA construct map for original pQBI25-GFP vector (Quantum Biotechnologies) prior to E-cadherin-GFP sequence insertion. (**B**) Agarose gel electrophoresis. The full length construct is 9438 Kb. The predicted fragment sizes after digest with Nhe1 and Xba1 were 748 and 8600Kb.

In a preliminary experiment the expression construct was transfected into HeLa cells according to the same protocol used for the pZEB1 construct, and a western blot performed of whole cell lysates after 48 hours to examine E-cadherin and ZEB1 expression in the transfected cells (figure 3.8).

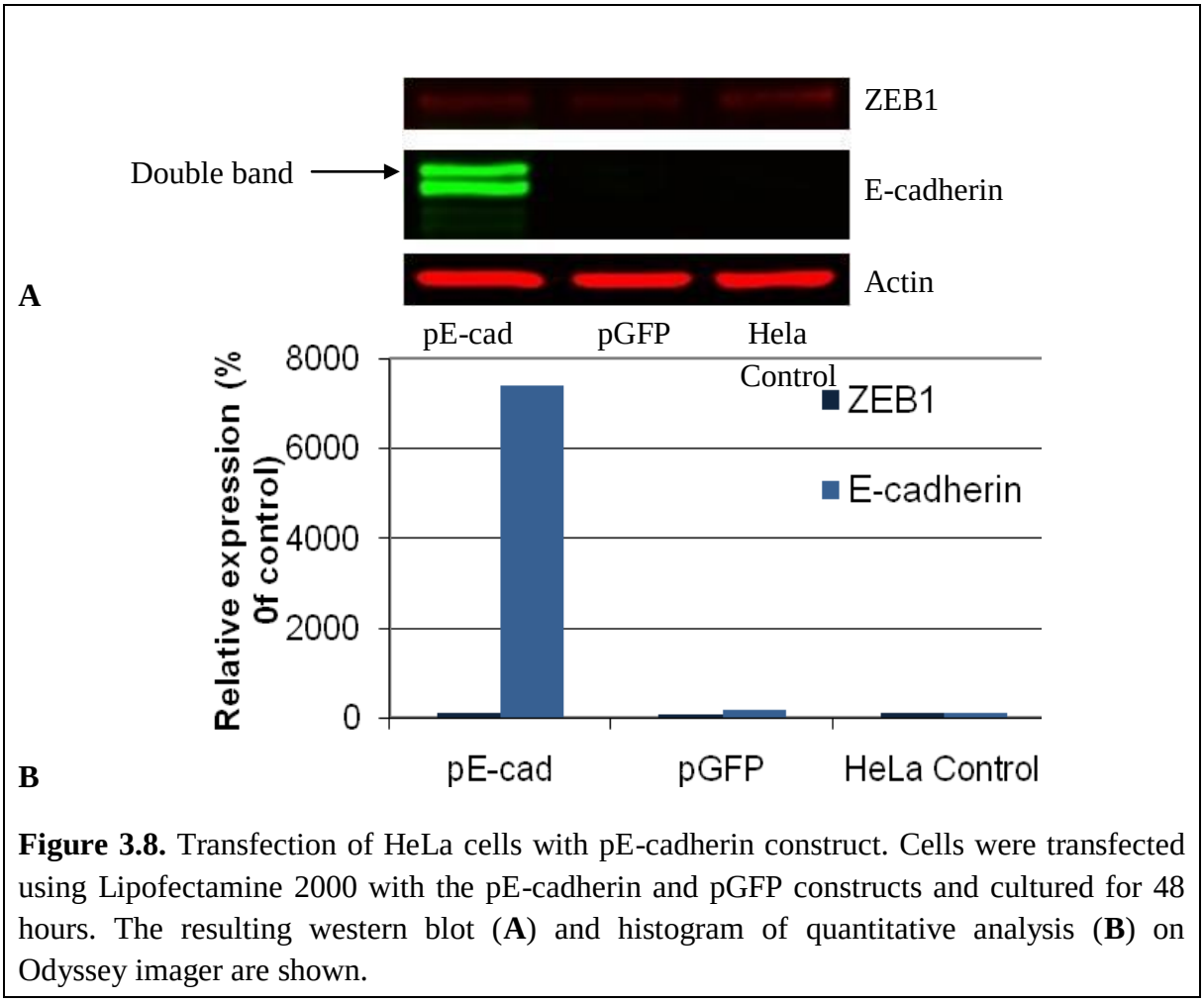

Figure 3.8. Transfection of HeLa cells with pE-cadherin construct. Cells were transfected using Lipofectamine 2000 with the pE-cadherin and pGFP constructs and cultured for 48 hours. The resulting western blot (**A**) and histogram of quantitative analysis (**B**) on Odyssey imager are shown.

Transfection of HeLa cells with the pE-cadherin construct resulted in expression of a protein doublet larger than the predicted molecular weight for endogenous E-cadherin of 134kDa. The increased size of the protein is likely to be due to the GFP element which is part of the E-cadherin construct and produces two E-cadherin proteins of slightly different conformational structure. This vector has previously been shown to cause this double-band

signature in some cell lines but produces fully functional E-cadherin protein[278, 279]. In the HeLa cells, which have little endogenous ZEB1 or E-cadherin, ZEB1 expression was unaffected by E-cadherin over-expression, consistent with observations in the literature in other cell lines[104].

After the successful transfection in HeLa cells, further experiments were performed in colon cell lines. HCT116 cells, which had previously been successfully transfected with the pZEB1 construct, have significant levels of endogenous E-cadherin. Thus to examine the effect of increased E-cadherin expression on ZEB1 levels it was desirable to transfect the pE-cadherin construct into SW480 cells which have little endogenous E-cadherin and high levels of ZEB1. This experiment was performed in order to check E-cadherin did not have any effect on ZEB1 expression. Therefore transfection of the pE-cadherin construct was attempted in the SW480 cells (figure 3.9).

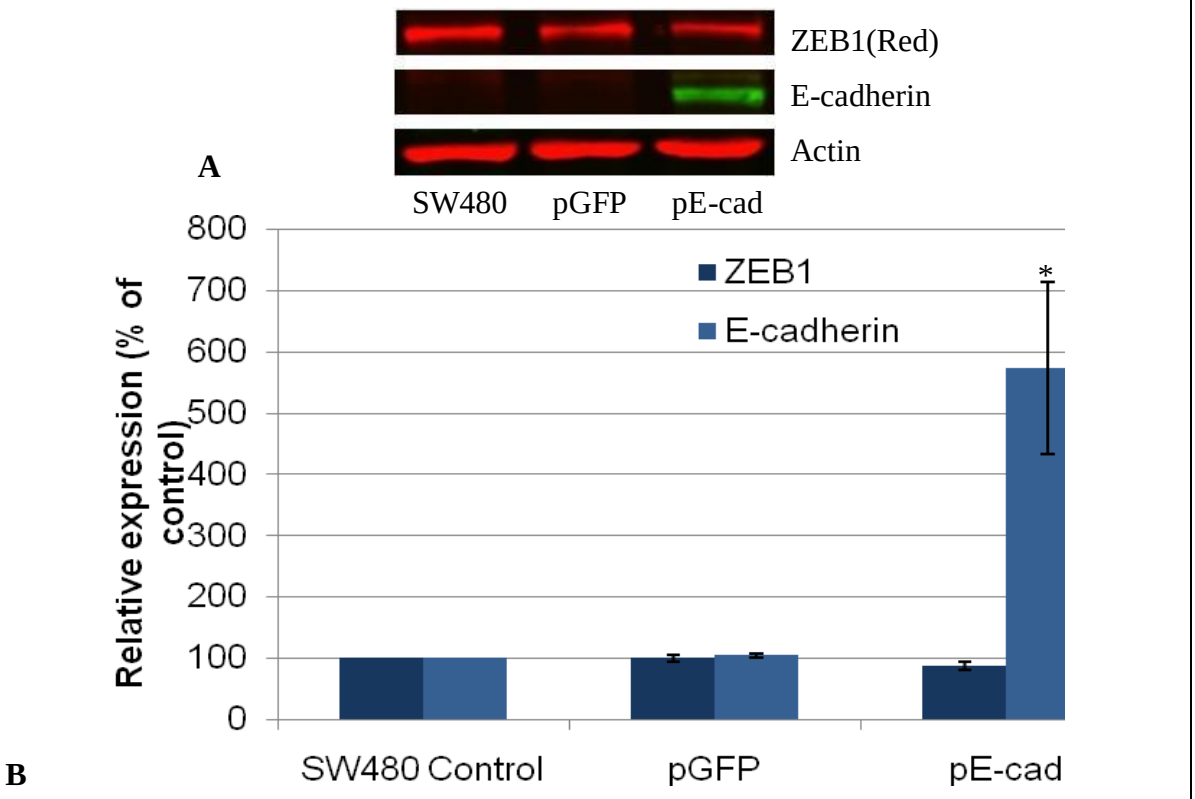

Figure 3.9. Effect of transfection with the pE-cadherin construct on ZEB1 and E-cadherin expression in SW480 cells. Representative western blot (**A**) and histogram of quantitative analysis (**B**) of ZEB1 and E-cadherin expression in SW480 cells using Lipofectamine 2000 and cultured for 48 hours. No significant change in ZEB1 expression was seen in any of the samples (One-way ANOVA). Transfection of the pE-cadherin plasmid caused a significant increase in E-cadherin expression (* indicates P=0.004; One-way ANOVA and Tukey post-hoc test, n=4, error bars=±SEM)

Transfection of the pE-cadherin construct was successful in SW480 cells and a 5.5-fold increase in expression was observed relative to control Lipofectamine-treated and GFP transfected cells. No changes in the microscopic appearance of the cells were observed in terms of growth, shape or distribution. Over-expression of E-cadherin had little effect on ZEB1 expression in these cells consistent with observations published elsewhere. ZEB1 expression therefore appears to be unaffected by E-cadherin over-expression in this cell line.

3.6 ZEB1 AND E-CADHERIN EXPRESSION *IN VIVO*

The formalin-fixed tissues from 101 colorectal cancer specimens, with their matched lymph node and liver metastases were investigated for ZEB1 expression using immunohistochemistry as described in methods.

3.6.1 Selection of positive control tissue for ZEB1

In order to find the optimal antibody concentration for use with the Envision detection system, and subsequently to confirm consistent results between runs, a positive control was required. Spoelstra and colleagues examined ZEB1 expression in endometrial tissues and found moderate levels in the stromal cells of proliferative phase tissue and high levels in secretory endometrium[86]. Anonymised sections from both secretory and proliferative phase normal endometrium were obtained from the Department of Pathology, Leicester Royal Infirmary and used to optimise conditions for use of the ZEB1 antibody with the Envision detection system (figure 3.10). In addition to these control tissues a transformed cell line - A431ZEB1 – was made available by Dr E. Tulchinsky (Cancer Studies and Molecular Medicine, University of Leicester) which expresses ZEB1 when exposed to doxycycline. The cell line was cultured with- and with-out doxycycline, pelletted using the Shandon cytospin kit, formalin-fixed and stained as described in methods. These sections were used as a further positive control (figure 3.11).

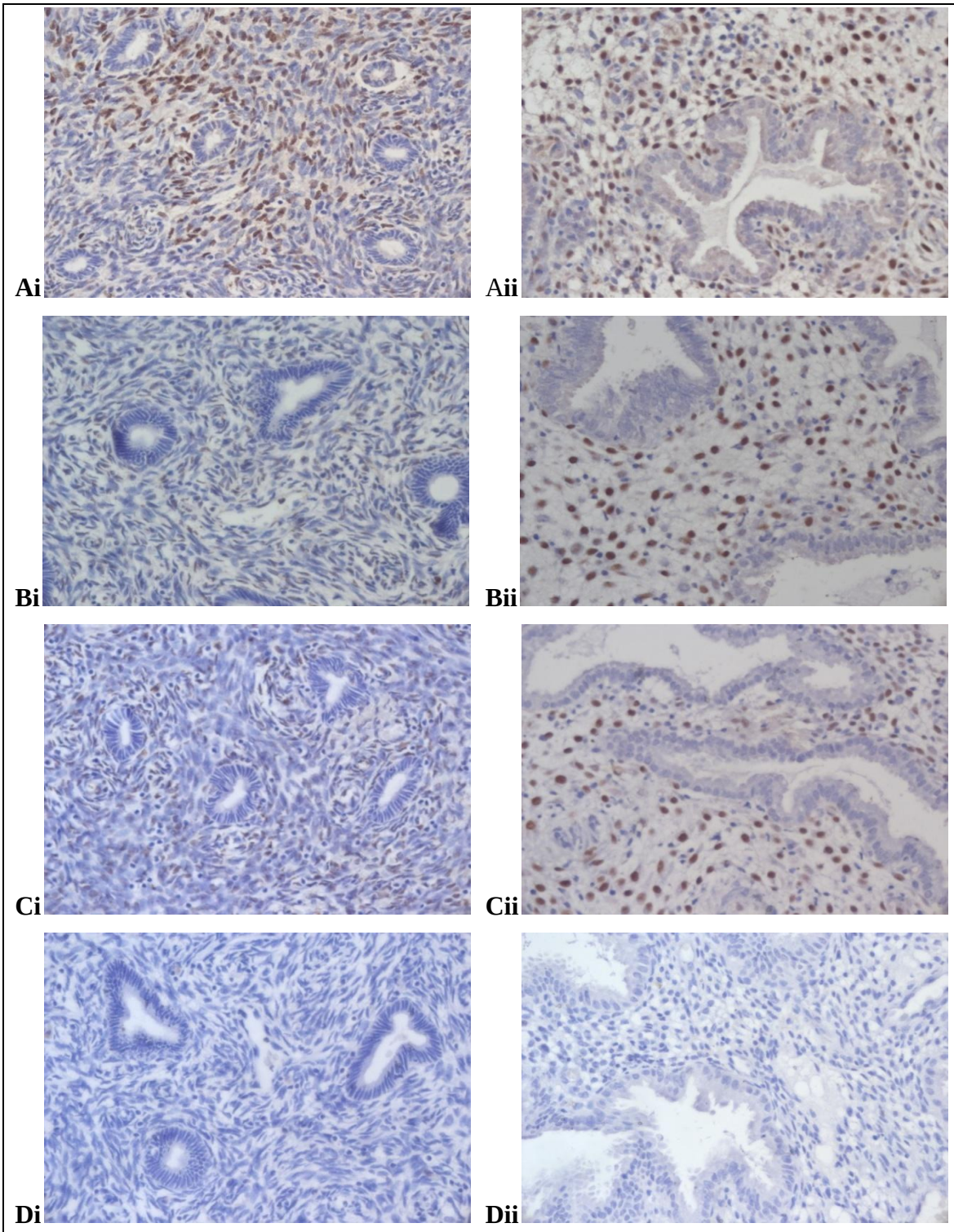

Figure 3.10. Optimisation of ZEB1 antibody in endometrial tissue. Sections of (**i**) proliferative and (**ii**) secretory phase endometrial tissue were stained according to the immunohistochemistry protocol described in methods, with varying ZEB1 antibody concentrations (**A**) 1:250 (**B**) 1:500 (**C**) 1:1000 (**D**) Non-specific rabbit immunoglobulin fraction negative control 1:500. (All magnifications are 40X).

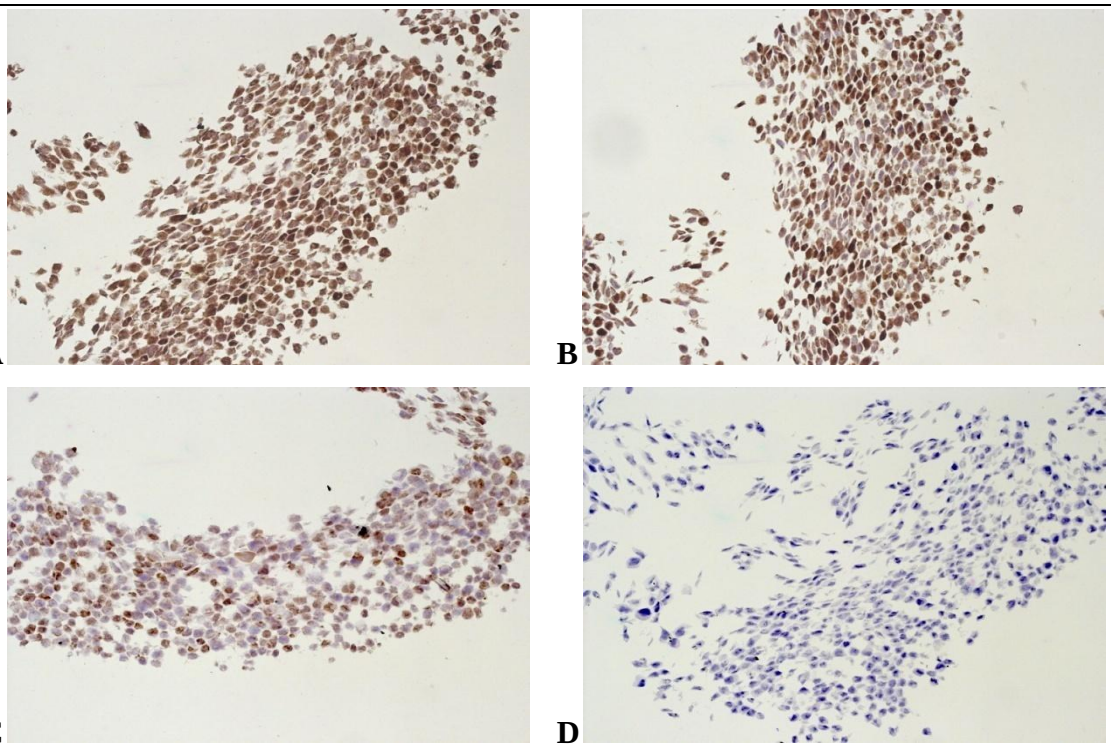

Figure 3.11. Optimisation of ZEB1 in A431-ZEB1 cells. A431-ZEB1 cells were treated with doxycycline (1µl/ml) for 48 hours, pelletted, formalin-fixed and paraffin embedded. Sections were then subjected to immunohistochemistry with ZEB1 antibody at varying concentrations. (**A**) 1:250 (**B**) 1:500 (**C**) 1:1000 (**D**) Non-specific rabbit immunoglobulin fraction negative control (1:500). (All magnifications are 20X).

Nuclear staining was observed as described by Spoelstra and colleagues in the endometrial tissues[86]. Stromal cells stained positively for ZEB1, with a stronger pattern being observed in the secretory phase tissues. Further optimisation in A431-ZEB1 cells confirmed the specificity of the antibody. A dilution of 1 in 500 was selected as having the least background staining with maintained specific nuclear staining.

3.6.2 ZEB1 in colorectal cancer specimens

Colorectal cancer specimens, along with patient matched normal colonic epithelium, lymph node and liver metastases, were stained using the Envision immunohistochemistry detection system with a 1:500 final antibody dilution (see methods). Representative sections of these tissues and the staining patterns observed are shown in figures 3.12 - 3.13.

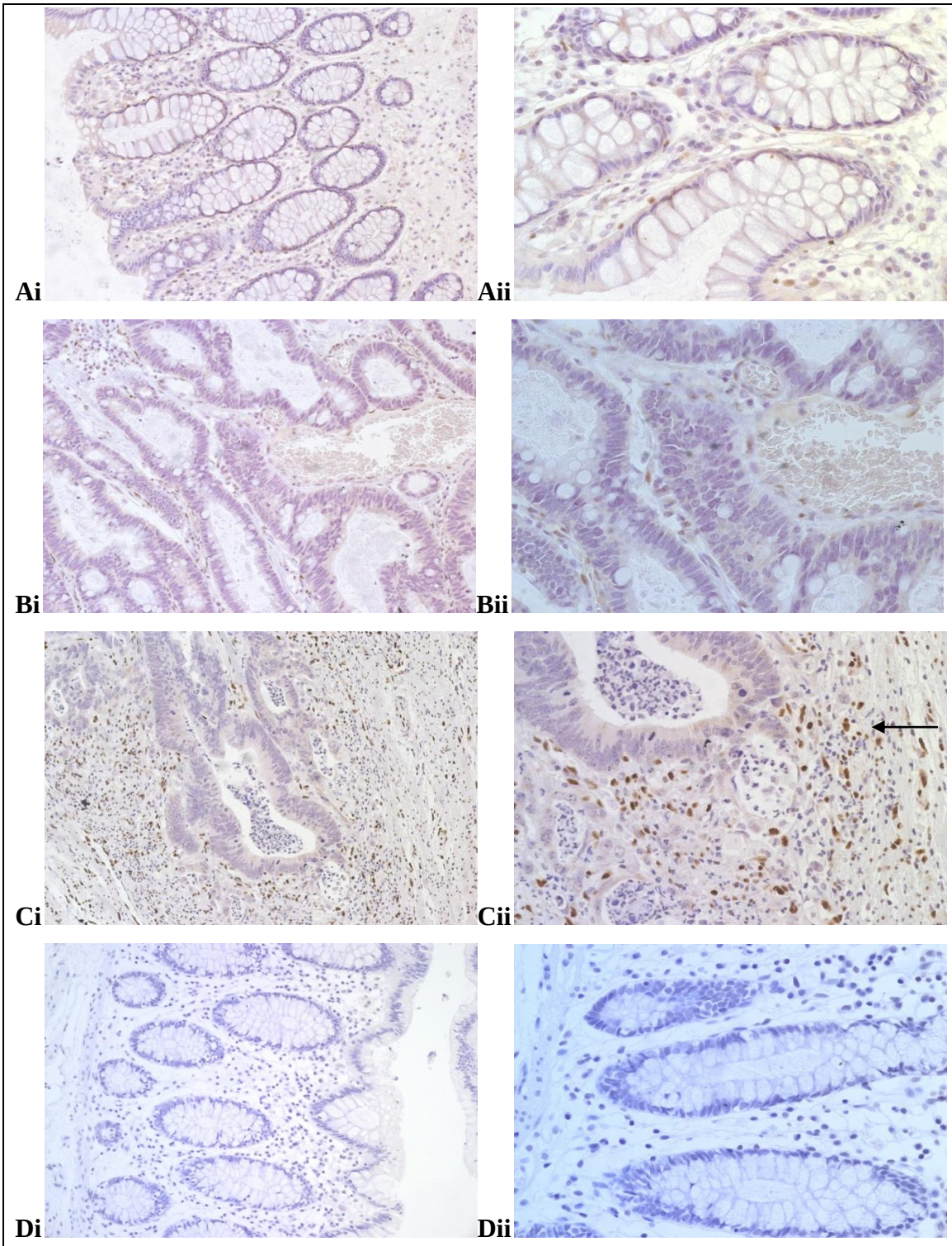

Figure 3.12. Immunohistochemical detection of ZEB1 in colonic specimens. Representative sections are shown of (**A**) normal colonic epithelium, (**B**) central primary colonic carcinoma and (**C**) invasive front of primary colonic tumour. (**D**) Non-specific rabbit immunoglobulin fraction negative control. (→=ZEB1 nuclear stain. **i**=20X magnification, **ii**=40X magnification.)

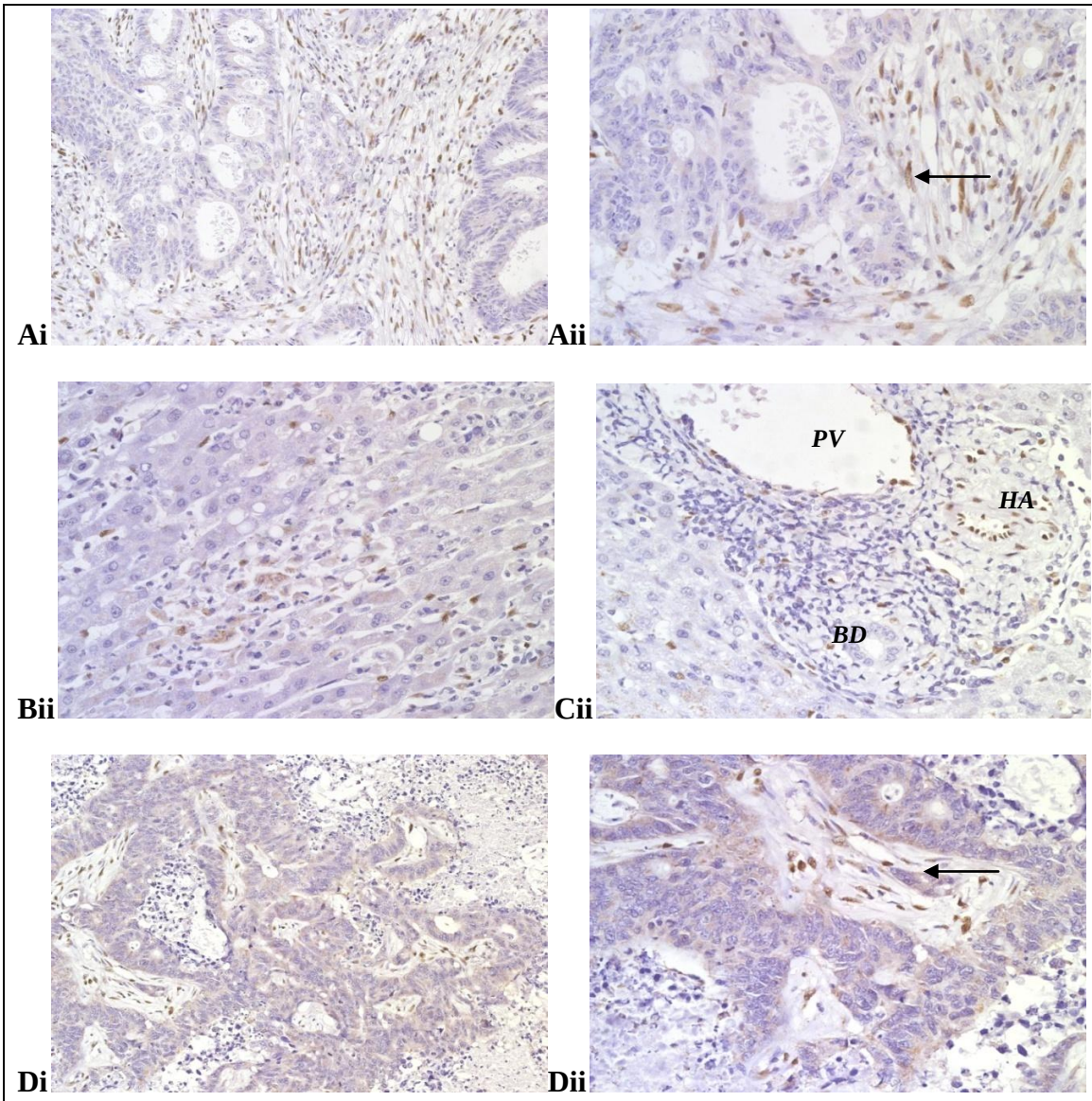

Figure 3.13. Immunohistochemical detection of ZEB1 in lymph node and liver specimens. Representative sections are shown of (**A**) lymph node metastasis, (**B**) normal liver, (**C**) portal tract in the liver and (**D**) liver metastasis. (→=ZEB1 nuclear stain; ***PV***=portal vein; ***HA***= hepatic artery; ***BD***= bile duct. **i**=20X magnification, **ii**=40X magnification.)

In normal colonic epithelium occasional stromal cell nuclei were positive for ZEB1, but this was an infrequent finding. None of the colonic epithelial cells demonstrated ZEB1 expression. The central colonic tumour cells showed little or no ZEB1 reactivity, but stromal cells in this area showed increased ZEB1 expression compared to normal epithelium. However, at the invasive front of the tumours significant up-regulation of

ZEB1 expression was noted in the stromal cells of a large proportion of tumours (43/101).

Normal liver sections demonstrated occasional ZEB1 expression in stromal cells in a distribution akin to that seen in normal colonic sections. In lymph node and liver metastases the pattern of ZEB1 expression seen in the central areas of primary tumours was maintained. Statistical analysis of ZEB1 expression is performed in chapter 6.

Chapter 4: Results – The relationship between ZEB1 and Wnt-Inducible Signalling Proteins (WISPs).

Introduction

Reports of up-regulated expression of ZEB1 in stroma-associated cells in CRC and other epithelial tissues led to a search for proteins which may be involved in stromal cell regulation and signalling, and may therefore be associated with ZEB1 expression[86, 115]. Recent evidence has suggested that WISPs may play a critical role as multi-functioning regulators of the extra-cellular matrix[280]. Members of the CCN family are thought to interact with cellular adhesion molecules and modify cellular responses to changes in the micro-environment through these associations, although the exact nature of these interactions remains to be elucidated[281].

In CRC, up to 90% of sporadic tumours carry genetic mutations which result in aberrant Wnt signalling activity[156]. WISP proteins are down-stream targets of the Wnt signalling cascade, and have been found to be differentially expressed in various malignancies. In inflammatory breast cancer, Huang and colleagues demonstrated that reduced WISP-3 expression correlated with a decrease in E-cadherin and an increase in lymph node metastases. This association was further examined in human mammary epithelial cells. siRNA-mediated knockdown of WISP-3 was found to result in up-regulation of ZEB1 and subsequent decreased E-cadherin expression[94]. These findings corroborated the hypothesised link between ZEB1 and WISP proteins in breast cancer, and instigated the investigations in CRC performed here.

4.1 WISP EXPRESSION IN CELL LINES

Western blots examining WISP-1, WISP-2 and WISP-3 protein expression in a panel of breast and colon cell lines were performed using whole cell lysates prepared from untreated cells cultured to approximately 70% confluency. Two breast cell lines with known expression patterns were included as positive controls.

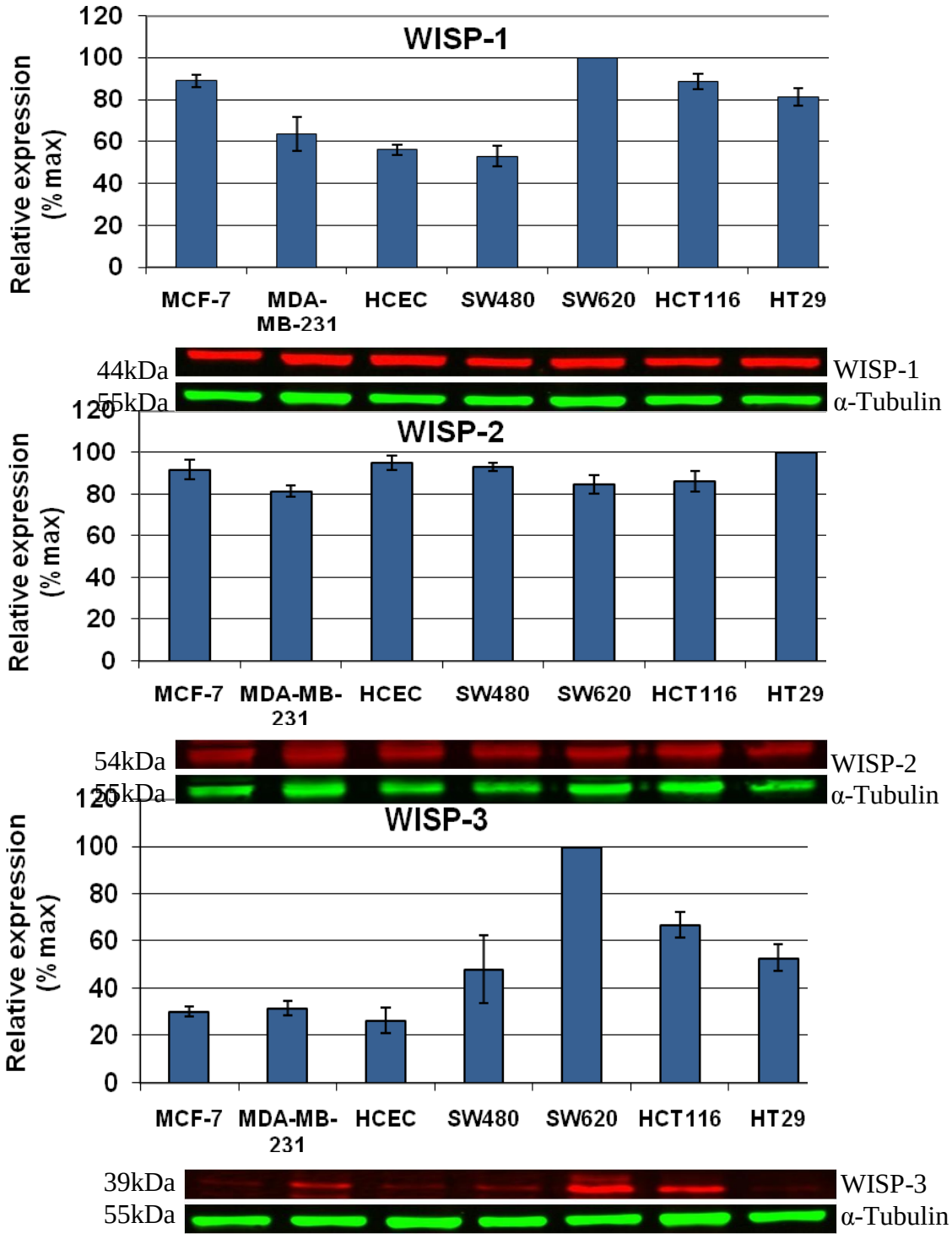

Figure 4.1. WISP-1, WISP-2 and WISP-3 expression in a panel of colorectal and breast cell lines. WISP-1, WISP-2 and WISP-3 protein expression levels are plotted as a percentage of the maximum level in any cell line, using alpha tubulin as a loading control and determined by Odyssey imager quantitative analysis. Representative western blots are also shown. (n=3, error bars +/- SEM.)

In figure 4.1 WISP-3 demonstrated differential expression profiles across the range of cell lines. It is expressed at low levels in the de-differentiated, SW480 cell line with metastatic potential, but at significantly higher levels in the SW620 cells which were derived from the same patient's lymph node metastasis. These findings were noted to be similar to the expression profile of E-cadherin in these cell lines. WISP-1 was found to have some variability in the cell lines examined, but this was not as pronounced as that seen for WISP-3. WISP-2 showed little variability of expression among all cell lines examined. The breast cell lines MCF-7 and MDA-MB231 were examined as positive controls for the various WISP proteins. The bands detected on western blotting matched the projected molecular weight of all the proteins. Given the previous evidence linking WISP-3 with ZEB1 and the variable expression profile of WISP-3 in the panel of colon cell lines demonstrated here, further investigations concentrated initially on WISP-3 and ZEB1 relationships[94].

4.2 EFFECT OF ZEB1 ON WISP EXPRESSION

The A431-ZEB1 cell line was a kind gift from Dr E. Tulchinsky (Leicester, UK). These cells, which are derived from a human epithelial squamous cell carcinoma, have been transfected with a DNA construct which causes ZEB1 expression when the cells are exposed to doxycycline at appropriate concentrations. As a simple model of the effect of ZEB1 on WISP protein expression these cells were examined. Cells were cultured in 10cm plates, as described in Chapter 2. After 24 hours, doxycycline (1µg/ml) was added to the treatment plates alongside untreated controls, and the cells cultured on for a further 48 hours. Whole cell lysates were prepared and western blots performed to examine protein expression. All experiments were repeated three times. Representative western blots and overall quantitative analysis using odyssey imager software are shown in figure 4.2.

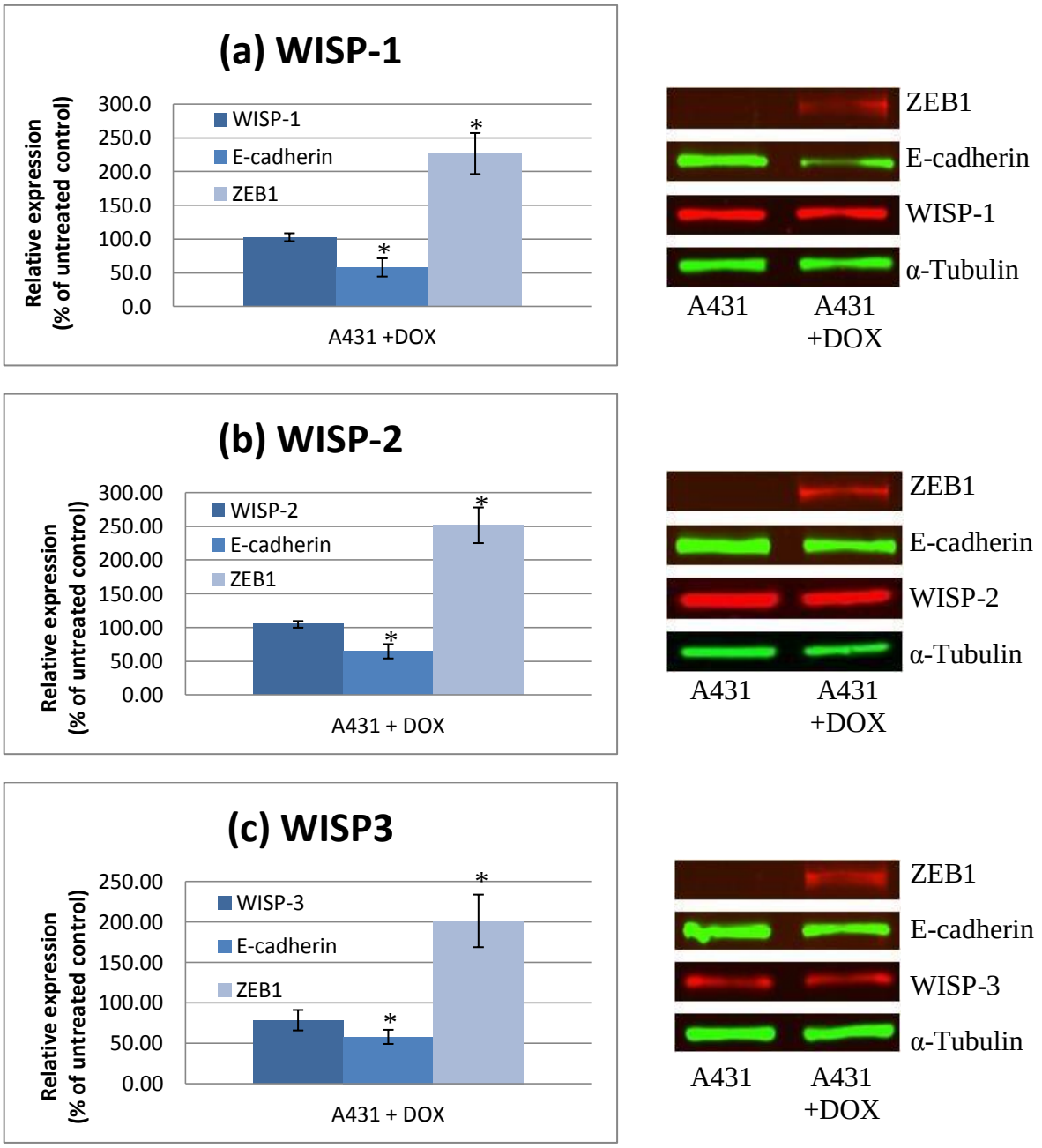

Figure 4.2. Effect of ZEB1 expression on WISP proteins in A431 cells. Representative western blots and histograms of relative expression of WISP proteins, ZEB1 and E-cadherin are shown in A431 cells after 48 hours treatment with doxycycline (1µg/ml). A significant increase in ZEB1 expression was accompanied by a significant decrease in E-cadherin expression on doxycycline treatment (*=P<0.05; One-way ANOVA and Tukey Post Hoc test). A decrease in WISP protein expression was observed for WISP-3, but this did not reach statistical significance (One-way ANOVA, n=3 for each WISP protein, ± SEM).

A significant increase in ZEB1 and decrease in E-cadherin expression was seen in all experiments, but no change was observed in WISP-1 and WISP-2 expression. However, WISP-3 expression was decreased by doxycycline treatment and ZEB1 over-expression. Although the change was not statistically significant, these initial experiments appeared to suggest a signalling link between ZEB1, E-cadherin and WISP-3, albeit in these skin epithelium-derived cells. Huang and colleagues previously reported an association between WISP-3 and ZEB1 expression in breast cell lines. They demonstrated the up-regulation of ZEB1 in response to WISP-3 knockdown, and the above experiment may suggest a negative feedback loop effect associated with ZEB1 expression on WISP-3[94].

4.3 MANIPULATION OF WISP PROTEIN EXPRESSION

In order to investigate the relationship between ZEB1 and WISP-3 in colorectal cell lines, HCT116 cells were selected for knockdown experiments using the Lipofectamine 2000 transfection reagent. This reagent has previously been used for transfection of these cells with both DNA and siRNA (according to the literature), and the ZEB1 plasmid had been successfully transfected according to the manufacturers' instructions (see Chapter 3). A specifically optimised transfection protocol for siRNA and HCT116 cells was available from the manufacturer and was followed in the initial experiments. HCT116 cells were shown to express all three WISP proteins by western blotting and were therefore suitable to study protein knockdown. They also possess little endogenous ZEB1 expression.

4.3.1 WISP-3

Initially four different WISP-3 siRNAs were transfected into HCT116 cells in order to identify the most effective. Cells were plated out in 6-well format as outlined in chapter 2. A control siRNA was also included in all experiments. As recommended by the

transfection reagent manufacturer, the concentration of siRNA in all experiments was 50nM. Cells were cultured for 48 hours after transfection in this initial experiment and then whole cell lysates prepared and WISP-3 expression assessed by western blot (figure 4.3).

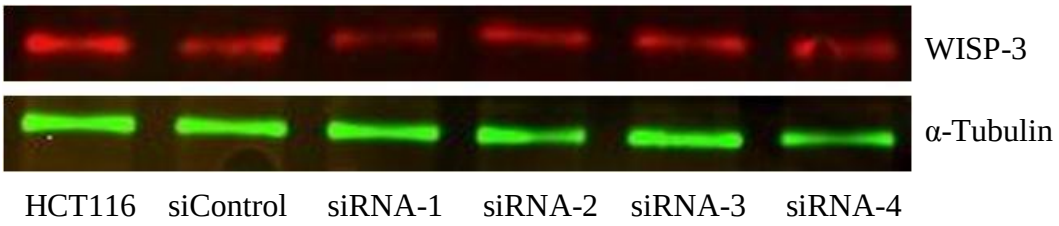

Figure 4.3. Initial test of 4 siRNAs to knockdown WISP-3 in HCT116 cells. HCT116 cells were transfected with siRNA to WISP-3 using Lipofectamine 2000, whole cell lysates prepared after 48 hours and western blotting performed. (n=1).

siRNA-1 appears to give some knockdown of WISP-3 protein and was selected for further experiments. Following this initial experiment it was apparent that even the most effective siRNA against WISP-3 out of those tested was only providing approximately 20-30% knockdown. Given the previous difficulties with DNA transfection, the possibility that the Lipofectamine 2000 chemical reagent was not providing sufficient transfection efficiency to deliver the siRNA into the cell was considered. Therefore 2 further chemical reagents were used in the subsequent experiment. These reagents were advertised by the manufacturer as being specifically designed for siRNA, as opposed to DNA, delivery (siPORT NeoFX [Ambion] and Codebreaker [Promega]). The half life of WISP-3 has not been reported in the literature and therefore it was also hypothesised that this may be another factor effecting protein knockdown. The experiments were carried out at various time points to examine whether this had any effect on protein expression. All experiments

included a control transfection with the pGFP plasmid to allow an estimate of transfection efficiency to be made.

The GFP well of each 6-well plate was examined after 24 hours under a fluorescent microscope, and transfection efficiency was estimated as a percentage of total cells per high-power field. This was found to be 60% for all the reagents. Western blots from the experiments are shown in figure 4.4.

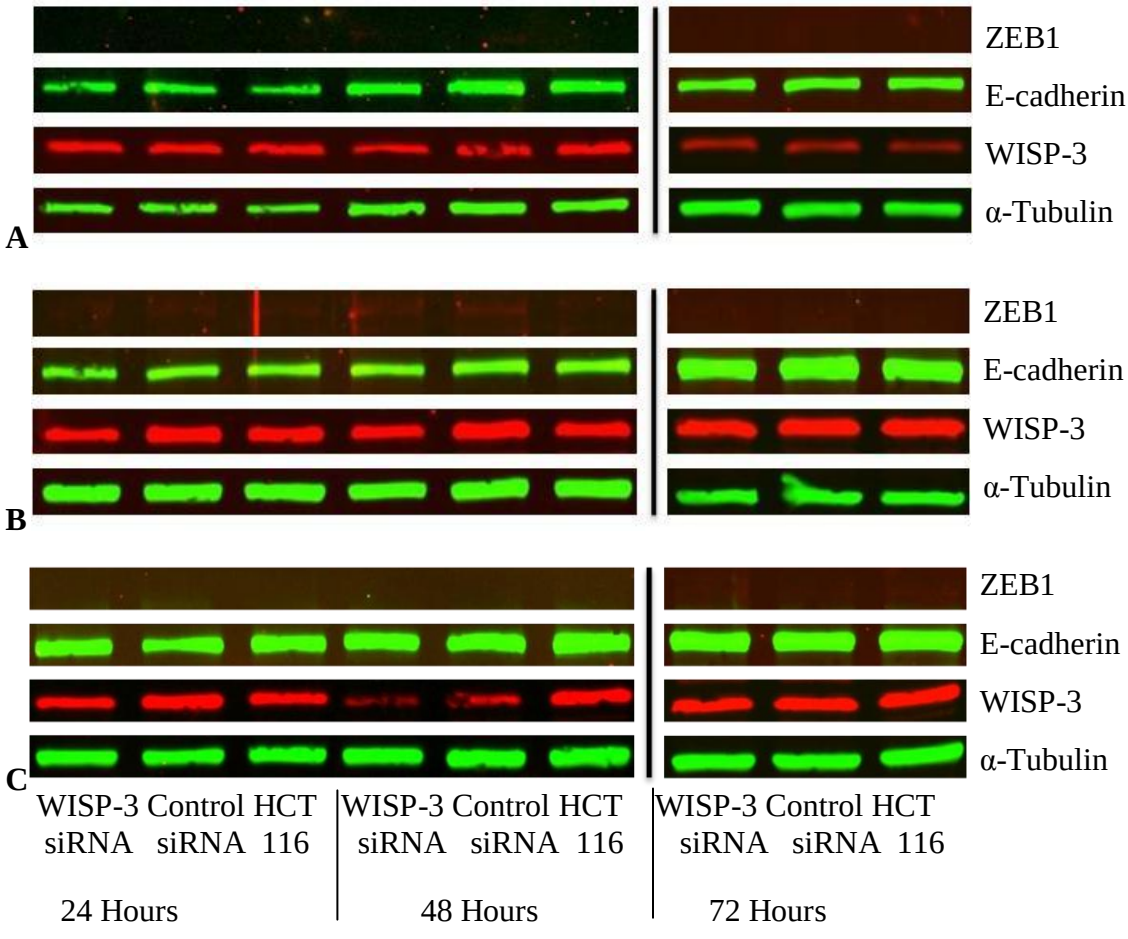

Figure 4.4. Transfection of WISP-3 siRNA into HCT116 cells using 3 different chemical agents. HCT116 cells were transfected with WISP-3 siRNA using (**A**) siPORT NeoFX, (**B**) Codebreaker, (**C**) Lipofectamine 2000 and cultured for 24, 48 and 72 hours. Whole cell lysates were prepared and western blots performed. (n=1 for all reagents)

Transient 80% knockdown of WISP-3 was seen at the 48 hour time point using Lipofectamine 2000, but some decrease in WISP-3 expression was also seen in the control siRNA treated lane at this point raising the suspicion that it may be a transfection or western blotting-related phenomenon. In addition WISP-3 was expressed at normal levels at 72 hours, indicating a very short-lived knockdown. There was no effect on E-cadherin and ZEB1 levels at any time point or with any of the reagents. Given the lack of successful knockdown of WISP-3 at almost all other time points with any of the reagents a further trouble-shooting experiment was attempted. Transfections were performed in HCT116 and SW620 cells to test whether there may be a specific problem relating to the HCT116 cell line. Amaxa transfection (combined chemical and electroporation transfection) was performed in an attempt to increase transfection efficiency. Western blots from these experiments are shown in figure 4.5.

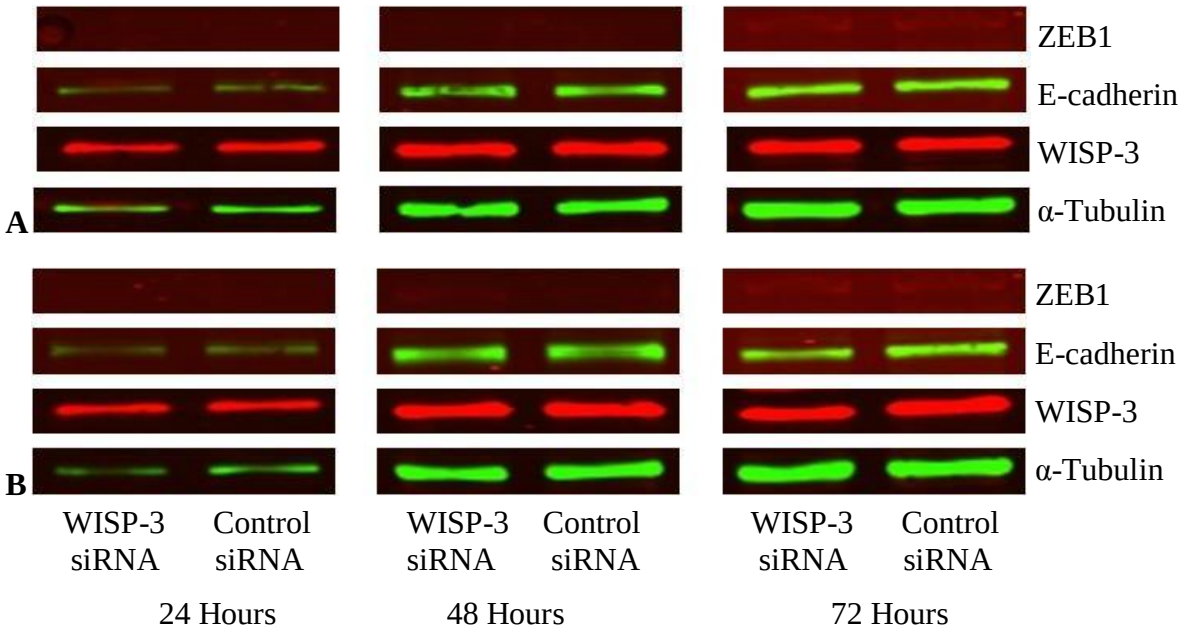

Figure 4.5. Transfection of WISP-3 siRNA into HCT116 and SW620 cells using Amaxa technique. WISP-3 siRNA was transfected into (**A**) HCT116 and (**B**) SW620 cells and cultured for 24, 48 and 72 hours. Whole cell lysates were prepared and western blots performed. (n=1)

No change in WISP-3, E-cadherin or ZEB1 expression was observed in either cell line. Despite the variation of transfection techniques, use of two cell lines and examination of three time-points there was still no significant success in WISP-3 knockdown with siRNA. Further examination of the literature indicated that other investigators had utilised shRNA vectors to achieve stable protein knockdown and selected clones for further study. This strategy may have been adopted in order to study the long term effects of protein loss, but may also indicate difficulties experienced by other researchers in the use of siRNA-mediated knockdown in these proteins.

4.3.2 WISP-1

As previously discussed evidence regarding the expression of WISP-1 in cell lines indicates its role as an oncogenic protein. Anti-apoptotic, increased migratory and proliferative effects have been demonstrated in several tumour cell lines over-expressing WISP-1, although Soon and colleagues found decreased invasive and migratory potential in lung carcinoma cells[182, 185, 196, 197]. Pennica and colleagues found high expression of WISP-1 mRNA in cell lines derived from colonic neoplasms, which included HCT116[184]. However, few investigators have examined WISP-1 expression in CRC cell lines at the protein level. Given the protein expression levels of WISP-1 shown here in HCT116 cells, siRNA transfection was attempted with a view to examination of end-point assays if successful knockdown could be achieved. Lipofectamine 2000 transfection was conducted as described in Chapter 2 in attempts to deliver WISP-1 siRNA and control siRNA into the cells. GFP transfected cells were again examined to check transfection efficiency in this experiment. Results of subsequent western blots at three time points are shown in figure 4.6.

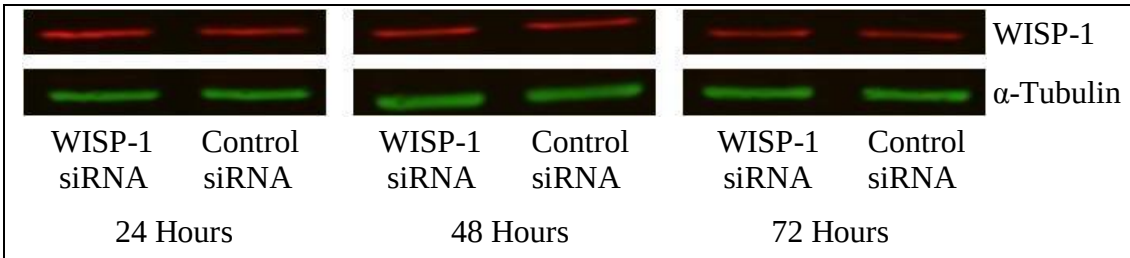

Figure 4.6. Transfection of WISP-1 siRNA into HCT116 cells using Lipofectamine 2000. HCT116 cells were transfected with WISP-1 siRNA and cultured for 24, 48 and 72hours. Whole cell lysates were prepared and western blots performed. (n=1)

When the GFP transfected cells were examined ≥75% transfection efficiency had been achieved as quantified by fluorescent cells as a proportion of the total population on light

microscopy. Western blotting demonstrated no change in WISP-1 expression at 24, 48 or 72 hours. The continued lack of protein knockdown prompted a further optimisation attempt using varying concentrations of siRNA in the experiment. A single time point of 48 hours was chosen. Figure 4.7 shows the result of this experiment.

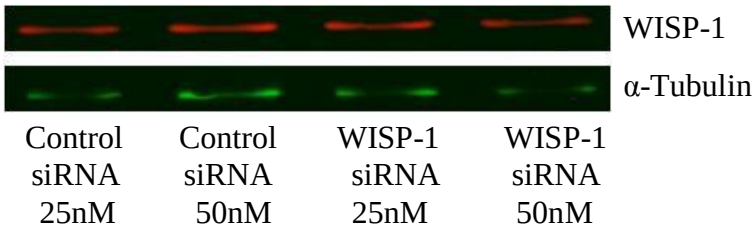

Figure 4.7. Effect of varying concentration of siRNA on knockdown of WISP-1. HCT116 cells were transfected with varying concentrations of WISP-1 and control siRNAs using Lipofectamine 2000. Cells were cultured for 48 hours, whole cell lysates prepared and western blotting performed. Final siRNA concentrations of 25nM and 50nM were tested. (n=1)

No change in WISP-1 expression was observed. The siRNA manufacturer's optimised protocol suggested a final concentration of 50nM would give optimum protein knockdown in HCT116 cells. This concentration of siRNA is relatively high in comparison to experience in other cell lines and with other reagents. However, a 0.5-fold reduction in concentration (25nM) had no effect on protein expression. It was clear that further attempts at protein knockdown using siRNA were likely to be unsuccessful with the continued use of chemical transfection in these cells.

4.3.3 WISP-2

WISP-2 is perhaps the most widely investigated of the WISP proteins, with several groups interested in its role in breast cancer. The majority of investigators have documented a

tumour suppressor role of WISP-2 in breast and other cancer cell lines[211, 212, 223, 241]. Expression of WISP-2 appears to engender anti-metastatic properties *in vitro*, with several investigators demonstrating WISP-2 knockdown leads to increased migration, invasion and proliferation[211, 212]. Of particular interest, Banerjee and colleagues found knockdown of WISP-2 in non-invasive MCF-7 cells to increase migratory and invasive potential via an EMT, with concurrent decrease of E-cadherin and up-regulation of SNAIL[212]. ZEB1 expression was not assessed in this study.

The lack of effective knockdown of WISP-1 and WISP-3 proteins using siRNA techniques in the previous experiments, despite attempts at transfection protocol optimisation, prompted investigation of other methods of protein knockdown. The pSilencer shRNA vector with shRNA to WISP-2 was a kind gift from Dr S. Banerjee (Minnesota, USA). This vector inserts DNA encoding WISP2shRNA (figure 4.8 (A)) into the cell of interest which is then replicated and causes stable knockdown of protein expression. A control vector with a sequence encoding non-targeting shRNA was also provided. Both the vectors were cloned as described in chapter 2 and analysed by agarose gel electrophoresis (figure 4.8(B)).

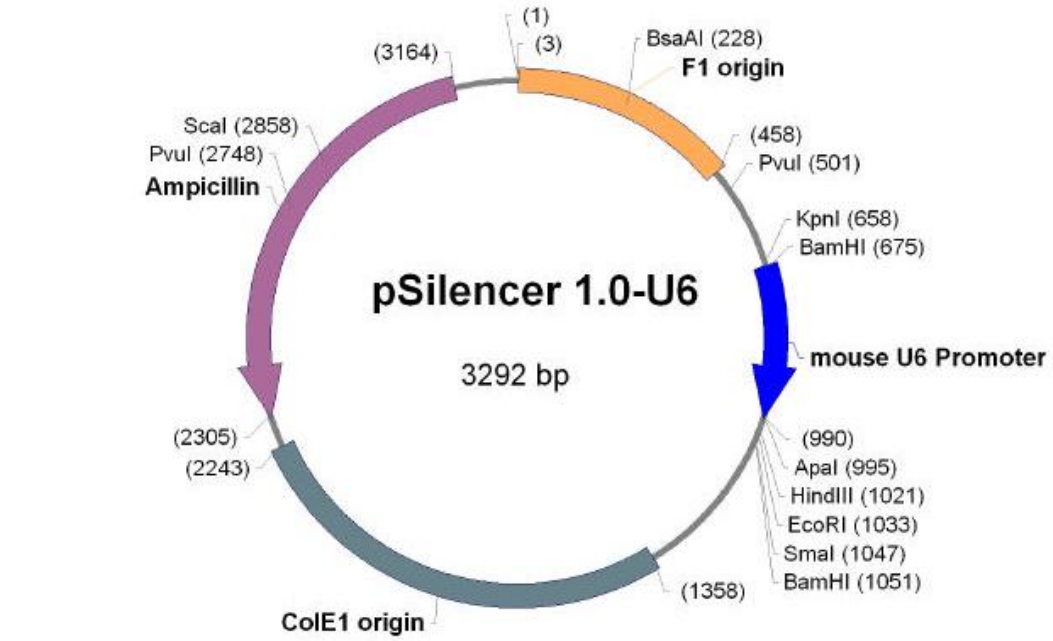

A

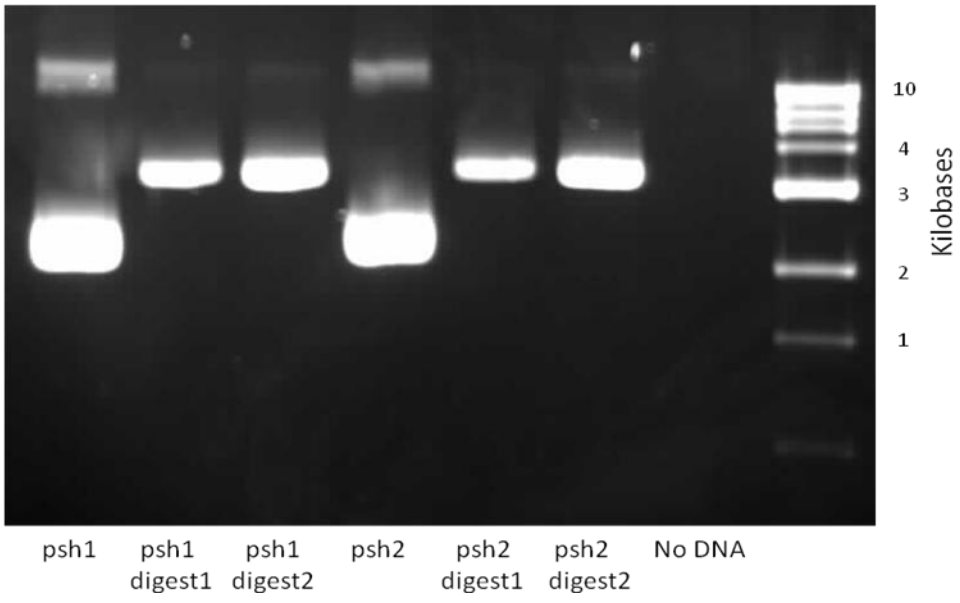

B

Figure 4.8. Schematic of the original pSilencer 1.0-U6 sh/siRNA expression vector (A) and analysis of cloned pshWISP2 and pshControl vectors by agarose gel electrophoresis (B). The cloned vectors were subjected to electrophoresis on a 0.8% agarose gel with appropriate digests. (psh1=pshControl vector, psh2=pshWISP2 vector. Digest 1 = DNA : Sma1 enzyme 1:1 ratio, digest 2= DNA : Sma1 enzyme 2:1 ratio.)

The super-coiled, undigested vector ran at a molecular weight of 2500bp. When cut with the Sma1 enzyme a single band was seen corresponding to the projected weight of approximately 3300bp.

The pshWISP2 vector was then transfected into two cell lines, HCT116 and SW620, which had been shown to express WISP-2, using Lipofectamine 2000 according to the previously successful DNA transfection protocol (see chapters 2 and 3). Protein expression was examined at two time points by western blot and with two different DNA: lipofectamine 2000 ratios. Quantitative analysis of western blots was performed on the Odyssey imager (figure 4.9).

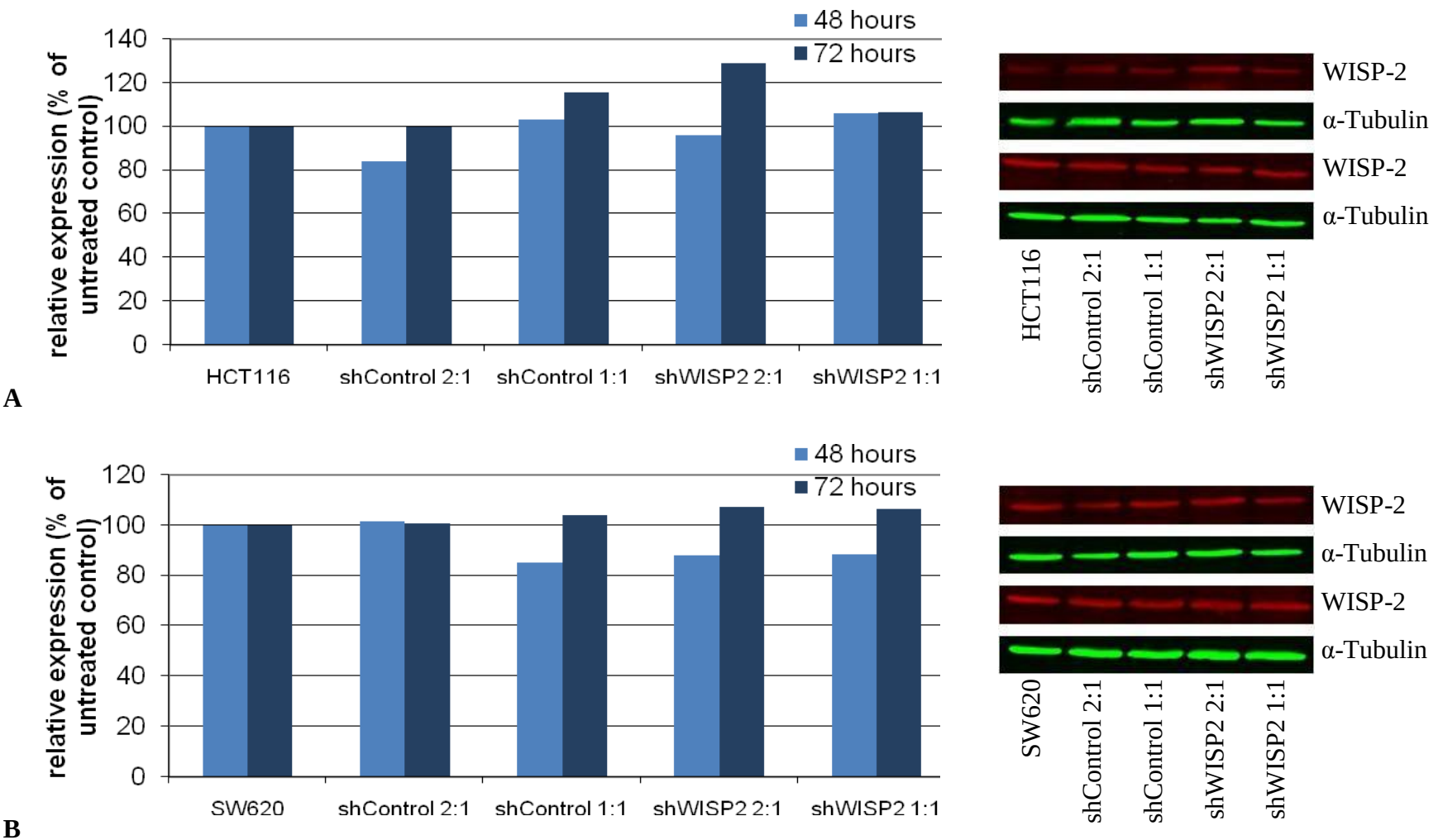

Figure 4.9. Attempted knockdown of WISP-2. Histograms and western blots showing WISP-2 expression after transfection of varying quantities of pshWISP2 and pshControl vectors using Lipofectamine 2000 in (**A**) HCT116 and (**B**) SW620 cells at 48 and 72 hours. (n=1 for each time point and cell line)

Despite confirmation of the correct DNA size of the vectors on electrophoresis, and attempts at optimisation with varying quantities of DNA, two time points and use of two cell lines, knockdown of WISP-2 was not achieved. The lack of success in modulating expression of any of the WISP proteins was difficult to explain. Delivery of DNA into the cells by chemical transfection had been confirmed using the pGFP plasmid and ZEB1 had been successfully expressed after transfection of the pZEB1 construct. Various different concentrations of both the siRNA and pshWISP2 constructs had been tried, and at various time-points. This raised concerns over the validity of the antibodies being used and the specificity of the band which was assumed to represent the protein of interest. A further experiment was conducted to test this theory.

Full length recombinant WISP-2 protein was purchased and used as a blocking agent in a western blotting experiment. Untreated lysates from the cell lines were loaded onto a gel and run as described in Chapter 2. Once transferred to the membrane non-specific blocking with odyssey solution was performed as previously. The full length WISP-2 recombinant protein was mixed with the primary WISP-2 antibody at a ratio of 2:1, the theory being that the protein should saturate all the specific antibody binding sites. If this were the case no antibody should bind the protein on the membrane and the previously seen WISP-2 band on the western blot should disappear, indicating antibody specificity. However, if the band remained then this must represent detection of a protein other than WISP-2. Figure 4.10 shows the resulting blot.

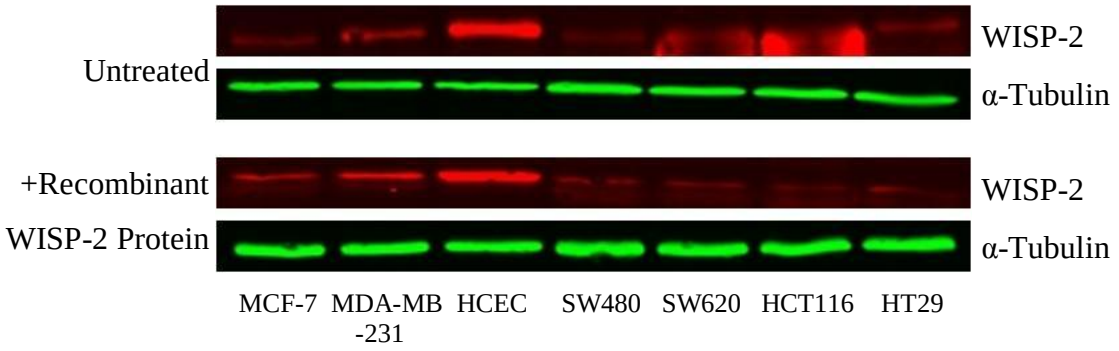

Figure 4.10. Effect of blocking WISP-2 antibody with recombinant protein. Western blots of whole cell lysates from breast and colorectal cell lines prepared. The first blot was probed with untreated WISP-2 antibody in the standard manner. WISP-2 antibody which had been treated with recombinant WISP-2 protein in order to block antibody binding sites was used on the second blot. (n=1)

The resulting western blot after blocking demonstrated that the antibody band which had been assumed to represent WISP-2 protein was not affected by incubation with the recombinant protein in several cell lines, although in SW620 and HCT116 the band did seem to decrease. Given these findings it is possible that the band being picked up on western blotting may not represent WISP-2. This result may explain the lack of success in the previous experiment when attempting knockdown. If the band on the western blot which was being examined was not specific for WISP-2 then no change would be observed, even if the WISP-2 protein knockdown were successful. As previously discussed, WISP proteins are prone to post-translation changes and various splice variants may exist of each protein. It is possible that this may contribute to the lack of change in protein expression seen on the western blot here.

4.4 WISP EXPRESSION *IN VIVO*

Alongside assessment of WISP protein expression in various cell lines, formalin-fixed tissues from 101 colorectal cancer specimens and matched lymph node and liver metastases were available for investigation.

4.4.1 Selection of Positive controls

In order to assess the best concentration of each antibody for use with the Envision immunohistochemistry detection system, and subsequently to confirm consistent results between runs, tissues known to express the protein of interest were selected and used to optimise each antibody.

4.4.1.1 WISP-1

Very few *in vivo* investigations examining WISP-1 expression at the protein level have been performed in human normal or malignant tissues. Yanagita and colleagues recorded WISP-1 expression in chondrocytes of the developing tibia of a mouse embryo[165]. Expression in a human chondrocyte cell line was also demonstrated by the same group of investigators. Expression of WISP-1 RNA was reported in normal cartilage samples by Yu and colleagues[202]. Human cartilage was therefore selected as the positive control tissue for WISP-1. Anonymised specimens were provided by the Pathology Department at the Leicester Royal Infirmary (LRI) and several optimisation experiments were attempted with these tissues. However, the blocks were extremely difficult to cut on the microtome due to the high calcium content of the bone associated with the cartilage. Despite attempts at de-calcification prior to fixation, the successfully cut sections also tended to lift off the slides during antigen retrieval, even though the slides contained a negative charge to attract the tissue. This meant that the stained sections were un-interpretable.

The results of investigations detailing weak expression of WISP-1 in normal colon have been previously published by two groups, both found weak cytoplasmic staining in the normal colonic epithelium[188, 192]. The lack of other suitable normal tissue as positive controls therefore led to optimisation of the antibody using normal colon sections. Examples of the varying results according to different antibody dilutions are shown in figure 4.11, with a non-specific rabbit immunoglobulin fraction used as a negative control.

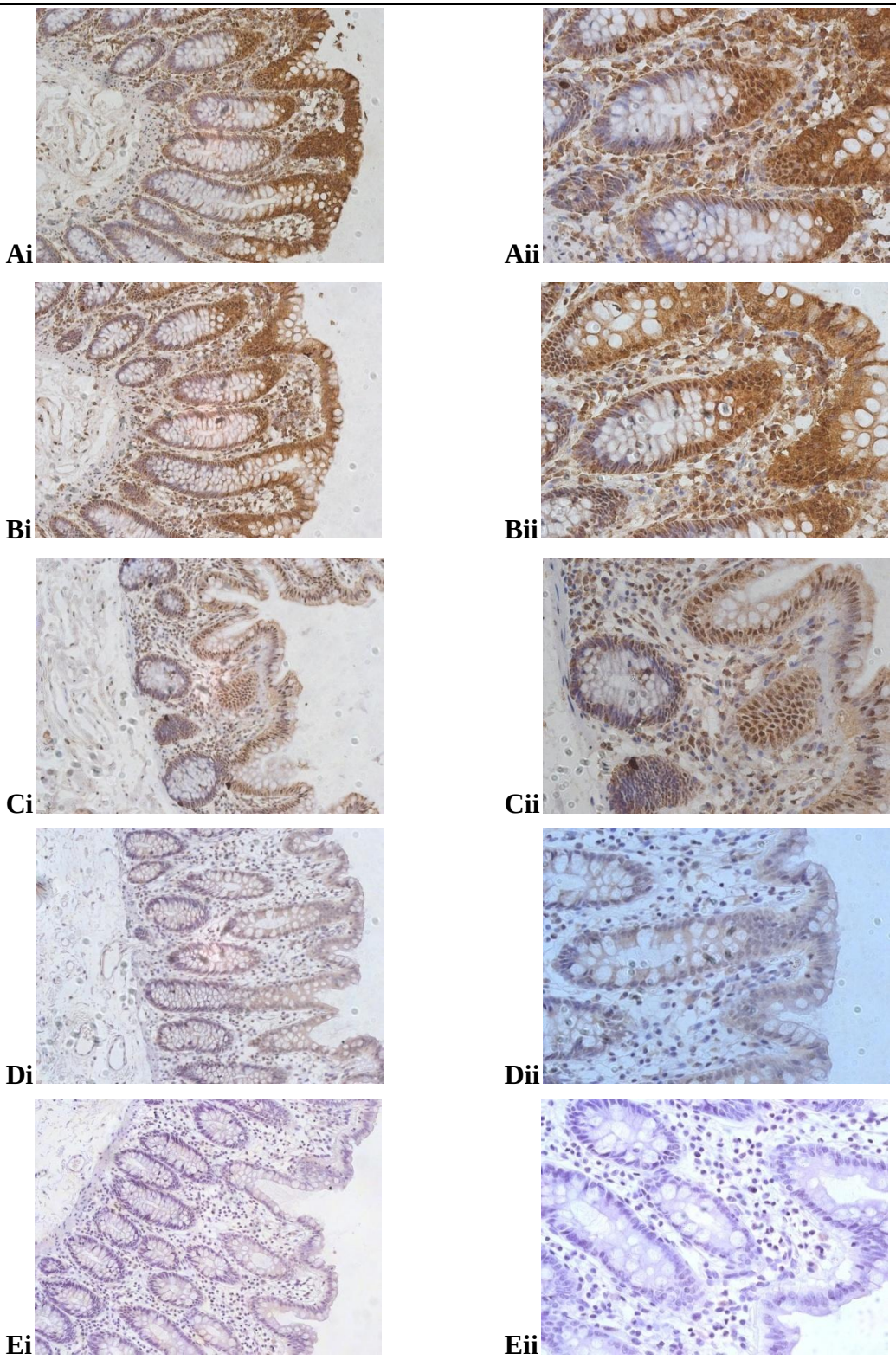

Figure 4.11. Optimisation of WISP-1 antibody in normal colon sections. (**A**) 1:100 (**B**) 1:250 (**C**) 1:500 (**D**) 1:1000 and (**E**) Negative control rabbit immunoglobulin fraction, 1:250. (**i**=20X magnification, **ii**=40X magnification)

WISP-1 was observed to weakly stain the cytoplasm of colonic epithelial cells. Significant background staining was seen at concentrations of antibody higher than 1 in 500. Moderate nuclear staining of cells in the upper epithelial layers was also observed which appeared very specific to the epithelium as no cell nuclei in the stroma were stained. Therefore a WISP-1 antibody concentration of 1:500 was selected for investigations of CRC specimens with immunohistochemistry. Examples of WISP-1 expression in colonic tissues and lymphatic / liver tissues are shown in figure 4.12 and 4.13 respectively.

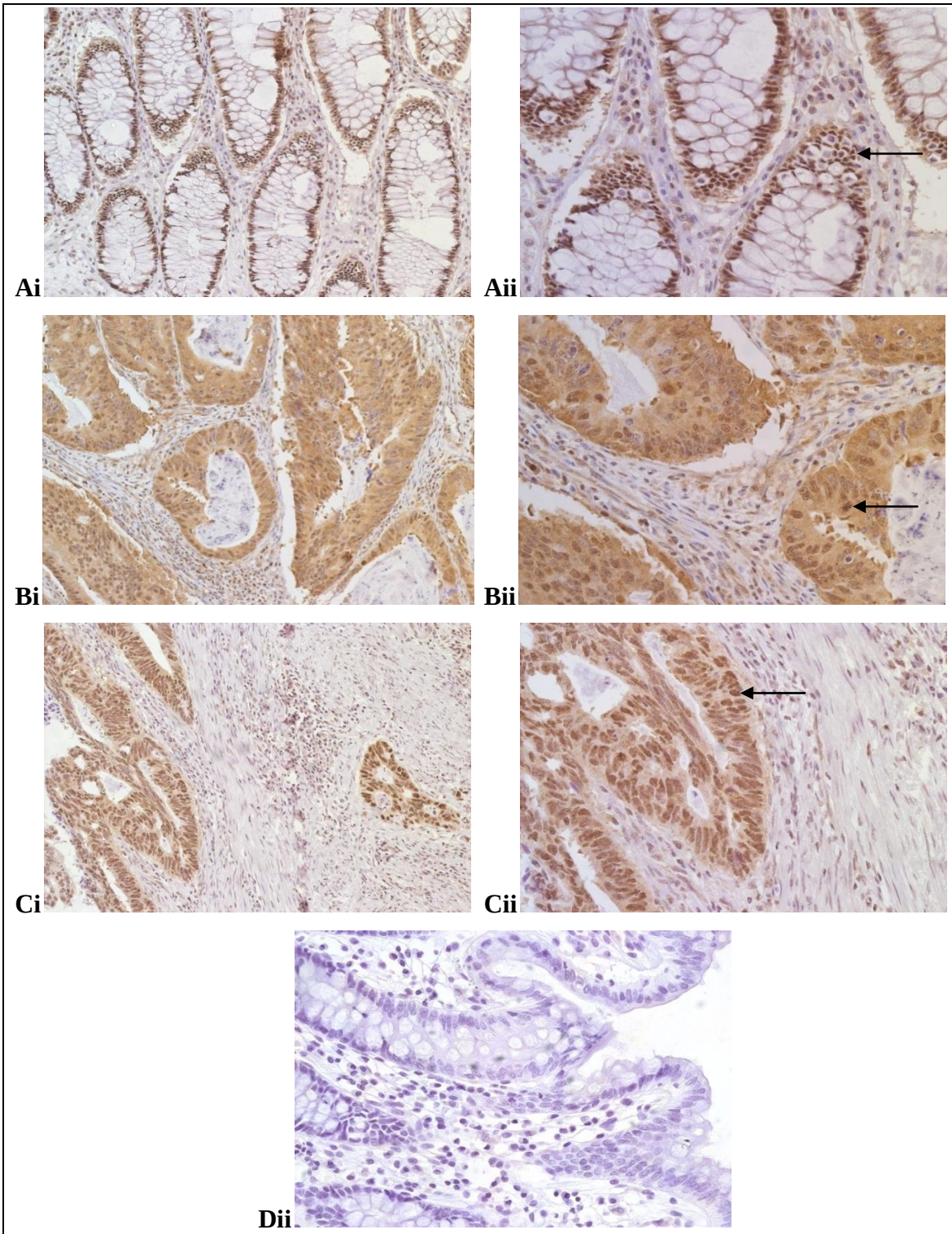

Figure 4.12. Immunohistochemical detection of WISP-1 in colonic specimens. Representative sections are shown of (**A**) normal colonic epithelium, (**B**) central primary colonic carcinoma and (**C**) invasive front of primary colonic tumour. (**D**) Non-specific rabbit immunoglobulin fraction negative control. (→=WISP-1 nuclear stain. **i**=20X magnification, **ii**=40X magnification.)

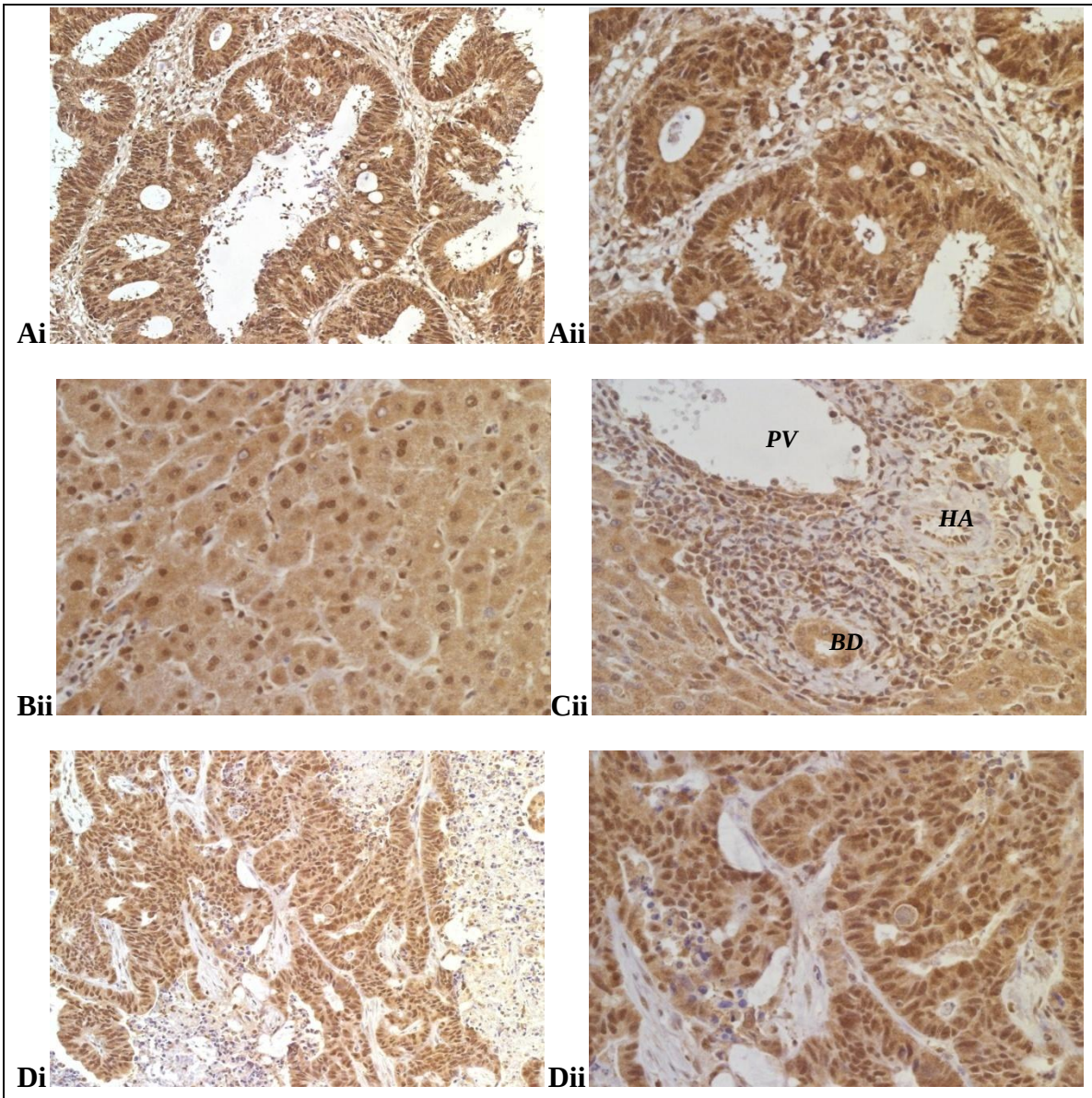

Figure 4.13. Immunohistochemical detection of WISP-1 in lymph node and liver specimens. Representative sections are shown of (**A**) lymph node metastasis, (**B**) normal liver, (**C**) portal triad in liver and (**D**) liver metastasis. (→=WISP-1 nuclear stain; ***PV***=portal vein; ***HA***= hepatic artery; ***BD***= bile duct. **i**=20X magnification, **ii**=40X magnification.)

Normal colonic epithelial nuclei stained differentially for WISP-1, cells in the basal crypts demonstrating weak or absent WISP-1 expression, with increasing positivity toward the

lumen. Cytoplasmic staining was noted throughout the majority of normal and neoplastic epithelial cells. The central colonic tumour cells showed significant WISP-1 reactivity; in only a small number of tumours (6/101) increased cytoplasmic WISP-1 expression was observed at the tumour invasive front. However, on scoring nuclear stain, 42 out of 101 tumours demonstrated increased WISP-1 reactivity at the invasive front.

Normal hepatocytes demonstrated weak cytoplasmic and moderate nuclear WISP-1 expression. Bile duct epithelial cells within portal triad sections were noted to be positive for WISP-1. In lymph node and liver metastases there was strong WISP-1 nuclear expression similar to that seen in the primary tumours. Statistical analysis of WISP-1 expression is further discussed in chapter 6.

4.4.1.2 WISP-2 and WISP-3.

WISP-2 and WISP-3 expression has been previously identified in fibroblasts of rheumatoid synovium and at the synovial intimal lining of joints affected by rheumatoid arthritis[172, 227]. Anonymised rheumatoid synovial tissues were supplied by the Department of Pathology at LRI. Examples of the staining achieved during optimisation experiments for WISP-2 are shown in figure 4.14.

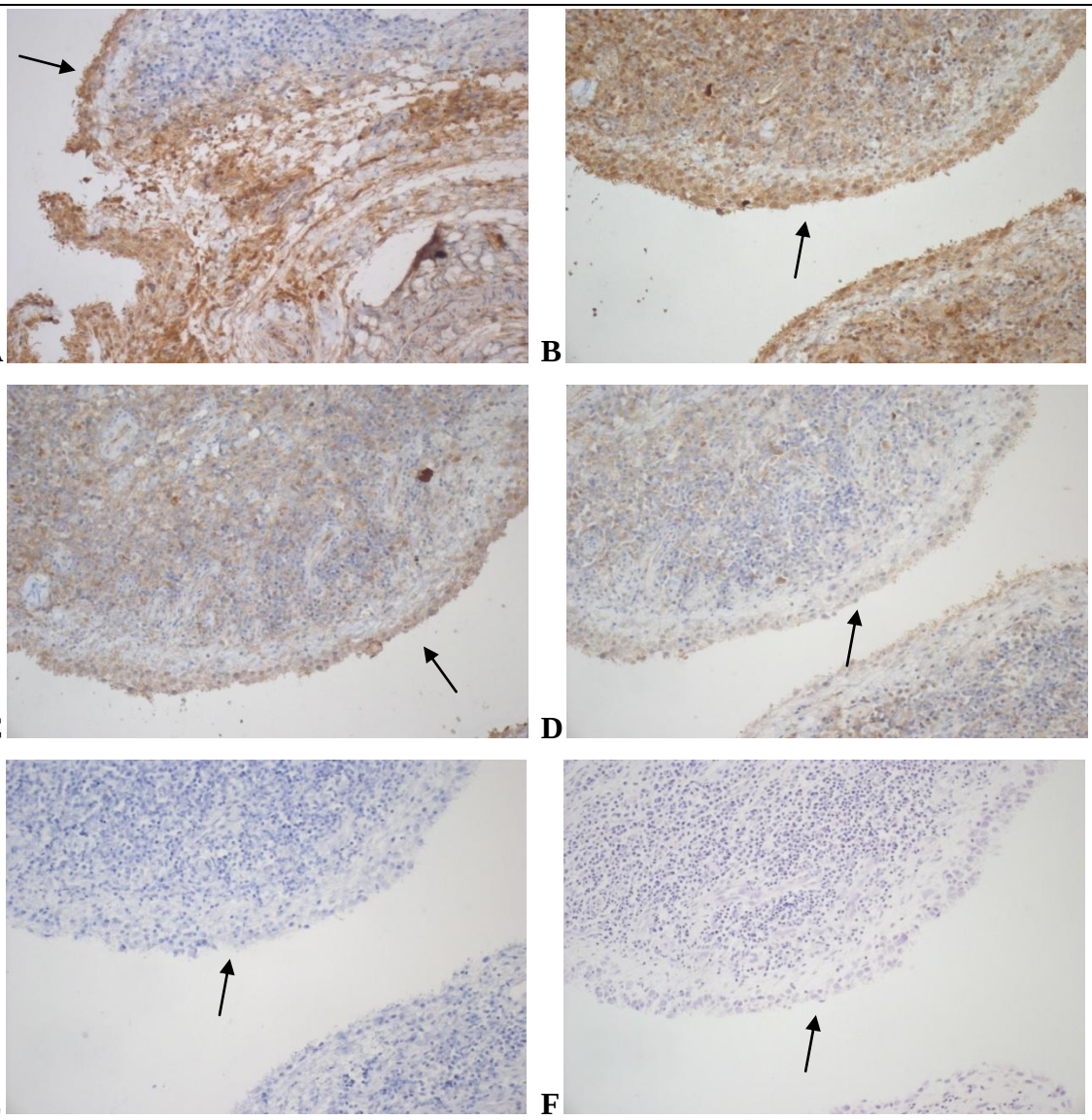

Figure 4.14. Optimisation of WISP-2 antibody in femoral head sections. Tissue sections were subjected to immunohistochemistry with varying WISP-2 antibody concentrations (**A**) 1:100 (**B**) 1:250 (**C**) 1:500 (**D**) 1:1000. (**E**) Non-specific rabbit immunoglobulin fraction negative control (1:250). (**F**) Haemotoxylin and Eosin stain. (→= synovial epithelium, all magnifications are 20X).

Non-specific cytoplasmic staining (brown areas) was observed throughout the sections at varying antibody concentrations, although cells at the synovial lining did appear to display stronger cytoplasmic staining. After this optimisation in synovial tissue, an antibody concentration of 1:500 was selected as the most appropriate as this gave the least

background with positive staining of cells at the synovial lining. The lack of specificity in synovial tissue along with the negative results of *in vitro* attempts at protein manipulation raised significant concerns as to the specificity of the antibody. However, 20 colonic sections were selected and stained to examine the antibody *in vivo*. Figure 4.15 shows typical examples of colon sections stained with WISP-2 antibody.

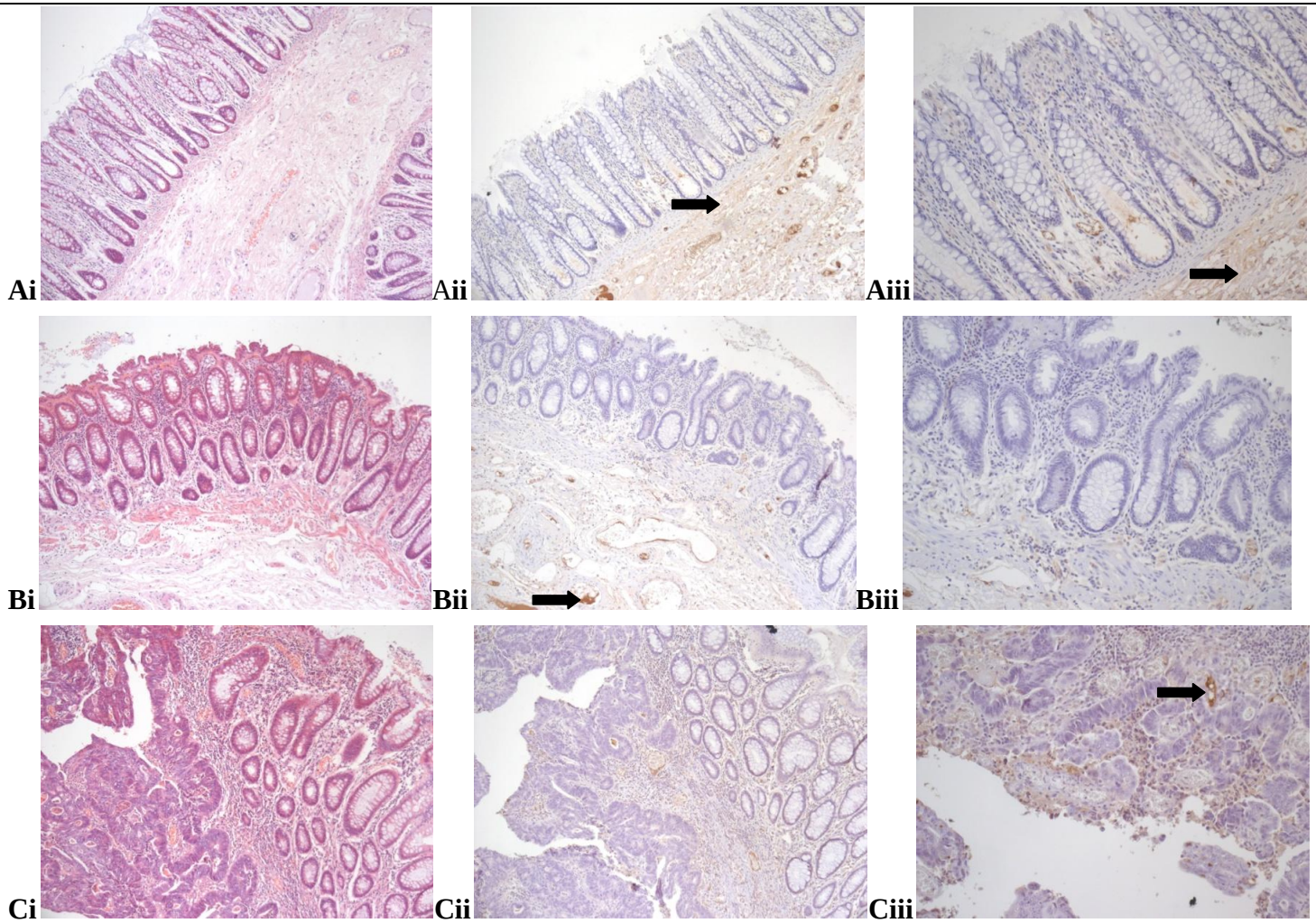

Figure 4.15. WISP-2 in normal colonic epithelium and colorectal cancers. Colonic tissue sections were subjected to immunohistochemistry and stained with WISP-2 (1:500). Representative sections are shown of normal colon (**A**,**B**) and normal colon/tumour interface (**C**). (→= non-specific stain, **i**=H & E, **ii**=10X magnification, **iii**=20Xmagnification)

The stain pattern produced by use of the WISP-2 antibody in colonic specimens appeared non-specific. No staining was observed in the epithelial cells, and various stromal cell and connective tissue components showed cytoplasmic staining. The results from optimisation in synovial sections and those from the colonic tissues were consistent with the *in vitro* experiments which had raised concerns regarding the specificity of the antibody. There were also significant concerns over the WISP-3 antibody subsequent to its *in vitro* use. However, an attempt at optimisation in synovial sections was also made (figure 4.16).

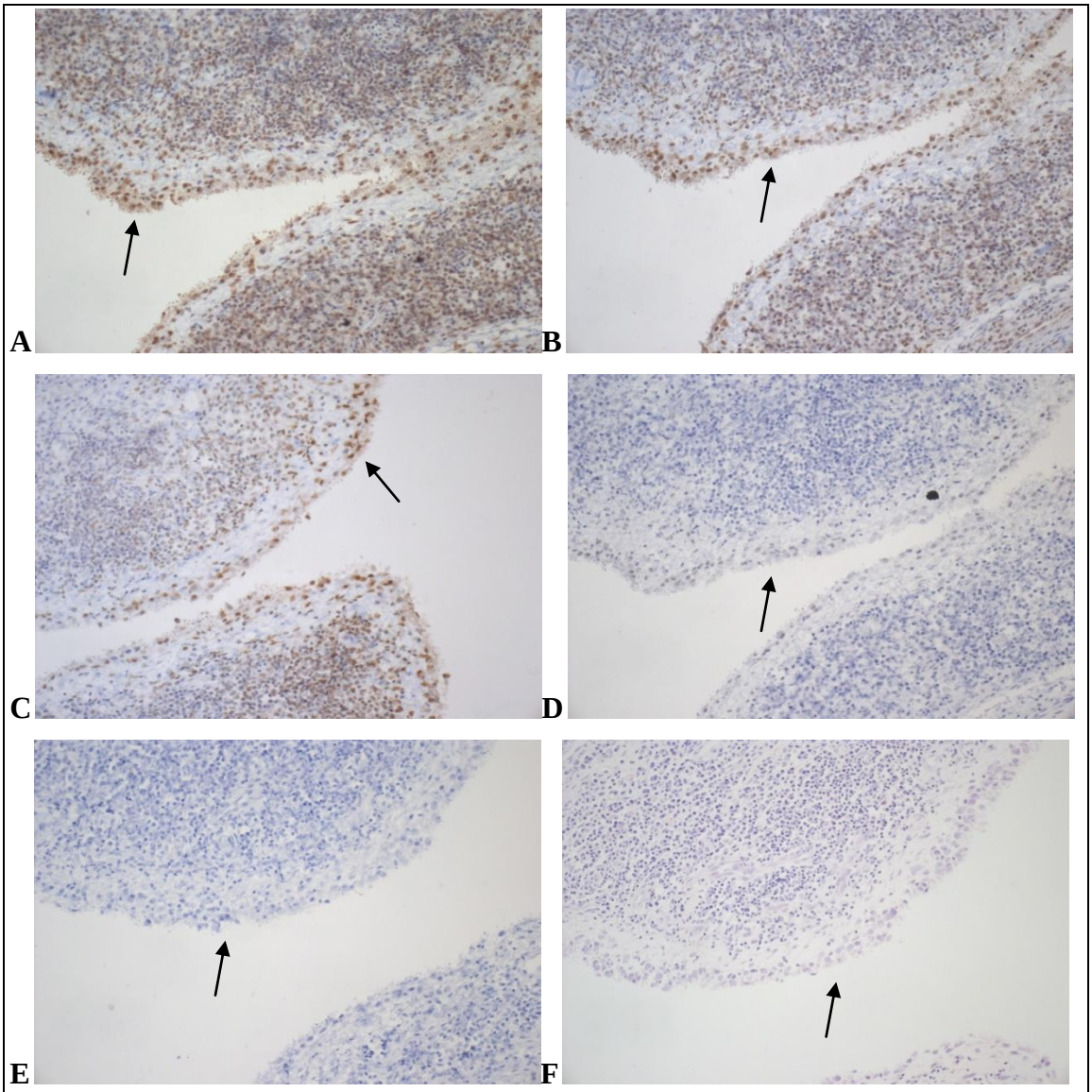

Figure 4.16. Optimisation of WISP-3 antibody in femoral head sections. Tissue sections were subjected to immunohistochemistry with varying WISP-3 antibody concentrations (**A**) 1:100 (**B**) 1:250 (**C**) 1:500 (**D**) 1:1000. (**E**) Non-specific rabbit immunoglobulin fraction negative control (1:250). (**F**) Haemotoxylin and Eosin stain. (→= synovial epithelium, all magnifications are 20X).

WISP-3 staining in this optimisation experiment was noted both in synovial epithelial and stromal cells and again appeared non-specific. Given the problems encountered using the WISP-2 antibody and the lack of successful *in vitro* experiments during investigation of both WISP-2 and WISP-3, the decision was taken not to perform any further immunohistochemistry with these antibodies.

Chapter 5: Results - Plakophilin-3.

Introduction

As previously discussed PKP-3 is a member of the p120ctn family of armadillo-related proteins whose expression has previously been shown to be down-regulated in some epithelial malignancies. PKP-3 participates in the formation of desmosomes, which are important in the maintenance of the structural and functional integrity of epithelial tissues. Aigner and colleagues have previously demonstrated that ZEB1 is able to associate with the PKP-3 promoter in MDA-MB-231 cells and via transcriptional repression is able to down-regulate PKP-3 in a similar manner to its effect on E-cadherin[104]. Other investigators have shown PKP-3 knockdown in HCT116 cells to cause a decrease in cellular adhesion *in vitro*, and increased propensity for metastatic behaviour in an animal model, indicating that PKP-3 may be involved in EMT[256]. Apart from its role in adhesion and cellular integrity, PKP-3 may also perform as a cellular signal mediator, given reports of its nuclear localisation in some cell types[247, 282].

The only investigation of PKP-3 in colorectal tissues to date constituted an examination of 10 colorectal cancer specimens by immunohistochemistry, and revealed high ZEB1 expression at the tumour invasive front in association with a decrease in PKP-3[104]. This relatively preliminary finding led to the selection of PKP-3 as the next ZEB1-related protein worthy of further investigation here.

5.1 EXPRESSION OF PKP-3 IN A PANEL OF COLORECTAL AND BREAST CELL LINES

Western blot experiments examining PKP-3, ZEB1 and E-cadherin protein expression in a panel of breast and colon cell lines were performed, using lysates prepared from untreated cells cultured to approximately 70% confluency. Figure 5.1(A) and (B) illustrate a typical western blot result and graphical representation of protein levels as quantified by Odyssey imager software after normalising to β actin.

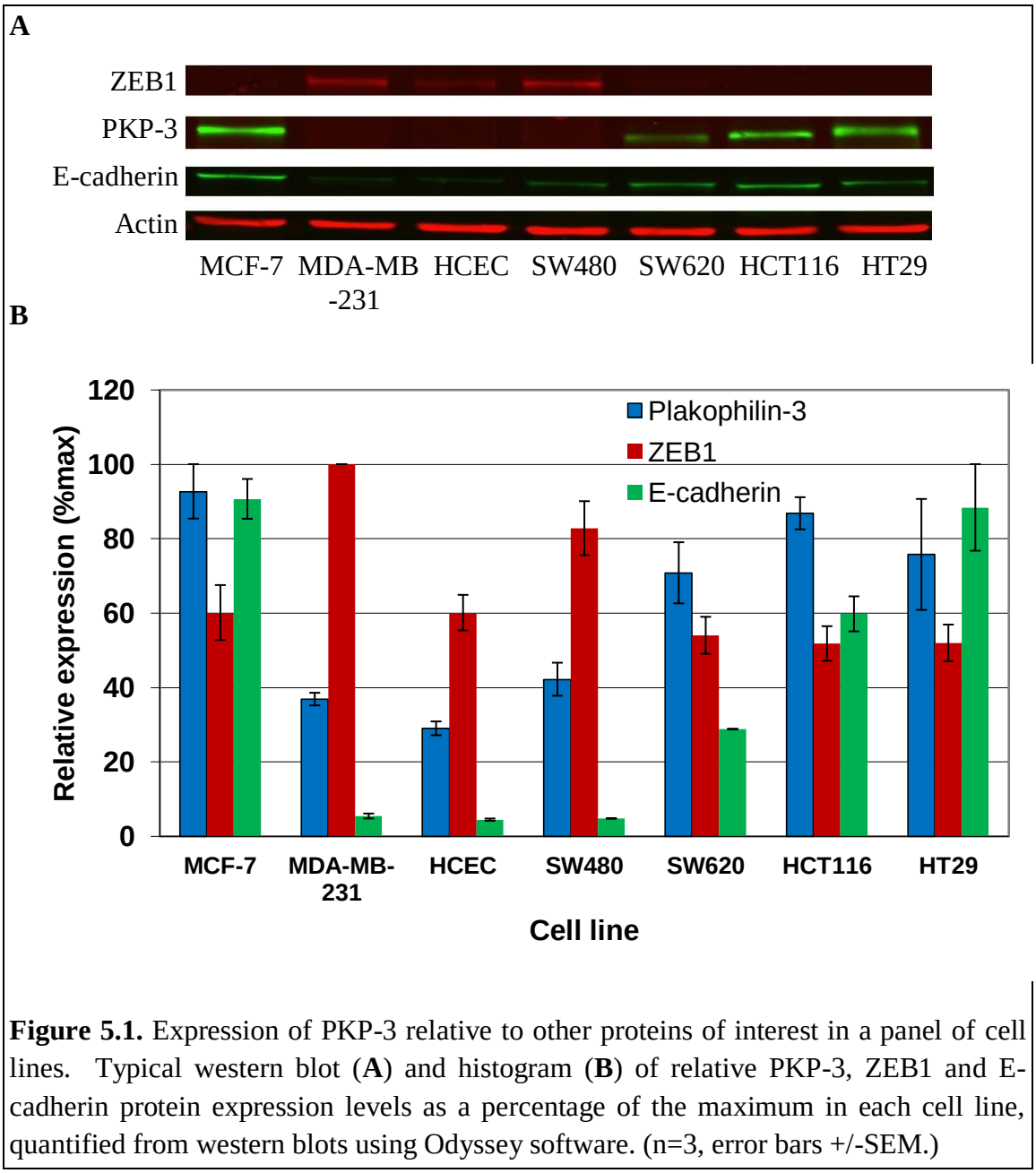

Figure 5.1. Expression of PKP-3 relative to other proteins of interest in a panel of cell lines. Typical western blot (**A**) and histogram (**B**) of relative PKP-3, ZEB1 and E-cadherin protein expression levels as a percentage of the maximum in each cell line, quantified from western blots using Odyssey software. (n=3, error bars +/-SEM.)

Investigation of the panel of cell lines indicated similarities between E-cadherin and PKP-3 expression, and a similar reciprocal relationship between PKP-3 and ZEB1 to that seen with E-cadherin. Cell lines with relatively high ZEB1 levels were those with mesenchymal characteristics (MDA-MB-231 and SW480) and these expressed low levels of E-cadherin and PKP-3, whereas those with epithelial morphology expressed lower levels of ZEB1 (MCF-7, HT29, HCT116) and demonstrated higher E-cadherin and PKP-3. These results are consistent with published findings[104, 247, 248].

5.2 KNOCKDOWN OF PKP-3 IN HCT116 CELLS

Following previous difficulties with siRNA-mediated knockdown of WISP proteins an optimisation experiment was carried out for knockdown of PKP-3. HCT116 cells were again selected due to their high level of expression of PKP-3 and the previous success of chemical transfection of plasmid DNA in this cell line. Cells were seeded in 6-well plates and transfected using Lipofectamine 2000, with varying concentrations of siRNA, and cultured up to 24 or 48 hour time points as described in methods. Whole cell lysates were prepared and expression of PKP-3 and ZEB1 assessed by western blotting, with actin as the loading control. Western blots from this experiment are shown in figure 5.2.

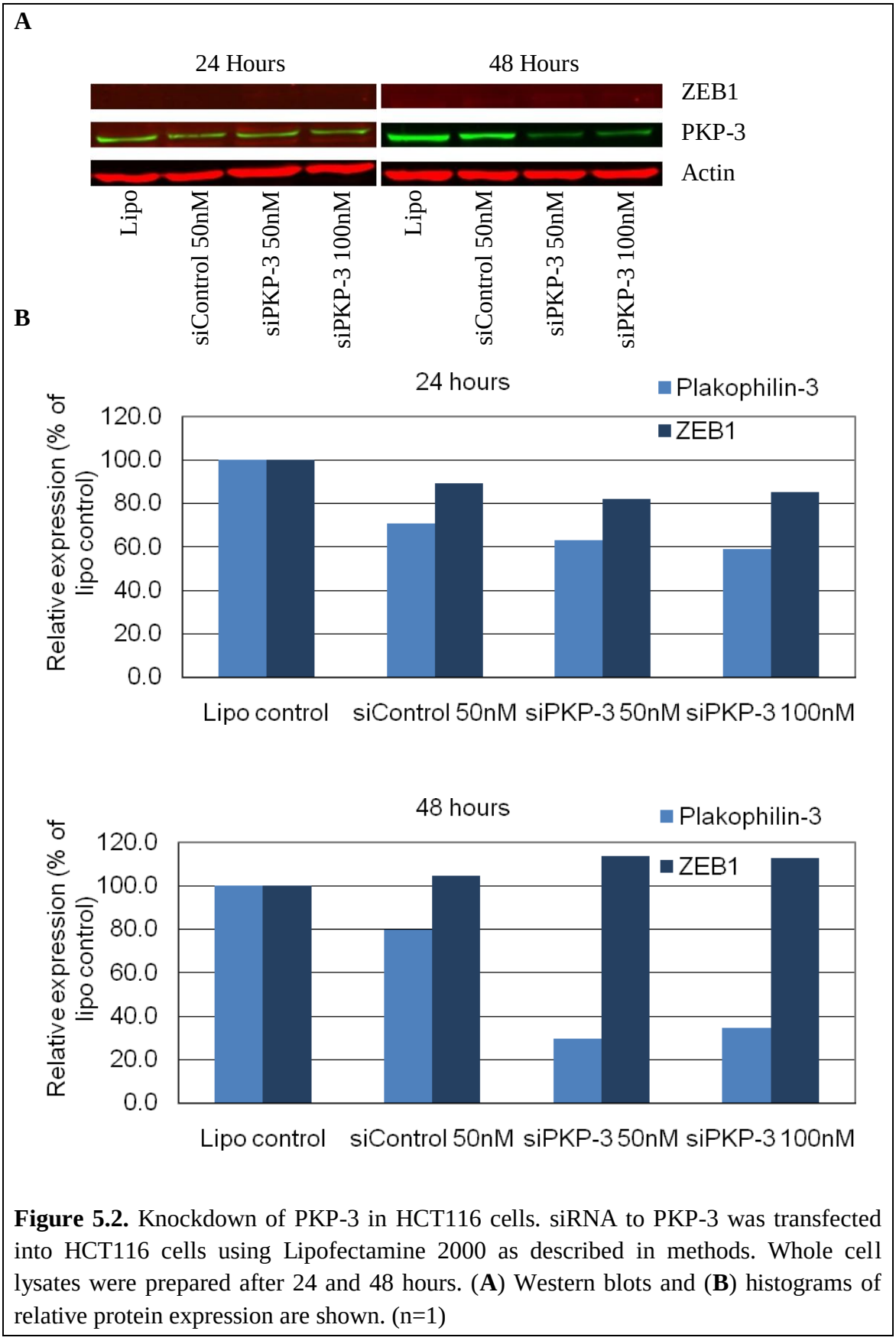

Figure 5.2. Knockdown of PKP-3 in HCT116 cells. siRNA to PKP-3 was transfected into HCT116 cells using Lipofectamine 2000 as described in methods. Whole cell lysates were prepared after 24 and 48 hours. (**A**) Western blots and (**B**) histograms of relative protein expression are shown. (n=1)

From this optimisation experiment the most effective knockdown of PKP-3 was achieved at 48hours after transfection of siRNA at 50nM concentration. Four further experiments were performed using these conditions. Whole cell lysates were prepared after 48 hours and expression of PKP-3, ZEB1 and E-cadherin assessed by western blotting as described in methods (figure 5.3).

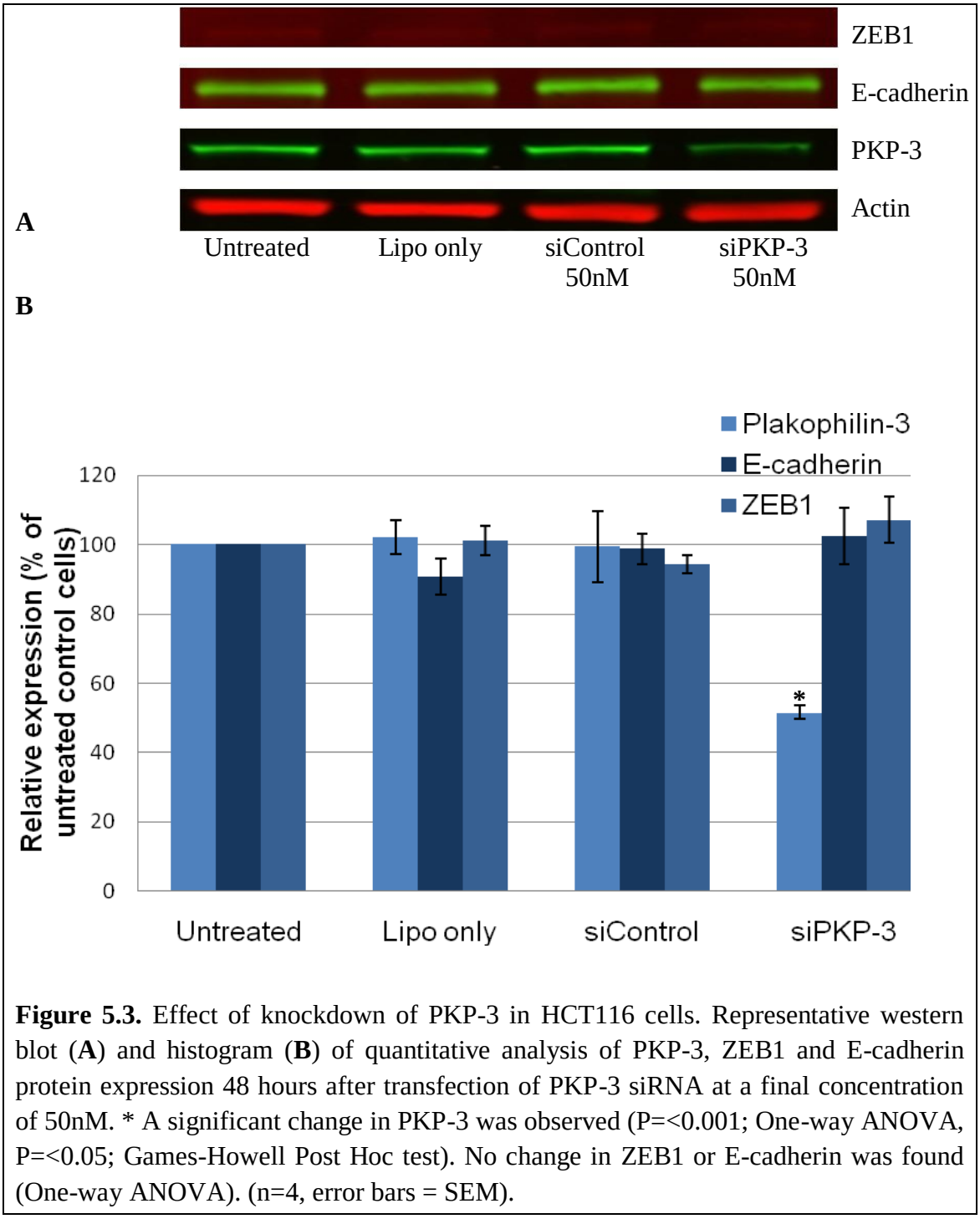

Figure 5.3. Effect of knockdown of PKP-3 in HCT116 cells. Representative western blot (**A**) and histogram (**B**) of quantitative analysis of PKP-3, ZEB1 and E-cadherin protein expression 48 hours after transfection of PKP-3 siRNA at a final concentration of 50nM. * A significant change in PKP-3 was observed (P=<0.001; One-way ANOVA, P=<0.05; Games-Howell Post Hoc test). No change in ZEB1 or E-cadherin was found (One-way ANOVA). (n=4, error bars = SEM).

Fifty percent knockdown of PKP-3 was achieved, but had little effect on ZEB1 or E-cadherin expression levels in HCT116 cells. However, on bright-field microscopic examination, an increase in the number of cells present in each plate was observed prior to lysis and protein extraction. Of particular note no change in the phenotype of the cells could be seen. Consistent with these observations Kundu and colleagues noted that HCT116 PKP-3 knockout clones grew to high density in culture and in soft agar assays in comparison to controls[256].

5.3 EFFECT OF ZEB1 KNOCKDOWN ON PKP-3 EXPRESSION

Examination of the invasive, breast carcinoma-derived cell line MDA-MB-231 has indicated that knockdown of ZEB1 causes strong up-regulation of PKP-3, as well as E-cadherin expression[104]. This relationship has not been examined in colorectal cell lines. The de-differentiated and invasive SW480 cell line was selected for its strong similarities to the MDA-MB-231 cell line. Both are aggressive, invasive cell lines with mesenchymal characteristics and fibroblastic morphology. The earlier investigations here had already shown these cells to have high expression of ZEB1, low PKP-3 and E-cadherin levels. SW480 cells were therefore transfected with the pshZEB1 construct (kind gift of Dr S Spaderna, Germany) or the vector with a non-coding shRNA sequence (pshControl). An experiment was also performed using MDA-MB-231 cells to confirm reproducibility of the published results and the expected function of the construct. Cells were cultured for 72 hours after transfection (as described by Aigner and colleagues[104]) and whole cell lysates prepared. Representative western blots and quantitative analyses using Odyssey imager software are shown in figure 5.4.

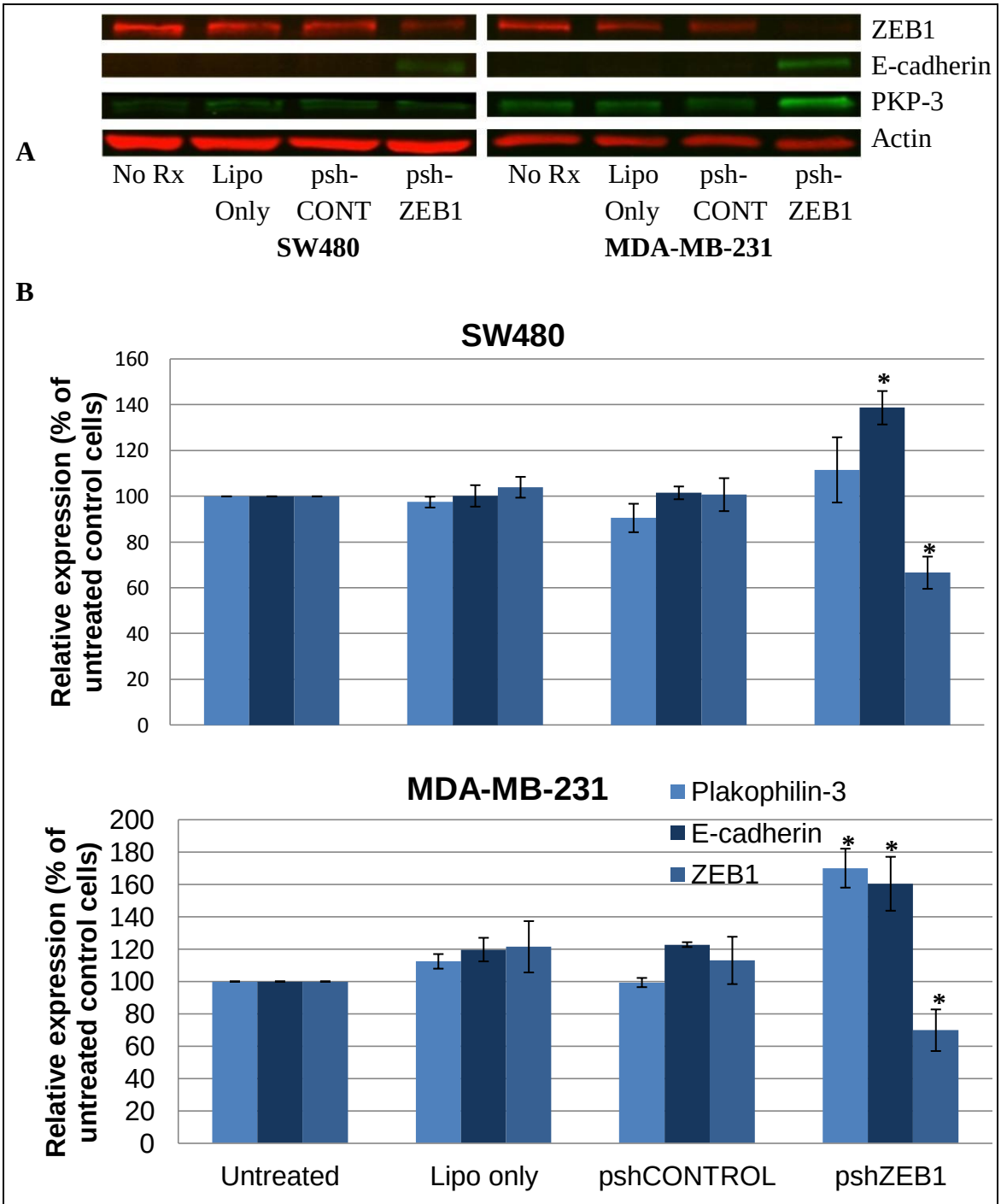

Figure 5.4. Effect of ZEB1 knockdown on PKP-3 expression in SW480 and MDA-MB-231 cells. Representative western blots (**A**) and histograms of quantitative analyses (**B**) are shown for SW480 and MDA-MB-231 cell lines after 72 hours knockdown of ZEB1 with pshZEB1 construct. In both cell lines significant changes in ZEB1 and E-cadherin expression were observed (P=<0.001 for both; One-way ANOVA, P<0.05 Games-Howell Post Hoc test). PKP-3 expression increased in both cell lines, but this was only significant in the MDA-MB-231 cells (SW480 P=0.334, MDA-MB-231 P=<0.01 ;One-way ANOVA, P=<0.001 Tukey Post Hoc test). (SW480 cells n=5, MDA-MB-231 cells n=4, error bars=SEM).

Thirty percent knockdown of ZEB1 was achieved in both cell lines. ZEB1 and E-cadherin expression was noted to increase with ZEB1 knockdown in the MDA-MB-231 cell line and, to a lesser extent, in the SW480 cells. This was consistent with previously published findings for the MDA-MB-231 cells, and suggested a similar relationship operating in the SW480 colorectal cells[104]. The reasons behind the less marked increase in PKP-3 in these cells upon ZEB1 knockdown are unclear. This may be explained by a decrease in transfection efficiency in this cell line compared to MDA-MB-231, and therefore a decrease in the population with PKP-3 up-regulation. The transient knockdown used to decrease ZEB1 levels here and relatively short time-point at cell lysis may also be a factor, leading to inability of the cells to undergo initiation of PKP-3 production and or stabilisation. Other cell-line specific factors may also be implicated which remain as yet undetermined. Further examination of this system is performed later in this chapter.

5.4 EFFECT OF E-CADHERIN EXPRESSION ON PKP-3

The repressive effect of ZEB1 expression on E-cadherin has been well documented. As well as its effect on cellular adherens junction formation and epithelial differentiation, E-cadherin has been shown to influence several cellular signalling pathways, such as the Wnt and receptor tyrosine kinase pathways (for a review see [283]). Knockdown of ZEB1 has been shown to lead to up-regulation of E-cadherin expression in several cell lines. To examine whether E-cadherin alone can effect PKP-3 expression, SW480 cells were transfected with the pE-cadherinGFP construct (kind gift from Dr E Tulchinsky). After 48 hours whole cell lysates were prepared and western blotting experiments performed (figure 5.5).

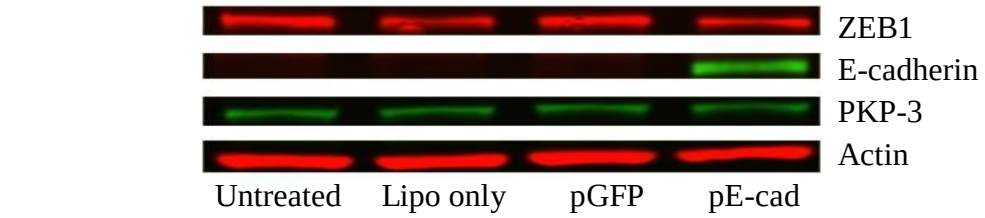

A

B

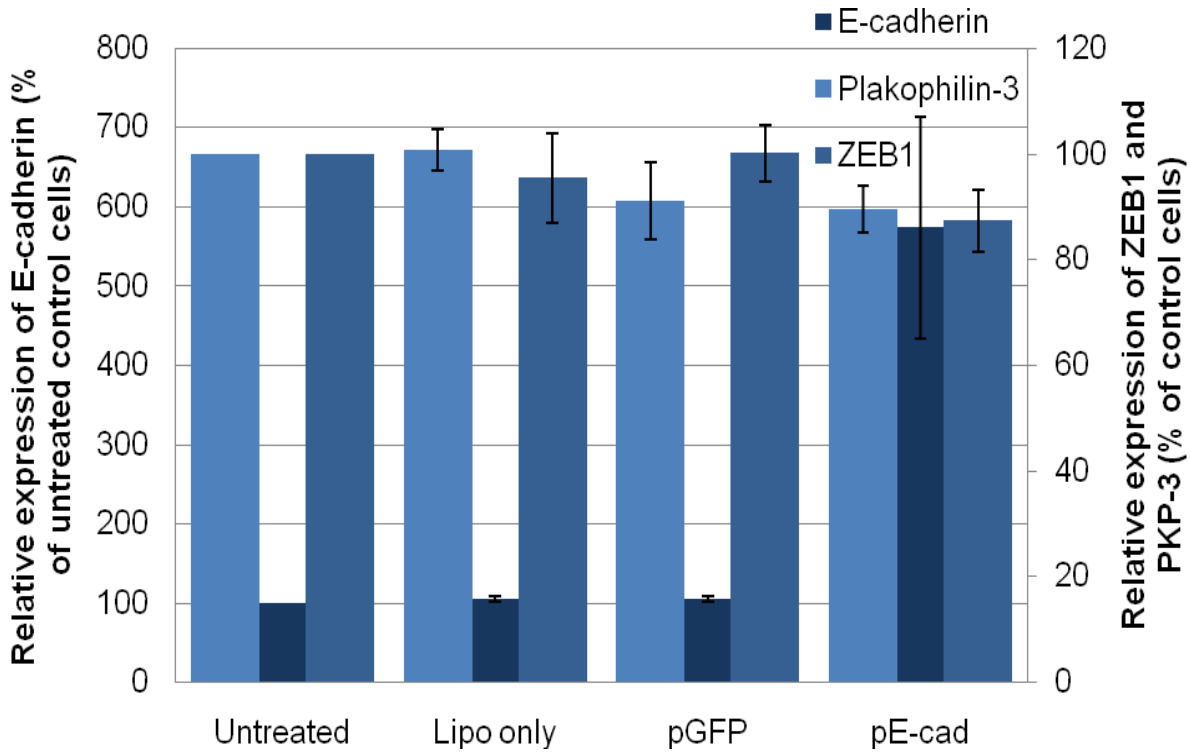

Figure 5.5. Effect of E-cadherin on PKP-3 expression in SW480 cells. Representative western blot (**A**) and quatitative analysis (**B**) after transfection of pE-cadherinGFP plasmid into SW480 cells. Cells were cultured for 48 hours and western blots performed on whole cell lysates. Note E-cadherin expression is displayed on the primary y axis, and PKP-3 and ZEB1 expression on the secondary y axis. A significant increase in E-cadherin expression was observed, with no significant change in ZEB1 or PKP-3 expression (P=0.001, 0.405 and 0.245 respectively; One-way ANOVA, P=0.002 Games-Howell Post Hoc test). (n=4, error bars=SEM)

A significant increase in E-cadherin expression was achieved, but no change in ZEB1 or PKP-3 was apparent. Therefore expression of E-cadherin alone does not appear to influence

either ZEB1 or PKP-3 protein levels. This is consistent with experimental evidence in the literature from the MDA-MB-231 cell line[104].

5.5 EFFECT OF ZEB1 EXPRESSION ON PKP-3

The preliminary investigation of PKP-3 expression in 10 colorectal cancer tissue specimens by Aigner and colleagues identified an inverse relationship between ZEB1 and PKP-3 expression at the invasive front[104]. Further *in vitro* investigation of this relationship using chromatin immunoprecipitation (ChIP) analysis in MDA-MB-231 breast cells confirmed that ZEB1 specifically binds the PKP-3 promoter and represses it. To examine if this relationship is in operation in CRC cell lines, HCT116 cells expressing relatively high levels of PKP-3 were transfected with the pZEB1 construct, cultured for 48 hours and whole cell lysates prepared. The effect on PKP-3 was then assessed by western blotting and quantitative Odyssey imager analysis (figure 5.5).

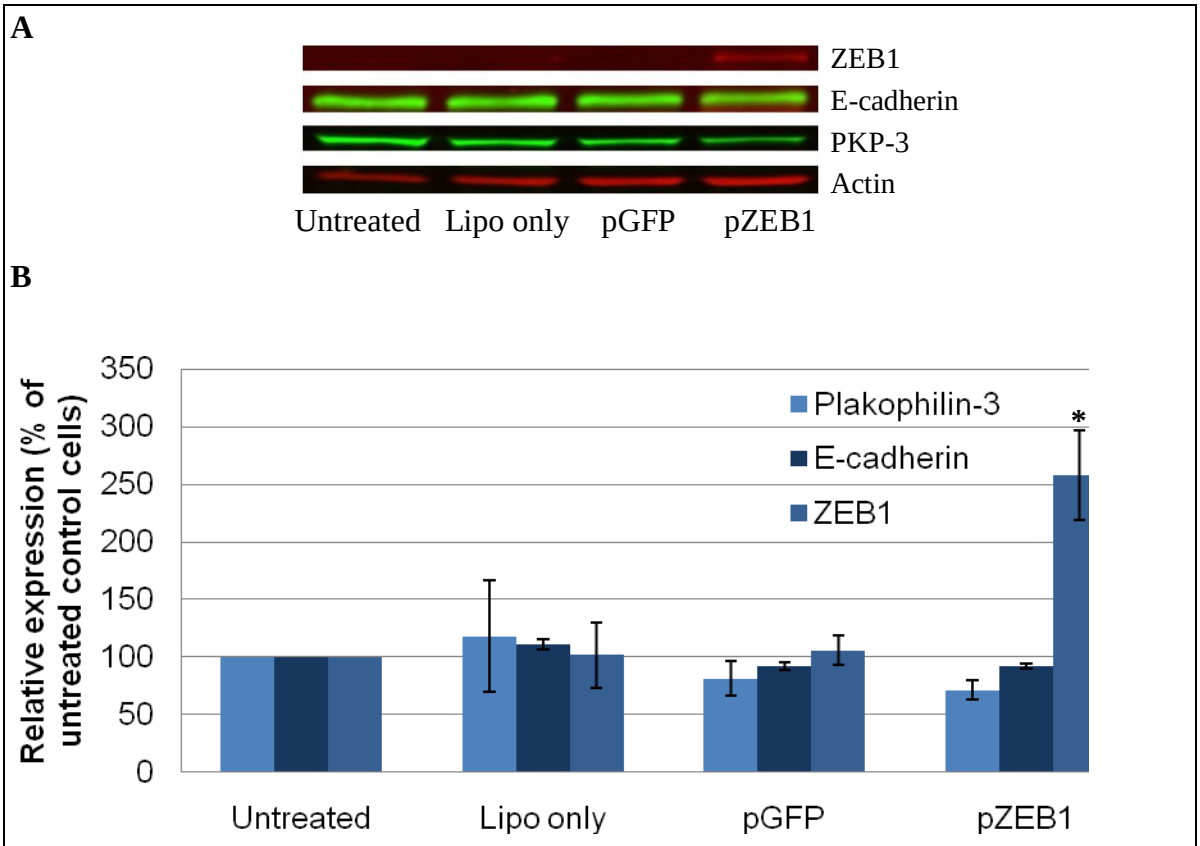

Figure 5.5. Effect of ZEB1 expression on PKP-3. Representative western blot (**A**) and histogram of quantitative analysis of PKP-3, ZEB1 and E-cadherin protein expression (**B**) in HCT116 cells 48 hours after transfection of pZEB1 construct. A significant increase in ZEB1 expression was observed (P=<0.001; One-way ANOVA and Tukey Post Hoc test). A decrease in E-cadherin and PKP-3 expression was also observed, but this was not statistically significant (P=0.102 and 0.378 respectively; One-way ANOVA). (n=3, error bars = SEM).

Over-expression of ZEB1 was successfully achieved, and a subsequent 40% decrease in PKP-3 expression was observed in comparison to control cells treated with Lipofectamine. It was noted that significant variability was present in the control population which may account for the lack of statistical significance.

5.6 ANALYSIS OF PROTEIN EXPRESSION AT THE CELLULAR LEVEL

Use of whole cell lysates and western blotting to examine protein expression changes after ZEB1 knockdown gave an indication of the changes within the whole cellular population. However, the 30-35% decrease in ZEB1 expression indicated that either the majority of cells were not being successfully transfected, or that complete silencing of the protein was not achieved by the shRNA construct. The differences in protein expression demonstrated by western blotting after knockdown of ZEB1 in MDA-MB-231 and SW480 cells merited further examination at the individual cell level. Immunocytochemistry was therefore performed as described in chapter 2 after transfection of the pshZEB1 construct. PKP-3, ZEB1 and E-cadherin expression were examined and representative images from 3 experiments are shown in figures 5.6 and 5.7.

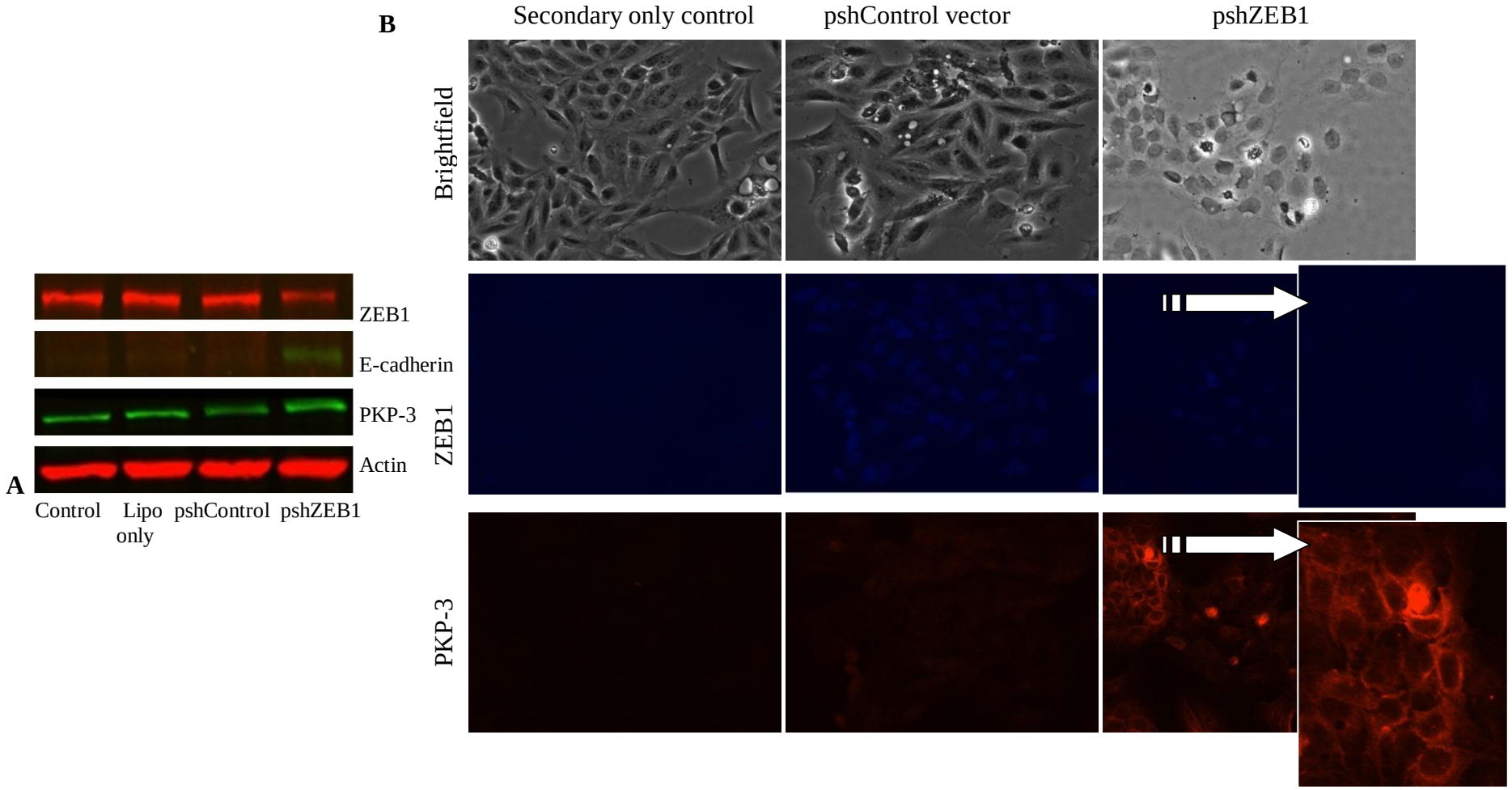

Figure 5.6. Effect of ZEB1 knockdown on PKP-3 expression in SW480 cells. Western blot confirming ZEB1 knockdown (**A**) and Immunocytochemistry brightfield, ZEB1 (blue) and PKP-3 (red) images (**B**) are shown. Cells (~50% confluent) were grown on cover slips in 6-well plates and transfected with pshControl or pshZEB1 constructs. After 72 hours cells were fixed with 4% paraformaldehyde, permeabilised with 0.1% Triton X-100 and stained with ZEB1 polyclonal rabbit (1:100) or PKP-3 monoclonal mouse (1:200) antibodies. Secondary antibodies to rabbit (AMCA 1:100) and mouse (Cy3 1:250) were applied and cover slips fixed onto slides with Prolong reagent. A control experiment was also performed in which the primary antibody was omitted. (Representative images from 3 experiments are shown).

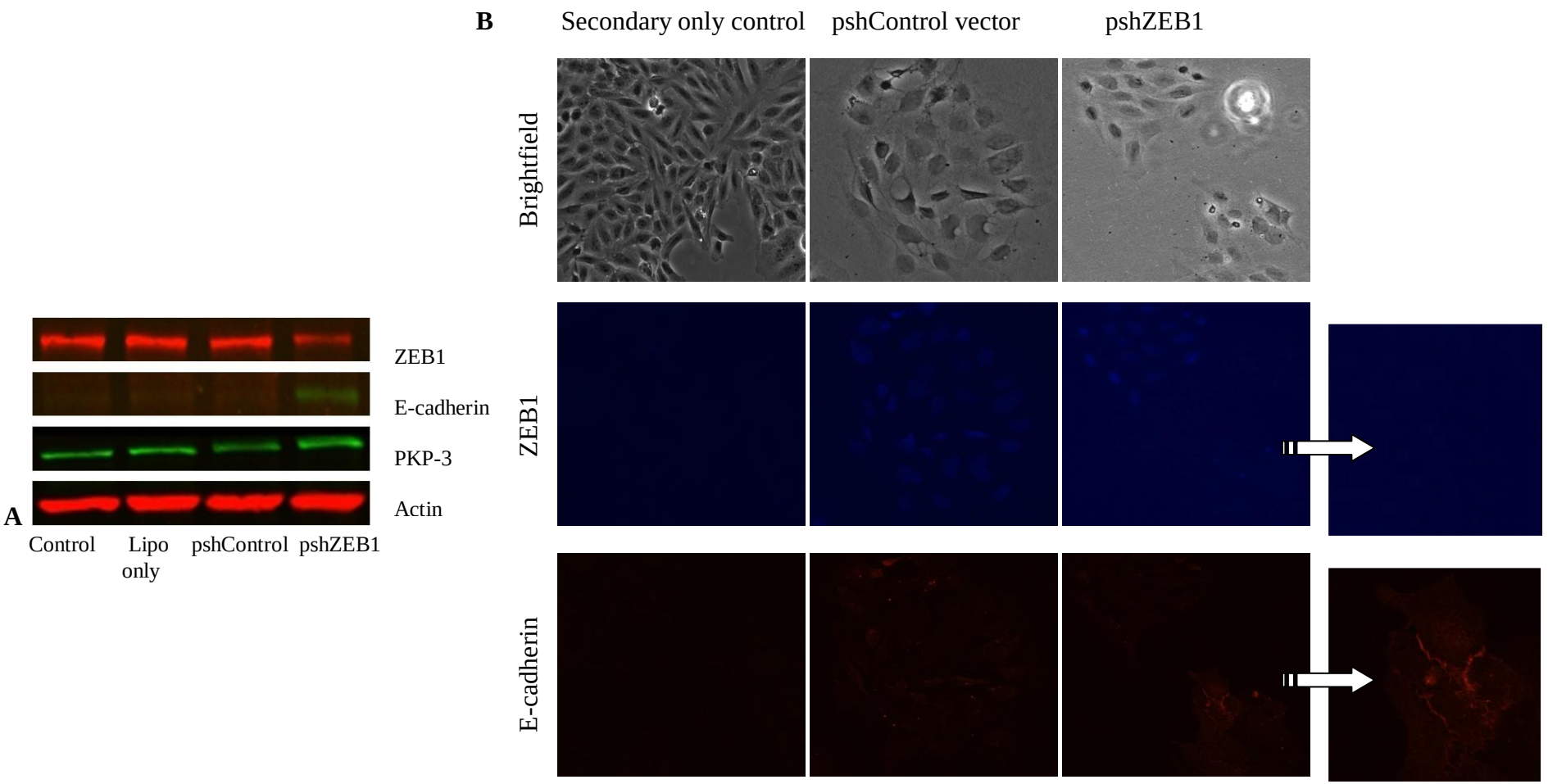

Figure 5.7. Effect of ZEB1 knockdown on E-cadherin expression in SW480 cells. (**A**) Western blot confirming ZEB1 knockdown and Immunocytochemistry brightfield, ZEB1 (blue) and E-cadherin (red) images (**B**) are shown. Cells (~50% confluent) were grown on cover slips in 6-well plates and transfected with pshControl or pshZEB1 constructs. After 72 hours cells were fixed with 4% paraformaldehyde, permeabilised with 0.1% Triton X-100 and stained with ZEB1 (1:100) or E-cadherin (1:200) antibodies. Secondary antibodies to rabbit (AMCA 1:100) and mouse (Cy3 1:250) were applied and cover slips fixed onto slides with Prolong reagent. A control experiment was also performed in which the primary antibody was omitted. (Representative images from 3 experiments are shown).

Immunofluorescence microscopy after transfection of the pshZEB1 construct confirmed knockdown of ZEB1 in approximately 30% of the cell population. PKP-3 expression was up-regulated in these cells and localised to the cell cytoplasm and membrane. In contrast, cells transfected with the control vector showed unchanged nuclear ZEB1 expression compared to non-transfected controls, and weak cytoplasmic and little membranous PKP-3 expression. Examination of E-cadherin expression demonstrated similar results. Successful ZEB1 knockdown was only seen in approximately 30% of the cell population. As discussed previously this may partially account for the lack of significant up-regulation of PKP-3 expression when examined on western blots from the whole cell lysates.

5.7 PKP-3 EXPRESSION *IN VIVO*

The formalin-fixed tissues from 101 colorectal cancer specimens, with their matched lymph node and liver metastases were investigated for PKP-3 expression using immunohistochemistry as described in chapter 2.

5.7.1 Selection of positive control tissue

In order to find the optimal antibody concentration for use with the Envision detection system, and subsequently to confirm consistent results between runs, the literature was consulted for normal tissue known to express PKP-3 to act as a positive control. Normal skin has been shown to express PKP-3 throughout the epidermal layer, though it is not expressed in the stratum corneum or dermis itself. In addition PKP-3 has been shown to be expressed in the hair follicle root sheaths[255]. Anonymised normal skin sections were obtained from the Department of Pathology, Leicester Royal Infirmary and used to optimise PKP-3 antibody conditions with the Envision detection system (figure 5.8).

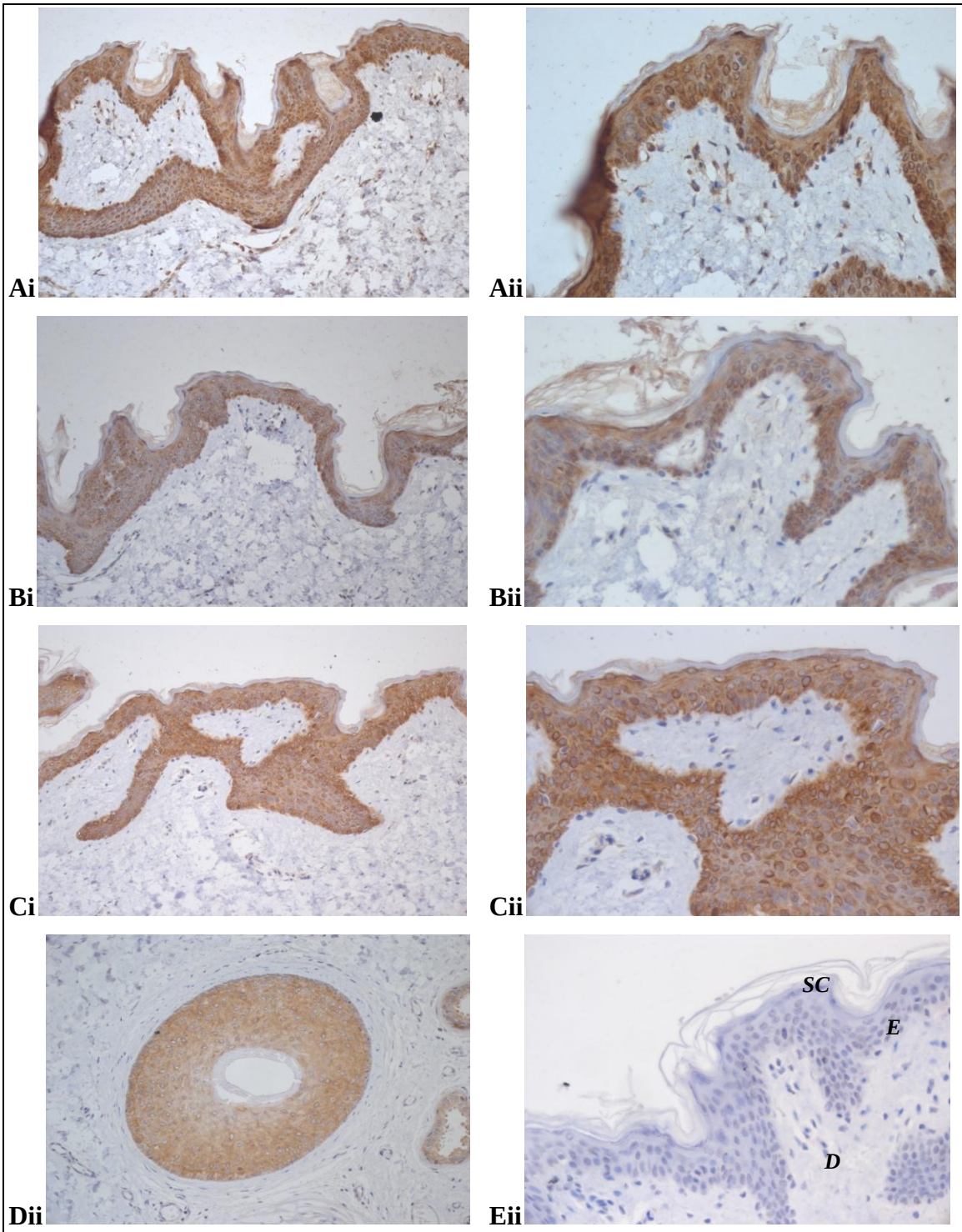

Figure 5.8. Optimisation of PKP-3 antibody in normal skin. Sections were stained according to the immunohistochemistry protocol described in methods, with varying PKP-3 antibody concentrations (**A**) 1:500 (**B**) 1:1000 (**C**) 1:3000 (**D**) Hair follicle root sheath (**E**) Non-specific mouse immunoglobulin fraction negative control. (**SC**=stratum corneum, **E**=epidermis, **D**=dermis, **i**=20X magnification, **ii**=40X magnification.)

The optimisation of the antibody in skin sections demonstrated expression of PKP-3 at the epidermal layer and in the hair follicle roots as previously described in the literature, with a dultion of 1 in 3000 giving the least non-specific background staining[255].

5.7.2 PKP-3 in colorectal cancer

Colorectal cancer specimens along with matched normal colonic epithelium, lymph node and liver metastases where available were stained using the Envision immunohistochemistry detection system. Representative sections of these tissues and the staining patterns observed are shown in figure 5.9.

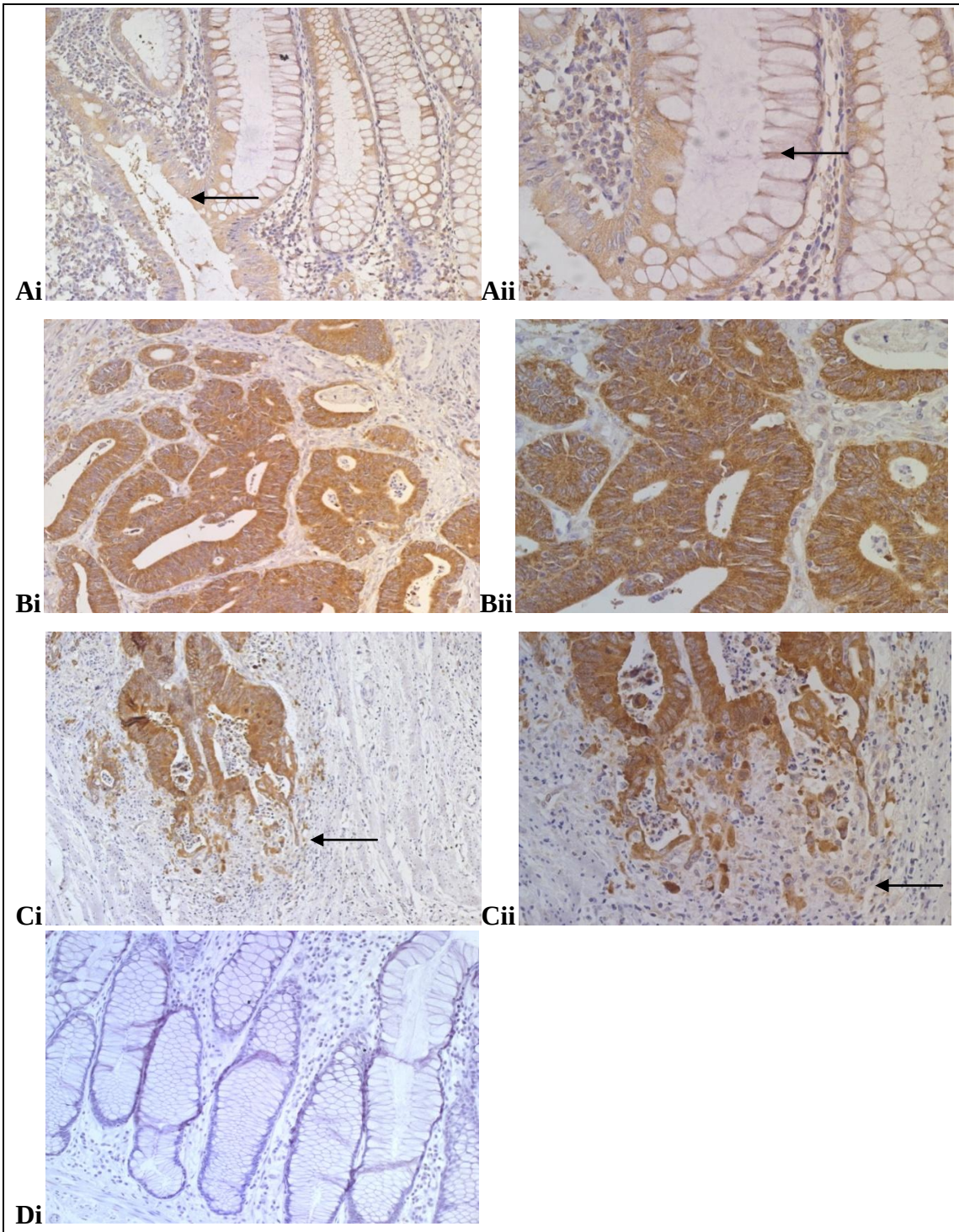

Figure 5.9. Immunohistochemical detection of PKP-3 in colonic specimens. Representative sections are shown of (**A**) normal colonic epithelium, cytoplasmic staining is indicated, (**B**) centre of primary colonic carcinoma and (**C**) invasive front of primary colonic tumour, loss of expression of PKP-3 is indicated. (**D**) Non-specific rabbit immunoglobulin fraction negative control. (**i**=20X magnification, **ii**=40X magnification.)

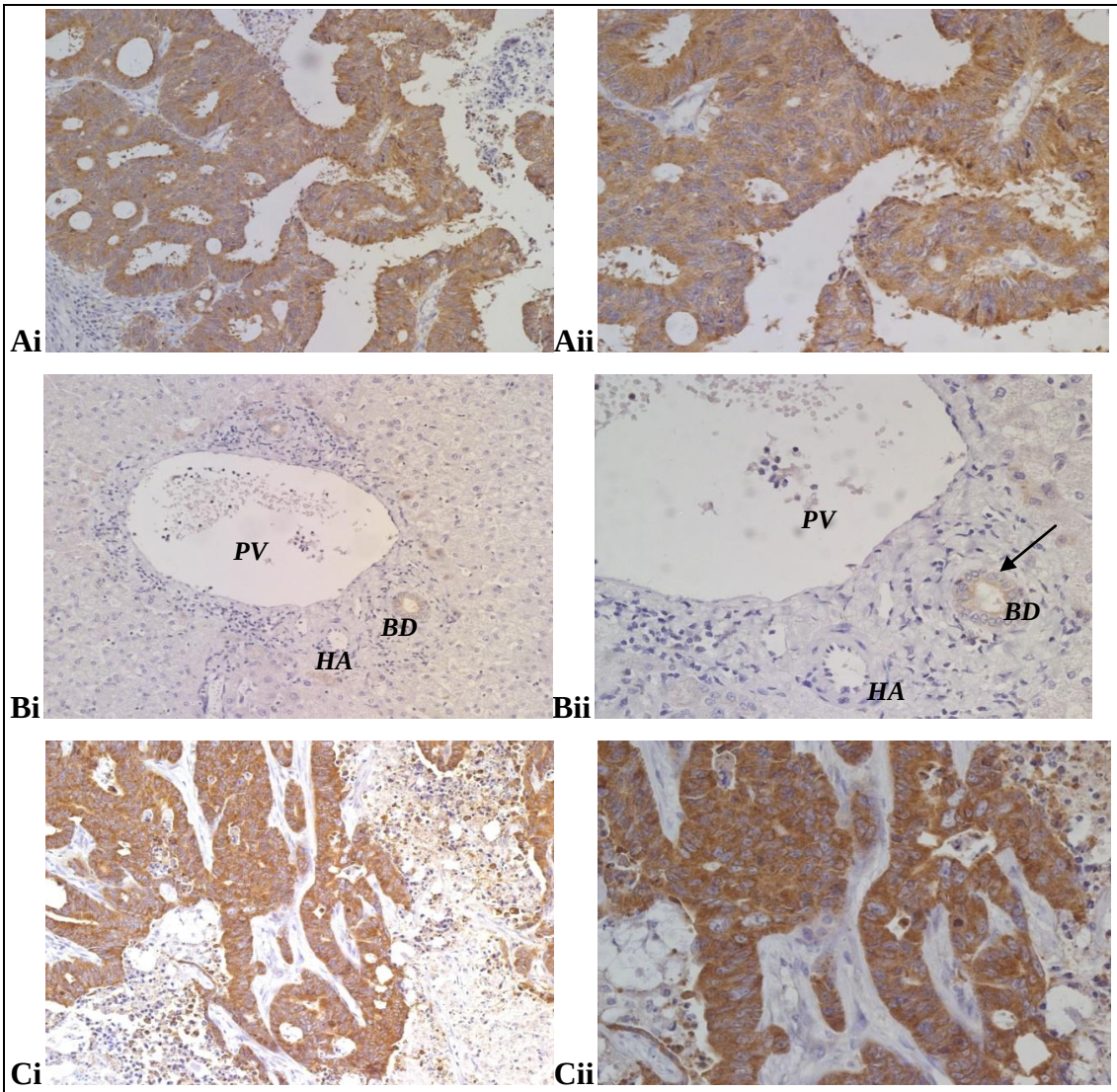

Figure 5.10. Immunohistochemical detection of PKP-3 in lymph node and liver specimens. Representative sections are shown of (**A**) lymph node metastasis, (**B**) normal liver portal triad and (**C**) liver metastasis. (→=PKP-3 stain; ***PV***=portal vein; ***HA***= hepatic artery; ***BD***= bile duct. **i**=20X magnification, **ii**=40X magnification.)

Weak to moderate cytoplasmic staining was observed in all normal colonic epithelia, and in the bile duct epithelium of portal tracts in the liver. These results were consistent with previous reports[259]. In the central area of colonic tumours PKP-3 was expressed at high levels in comparison to the normal epithelium. However, at the invasive front of several tumours (29/101) expression was observed to be patchy and in some cases lost completely. In metastatic areas, such as lymph nodes and liver tumours, PKP-3 expression was similar to that seen in the central primary tumour. Little PKP-3

expression was observed in hepatocytes, as previously described by Schwartz and colleagues[259].

Statistical analysis of PKP-3 expression related to ZEB1, WISP-1 and clinico-pathological data are reported in chapter 6.

Chapter 6: Results – The relationship between ZEB1, WISP-1, Plakophilin-3 and clinicopathological data.

Introduction

Few studies exist examining the expression of ZEB1, WISP1, WISP2, WISP3 and PKP-3 in CRC tissues, and only one of these groups examined a significant cohort of samples at the protein level[114, 115] (table 1.3). In particular none of these published series have directly examined the relationship between expression of these markers and survival in CRC.

Several investigators have found associations between ZEB1 expression and tumour characteristics, such as stage and differentiation, in several different tumour types[85, 104, 111, 114, 265], although others have found no such associations (table 1.3)[93, 123]. The only two studies examining ZEB1 expression in relation to survival have been in bladder and breast cancer. Sayan and colleagues found no correlation with survival in their series, and Hugo and colleagues found **decreased** ZEB1 gene expression to correlate with decreased overall and disease-free survival in breast tumours (the opposite finding to that which would be expected if expression of ZEB1 leads to an increased propensity to dys-adhesion, invasion and metastases)[93, 105].

Three studies examining WISP-1 expression in CRC tumour tissues have found significant correlations between WISP-1 expression and pathological factors, however none of these examined survival associations (table 1.5)[188, 191, 192]. Correlation of WISP-1 expression and pathological variables have also been found in other tumour tissues such as breast and cholangiocarcinoma and in addition with survival[193, 194,

197, 198]. However other groups failed to confirm association with pathological factors and survival in gastric, ovarian and non-small cell lung cancer[187, 196, 203].

There have been two studies on the expression of WISP-2 in CRC, but only Davies and colleagues examined protein expression by IHC[184, 191]. They found significant correlations between low WISP-2 expression and increased tumour stage, poorly differentiated and node positive tumours[191]. However, in 120 breast tumours the same group found high WISP-2 mRNA expression correlated with lymph node metastases, poor Nottingham Prognostic Index, high grade tumours and the development of metastases, although there was no association with survival[193]. In gastric, prostate, ovarian and salivary gland tumours WISP-2 expression has been shown to be decreased in tumours compared to normal control tissues, but no correlation with clinicopathological factors has been found[196, 203, 212, 223, 241]. This may be due to the low numbers of tumours examined, or the different methods used to evaluate expression (table 1.7).

WISP-3 has rarely been examined in tumour tissues and data are conflicting as to its role (table 1.9). Davies and colleagues found no significant variation in expression compared to control tissues in CRC, and similarly in breast tumours found no correlation with clinicopathological factors[191, 193]. In other tumours investigators have noted similar findings, showing variable WISP-3 expression in different tumour types and no association with tumour characteristics[196, 203, 241]. However, Huang and colleagues did find correlation between low WISP-3 expression in tumours and lymph node metastases[94].

Minimal data exist on PKP-3 expression in tumour tissues (table 1.10). High grade oral SCCs expressed low levels of PKP-3 which were inversely correlated with tumour

grade and survival[258, 259]. Conversely in NSCLC high PKP-3 expression was associated with increased lymph node metastases and decreased survival[260]. No studies exist correlating clinicopathological factors and PKP-3 expression in CRC.

Conflicting data for the various proteins under examination in this project suggest further analysis of their expression *in vivo* and in relation to clinicopathological variables is desirable. The importance of ZEB1, WISP1, and PKP-3 expression in CRC *in vivo* was assessed in 101 tumour specimens along with any available matched normal colonic tissue, lymph node and liver metastases specimens. Information on patient demographics was extracted from case notes in a retrospective manner and tumour characteristics such as stage, differentiation and type were examined by a single pathologist. As discussed previously WISP-2 and WISP-3 expression was not assessed because of apparent lack of specificity of the relevant antibodies.

6.1 PATIENT AND TUMOUR CHARACTERISTICS

Table 6.1 shows the demographics and tumour characteristics of the patients included in the IHC analysis. After processing 101 tumour samples were available for scoring of all three protein markers, with 31 matched lymph node and 5 liver metastases specimens. The patients comprised 56 males and 45 females, with a mean age of 70 (range 35-88) years. The proportion of tumours according to anatomical site included 23 rectal, 8 recto-sigmoid, 38 left, 3 transverse and 28 right colonic malignancies. Histologically 12, 58 and 26 tumours were well, moderately and poorly differentiated respectively. Five tumours were ungraded mucinous differentiation. Synchronous liver metastases were present in 15 patients, the others comprising 16 Duke's A, 42 Duke's B, 28 Duke's C1 and 15 Duke's C2 tumours. Vascular invasion was present in 17 tumours and lymph node metastases in 43. Median follow up for all patients was 96 (range 2-138) months. Median overall survival was 77 (range 2-138) months.

Table 6.1. Demographics and tumour related variables of patients included in study.

Variable		N	%
Total patients		101	100
Gender	Male	56	56
	Female	45	45
Age (years)	Mean	70	
	Median [Range]	71 [35-88]	
Type of operation	Elective	83	82
	Emergency	18	18
Site of Tumour	Low rectum	2	2
	Mid rectum	21	21
	Recto-sigmoid	8	8
	Left colon	38	38
	Transverse colon	3	3
	Right colon	28	28
Primary tumour size (mm)	Mean	47	
	Median [Range]	45 [15-110]	
Differentiation	Well	12	12
	Moderate	58	57
	Poor	26	26
	Mucinous	5	5
Duke's stage of primary	A	16	15
	B	42	42
	C1	28	28
	C2	15	15
Liver metastases at presentation (Duke's D)		15	15
T stage	T1	6	6
	T2	15	15
	T3	53	52
	T4	27	27
Vascular invasion	Yes	17	17
	No	68	67
	Not stated	16	16
Lymph node stage	N0	58	57
	N1	22	22
	N2	21	21
Lymph nodes collected	Mean	12	
	Median [Range]	11 [1-33]	
Lymph nodes positive	Mean	2	
	Median [Range]	0 [0-19]	
Follow up (months)	Mean	77.6	
	Median [Range]	75 [2-138]	
Disease free survival (months)	Mean	62.3	
	Median [Range]	69 [0-138]	
Overall survival (months)	Mean	68.2	
	Median [Range]	77 [2-138]	

6.2 IMMUNOHISTOCHEMISTRY SCORING CORRELATIONS

As described in chapter 2, each protein was scored independently by two researchers blinded to the patient's clinical parameters and tumour characteristics as assessed by the

independent pathologist. In order to assess agreement between the two observers' scores the intra-class correlation coefficient was calculated for each protein examined (table 6.2).

Table 6.2. Intraclass correlation coefficient agreement between immunohistochemistry scores.

Protein	Intraclass correlation coefficient	95% confidence interval	P
ZEB1	0.996	0.995-0.997	<0.001
Plakophilin-3	0.996	0.995-0.997	<0.001
WISP-1	0.996	0.995-0.997	<0.001

Intraclass correlation coefficient, one-way random model was used to compare scores between the two observers

There was a high level of agreement between observers in all the proteins examined. In cases of disagreement the average scores between the two observers were used for analysis.

6.3 EXPRESSION PATTERNS AND RELATIONSHIP BETWEEN ZEB1, WISP-1 AND PKP-3

6.3.1 ZEB1, WISP-1 and PKP-3 expression patterns

The expression patterns were described in detail in the relevant sections of Chapters 3, 4 and 5.

6.3.2 Statistical relationship between ZEB1, WISP-1 and PKP-3 at the invasive front

Univariable analysis of the relationship between ZEB1, WISP-1 and PKP-3 expression was performed using chi square test. For ZEB1 and WISP-1, both proteins previously demonstrated to be over-expressed in malignant cells, tumours were divided into high expressors (H score ≥ 200) and low/moderate expressors (H score ≤199). PKP-3 is thought

to have a tumour-suppressor role and appears to be lost in malignant transformation. Therefore the tumours were divided into a low expression group (H score ≤75) and moderate / high expression group (H score ≥76). All markers were analysed in both the central tumour and at the invasive front. In addition ZEB1, WISP-1 and PKP-3 were divided into a further two groups according to whether expression was lost or gained at the invasive front compared with the central tumour.

Table 6.3. Univariable analysis of correlations between ZEB1, WISP-1 and PKP-3 scores in varying tumour locations.

Markers examined	P value	Markers examined	P value
ZEB1 CT vs ZEB1 IF	**<0.001**	WISP-1 CYTO CT vs WISP-1 NUC CT	**0.002**
ZEB1 CT vs WISP-1 CYTO CT	0.909	WISP-1 CYTO CT vs WISP-1 NUC IF	**<0.001**
ZEB1 CT vs WISP-1 CYTO IF	0.816	WISP-1 CYTO CT vs PKP-3 CT	**<0.001**
ZEB1 CT vs WISP-1 NUC CT	0.869	WISP-1 CYTO CT vs PKP-3 IF	0.955
ZEB1 CT vs WISP-1 NUC IF	0.574	WISP-1 CYTO IF vs WISP-1 NUC CT	**0.024**
ZEB1 CT vs PKP-3 CT	**<0.001**	WISP-1 CYTO IF vs WISP-1 NUC IF	**0.019**
ZEB1 CT vs PKP-3 IF	0.151	WISP-1 CYTO IF vs PKP-3 CT	0.311
ZEB1 IF vs WISP-1 CYTO CT	**0.019**	WISP-1 CYTO IF vs PKP-3 IF	**0.002**
ZEB1 IF vs WISP-1 CYTO IF	0.718	WISP-1 NUC CT vs WISP-1 NUC IF	**0.028**
ZEB1 IF vs WISP-1 NUC CT	0.426	WISP-1 NUC CT vs PKP-3 CT	0.615
ZEB1 IF vs WISP-1 NUC IF	**0.007**	WISP-1 NUC CT vs PKP-3 IF	0.924
ZEB1 IF vs PKP-3 CT	**0.001**	WISP-1 NUC IF vs PKP-3 CT	**0.035**
ZEB1 IF vs PKP-3 IF	**0.061**	WISP-1 NUC IF vs PKP-3 IF	0.979
ZEB1 UP AT IF vs ZEB1 CT	**0.033**	WISP-1 CYTO UP AT IF vs WISP-1 NUC CT	**0.083**
ZEB1 UP AT IF vs ZEB1 IF	0.477	WISP-1 CYTO UP AT IF vs WISP-1 NUC IF	0.104
ZEB1 UP AT IF vs WISP-1 CYTO CT	0.398	WISP-1 CYTO UP AT IF vs WISP-1 NUC UP AT IF	**0.094**
ZEB1 UP AT IF vs WISP-1 CYTO IF	0.473	WISP-1 CYTO UP AT IF vs PKP-3 CT	**0.012**
ZEB1 UP AT IF vs WISP-1 CYTO UP AT IF	0.918	WISP-1 CYTO UP AT IF vs PKP-3 IF	0.581
ZEB1 UP AT IF vs WISP-1 NUC CT	0.358	WISP-1 CYTO UP AT IF vs PKP-3 DOWN AT IF	0.298
ZEB1 UP AT IF vs WISP-1 NUC IF	**0.094**	WISP-1 NUC UP AT IF vs WISP-1 NUC CT	0.130
ZEB1 UP AT IF vs WISP-1 NUC UP AT IF	0.760	WISP-1 NUC UP AT IF vs WISP-1 NUC IF	**0.094**
ZEB1 UP AT IF vs PKP-3 CT	**0.085**	WISP-1 NUC UP AT IF vs PKP-3 CT	0.344
ZEB1 UP AT IF vs PKP-3 IF	**0.063**	WISP-1 NUC UP AT IF vs PKP-3 IF	0.249
ZEB1 UP AT IF vs PKP-3 DOWN AT IF	0.246	WISP-1 NUC UP AT IF vs PKP-3 DOWN AT IF	0.480
WISP-1 CYTO UP AT IF vs WISP-1 CYTO CT	**0.021**	PKP-3 CT vs PKP-3 IF	**<0.001**
WISP-1 CYTO UP AT IF vs WISP-1 CYTO IF	0.511	PKP-3 DOWN AT IF vs PKP-3 CT	**0.001**
WISP-1 CYTO CT vs WISP-1 CYTO IF	**<0.001**	PKP-3 DOWN AT IF vs PKP-3 IF	0.200

CT, central tumour; IF, invasive front; CYTO, cytoplasmic expression; NUC, nuclear expression. All P values are Chi square test. Results where P<0.1 are shown in bold.

High expression of ZEB1 in the central tumour correlated with high expression at the invasive front and low PKP-3 in the central tumour. High ZEB1 at the invasive front correlated with high cytoplasmic WISP-1 in the central tumour, nuclear WISP-1 at the invasive front, low PKP-3 in the central tumour and showed a trend towards significance with low PKP-3 at the invasive front (P=0.061). An increase in ZEB1 expression at the invasive front in comparison to the central tumour correlated with high ZEB1 in the central tumour, high nuclear WISP-1 at the invasive front and demonstrated a trend towards significance with low PKP-3 expression in both the central tumour and at the invasive front (P=0.085 and 0.063 respectively).

High cytoplasmic WISP-1 expression in the central tumour and at the invasive front correlated with high nuclear WISP-1 in the central tumour and at the invasive front. Central cytoplasmic WISP-1 expression also correlated with low PKP-3 in the central tumour, and expression at the invasive front with low PKP-3 at the invasive front. High nuclear WISP-1 expression in the central tumour correlated with high expression at the invasive front. High nuclear WISP-1 at the invasive front correlated with low PKP-3 in the central tumour.

An increase in cytoplasmic WISP-1 expression at the invasive front compared with the central tumour correlated with high cytoplasmic WISP-1 and low PKP-3 expression in the central tumour; and showed a trend towards correlation with high nuclear WISP-1 in the central tumour and an increase in nuclear WISP-1 expression at the invasive front compared to the central tumour (P=0.083 and 0.094 respectively). Increased nuclear WISP-1 expression at the invasive front compared to the central tumour also tended to correlate with nuclear WISP-1 expression at the invasive front (P=0.094).

Low PKP-3 in the central tumour correlated with low expression at the invasive front, and loss of PKP-3 at the invasive front compared to expression in the central tumour correlated with low PKP expression in the central tumour.

6.4 THE RELATIONSHIP BETWEEN ZEB1, WISP-1, PKP-3 AND CLINICOPATHOLOGICAL VARIABLES.

For each protein marker univariable analysis was performed by dividing the tumours into two groups according to their H-scores as described above for the marker correlation analysis. All clinicopathological data were then analysed against these groups using Chi square test (tables 6.4 - 6.7).

6.4.1 ZEB1

Table 6.4. Univariable analysis of ZEB1 scores and clinicopathological variables.

Variable	CT High vs None/Low/Mod	IF High vs None/Low/Mod	Increase in ZEB1 at IF vs CT
	p-value	p-value	p-value
Clinicopathological variables			
Gender: Male/Female	0.790	**0.085**	0.433
Age: >65/≤65years	0.203	0.659	0.382
Elective / Emergency	0.244	0.236	**0.008**
Rectal / Colonic tumour	0.501	0.934	0.676
Duke's stage A/B/C_1/C_2	0.242	0.644	0.283
Tumour stage: T_3/T_{1-2}	0.446	0.597	0.749
Histological grade G_3/G_{1-2}	0.836	0.246	0.307
Mucinous tumour Yes/No	0.261	0.420	0.562
Nodal Stage N_0/N_1/N_2	**0.040**	0.392	0.306
Lymph nodes: +/-	0.256	0.955	0.165
Vascular invasion V_1/V_0	**0.022**	0.113	0.103
Pathological R_1 resection	0.538	0.775	0.700
Surgical R_1 resection	0.366	0.404	0.695
Chemotherapy Yes / No	0.831	0.715	0.177
Synchronous liver metastases	0.366	0.404	0.695
Metachronous liver metastases	0.491	0.924	0.718

CT, Central Tumour; IF, Invasive Front. P values are Pearson's Chi square test.

On univariable analysis high central tumour ZEB1 score significantly correlated with vascular invasion and increasing nodal stage. High ZEB1 expression at the invasive front showed few associations with clinicopathological factors, only gender having any significant correlation. An increase in ZEB1 expression at the invasive front over the central tumour score correlated with emergency resection surgery, but no other factors.

6.4.2 Nuclear WISP-1

Table 6.5. Univariable analysis of nuclear WISP-1 scores and clinicopathological variables.

Variable	CT High vs None/Low/Mod	IF High vs None/Low/Mod	Increase in WISP-1 at IF vs CT
	p-value	p-value	p-value
Clinicopathological variables			
Gender: Male/Female	0.288	0.724	**0.054**
Age: >65/≤65years	0.997	0.800	0.602
Elective / Emergency	0.919	0.276	0.458
Rectal / Colonic tumour	0.261	**0.071**	**0.031**
Duke's stage A/B/C_1/C_2	0.138	0.797	**0.022**
Tumour stage: T_3/T_{1-2}	**0.021**	0.452	0.159
Histological grade G_3/G_{1-2}	0.168	0.800	0.234
Mucinous tumour Yes/No	0.310	0.285	0.974
Nodal Stage N_0/N_1/N_2	0.156	0.719	**0.065**
Lymph nodes: +/-	**0.082**	0.423	0.268
Vascular invasion V_1/V_0	**0.047**	0.996	0.170
Pathological R_1 resection	**0.010**	0.281	**0.049**
Surgical R_1 resection	**0.089**	0.261	**0.015**
Chemotherapy Yes / No	0.153	0.984	0.935
Synchronous liver metastases	**0.089**	0.261	**0.015**
Metachronous liver metastases	0.497	0.278	0.555

CT, Central Tumour; IF, Invasive Front. P values are Pearson's Chi square test.

High nuclear WISP-1 in the central tumour correlated with increasing tumour T stage, vascular invasion and pathological R_1 resection, perhaps suggesting a role for WISP-1 in local advanced disease status and invasion. Trends were also noted ($p<0.1$) in association with lymph node and liver metastases. When scored on its own at the invasive front high

WISP-1 did not significantly correlate with any of the factors examined. When an increase in nuclear WISP-1 expression was seen at the invasive front in comparison to expression in the central tumour, significant correlations were noted with male gender, rectal tumour, advancing Duke's stage, surgical R_1 resection and formation of liver metastases. An association with lymph node metastases was also seen (p=0.065). These data suggest high expression of nuclear WISP-1 plays an oncogenic role and encourages local invasion and metastasis, in agreement with some of the previous studies in CRC and other tumours discussed above[188, 191-194, 197].

6.4.3 Cytoplasmic WISP-1

Table 6.6. Univariable analysis of cytoplasmic WISP-1 scores and clinicopathological variables.

Variable	CT High vs None/Low/Mod	IF High vs None/Low/Mod	Increase in WISP-1 at IF vs CT
	p-value	p-value	p-value
Clinicopathological variables			
Gender: Male/Female	**0.001**	0.160	**0.099**
Age: >65/≤65years	0.132	0.739	0.328
Elective / Emergency	**0.017**	0.157	0.225
Rectal / Colonic tumour	0.245	0.421	0.651
Duke's stage A/B/C_1/C_2	0.451	0.888	**0.011**
Tumour stage: T_3/T_{1-2}	0.154	0.369	0.645
Histological grade G_3/G_{1-2}	0.415	0.264	0.328
Mucinous tumour Yes/No	0.216	0.286	0.105
Nodal Stage N_0/N_1/N_2	0.379	0.912	**0.014**
Lymph nodes: +/-	0.443	0.668	**0.060**
Vascular invasion V_1/V_0	0.218	0.206	0.551
Pathological R_1 resection	0.570	0.209	0.248
Surgical R_1 resection	0.783	0.524	0.512
Chemotherapy Yes / No	0.937	0.381	**0.015**
Synchronous liver metastases	0.783	0.524	0.512
Metachronous liver metastases	**0.075**	0.577	0.461

CT, Central Tumour; IF, Invasive Front. P values are Pearson's Chi square test.

High cytoplasmic WISP-1 in central tumour areas showed fewer correlations with clinicopathological factors, only male gender and emergency surgery showing significant associations. Over-expression of cytoplasmic WISP-1 at the invasive front did not show any relationship with the factors examined. However, an increase in cytoplasmic WISP-1 at the invasive front versus the central tumour correlated with increased Duke's and lymph node stage, lymph node metastases and the use of adjuvant chemotherapy, suggesting, as with nuclear WISP-1 expression, an oncogenic role for WISP-1, perhaps encouraging advanced local disease and lymph node metastasis.

6.4.4 PKP-3

Table 6.7. Univariable analysis of PKP-3 scores and clinicopathological variables.

Variable	CT None/Low vs Mod/High	IF None/Low vs Mod/High	Decrease in PKP-3 at IF vs CT
	p-value	p-value	p-value
Clinicopathological variables			
Gender: Male/Female	0.746	0.371	0.217
Age: >65/≤65years	0.813	0.547	0.256
Elective / Emergency	0.182	0.200	0.340
Rectal / Colonic tumour	0.159	0.155	0.273
Duke's stage A/B/C_1/C_2	0.103	0.689	0.337
Tumour stage: T_3/T_{1-2}	0.779	**0.098**	**0.093**
Histological grade G_3/G_{1-2}	0.158	0.758	0.577
Mucinous tumour Yes/No	0.244	0.459	0.715
Nodal Stage N_0/N_1/N_2	**0.004**	0.625	**0.008**
Lymph nodes: +/-	0.107	0.422	0.644
Vascular invasion V_1/V_0	0.378	0.277	0.698
Pathological R_1 resection	0.218	0.768	**0.073**
Surgical R_1 resection	0.666	0.428	0.481
Chemotherapy Yes / No	0.690	0.306	0.776
Synchronous liver metastases	0.666	0.428	0.481
Metachronous liver metastases	0.631	0.495	0.473

CT, Central Tumour; IF, Invasive Front. P values are Pearson's Chi square test.

A low PKP-3 score in the central tumour showed significant correlation with increased nodal stage and this was also the case when a decrease in PKP-3 score at the invasive front

was seen compared to the central tumour. A decrease in PKP-3 score at the invasive front versus the central tumour also showed trends to correlate with increased T stage and pathological R_1 resection, although this was not statistically significant (p=0.093 and 0.073 respectively). Low PKP-3 score at the invasive front was associated with advancing T stage, although again this lacked statistical significance (P=0.098). These correlations may suggest that loss of PKP-3 at the invasive front correlates with advanced loco-regional disease given the increased T and nodal stage.

6.5 THE RELATIONSHIP BETWEEN CLINICOPATHOLOGICAL VARIABLES, THE DEVELOPMENT OF LIVER METASTASES AND SURVIVAL.

All clinicopathological data were analysed using log rank and Kaplan Meier tests in relation to the presence or development of liver metastases and overall or disease-specific survival (table 6.8).

Table 6.8. Univariable analysis of clinicopathological factors according to the presence or subsequent formation of liver metastases, overall and disease-specific survival.

Variable	Synchronous Liver Metastases	Metachronous Liver Metastases	Overall Survival			Disease Specific Survival		
	p-value	p-value	HR	95% C.I.	p-value	HR	95% C.I.	p-value
Clinicopathological variables								
Gender: Male/Female	0.800	0.584	0.800	0.509-1.259	0.330	1.087	0.623-1.896	0.769
Age: >65/≤65years	0.464	0.230	0.895	0.532-1.506	0.674	0.751	0.419-1.345	0.335
Elective / Emergency	**0.031**	1.000	0.716	0.400-1.281	0.254	1.286	0.625-2.646	0.495
Rectal / Colonic tumour	0.795	0.383	0.877	0.498-1.545	0.646	1.280	0.622-2.635	0.502
Duke's stage A/B/C_1/C_2	**<0.001**	**<0.001**	3.172	2.264-4.445	**<0.001**	5.410	3.396-8.617	**<0.001**
Tumour stage: T_3/T_{1-2}	**<0.001**	0.386	2.021	1.425-2.865	**<0.001**	2.469	1.581-3.855	**<0.001**
Histological grade G_3/G_{1-2}	**0.042**	0.715	1.132	0.679-1.887	0.631	1.438	0.795-2.599	0.229
Mucinous tumour Yes/No	0.590	0.122	1.321	0.679-2.570	0.407	2.090	1.046-4.175	**0.037**
Nodal Stage N_0/N_1/N_2	**<0.001**	**<0.001**	2.668	1.995-3.569	**<0.001**	3.773	2.582-5.513	**<0.001**
Lymph nodes: +/-	**<0.001**	**<0.001**	3.187	1.958-5.188	**<0.001**	6.427	3.118-13.249	**<0.001**
Vascular invasion V_1/V_0	**0.001**	**0.028**	2.877	1.642-5.042	**<0.001**	3.925	2.075-7.424	**<0.001**
Pathological R_1 resection	**0.002**	0.375	0.551	0.297-1.024	0.054	2.232	1.115-4.468	**0.023**
Chemotherapy Yes / No	0.115	**0.004**	1.386	0.883-2.176	0.150	2.372	1.343-4.190	**0.003**
Synchronous liver mets	N/A	**<0.001**	10.243	5.831-17.993	**<0.001**	18.893	9.723-36.711	**<0.001**

HR, Hazards Ratio; CI, Confidence Interval. For liver metastases analysis binary logistic regression was used. For Survival log rank and Kaplan Meier analyses were performed.

6.5.1 Liver Metastases

Factors found to significantly correlate with the presence of liver metastases at the initial diagnosis of CRC (synchronous metastases) include emergency surgery, increased Duke's stage of the primary tumour and T stage, poor tumour differentiation, increased nodal stage, pathological R_1 resection, lymph node metastases and vascular invasion. The development of liver metastases after removal of the primary tumour (metachronous) was associated with increasing Duke's and nodal stage of the primary tumour, vascular invasion, lymph node metastases and previous synchronous liver metastases. Use of adjuvant chemotherapy was also associated with the development of metachronous liver metastases, although it is likely that this is merely a reflection of the fact that patients with a high primary Duke's stage are more likely to be offered chemotherapy.

6.5.2 Survival

Increasing Duke's, T and lymph node stage and the presence of vascular invasion or synchronous liver metastases were all very significantly correlated with overall and disease-specific survival ($p<0.001$ in all cases). In addition mucinous differentiation, pathological R_1 resection and the receipt of adjuvant chemotherapy all correlated with decreased disease-specific survival.

6.6 THE RELATIONSHIP BETWEEN ZEB1, WISP-1, PKP-3 AND SURVIVAL IN COLORECTAL CANCER.

Univariable survival analyses were performed using log rank and Kaplan Meier tests with regard to survival and the expression of ZEB1, WISP-1 and PKP-3 in the central tumour, at the invasive front and changes in expression between the two areas (table 6.9).

Table 6.9. Univariable analysis of immunohistochemical markers (H score) according to overall and disease-specific survival.

Variable		Overall Survival			Disease Specific Survival		
		HR	**95% C.I.**	**p-value**	**HR**	**95% C.I.**	**p-value**
Immunohistochemical Marker							
ZEB1	CT High vs None/Low/Mod	1.831	0.875-3.831	0.108	1.375	0.659-2.868	0.396
	IF High vs None/Low/Mod	1.274	0.685-2.370	0.444	1.265	0.680-2.353	0.457
	Increased at IF vs CT	0.974	0.619-1.534	0.910	1.133	0.720-1.784	0.589
CytoplasmicWISP-1	CT High vs None/Low/Mod	0.466	0.170-1.278	0.138	0.586	0.213-1.607	0.299
	IF High vs None/Low/Mod	0.431	0.135-1.371	0.154	0.597	0.188-1.900	0.383
	Increased at IF vs CT	0.848	0.309-2.333	0.750	0.715	0.260-1.966	0.516
Nuclear WISP-1	CT High vs None/Low/Mod	1.441	0.869-2.389	0.157	0.920	0.555-1.526	0.748
	IF High vs None/Low/Mod	1.354	0.837-2.189	0.217	1.056	0.654-1.706	0.823
	Increased at IF vs CT	**1.852**	**1.115-3.018**	**0.017**	**0.907**	**0.547-1.504**	**0.073**
PKP-3	CT None/Low vs Mod/High	1.419	0.777-2.592	0.255	0.968	0.529-1.771	0.916
	IF None/Low vs Mod/High	1.365	0.835-2.231	0.215	1.107	0.677-1.809	0.685
	Decreased at IF vs CT	1.277	0.738-2.209	0.382	1.131	0.654-1.956	0.659

CT, central tumour; IF, invasive front; HR, Hazards Ratio; CI, Confidence Interval; PKP-3, Plakophilin-3; WISP-1, Wnt-inducible Signalling Protein-1. Survival analyses were performed by log rank and Kaplein Meier tests.

Neither expression of ZEB1, WISP-1 or PKP-3 at the invasive front or in the central tumour alone correlated with overall or disease-specific survival. However, as previously discussed it is postulated that the tumour micro-environment is dynamic in different areas, and therefore changes in expression of the proteins between the central tumour and the invasive front may be important. On Kaplan Meier and log rank analysis increased nuclear WISP-1 at the invasive front over the central tumour significantly correlated with decreased overall survival, and a trend was also noted towards significance in decreased disease-specific survival (Figure 6.1).

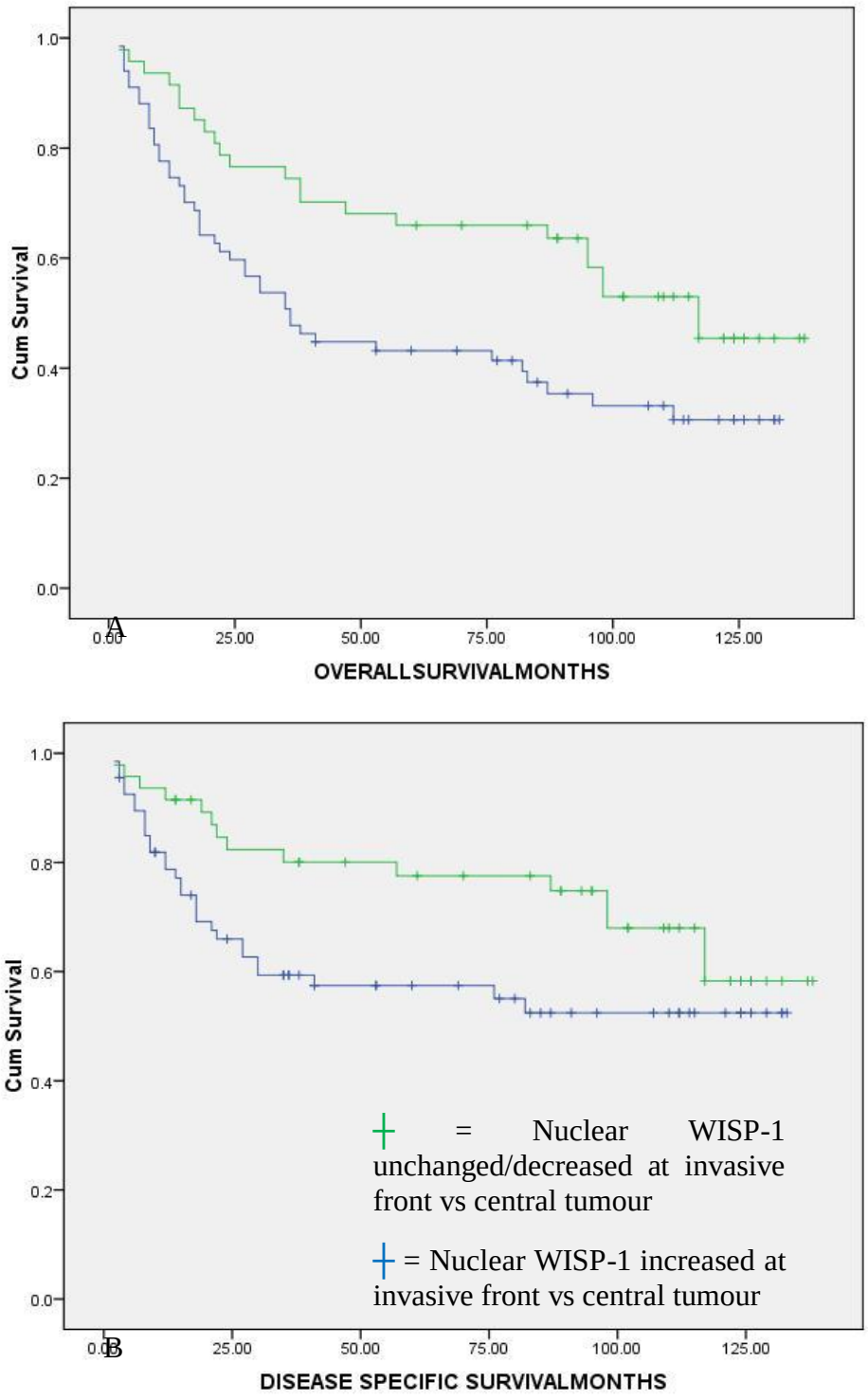

Figure 6.1. Kaplan Meier survival curves for increased nuclear WISP-1 at the invasive front.

6.7 MULTIVARIABLE ANALYSIS OF FACTORS PREDICTIVE OF THE DEVELOPMENT OF LIVER METASTASES, OVERALL AND DISEASE-SPECIFIC SURVIVAL.

All clinicopathological factors and protein markers found to be correlated with the formation of metachronous liver metastases, overall and disease-specific survival at the $p \leq 0.1$ level in univariable analysis were entered into multivariable backward logistic cox regression models to establish any which may be individually predictive of outcome. Therefore in the metachronous liver metastases model markers entered into the analysis included Duke's stage of the primary tumour, presence of lymph node metastases, nodal stage (N_0 / N_1 / N_2), vascular invasion, receipt of adjuvant chemotherapy and synchronous liver metastases. For overall survival analysis, factors entered into the model included Duke's stage of the primary tumour, T stage, presence of lymph node metastases, nodal stage (N_0 / N_1 / N_2), vascular invasion, synchronous liver metastases and increased nuclear WISP-1 score at the invasive front versus the central tumour. For disease specific survival the same factors as those for overall survival were included with the addition of mucinous tumour differentiation, pathological R_1 resection and receipt of adjuvant chemotherapy. The results are shown in table 6.10.

Table 6.10. Multivariable analysis of clincopathological and immunohistochemical factors predictive of the formation of liver metastases, overall and disease-specific survival.

Variable		Metachronous Liver Metastases			Overall Survival			Disease Specific Survival		
		HR	**95% C.I.**	**p-value**	**HR**	**95% C.I.**	**p-value**	**HR**	**95% C.I.**	**p-value**
Clinicopathological variables										
Duke's stage A/B/C_1/C_2				NS			**0.005**			**0.002**
- Duke's B	Risk relative to Duke's A as 1st categorical variable	NS	NS	NS	**1.213**	**0.400-3.677**	**0.733**	**1.494**	**0.172-12.958**	**0.716**
- Duke's C_1		NS	NS	NS	**2.282**	**0.743-7.015**	**0.150**	**4.716**	**0.596-37.317**	**0.142**
- Duke's C_2		NS	NS	NS	**7.393**	**1.943-28.134**	**0.003**	**16.875**	**1.828-155.761**	**0.013**
Tumour stage: T_3/T_{1-2}		-	-	-	NS	NS	NS	NS	NS	NS
Mucinous tumour Yes/No		-	-	-	-	-	-	NS	NS	NS
Nodal Stage N_0/N_1/N_2		NS	NS	NS	NS	NS	NS	NS	NS	NS
Lymph nodes: +/-		NS	NS	NS	NS	NS	NS	NS	NS	NS
Vascular invasion V_1/V_0		NS	NS	NS	NS	NS	NS	2.161	0.948-4.927	0.067
Pathological R_1 resection		-	-	-	-	-	-	NS	NS	NS
Chemotherapy Yes / No		NS	NS	NS	-	-	-	NS	NS	NS
Synchronous liver mets		**25.799**	**5.879-113.208**	**<0.001**	**9.040**	**3.242-25.209**	**<0.001**	**15.377**	**4.359-54.250**	**<0.001**
Immunohistochemical markers										
Increased nuclear WISP-1 at IF vs CT		-	-	-	**1.957**	**1.031-3.704**	**0.040**	NS	NS	NS
High cytoplasmic WISP-1 in central tumour		NS	NS	NS	-	-	-	-	-	-

HR, Hazards Ratio; CI, Confidence Interval; NS, Not Significant; -, not entered into this analysis as p>0.1 on univariable testing. Analysis was performed using a backward stepwise cox regression model. All factors with p≤0.1 on univariable analysis were entered into the equation. Independent prognostic indicators are those with p<0.05 and are shown in bold. Factors with a trend toward significance (p<0.1) are shown in normal type. Factors where p>0.1 are stated as not significant (NS).

As can be seen in table 6.10, and as expected, Duke's stage is an independent prognostic factor predicting overall and disease specific survival. The presence of liver metastases at presentation is also an independent predictor of poor overall and disease specific survival, as is the formation of metachronous liver metastases after resection. The presence of synchronous liver metastases is a very poor prognostic sign in this series, as delineated by the hazard ratios which indicate 9 and 15 fold higher disease specific and overall risk of death compared to those patients without synchronous metastases. An increase in nuclear WISP-1 expression at the invasive front versus the central tumour also independently predicted decreased overall, but not disease specific survival.

Chapter 7: Discussion, summary and future directions.

7.1 DISCUSSION

Several theories on the importance of ZEB1 as a signalling protein in development and malignant disease processes have been published in recent years. These papers have highlighted multiple potential targets of this transcriptional repressor and opened the door to wide-ranging avenues of investigation in several different signalling systems. This project aimed to investigate the relationship between ZEB1 and other proteins thought to be of importance in CRC, and which may lead to the identification of targets for therapeutic modulation in the future. To this end, *in vitro* and *in vivo* techniques were used to try and relate ZEB1 signalling pathways seen to operate in cellular culture systems with protein expression in patient tissues.

7.1.1 Expression of markers *in vitro* – ZEB1 and E-cadherin

Previous analyses in the literature have suggested that ZEB1 is expressed in CRC and breast cancer cell lines. The immortalised colorectal and breast-derived cells examined here demonstrated high levels of ZEB1 expression in those with an aggressive, mesenchymal-like phenotype such as MDA-MB-231 and SW480, with lower expression noted in HCEC and MCF-7 cells which present a more typical epithelial phenotype. On further investigation most cell lines appeared to demonstrate an inversely correlated expression pattern between ZEB1 and adhesional complex proteins such as E-cadherin and PKP-3. This was consistent with the suggestion that ZEB1 acts as a repressor of these proteins and is involved in their down-regulation in order to achieve dysadhesion and invasive / metastatic behaviour.

In order to further investigate this relationship a ZEB1 construct was used to express the protein in epithelial-type cell lines and ascertain its effect on the various proteins of interest. Initial experimentation confirmed successful cloning of the ZEB1 construct and its expression in easily transfected HeLa cells. Three immortalised cell lines derived from CRC tissues were then selected for further study, each with differing levels of E-cadherin expression. Initially chemical transfection of these cell lines proved problematic and only a maximum of 60% transfection efficiency could be achieved. Despite this, on western blot a 100% increase in ZEB1 expression was observed in HCT116 cells compared to controls, but with little discernable change in E-cadherin expression.

The results with respect to E-cadherin of these initial experiments to over-express ZEB1 were contrary to observations in other epithelial malignancies [93, 96]. There may be several reasons for this. Ireton and colleagues demonstrated that p120 is crucial in the control of E-cadherin expression in SW480 cells; and CtBP and p300 expression have also been shown to directly influence E-cadherin levels in T cells and to correlate with E-cadherin and ZEB1 levels *in vivo*[90, 276, 277]. It is therefore possible that, in the HCT116 cell line, alterations in p120, p300 or CtBP levels may account for the lack of E-cadherin response to ZEB1 manipulation. It is also conceivable that the ZEB1 expression construct used here did not produce fully functional ZEB1 protein. The construct was tested prior to use by molecular weight analysis on agarose gel and by demonstration of the correct band detected on western blotting of the over-expressed protein, but full DNA sequence analysis of the construct was not performed.

In order to investigate the effect of increased E-cadherin levels on ZEB1 expression, E-cadherin was overexpressed in SW480 cells which have negligible inherent E-cadherin expression and high levels of ZEB1. Successful over-expression was achieved with

little discernable effect on ZEB1 levels, consistent with previous observations in breast cancer cell lines[104]. In addition the macroscopic phenotype of the cells on culture plates was unchanged, indicating that despite E-cadherin expression as confirmed on western blot, the cells retained a mesenchymal phenotype and the expressed E-cadherin protein was unable to function in forming normal adherens complexes. Aigner and colleagues noted that this effect was likely to be due to ZEB1's ability to repress epithelial polarity proteins such as CRUMBS, PATJ and HUGL2 in MDA-MB-231 cells, important in the assembly of such adhesion complexes[104]. This experiment suggested similar effects in CRC cells, suggesting ZEB1 may be influential over polarity genes in this cell line.

7.1.2 Expression of markers *in vitro* – ZEB1, WISP-1, WISP-2 and WISP-3

Little is known about the relationship between WISP proteins and ZEB1. To date only one group have identified a direct connection between them, and that study was conducted in breast carcinoma cells[94]. However, the role of CCN proteins in malignancy has been widely discussed and it is thought that they may play a pivotal role in the interaction between epithelium and stroma. Given that previous investigators had highlighted the presence of high ZEB1 expression in CRC and stromal cells in other epithelial malignancies, and in the light of a study by Huang and colleagues, making a connection between ZEB1 and WISP-3 in breast tumours, it seemed feasible that WISP proteins may contribute to ZEB1 signalling in CRC[86, 94, 115].

As few data exist on the levels of WISP expression in CRC cell lines, initially two breast and the available colorectal cell lines were characterised for WISP protein expression.

Given the previous problems with ZEB1 over-expression in HCT116 cells, a different approach was taken to examine the effect of ZEB1 on the WISP proteins. A431 cells (originally derived from a human skin cancer) which had previously been transfected with a ZEB1 construct were grown and treated with Doxycycline in order to induce ZEB1 expression. On western blot ZEB1 expression was clearly increased and down-regulation of E-cadherin was observed, but little effect was seen on WISP-1 or WISP-2 expression. However, the inhibition of WISP-3 by ZEB1, suggested a feed-back loop with signalling opposite to that reported by Huang and colleagues who found that inhibition of WISP-3 caused up-regulation of ZEB1 (figure 7.1)[94].

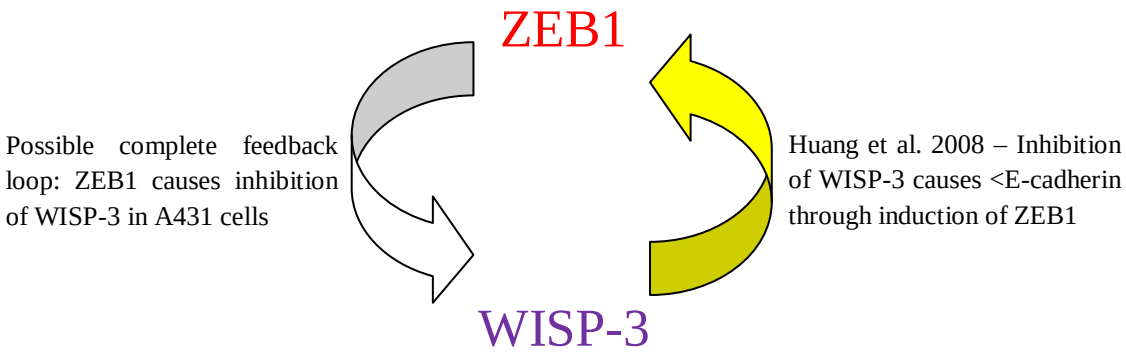

Figure 7.1. Possible signalling interaction between ZEB1 and WISP-3.

In order to test whether WISP-3 affects ZEB1 in CRC cell lines, knockdown of WISP-3 was attempted. Chemical transfection of WISP-3 siRNA using three different reagents failed to cause significant knockdown. Further attempts at transfection of the siRNA with nucleofection (Amaxa technique) also failed to knockdown the protein. Of interest, Huang and colleagues utilised a lentiviral vector to deliver knockdown of WISP-3 in HME cells, and when contacted to ask for advice it was clear that WISP-3 knockdown had been extremely challenging.

Previous investigation of WISP-1 in CRC has demonstrated high expression levels in cancer tissues. No expression constructs for WISP-1 were commercially available at the

time of experimentation and therefore the decision was taken to examine knockdown of WISP-1 in CRC cells which showed a high expression pattern. However knockdown of WISP-1 failed despite further attempts at optimisation with varying concentrations of siRNA. It was not clear why knockdown of either WISP-3 or WISP-1 could not be achieved.

Due to the difficulties experienced with siRNA-mediated protein silencing a knockdown DNA construct for WISP-2 was acquired as a kind gift from Dr S. Banerjee (Minnesota, USA). Banerjee and colleagues had successfully used this construct in MCF-7 breast cells, observing an EMT with decreased E-cadherin expression[212]. ZEB1 was not assessed in their study, although another transcriptional repressor of E-cadherin, SNAIL, was up-regulated in response to WISP-2 knockdown. Despite performing an optimisation experiment with several different concentrations of DNA, Lipofectamine and two cell lines effective knockdown of WISP-2 as assessed by western blot could not be achieved. When analysis was undertaken to test the specificity of the WISP-2 antibody, significant concerns were raised and further experiments requiring it were abandoned.

The results encountered during these *in vitro* WISP studies may have several explanations. The failure of siRNA delivery into the cells may account for lack of gene silencing and it is important to conduct optimisation experiments to achieve maximal siRNA delivery. The conditions for efficient transfection vary for each cell line, although several of the lines have published transfection protocols which have been optimised by the reagent manufacturer. Initial success was achieved in HCT116 cells delivering a GFP construct using a published protocol for transfection of DNA vectors, with approximately 60% efficiency as assessed by fluorescent microscopy. However this protocol failed to achieve successful siRNA knockdown in these cells, and no

published protocol existed for the delivery of siRNA into HCT116 cells using any of the reagents examined here. Several experiments were therefore performed in order to try and achieve successful siRNA delivery, varying reagent and siRNA ratios and concentrations, time-points for examination and the use of two different cell lines, but without success.

7.1.3 Expression of markers *in vitro* – ZEB1 and PKP-3

The desmosomal adhesion complex protein PKP-3 has yet to be widely investigated in malignant disease. Aigner and colleagues demonstrated that ZEB1 associates with the PKP-3 promoter complex in MDA-MB-231 breast cancer cells and transcriptionally represses its activity in a similar fashion to that seen with E-cadherin. This study has investigated the relationship between ZEB1 and PKP-3 in CRC. Initial characterisation of a panel of cell lines demonstrated variable expression of PKP-3; loss of expression being noted in the invasive, metastatic mesenchymal phenotype SW480 cell line and higher levels in the lymph node metastasis-derived SW620 cell line from the same patient. Interestingly this expression pattern was almost the same as that of E-cadherin, and inversely correlated with ZEB1 expression.

In contrast to the previous problems with siRNA-mediated protein knockdown, PKP-3 siRNA was transfected into HCT116 cells and successfully delivered up to 60% reduction in PKP-3 expression. No discernable change in E-cadherin or ZEB1 expression was seen on western blots, although, on light microscope examination, increases in the number of cells per high power field were observed, perhaps indicating an increase in cell division. The HCT116 PKP-3 knockdown clones appeared to be growing more rapidly, although no change in morphology was seen, indicating that loss of PKP-3 expression may affect cell turnover but not morphology in its own right. This

is consistent with Kundu and colleagues' previous observations in HCT116 PKP-3 knockdown cells[256].

Further to the successful knockdown of PKP-3, of interest was the effect of loss of ZEB1 on expression of PKP-3 and whether this would cause phenotypic changes in the aggressive metastatic cell lines SW480 and MDA-MB-231. A pshZEB1 construct was therefore used successfully to knockdown ZEB1 in these cells. Increases in both PKP-3 and E-cadherin expression were observed in both cell lines, although the increase in PKP-3 was of a lesser degree in SW480 to that seen in MDA-MB-231 cells. On light microscopy the cells were also seen to grow in a more typical epithelial morphology, changes typical of an MET. In order to establish that the down-regulation of ZEB1 was responsible for the increase in PKP-3 expression, and not the increase in E-cadherin expression, SW480 cells were transfected with an E-cadherin construct. No significant change in PKP-3, or ZEB1 expression (as described earlier in chapter 3), was observed on E-cadherin over-expression. In addition over-expression of ZEB1 in HCT116 cells caused a significant decrease in PKP-3 expression. These experiments indirectly confirmed the specificity of ZEB1 in the signalling cascade controlling PKP-3 expression.

The changes in E-cadherin and PKP-3 expression on ZEB1 knockdown were further examined at the cellular level by immunocytochemistry. Spaderna and colleagues previously performed a similar experiment in SW480 cells to analyse changes in the Lama3 protein upon ZEB1 knockdown. They noted a dramatic change in the SW480 cell phenotype, with increased adhesion and clustering of cells consistent with an MET. E-cadherin expression was assessed and seen to increase at sites of cell contact where adherens junctions were formed. These findings were confirmed in the experiments performed here, but with assessment of PKP-3 expression. In cell clusters in which

ZEB1 knockdown had been successful PKP-3 expression was significantly increased, along with E-cadherin at sites of cell-cell contact. The re-expression of these proteins involved in cell adhesion on ZEB1 knockdown explains the phenotypic changes observed in MDA-MB-231 and SW480, and raises the question as to whether or not other such adhesional-related molecules may also be involved in ZEB1 signalling.

7.1.4 Expression of markers *in vivo* – ZEB1, WISP-1 and PKP-3.

Consistent with the *in vitro* findings significant correlations were found between the over-expression of ZEB1, both in the central tumour and at the invasive front, and low PKP-3 expression in both these areas. High expression of cytoplasmic and nuclear WISP-1 also demonstrated correlations with high ZEB1 expression and low PKP-3 expression in the central tumour and at the invasive front. These correlations between the tumour markers were encouraging and suggest that the positive *in vitro* results may reflect what is happening in the tumour itself.

The results from demographic and survival comparisons with ZEB1 expression were less convincing. Expression in the central tumour correlated with increasing nodal stage and vascular invasion. But change in ZEB1 expression at the invasive front, which from previous reports appears to be an important factor for metastasis and tumour stage, did not correlate with either of these features[115].

Over-expression or increased expression of WISP-1 at the invasive front showed correlations with several tumour-related factors on univariable analysis. High nuclear WISP-1 expression in the central tumour correlated with T stage, vascular invasion, pathological R1 resection and there were trends of association with lymph node metastases, surgical R1 resection and synchronous liver metastases. Increased nuclear WISP-1 expression at the invasive front also correlated with Duke's stage and several of

these factors. Similarly increased cytoplasmic WISP-1 expression at the invasive front correlated with Duke's stage, nodal stage and lymph node mestastases. The correlations seen here with clinicopathological factors on univariable analysis are in-keeping with other studies of WISP-1 in CRC[188, 191, 192].

Loss of PKP-3 expression in tumour tissues has been described in a few small series to date, but none of these examined the relationship with clinicopathological factors. The statistical analysis performed in this study indicated correlations between loss of PKP-3 at the invasive front and increasing T stage, lymph node metastases and pathological R1 resection. These findings would be consistent with the *in vitro* experiments and previously published studies which suggest a more aggressive cellular phenotype when PKP-3 is knocked down[124].

Despite these correlations between ZEB1, WISP-1 and PKP-3 expression and the clinicopathological variables, univariable survival analyses revealed that only increased nuclear WISP-1 at the invasive front had any relationship with survival. When multivariable survival analysis was undertaken both Duke's stage and the presence of synchronous liver metastases independently predicted poor survival, as has been validated in previous studies. Interestingly the correlations between increased nuclear WISP-1 at the invasive front and survival also held true in the multivariable analysis; increased nuclear WISP-1 at the invasive front being an independent predictor of poor overall survival.

7.2 SUMMARY

This study was designed to analyse the role of ZEB1 and other potentially related proteins in CRC cell signalling. The results indicate that ZEB1 plays a significant role in the control of E-cadherin and PKP-3 expression and in modulating cell adhesion

through the control of these adhesion proteins. In particular ZEB1 is over-expressed at the invasive front of some tumours and this is associated with an increase in WISP-1 and decrease in PKP-3 expression. Increased WISP-1 expression at the invasive front is an independent predictor of poor overall survival in CRC.

7.3 FUTURE DIRECTIONS

Metastatic disease remains the primary cause of death and morbidity in CRC. The identification and detailed understanding of cellular signalling pathways related to tumour metastasis is the key to the discovery of novel therapeutic targets which may influence patient survival and outcome. ZEB1 appears to be involved in several signalling systems related to adhesion and the maintenance of the epithelial phenotype. The work performed here demonstrates that this relationship is by no means a linear one, with complex mechanisms orchestrating the overall cellular phenotype and ability to invade and metastasise. It would appear that ZEB1 has significant relationships with at least two adhesion-related proteins in E-cadherin and PKP-3 and may be a master regulator of the epithelial phenotype in CRC. It would be easy to envisage that ZEB1 may have other such interactions with the cell adhesion complex and other molecules involved in this system would be worthy of further investigation in this regard. The Desmoplakins and Plakophilins 1 and 2, other proteins involved on the desmosomal adhesion complex, may be such candidates.

In the experiments in which PKP-3 was knocked down the cells were observed to increase their growth rate. This phenomenon has previously been recognised by Kundu and colleagues, but never formally assessed as far as the author is aware[256]. This increase in cell turnover is of interest as it may have ramifications for both therapeutic targeting and tumour aggressiveness. Thus further *in vitro* analysis of cellular turnover on PKP-3 knockdown would be of interest. In addition, few studies have examined the

expression of PKP-3 *in vivo* and further validation of the results seen here would be of great interest, both in CRC and other tumours.

It is also worth noting that the interaction of ZEB1, as well as several of the previously investigated transcriptional repressors, such as SNAIL, SLUG, TWIST, E12/47, Kruppel-like factor 8 with E-cadherin and other adhesion complex proteins such as PKP-3, appears to be tumour and even cell-line specific. This may in some way account for the significant variation in the reports of ZEB1 expression in CRC to date. No group has analysed a significant number of tumours for expression of a panel of these repressors in the same study. The application of a proteomic or micro-array based approach should allow accurate quantification of expression of several of these molecules in the same cohort of tumours, allowing further understanding of their individual roles.

Finally the discovery that WISP-1 over-expression correlates with poor survival prompts further questions as to the role of the WISP proteins in tumourigenesis and progression. These molecules have been scantily investigated to date and warrant further attention. Studies to examine their expression *in vitro* and *in vivo* should be initiated, either with new validated antibodies or using DNA / RNA based approaches to expression analysis, in order to establish the exact nature of their role in malignant disease.

REFERENCES

1. Boyle, P. and J. Ferlay, *Cancer incidence and mortality in Europe, 2004.* Ann Oncol, 2005. **16**(3): p. 481-8.
2. Fegiz, G., et al., *Hepatic resections for colorectal metastases: the Italian multicenter experience.* J Surg Oncol Suppl, 1991. **2**: p. 144-54.
3. Jatzko, G.R., et al., *Hepatic resection for metastases from colorectal carcinoma--a survival analysis.* Eur J Cancer, 1995. **31A**(1): p. 41-6.
4. Fuhrman, G.M., et al., *Improved survival after resection of colorectal liver metastases.* Ann Surg Oncol, 1995. **2**(6): p. 537-41.
5. Adam, R., et al., *Five-year survival following hepatic resection after neoadjuvant therapy for nonresectable colorectal [liver] metastases.* Annals of Surgical Oncology, 2001. **8**(4): p. 347-353.
6. Rockey, D.C., et al., *Analysis of air contrast barium enema, computed tomographic colonography, and colonoscopy: prospective comparison.* Lancet, 2005. **365**(9456): p. 305-11.
7. O'Connell, J.B., M.A. Maggard, and C.Y. Ko, *Colon cancer survival rates with the new American Joint Committee on cancer sixth edition staging.* Journal of the National Cancer Institute, 2004. **96**(19): p. 1420-1425.
8. Campbell, N.C., et al., *Rural and urban differences in stage at diagnosis of colorectal and lung cancers.* Br J Cancer, 2001. **84**(7): p. 910-4.
9. Heald, R.J., et al., *Rectal cancer: the Basingstoke experience of total mesorectal excision, 1978-1997.* Arch Surg, 1998. **133**(8): p. 894-9.
10. Heald, R.J. and R.D. Ryall, *Recurrence and survival after total mesorectal excision for rectal cancer.* Lancet, 1986. **1**(8496): p. 1479-82.
11. [Anon], *Prolongation of the Disease-Free Interval in Surgically Treated Rectal-Carcinoma.* New England Journal of Medicine, 1985. **312**(23): p. 1465-1472.
12. Kapiteijn, E., et al., *Preoperative radiotherapy combined with total mesorectal excision for resectable rectal cancer.* New England Journal of Medicine, 2001. **345**(9): p. 638-646.
13. O'Dwyer P, J., et al., *Priorities in colorectal cancer research: recommendations from the Gastrointestinal Scientific Leadership Council of the Coalition of Cancer Cooperative Groups.* J Clin Oncol, 2007. **25**(16): p. 2313-21.
14. Thiery, J.P. and J.P. Sleeman, *Complex networks orchestrate epithelial-mesenchymal transitions.* Nat Rev Mol Cell Biol, 2006. **7**(2): p. 131-42.
15. Guarino, M., *Epithelial-to-mesenchymal change of differentiation. From embryogenetic mechanism to pathological patterns.* Histol Histopathol, 1995. **10**(1): p. 171-84.
16. Guarino, M., et al., *Pathological relevance of epithelial and mesenchymal phenotype plasticity.* Pathol Res Pract, 1999. **195**(6): p. 379-89.
17. Thiery, J.P., *Epithelial-mesenchymal transitions in tumour progression.* Nat Rev Cancer, 2002. **2**(6): p. 442-54.
18. Thiery, J.P., *Epithelial-mesenchymal transitions in development and pathologies.* Curr Opin Cell Biol, 2003. **15**(6): p. 740-6.
19. Schneeberger, E.E. and R.D. Lynch, *The tight junction: a multifunctional complex.* Am J Physiol Cell Physiol, 2004. **286**(6): p. C1213-28.
20. Kojima, T., et al., *Connexins induce and maintain tight junctions in epithelial cells.* J Membr Biol, 2007. **217**(1-3): p. 13-9.

21. Chidgey, M. and C. Dawson, *Desmosomes: a role in cancer?* Br J Cancer, 2007. **96**(12): p. 1783-7.
22. Getsios, S., A.C. Huen, and K.J. Green, *Working out the strength and flexibility of desmosomes.* Nat Rev Mol Cell Biol, 2004. **5**(4): p. 271-81.
23. Hartsock, A. and W.J. Nelson, *Adherens and tight junctions: structure, function and connections to the actin cytoskeleton.* Biochim Biophys Acta, 2008. **1778**(3): p. 660-9.
24. Berx, G. and F. Van Roy, *The E-cadherin/catenin complex: an important gatekeeper in breast cancer tumorigenesis and malignant progression.* Breast Cancer Res, 2001. **3**(5): p. 289-93.
25. Conacci-Sorrell, M., J. Zhurinsky, and A. Ben-Ze'ev, *The cadherin-catenin adhesion system in signalling and cancer.* J Clin Invest, 2002. **109**(8): p. 987-91.
26. Cowin, P., T.M. Rowlands, and S.J. Hatsell, *Cadherins and catenins in breast cancer.* Curr Opin Cell Biol, 2005. **17**(5): p. 499-508.
27. Van Aken, E., et al., *Defective E-cadherin/catenin complexes in human cancer.* Virchows Arch, 2001. **439**(6): p. 725-51.
28. Strathdee, G., *Epigenetic versus genetic alterations in the inactivation of E-cadherin.* Semin Cancer Biol, 2002. **12**(5): p. 373-9.
29. Kanai, Y., et al., *Point mutation of the E-cadherin gene in invasive lobular carcinoma of the breast.* Jpn J Cancer Res, 1994. **85**(10): p. 1035-9.
30. Berx, G., et al., *E-cadherin is inactivated in a majority of invasive human lobular breast cancers by truncation mutations throughout its extracellular domain.* Oncogene, 1996. **13**(9): p. 1919-25.
31. Becker, K.F., et al., *Identification of eleven novel tumor-associated E-cadherin mutations. Mutations in brief no. 215. Online.* Hum Mutat, 1999. **13**(2): p. 171.
32. Muta, H., et al., *E-cadherin gene mutations in signet ring cell carcinoma of the stomach.* Jpn J Cancer Res, 1996. **87**(8): p. 843-8.
33. Becker, K.F., et al., *E-cadherin gene mutations provide clues to diffuse type gastric carcinomas.* Cancer Res, 1994. **54**(14): p. 3845-52.
34. Risinger, J.I., et al., *Mutations of the E-cadherin gene in human gynecologic cancers.* Nat Genet, 1994. **7**(1): p. 98-102.
35. Wijnhoven, B.P., et al., *E-cadherin gene mutations are rare in adenocarcinomas of the oesophagus.* Br J Cancer, 1999. **80**(10): p. 1652-7.
36. Schuhmacher, C., et al., *Loss of immunohistochemical E-cadherin expression in colon cancer is not due to structural gene alterations.* Virchows Arch, 1999. **434**(6): p. 489-95.
37. Soares, P., et al., *E-cadherin gene alterations are rare events in thyroid tumors.* Int J Cancer, 1997. **70**(1): p. 32-8.
38. Costello, J.F. and C. Plass, *Methylation matters.* J Med Genet, 2001. **38**(5): p. 285-303.
39. Bird, A., *DNA methylation patterns and epigenetic memory.* Genes Dev, 2002. **16**(1): p. 6-21.
40. Turner, B.M., *Cellular memory and the histone code.* Cell, 2002. **111**(3): p. 285-91.
41. Bird, A.P., *The relationship of DNA methylation to cancer.* Cancer Surv, 1996. **28**: p. 87-101.
42. Bird, A.P. and A.P. Wolffe, *Methylation-induced repression--belts, braces, and chromatin.* Cell, 1999. **99**(5): p. 451-4.

43. Yoshiura, K., et al., *Silencing of the E-cadherin invasion-suppressor gene by CpG methylation in human carcinomas.* Proc Natl Acad Sci U S A, 1995. **92**(16): p. 7416-9.
44. Behrens, J., et al., *The E-cadherin promoter: functional analysis of a G.C-rich region and an epithelial cell-specific palindromic regulatory element.* Proc Natl Acad Sci U S A, 1991. **88**(24): p. 11495-9.
45. Giroldi, L.A., et al., *Role of E boxes in the repression of E-cadherin expression.* Biochem Biophys Res Commun, 1997. **241**(2): p. 453-8.
46. Batlle, E., et al., *The transcription factor snail is a repressor of E-cadherin gene expression in epithelial tumour cells.* Nat Cell Biol, 2000. **2**(2): p. 84-9.
47. Cano, A., et al., *The transcription factor snail controls epithelial-mesenchymal transitions by repressing E-cadherin expression.* Nat Cell Biol, 2000. **2**(2): p. 76-83.
48. Comijn, J., et al., *The two-handed E box binding zinc finger protein SIP1 downregulates E-cadherin and induces invasion.* Mol Cell, 2001. **7**(6): p. 1267-78.
49. Cowell, I.G., *Repression versus activation in the control of gene transcription.* Trends Biochem Sci, 1994. **19**(1): p. 38-42.
50. Ng, H.H. and A. Bird, *Histone deacetylases: silencers for hire.* Trends Biochem Sci, 2000. **25**(3): p. 121-6.
51. Peinado, H., F. Portillo, and A. Cano, *Transcriptional regulation of cadherins during development and carcinogenesis.* Int J Dev Biol, 2004. **48**(5-6): p. 365-75.
52. Peinado, H., D. Olmeda, and A. Cano, *Snail, Zeb and bHLH factors in tumour progression: an alliance against the epithelial phenotype?* Nat Rev Cancer, 2007. **7**(6): p. 415-28.
53. Perez-Moreno, M.A., et al., *A new role for E12/E47 in the repression of E-cadherin expression and epithelial-mesenchymal transitions.* J Biol Chem, 2001. **276**(29): p. 27424-31.
54. Kang, Y. and J. Massague, *Epithelial-mesenchymal transitions: twist in development and metastasis.* Cell, 2004. **118**(3): p. 277-9.
55. Venkov, C.D., et al., *A proximal activator of transcription in epithelial-mesenchymal transition.* J Clin Invest, 2007. **117**(2): p. 482-91.
56. Mani, S.A., et al., *Mesenchyme Forkhead 1 (FOXC2) plays a key role in metastasis and is associated with aggressive basal-like breast cancers.* Proc Natl Acad Sci U S A, 2007. **104**(24): p. 10069-74.
57. Wu, X., et al., *HOXB7, a homeodomain protein, is overexpressed in breast cancer and confers epithelial-mesenchymal transition.* Cancer Res, 2006. **66**(19): p. 9527-34.
58. Wang, X., et al., *Kruppel-like factor 8 induces epithelial to mesenchymal transition and epithelial cell invasion.* Cancer Res, 2007. **67**(15): p. 7184-93.
59. Vandewalle, C., F. Van Roy, and G. Berx, *The role of the ZEB family of transcription factors in development and disease.* Cell Mol Life Sci, 2009. **66**(5): p. 773-87.
60. Funahashi, J., et al., *Delta-crystallin enhancer binding protein delta EF1 is a zinc finger-homeodomain protein implicated in postgastrulation embryogenesis.* Development, 1993. **119**(2): p. 433-46.
61. Remacle, J.E., et al., *New mode of DNA binding of multi-zinc finger transcription factors: deltaEF1 family members bind with two hands to two target sites.* EMBO J, 1999. **18**(18): p. 5073-84.

62. Smith, G.E. and D.S. Darling, *Combination of a zinc finger and homeodomain required for protein-interaction.* Mol Biol Rep, 2003. **30**(4): p. 199-206.
63. Furusawa, T., et al., *Identification of CtBP1 and CtBP2 as corepressors of zinc finger-homeodomain factor deltaEF1.* Mol Cell Biol, 1999. **19**(12): p. 8581-90.
64. Darling, D.S., et al., *Expression of Zfhep/deltaEF1 protein in palate, neural progenitors, and differentiated neurons.* Gene Expr Patterns, 2003. **3**(6): p. 709-17.
65. Higashi, Y., et al., *Impairment of T cell development in deltaEF1 mutant mice.* J Exp Med, 1997. **185**(8): p. 1467-79.
66. Tylzanowski, P., et al., *Zfhx1a and Zfhx1b mRNAs have non-overlapping expression domains during chick and mouse midgestation limb development.* Gene Expr Patterns, 2003. **3**(1): p. 39-42.
67. Davies, S.R., et al., *Distribution of the transcription factors Sox9, AP-2, and [delta]EF1 in adult murine articular and meniscal cartilage and growth plate.* J Histochem Cytochem, 2002. **50**(8): p. 1059-65.
68. Takagi, T., et al., *DeltaEF1, a zinc finger and homeodomain transcription factor, is required for skeleton patterning in multiple lineages.* Development, 1998. **125**(1): p. 21-31.
69. Miyoshi, T., et al., *Complementary expression pattern of Zfhx1 genes Sip1 and deltaEF1 in the mouse embryo and their genetic interaction revealed by compound mutants.* Dev Dyn, 2006. **235**(7): p. 1941-52.
70. Moribe, H., et al., *Suppression of polydactyly of the Gli3 mutant (extra toes) by deltaEF1 homozygous mutation.* Dev Growth Differ, 2000. **42**(4): p. 367-76.
71. Liu, Y., et al., *Zeb1 links epithelial-mesenchymal transition and cellular senescence.* Development, 2008. **135**(3): p. 579-88.
72. Sooy, K. and M.B. Demay, *Transcriptional repression of the rat osteocalcin gene by deltaEF1.* Endocrinology, 2002. **143**(9): p. 3370-5.
73. Kato, M., et al., *MicroRNA-192 in diabetic kidney glomeruli and its function in TGF-beta-induced collagen expression via inhibition of E-box repressors.* Proc Natl Acad Sci U S A, 2007. **104**(9): p. 3432-7.
74. Murray, D., et al., *The transcription factor deltaEF1 is inversely expressed with type II collagen mRNA and can repress Col2a1 promoter activity in transfected chondrocytes.* J Biol Chem, 2000. **275**(5): p. 3610-8.
75. Nishimura, G., et al., *DeltaEF1 mediates TGF-beta signalling in vascular smooth muscle cell differentiation.* Dev Cell, 2006. **11**(1): p. 93-104.
76. Krafchak, C.M., et al., *Mutations in TCF8 cause posterior polymorphous corneal dystrophy and ectopic expression of COL4A3 by corneal endothelial cells.* Am J Hum Genet, 2005. **77**(5): p. 694-708.
77. Liskova, P., et al., *Novel mutations in the ZEB1 gene identified in Czech and British patients with posterior polymorphous corneal dystrophy.* Hum Mutat, 2007. **28**(6): p. 638.
78. Aldave, A.J., et al., *Posterior polymorphous corneal dystrophy is associated with TCF8 gene mutations and abdominal hernia.* Am J Med Genet A, 2007. **143A**(21): p. 2549-56.
79. Nguyen, D.Q., et al., *Clinical phenotype of posterior polymorphous corneal dystrophy in a family with a novel ZEB1 mutation.* Acta Ophthalmol, 2009.
80. Liu, Y., et al., *Zeb1 mutant mice as a model of posterior corneal dystrophy.* Invest Ophthalmol Vis Sci, 2008. **49**(5): p. 1843-9.

81. Wacker, I., et al., *zag-1, a Zn-finger homeodomain transcription factor controlling neuronal differentiation and axon outgrowth in C. elegans.* Development, 2003. **130**(16): p. 3795-805.
82. Yen, G., et al., *Developmental and functional evidence of a role for Zfhep in neural cell development.* Brain Res Mol Brain Res, 2001. **96**(1-2): p. 59-67.
83. van Grunsven, L.A., et al., *Interaction between Smad-interacting protein-1 and the corepressor C-terminal binding protein is dispensable for transcriptional repression of E-cadherin.* J Biol Chem, 2003. **278**(28): p. 26135-45.
84. van Grunsven, L.A., et al., *deltaEF1 and SIP1 are differentially expressed and have overlapping activities during Xenopus embryogenesis.* Dev Dyn, 2006. **235**(6): p. 1491-500.
85. Hurt, E.M., et al., *Expression of the ZEB1 (deltaEF1) transcription factor in human: additional insights.* Mol Cell Biochem, 2008. **318**(1-2): p. 89-99.
86. Spoelstra, N.S., et al., *The transcription factor ZEB1 is aberrantly expressed in aggressive uterine cancers.* Cancer Res, 2006. **66**(7): p. 3893-902.
87. Chamberlain, E.M. and M.M. Sanders, *Identification of the novel player deltaEF1 in estrogen transcriptional cascades.* Mol Cell Biol, 1999. **19**(5): p. 3600-6.
88. Dillner, N.B. and M.M. Sanders, *The zinc finger/homeodomain protein deltaEF1 mediates estrogen-specific induction of the ovalbumin gene.* Mol Cell Endocrinol, 2002. **192**(1-2): p. 85-91.
89. Eger, A., et al., *DeltaEF1 is a transcriptional repressor of E-cadherin and regulates epithelial plasticity in breast cancer cells.* Oncogene, 2005. **24**(14): p. 2375-85.
90. Pena, C., et al., *The expression levels of the transcriptional regulators p300 and CtBP modulate the correlations between SNAIL, ZEB1, E-cadherin and vitamin D receptor in human colon carcinomas.* Int J Cancer, 2006. **119**(9): p. 2098-104.
91. Buck, E., et al., *Loss of homotypic cell adhesion by epithelial-mesenchymal transition or mutation limits sensitivity to epidermal growth factor receptor inhibition.* Mol Cancer Ther, 2007. **6**(2): p. 532-41.
92. Cochrane, D.R., et al., *MicroRNA-200c mitigates invasiveness and restores sensitivity to microtubule-targeting chemotherapeutic agents.* Mol Cancer Ther, 2009.
93. Sayan, A.E., et al., *SIP1 protein protects cells from DNA damage-induced apoptosis and has independent prognostic value in bladder cancer.* Proc Natl Acad Sci U S A, 2009. **106**(35): p. 14884-9.
94. Huang, W., et al., *Inhibition of CCN6 (Wnt-1-induced signalling protein 3) down-regulates E-cadherin in the breast epithelium through induction of snail and ZEB1.* Am J Pathol, 2008. **172**(4): p. 893-904.
95. Yang, S., et al., *BMP-6 promotes E-cadherin expression through repressing deltaEF1 in breast cancer cells.* BMC Cancer, 2007. **7**: p. 211.
96. Guaita, S., et al., *Snail induction of epithelial to mesenchymal transition in tumor cells is accompanied by MUC1 repression and ZEB1 expression.* J Biol Chem, 2002. **277**(42): p. 39209-16.
97. Ohira, T., et al., *WNT7a induces E-cadherin in lung cancer cells.* Proc Natl Acad Sci U S A, 2003. **100**(18): p. 10429-34.
98. Pena, C., et al., *E-cadherin and vitamin D receptor regulation by SNAIL and ZEB1 in colon cancer: clinicopathological correlations.* Hum Mol Genet, 2005. **14**(22): p. 3361-70.

99. Singh, M., et al., *ZEB1 expression in type I vs type II endometrial cancers: a marker of aggressive disease.* Mod Pathol, 2008. **21**(7): p. 912-23.
100. Haddad, Y., W. Choi, and D.J. McConkey, *Delta-crystallin enhancer binding factor 1 controls the epithelial to mesenchymal transition phenotype and resistance to the epidermal growth factor receptor inhibitor erlotinib in human head and neck squamous cell carcinoma lines.* Clin Cancer Res, 2009. **15**(2): p. 532-42.
101. Chua, H.L., et al., *NF-kappaB represses E-cadherin expression and enhances epithelial to mesenchymal transition of mammary epithelial cells: potential involvement of ZEB-1 and ZEB-2.* Oncogene, 2007. **26**(5): p. 711-24.
102. Anose, B.M., L. LaGoo, and J. Schwendinger, *Characterization of androgen regulation of ZEB-1 and PSA in 22RV1 prostate cancer cells.* Adv Exp Med Biol, 2008. **617**: p. 541-6.
103. Kirschmann, D.A., et al., *Differentially expressed genes associated with the metastatic phenotype in breast cancer.* Breast Cancer Res Treat, 1999. **55**(2): p. 127-36.
104. Aigner, K., et al., *The transcription factor ZEB1 (deltaEF1) promotes tumour cell dedifferentiation by repressing master regulators of epithelial polarity.* Oncogene, 2007. **26**(49): p. 6979-88.
105. Hugo, H.J., et al., *Staurosporine augments EGF-mediated EMT in PMC42-LA cells through actin depolymerisation, focal contact size reduction and Snail1 induction - a model for cross-modulation.* BMC Cancer, 2009. **9**: p. 235.
106. McPhee, T.R., et al., *Integrin-linked kinase regulates E-cadherin expression through PARP-1.* Dev Dyn, 2008. **237**(10): p. 2737-47.
107. Kleer, C.G., et al., *WISP3 (CCN6) is a secreted tumor-suppressor protein that modulates IGF signalling in inflammatory breast cancer.* Neoplasia, 2004. **6**(2): p. 179-85.
108. Kleer, C.G., Y. Zhang, and S.D. Merajver, *CCN6 (WISP3) as a new regulator of the epithelial phenotype in breast cancer.* Cells Tissues Organs, 2007. **185**(1-3): p. 95-9.
109. Zhang, Y., et al., *Inhibition of CCN6 (WISP3) expression promotes neoplastic progression and enhances the effects of insulin-like growth factor-1 on breast epithelial cells.* Breast Cancer Res, 2005. **7**(6): p. R1080-9.
110. Clarhaut, J., et al., *ZEB-1, a repressor of the semaphorin 3F tumor suppressor gene in lung cancer cells.* Neoplasia, 2009. **11**(2): p. 157-66.
111. Dohadwala, M., et al., *Cyclooxygenase-2-dependent regulation of E-cadherin: prostaglandin E(2) induces transcriptional repressors ZEB1 and snail in non-small cell lung cancer.* Cancer Res, 2006. **66**(10): p. 5338-45.
112. Veena, M.S., et al., *CAR mediates efficient tumor engraftment of mesenchymal type lung cancer cells.* Lab Invest, 2009. **89**(8): p. 875-86.
113. Fontemaggi, G., et al., *The transcriptional repressor ZEB regulates p73 expression at the crossroad between proliferation and differentiation.* Mol Cell Biol, 2001. **21**(24): p. 8461-70.
114. Spaderna, S., et al., *The transcriptional repressor ZEB1 promotes metastasis and loss of cell polarity in cancer.* Cancer Res, 2008. **68**(2): p. 537-44.
115. Spaderna, S., et al., *A transient, EMT-linked loss of basement membranes indicates metastasis and poor survival in colorectal cancer.* Gastroenterology, 2006. **131**(3): p. 830-40.

116. Wang, W.S., et al., *Overexpression of the thymosin beta-4 gene is associated with malignant progression of SW480 colon cancer cells.* Oncogene, 2003. **22**(21): p. 3297-306.
117. Huang, H.C., et al., *Thymosin beta4 triggers an epithelial-mesenchymal transition in colorectal carcinoma by upregulating integrin-linked kinase.* Oncogene, 2007. **26**(19): p. 2781-90.
118. Alvarez-Diaz, S., et al., *Cystatin D is a candidate tumor suppressor gene induced by vitamin D in human colon cancer cells.* J Clin Invest, 2009. **119**(8): p. 2343-58.
119. Kallay, E., et al., *Vitamin D receptor activity and prevention of colonic hyperproliferation and oxidative stress.* Food Chem Toxicol, 2002. **40**(8): p. 1191-6.
120. Larriba, M.J., et al., *Snail2 cooperates with Snail1 in the repression of vitamin D receptor in colon cancer.* Carcinogenesis, 2009. **30**(8): p. 1459-68.
121. Arima, Y., et al., *Rb depletion results in deregulation of E-cadherin and induction of cellular phenotypic changes that are characteristic of the epithelial-to-mesenchymal transition.* Cancer Res, 2008. **68**(13): p. 5104-12.
122. Wei, P.L., et al., *Tobacco-specific carcinogen enhances colon cancer cell migration through alpha7-nicotinic acetylcholine receptor.* Ann Surg, 2009. **249**(6): p. 978-85.
123. Dominguez, G., et al., *The presence of an intronic deletion in p73 and high levels of ZEB1 alter the TAp73/DeltaTAp73 ratio in colorectal carcinomas.* J Pathol, 2006. **210**(4): p. 390-7.
124. Aigner, K., et al., *The transcription factor ZEB1 (deltaEF1) represses Plakophilin 3 during human cancer progression.* FEBS Lett, 2007. **581**(8): p. 1617-24.
125. Wang, F., et al., *Membrane-bound heparin-binding epidermal growth factor like growth factor regulates E-cadherin expression in pancreatic carcinoma cells.* Cancer Res, 2007. **67**(18): p. 8486-93.
126. Wang, Z., et al., *Acquisition of epithelial-mesenchymal transition phenotype of gemcitabine-resistant pancreatic cancer cells is linked with activation of the notch signalling pathway.* Cancer Res, 2009. **69**(6): p. 2400-7.
127. Taki, M., et al., *Down-regulation of Wnt-4 and up-regulation of Wnt-5a expression by epithelial-mesenchymal transition in human squamous carcinoma cells.* Cancer Sci, 2003. **94**(7): p. 593-7.
128. Takkunen, M., et al., *Snail-dependent and -independent epithelial-mesenchymal transition in oral squamous carcinoma cells.* J Histochem Cytochem, 2006. **54**(11): p. 1263-75.
129. Filipowicz, W., S.N. Bhattacharyya, and N. Sonenberg, *Mechanisms of post-transcriptional regulation by microRNAs: are the answers in sight?* Nat Rev Genet, 2008. **9**(2): p. 102-14.
130. Bartel, D.P., *MicroRNAs: target recognition and regulatory functions.* Cell, 2009. **136**(2): p. 215-33.
131. Cano, A. and M.A. Nieto, *Non-coding RNAs take centre stage in epithelial-to-mesenchymal transition.* Trends Cell Biol, 2008. **18**(8): p. 357-9.
132. Hurteau, G.J., S.D. Spivack, and G.J. Brock, *Potential mRNA degradation targets of hsa-miR-200c, identified using informatics and qRT-PCR.* Cell Cycle, 2006. **5**(17): p. 1951-6.

133. Hurteau, G.J., et al., *Overexpression of the microRNA hsa-miR-200c leads to reduced expression of transcription factor 8 and increased expression of E-cadherin.* Cancer Res, 2007. **67**(17): p. 7972-6.
134. Yang, S., et al., *Dual mechanism of deltaEF1 expression regulated by bone morphogenetic protein-6 in breast cancer.* Int J Biochem Cell Biol, 2009. **41**(4): p. 853-61.
135. Park, S.M., et al., *The miR-200 family determines the epithelial phenotype of cancer cells by targeting the E-cadherin repressors ZEB1 and ZEB2.* Genes Dev, 2008. **22**(7): p. 894-907.
136. Korpal, M., et al., *The miR-200 family inhibits epithelial-mesenchymal transition and cancer cell migration by direct targeting of E-cadherin transcriptional repressors ZEB1 and ZEB2.* J Biol Chem, 2008. **283**(22): p. 14910-4.
137. Gregory, P.A., et al., *The miR-200 family and miR-205 regulate epithelial to mesenchymal transition by targeting ZEB1 and SIP1.* Nat Cell Biol, 2008. **10**(5): p. 593-601.
138. Adam, L., et al., *miR-200 expression regulates epithelial-to-mesenchymal transition in bladder cancer cells and reverses resistance to epidermal growth factor receptor therapy.* Clin Cancer Res, 2009. **15**(16): p. 5060-72.
139. Saydam, O., et al., *Downregulated microRNA-200a in meningiomas promotes tumor growth by reducing E-cadherin and activating the Wnt/beta-catenin signalling pathway.* Mol Cell Biol, 2009. **29**(21): p. 5923-40.
140. Burk, U., et al., *A reciprocal repression between ZEB1 and members of the miR-200 family promotes EMT and invasion in cancer cells.* EMBO Rep, 2008. **9**(6): p. 582-9.
141. Bracken, C.P., et al., *A double-negative feedback loop between ZEB1-SIP1 and the microRNA-200 family regulates epithelial-mesenchymal transition.* Cancer Res, 2008. **68**(19): p. 7846-54.
142. Katoh, Y. and M. Katoh, *Hedgehog signalling, epithelial-to-mesenchymal transition and miRNA (review).* Int J Mol Med, 2008. **22**(3): p. 271-5.
143. Thomson, S., et al., *Epithelial to mesenchymal transition is a determinant of sensitivity of non-small-cell lung carcinoma cell lines and xenografts to epidermal growth factor receptor inhibition.* Cancer Res, 2005. **65**(20): p. 9455-62.
144. Witta, S.E., et al., *Restoring E-cadherin expression increases sensitivity to epidermal growth factor receptor inhibitors in lung cancer cell lines.* Cancer Res, 2006. **66**(2): p. 944-50.
145. Li, Y., et al., *Up-regulation of miR-200 and let-7 by natural agents leads to the reversal of epithelial-to-mesenchymal transition in gemcitabine-resistant pancreatic cancer cells.* Cancer Res, 2009. **69**(16): p. 6704-12.
146. Gravalos, C., et al., *Adjuvant chemotherapy for stages II, III and IV of colon cancer.* Clin Transl Oncol, 2009. **11**(8): p. 526-33.
147. Tang, H., et al., *Establishment and gene analysis of an oxaliplatin-resistant colon cancer cell line THC8307/L-OHP.* Anticancer Drugs, 2007. **18**(6): p. 633-9.
148. Reckamp, K.L., et al., *Tumor response to combination celecoxib and erlotinib therapy in non-small cell lung cancer is associated with a low baseline matrix metalloproteinase-9 and a decline in serum-soluble E-cadherin.* J Thorac Oncol, 2008. **3**(2): p. 117-24.

149. de Souza Pereira, R., *Selective cyclooxygenase-2 (COX-2) inhibitors used for preventing or regressing cancer.* Recent Pat Anticancer Drug Discov, 2009. **4**(2): p. 157-63.
150. Moody, T.W., et al., *Dithiolethione modified valproate and diclofenac increase E-cadherin expression and decrease proliferation of non-small cell lung cancer cells.* Lung Cancer. **68**(2): p. 154-60.
151. Postigo, A.A., *Opposing functions of ZEB proteins in the regulation of the TGFbeta/BMP signalling pathway.* EMBO J, 2003. **22**(10): p. 2443-52.
152. Postigo, A.A. and D.C. Dean, *Independent repressor domains in ZEB regulate muscle and T-cell differentiation.* Mol Cell Biol, 1999. **19**(12): p. 7961-71.
153. Costantino, M.E., et al., *Cell-specific phosphorylation of Zfhep transcription factor.* Biochem Biophys Res Commun, 2002. **296**(2): p. 368-73.
154. Cabanillas, A.M. and D.S. Darling, *Alternative splicing gives rise to two isoforms of Zfhep, a zinc finger/homeodomain protein that binds T3-response elements.* DNA Cell Biol, 1996. **15**(8): p. 643-51.
155. Manavella, P.A., et al., *The ZFHX1A gene is differentially autoregulated by its isoforms.* Biochem Biophys Res Commun, 2007. **360**(3): p. 621-6.
156. Doucas, H., et al., *Changes in the Wnt signalling pathway in gastrointestinal cancers and their prognostic significance.* Eur J Cancer, 2005. **41**(3): p. 365-79.
157. Giles, R.H., J.H. van Es, and H. Clevers, *Caught up in a Wnt storm: Wnt signalling in cancer.* Biochim Biophys Acta, 2003. **1653**(1): p. 1-24.
158. Barker, N. and H. Clevers, *Mining the Wnt pathway for cancer therapeutics.* Nat Rev Drug Discov, 2006. **5**(12): p. 997-1014.
159. Janssens, N., M. Janicot, and T. Perera, *The Wnt-dependent signalling pathways as target in oncology drug discovery.* Invest New Drugs, 2006. **24**(4): p. 263-80.
160. Yeger, H. and B. Perbal, *The CCN family of genes: a perspective on CCN biology and therapeutic potential.* J Cell Commun Signal, 2007. **1**(3-4): p. 159-64.
161. Holbourn, K.P., K.R. Acharya, and B. Perbal, *The CCN family of proteins: structure-function relationships.* Trends Biochem Sci, 2008. **33**(10): p. 461-73.
162. Perbal, B., *The CCN family of genes: a brief history.* Mol Pathol, 2001. **54**(2): p. 103-4.
163. Perbal, B., *CCN proteins: multifunctional signalling regulators.* Lancet, 2004. **363**(9402): p. 62-4.
164. French, D.M., et al., *WISP-1 is an osteoblastic regulator expressed during skeletal development and fracture repair.* Am J Pathol, 2004. **165**(3): p. 855-67.
165. Yanagita, T., et al., *Expression and physiological role of CCN4/Wnt-induced secreted protein 1 mRNA splicing variants in chondrocytes.* FEBS J, 2007. **274**(7): p. 1655-65.
166. Case, N., et al., *Beta-catenin levels influence rapid mechanical responses in osteoblasts.* J Biol Chem, 2008. **283**(43): p. 29196-205.
167. Inkson, C.A., et al., *TGF-beta1 and WISP-1/CCN-4 can regulate each other's activity to cooperatively control osteoblast function.* J Cell Biochem, 2008. **104**(5): p. 1865-78.
168. Inkson, C.A., et al., *The potential functional interaction of biglycan and WISP-1 in controlling differentiation and proliferation of osteogenic cells.* Cells Tissues Organs, 2009. **189**(1-4): p. 153-7.
169. Djouad, F., et al., *Microenvironmental changes during differentiation of mesenchymal stem cells towards chondrocytes.* Arthritis Res Ther, 2007. **9**(2): p. R33.

170. Parisi, M.S., et al., *Expression and regulation of CCN genes in murine osteoblasts.* Bone, 2006. **38**(5): p. 671-7.
171. Mori, H., et al., *Expression of WISP-1 (ccn4), WISP-2 (ccn5) and WISP-3 (ccn6) in Rheumatoid Athritic Synovium Evaluated by DNA Microarrays.* Journal of Hard Tissue Biology, 2006. **15**(2): p. 89-95.
172. Tanaka, I., et al., *Expression and regulation of WISP2 in rheumatoid arthritic synovium.* Biochem Biophys Res Commun, 2005. **334**(4): p. 973-8.
173. Blom, A.B., et al., *Involvement of the Wnt signalling pathway in experimental and human osteoarthritis: prominent role of Wnt-induced signalling protein 1.* Arthritis Rheum, 2009. **60**(2): p. 501-12.
174. Geyer, M., et al., *Differential transcriptome analysis of intraarticular lesional vs intact cartilage reveals new candidate genes in osteoarthritis pathophysiology.* Osteoarthritis Cartilage, 2009. **17**(3): p. 328-35.
175. Wang, H., et al., *Nitric oxide increases Wnt-induced secreted protein-1 (WISP-1/CCN4) expression and function in colitis.* J Mol Med, 2009. **87**(4): p. 435-45.
176. Konigshoff, M., et al., *WNT1-inducible signalling protein-1 mediates pulmonary fibrosis in mice and is upregulated in humans with idiopathic pulmonary fibrosis.* J Clin Invest, 2009. **119**(4): p. 772-87.
177. Kapasa, M., et al., *Identification of phylogenetically conserved enhancer elements implicated in pancreas development in the WISP1 and CTGF orthologs.* Genomics, 2008. **92**(5): p. 301-8.
178. Shimomura, T., et al., *Hepatic differentiation of human bone marrow-derived UE7T-13 cells: Effects of cytokines and CCN family gene expression.* Hepatol Res, 2007. **37**(12): p. 1068-79.
179. Xu, L., et al., *WISP-1 is a Wnt-1- and beta-catenin-responsive oncogene.* Genes Dev, 2000. **14**(5): p. 585-95.
180. Taneyhill, L. and D. Pennica, *Identification of Wnt responsive genes using a murine mammary epithelial cell line model system.* BMC Dev Biol, 2004. **4**: p. 6.
181. Su, F., et al., *WISP-1 attenuates p53-mediated apoptosis in response to DNA damage through activation of the Akt kinase.* Genes Dev, 2002. **16**(1): p. 46-57.
182. You, Z., et al., *Wnt signalling promotes oncogenic transformation by inhibiting c-Myc-induced apoptosis.* J Cell Biol, 2002. **157**(3): p. 429-40.
183. Colston, J.T., et al., *Wnt-induced secreted protein-1 is a prohypertrophic and profibrotic growth factor.* Am J Physiol Heart Circ Physiol, 2007. **293**(3): p. H1839-46.
184. Pennica, D., et al., *WISP genes are members of the connective tissue growth factor family that are up-regulated in wnt-1-transformed cells and aberrantly expressed in human colon tumors.* Proc Natl Acad Sci U S A, 1998. **95**(25): p. 14717-22.
185. Soon, L.L., et al., *Overexpression of WISP-1 down-regulated motility and invasion of lung cancer cells through inhibition of Rac activation.* J Biol Chem, 2003. **278**(13): p. 11465-70.
186. Margalit, O., et al., *Overexpression of a set of genes, including WISP-1, common to pulmonary metastases of both mouse D122 Lewis lung carcinoma and B16-F10.9 melanoma cell lines.* Br J Cancer, 2003. **89**(2): p. 314-9.
187. Chen, P.P., et al., *Expression of Cyr61, CTGF, and WISP-1 correlates with clinical features of lung cancer.* PLoS One, 2007. **2**(6): p. e534.

188. Khor, T.O., et al., *A comparative study of the expression of Wnt-1, WISP-1, survivin and cyclin-D1 in colorectal carcinoma.* Int J Colorectal Dis, 2006. **21**(4): p. 291-300.
189. Desnoyers, L., D. Arnott, and D. Pennica, *WISP-1 binds to decorin and biglycan.* J Biol Chem, 2001. **276**(50): p. 47599-607.
190. Fischer, H., et al., *COL11A1 in FAP polyps and in sporadic colorectal tumors.* BMC Cancer, 2001. **1**: p. 17.
191. Davies, S.R., et al., *Differential expression of the CCN family member WISP-1, WISP-2 and WISP-3 in human colorectal cancer and the prognostic implications.* Int J Oncol, 2010. **36**(5): p. 1129-36.
192. Tian, C., et al., *Overexpression of connective tissue growth factor WISP-1 in Chinese primary rectal cancer patients.* World J Gastroenterol, 2007. **13**(28): p. 3878-82.
193. Davies, S.R., et al., *Differential expression and prognostic implications of the CCN family members WISP-1, WISP-2, and WISP-3 in human breast cancer.* Ann Surg Oncol, 2007. **14**(6): p. 1909-18.
194. Xie, D., et al., *Elevated levels of connective tissue growth factor, WISP-1, and CYR61 in primary breast cancers associated with more advanced features.* Cancer Res, 2001. **61**(24): p. 8917-23.
195. Perbal, B., *Alternative splicing of CCN mRNAs .... it has been upon us.* J Cell Commun Signal, 2009. **3**(2): p. 153-7.
196. Tanaka, S., et al., *A novel variant of WISP1 lacking a Von Willebrand type C module overexpressed in scirrhous gastric carcinoma.* Oncogene, 2001. **20**(39): p. 5525-32.
197. Tanaka, S., et al., *Human WISP1v, a member of the CCN family, is associated with invasive cholangiocarcinoma.* Hepatology, 2003. **37**(5): p. 1122-9.
198. Yamashita, Y., et al., *Predictive factors and molecular markers of postoperative prognosis for patients with intrahepatic cholangiocarcinoma.*, in *ASCO Gastrointestinal Cancers Symposium*. 2006: Atlanta, Georgia.
199. Bacac, M., et al., *A gene expression signature that distinguishes desmoid tumours from nodular fasciitis.* J Pathol, 2006. **208**(4): p. 543-53.
200. Skubitz, K.M. and A.P. Skubitz, *Gene expression in aggressive fibromatosis.* J Lab Clin Med, 2004. **143**(2): p. 89-98.
201. Cho, Y.L., et al., *Array comparative genomic hybridization analysis of uterine leiomyosarcoma.* Gynecol Oncol, 2005. **99**(3): p. 545-51.
202. Yu, C., et al., *NOV (CCN3) regulation in the growth plate and CCN family member expression in cartilage neoplasia.* J Pathol, 2003. **201**(4): p. 609-15.
203. Gery, S., et al., *Ovarian carcinomas: CCN genes are aberrantly expressed and CCN1 promotes proliferation of these cells.* Clin Cancer Res, 2005. **11**(20): p. 7243-54.
204. Hawizy, A.M., et al., *Overexpression of WISP-2 (Wnt induced secreted protein-2) reduces HGF/SF induced in vitro invasion in prostate cancer cells.*, in *ASCO Prostate Cancer Symposium.* 2006: San Francisco, California.
205. Schutze, N., et al., *Differential expression of CCN-family members in primary human bone marrow-derived mesenchymal stem cells during osteogenic, chondrogenic and adipogenic differentiation.* Cell Commun Signal, 2005. **3**(1): p. 5.
206. Jones, J.A., et al., *CCN5 expression in mammals : I. Embryonic and fetal tissues of mouse and human.* J Cell Commun Signal, 2007. **1**(2): p. 127-43.

207. Inadera, H., A. Shimomura, and S. Tachibana, *Effect of Wnt-1 inducible signalling pathway protein-2 (WISP-2/CCN5), a downstream protein of Wnt signalling, on adipocyte differentiation.* Biochem Biophys Res Commun, 2009. **379**(4): p. 969-74.
208. Dhar, G., et al., *Gain of oncogenic function of p53 mutants induces invasive phenotypes in human breast cancer cells by silencing CCN5/WISP-2.* Cancer Res, 2008. **68**(12): p. 4580-7.
209. Saxena, N., et al., *Differential expression of WISP-1 and WISP-2 genes in normal and transformed human breast cell lines.* Mol Cell Biochem, 2001. **228**(1-2): p. 99-104.
210. Banerjee, S., et al., *Epidermal growth factor induces WISP-2/CCN5 expression in estrogen receptor-alpha-positive breast tumor cells through multiple molecular cross-talks.* Mol Cancer Res, 2005. **3**(3): p. 151-62.
211. Fritah, A., et al., *Role of WISP-2/CCN5 in the maintenance of a differentiated and noninvasive phenotype in human breast cancer cells.* Mol Cell Biol, 2008. **28**(3): p. 1114-23.
212. Banerjee, S., et al., *CCN5/WISP-2 expression in breast adenocarcinoma is associated with less frequent progression of the disease and suppresses the invasive phenotypes of tumor cells.* Cancer Res, 2008. **68**(18): p. 7606-12.
213. Banerjee, S., et al., *WISP-2 gene in human breast cancer: estrogen and progesterone inducible expression and regulation of tumor cell proliferation.* Neoplasia, 2003. **5**(1): p. 63-73.
214. Dhar, K., et al., *Insulin-like growth factor-1 (IGF-1) induces WISP-2/CCN5 via multiple molecular cross-talks and is essential for mitogenic switch by IGF-1 axis in estrogen receptor-positive breast tumor cells.* Cancer Res, 2007. **67**(4): p. 1520-6.
215. Sengupta, K., et al., *WISP-2/CCN5 is involved as a novel signalling intermediate in phorbol ester-protein kinase Calpha-mediated breast tumor cell proliferation.* Biochemistry, 2006. **45**(35): p. 10698-709.
216. Aprelikova, O., et al., *Role of ETS transcription factors in the hypoxia-inducible factor-2 target gene selection.* Cancer Res, 2006. **66**(11): p. 5641-7.
217. Inadera, H., *Estrogen-induced genes, WISP-2 and pS2, respond divergently to protein kinase pathway.* Biochem Biophys Res Commun, 2003. **309**(2): p. 272-8.
218. Fritah, A., et al., *p21WAF1/CIP1 selectively controls the transcriptional activity of estrogen receptor alpha.* Mol Cell Biol, 2005. **25**(6): p. 2419-30.
219. Fritah, A., G. Redeuilh, and M. Sabbah, *Molecular cloning and characterization of the human WISP-2/CCN5 gene promoter reveal its upregulation by oestrogens.* J Endocrinol, 2006. **191**(3): p. 613-24.
220. Mason, H.R., et al., *Estrogen induces CCN5 expression in the rat uterus in vivo.* Endocrinology, 2004. **145**(2): p. 976-82.
221. Lake, A.C. and J.J. Castellot, Jr., *CCN5 modulates the antiproliferative effect of heparin and regulates cell motility in vascular smooth muscle cells.* Cell Commun Signal, 2003. **1**(1): p. 5.
222. Lake, A.C., et al., *CCN5 is a growth arrest-specific gene that regulates smooth muscle cell proliferation and motility.* Am J Pathol, 2003. **162**(1): p. 219-31.
223. Kouzu, Y., et al., *WISP-2 expression in human salivary gland tumors.* Int J Mol Med, 2006. **17**(4): p. 567-73.

224. Davis, L., Y. Chen, and M. Sen, *WISP-3 functions as a ligand and promotes superoxide dismutase activity.* Biochem Biophys Res Commun, 2006. **342**(1): p. 259-65.
225. Sen, M., et al., *WISP3-dependent regulation of type II collagen and aggrecan production in chondrocytes.* Arthritis Rheum, 2004. **50**(2): p. 488-97.
226. Miller, D.S. and M. Sen, *Potential role of WISP3 (CCN6) in regulating the accumulation of reactive oxygen species.* Biochem Biophys Res Commun, 2007. **355**(1): p. 156-61.
227. Cheon, H., D.L. Boyle, and G.S. Firestein, *Wnt1 inducible signalling pathway protein-3 regulation and microsatellite structure in arthritis.* J Rheumatol, 2004. **31**(11): p. 2106-14.
228. Schutze, N., et al., *CYR61/CCN1 and WISP3/CCN6 are chemoattractive ligands for human multipotent mesenchymal stroma cells.* BMC Cell Biol, 2007. **8**: p. 45.
229. Yang, Y. and E. Liao, *Mutant WISP3 triggers the phenotype shift of articular chondrocytes by promoting sensitivity to IGF-1 hypothesis of spondyloepiphyseal dysplasia tarda with progressive arthropathy (SEDT-PA).* Med Hypotheses, 2007. **68**(6): p. 1406-10.
230. Delague, V., et al., *Molecular study of WISP3 in nine families originating from the Middle-East and presenting with progressive pseudorheumatoid dysplasia: identification of two novel mutations, and description of a founder effect.* Am J Med Genet A, 2005. **138A**(2): p. 118-26.
231. Ehl, S., et al., *Clinical, radiographic, and genetic diagnosis of progressive pseudorheumatoid dysplasia in a patient with severe polyarthropathy.* Rheumatol Int, 2004. **24**(1): p. 53-6.
232. Hurvitz, J.R., et al., *Mutations in the CCN gene family member WISP3 cause progressive pseudorheumatoid dysplasia.* Nat Genet, 1999. **23**(1): p. 94-8.
233. Yue, H., Z.L. Zhang, and J.W. He, *Identification of novel mutations in WISP3 gene in two unrelated Chinese families with progressive pseudorheumatoid dysplasia.* Bone, 2009. **44**(4): p. 547-54.
234. Zhou, H.D., et al., *Cellular and molecular responses in progressive pseudorheumatoid dysplasia articular cartilage associated with compound heterozygous WISP3 gene mutation.* J Mol Med, 2007. **85**(9): p. 985-96.
235. Lamb, R., et al., *Wnt-1-inducible signalling pathway protein 3 and susceptibility to juvenile idiopathic arthritis.* Arthritis Rheum, 2005. **52**(11): p. 3548-53.
236. Kutz, W.E., Y. Gong, and M.L. Warman, *WISP3, the gene responsible for the human skeletal disease progressive pseudorheumatoid dysplasia, is not essential for skeletal function in mice.* Mol Cell Biol, 2005. **25**(1): p. 414-21.
237. Nakamura, Y., et al., *Normal growth and development in mice over-expressing the CCN family member WISP3.* J Cell Commun Signal, 2009. **3**(2): p. 105-13.
238. Kleer, C.G., et al., *WISP3 and RhoC guanosine triphosphatase cooperate in the development of inflammatory breast cancer.* Breast Cancer Res, 2004. **6**(1): p. R110-5.
239. Kleer, C.G., et al., *WISP3 is a novel tumor suppressor gene of inflammatory breast cancer.* Oncogene, 2002. **21**(20): p. 3172-80.
240. Huang, C.L., et al., *MRP-1/CD9 gene transduction downregulates Wnt signal pathways.* Oncogene, 2004. **23**(45): p. 7475-83.
241. Hawizy, A.M., et al., *Expression of Wnt induced Secreted Proteins (WISP's) in prostate tissues and cancer cell lines and their role in the action of HGF/SF.*, in *ASCO Prostate Cancer Symposium.* 2005: Orlando, Florida.

242. Hayes, M.J., et al., *Genetic changes of Wnt pathway genes are common events in metaplastic carcinomas of the breast.* Clin Cancer Res, 2008. **14**(13): p. 4038-44.
243. Thorstensen, L., et al., *WNT1 inducible signalling pathway protein 3, WISP-3, a novel target gene in colorectal carcinomas with microsatellite instability.* Gastroenterology, 2001. **121**(6): p. 1275-80.
244. Thorstensen, L., et al., *WNT-inducible signalling pathway protein 3, WISP-3, is mutated in microsatellite unstable gastrointestinal carcinomas but not in endometrial carcinomas.* Gastroenterology, 2003. **124**(1): p. 270-1.
245. Thorstensen, L., et al., *Genetic and epigenetic changes of components affecting the WNT pathway in colorectal carcinomas stratified by microsatellite instability.* Neoplasia, 2005. **7**(2): p. 99-108.
246. Hatzfeld, M., *Plakophilins: Multifunctional proteins or just regulators of desmosomal adhesion?* Biochim Biophys Acta, 2007. **1773**(1): p. 69-77.
247. Bonne, S., et al., *Plakophilin-3, a novel armadillo-like protein present in nuclei and desmosomes of epithelial cells.* J Cell Sci, 1999. **112 (Pt 14)**: p. 2265-76.
248. Schmidt, A., et al., *Plakophilin 3--a novel cell-type-specific desmosomal plaque protein.* Differentiation, 1999. **64**(5): p. 291-306.
249. North, A.J., et al., *Molecular map of the desmosomal plaque.* J Cell Sci, 1999. **112 (Pt 23)**: p. 4325-36.
250. Chen, X., et al., *Protein binding and functional characterization of plakophilin 2. Evidence for its diverse roles in desmosomes and beta -catenin signalling.* J Biol Chem, 2002. **277**(12): p. 10512-22.
251. Huen, A.C., et al., *Intermediate filament-membrane attachments function synergistically with actin-dependent contacts to regulate intercellular adhesive strength.* J Cell Biol, 2002. **159**(6): p. 1005-17.
252. McGrath, J.A., et al., *Mutations in the plakophilin 1 gene result in ectodermal dysplasia/skin fragility syndrome.* Nat Genet, 1997. **17**(2): p. 240-4.
253. Sklyarova, T., et al., *Plakophilin-3-deficient mice develop hair coat abnormalities and are prone to cutaneous inflammation.* J Invest Dermatol, 2008. **128**(6): p. 1375-85.
254. Hofmann, I., et al., *Identification of the junctional plaque protein plakophilin 3 in cytoplasmic particles containing RNA-binding proteins and the recruitment of plakophilins 1 and 3 to stress granules.* Mol Biol Cell, 2006. **17**(3): p. 1388-98.
255. Bonne, S., et al., *Defining desmosomal plakophilin-3 interactions.* J Cell Biol, 2003. **161**(2): p. 403-16.
256. Kundu, S.T., et al., *Plakophilin3 downregulation leads to a decrease in cell adhesion and promotes metastasis.* Int J Cancer, 2008. **123**(10): p. 2303-14.
257. Valladares-Ayerbes, M., et al., *Bioinformatics approach to mRNA markers discovery for detection of circulating tumor cells in patients with gastrointestinal cancer.* Cancer Detect Prev, 2008. **32**(3): p. 236-50.
258. Papagerakis, S., et al., *Immunohistochemical localization of plakophilins (PKP1, PKP2, PKP3, and p0071) in primary oropharyngeal tumors: correlation with clinical parameters.* Hum Pathol, 2003. **34**(6): p. 565-72.
259. Schwarz, J., et al., *Differential expression of desmosomal plakophilins in various types of carcinomas: correlation with cell type and differentiation.* Hum Pathol, 2006. **37**(5): p. 613-22.
260. Furukawa, C., et al., *Plakophilin 3 oncogene as prognostic marker and therapeutic target for lung cancer.* Cancer Res, 2005. **65**(16): p. 7102-10.

261. Bui, T., et al., *ZEB1 links p63 and p73 in a novel neuronal survival pathway rapidly induced in response to cortical ischemia.* PLoS One, 2009. **4**(2): p. e4373.
262. Genetta, T. and T. Kadesch, *Cloning of a cDNA encoding a mouse transcriptional repressor displaying striking sequence conservation across vertebrates.* Gene, 1996. **169**(2): p. 289-90.
263. Mehta, J.S., et al., *Analysis of the posterior polymorphous corneal dystrophy 3 gene, TCF8, in late-onset Fuchs endothelial corneal dystrophy.* Invest Ophthalmol Vis Sci, 2008. **49**(1): p. 184-8.
264. Darling, D.S., N.K. Gaur, and B. Zhu, *A zinc finger homeodomain transcription factor binds specific thyroid hormone response elements.* Mol Cell Endocrinol, 1998. **139**(1-2): p. 25-35.
265. Graham, T.R., et al., *Insulin-like growth factor-I-dependent up-regulation of ZEB1 drives epithelial-to-mesenchymal transition in human prostate cancer cells.* Cancer Res, 2008. **68**(7): p. 2479-88.
266. Hidaka, T., et al., *Down-regulation of TCF8 is involved in the leukemogenesis of adult T-cell leukemia/lymphoma.* Blood, 2008. **112**(2): p. 383-93.
267. Inuzuka, T., et al., *Integral role of transcription factor 8 in the negative regulation of tumor angiogenesis.* Cancer Res, 2009. **69**(4): p. 1678-84.
268. Vermeer, M.H., et al., *Novel and highly recurrent chromosomal alterations in Sezary syndrome.* Cancer Res, 2008. **68**(8): p. 2689-98.
269. Adachi, Y., et al., *Zeb1-mediated T-cadherin repression increases the invasive potential of gallbladder cancer.* FEBS Lett, 2009. **583**(2): p. 430-6.
270. Fisher, E.R., et al., *Solving the dilemma of the immunohistochemical and other methods used for scoring estrogen receptor and progesterone receptor in patients with invasive breast carcinoma.* Cancer, 2005. **103**(1): p. 164-73.
271. McCarty, K.S., Jr., et al., *Estrogen receptor analyses. Correlation of biochemical and immunohistochemical methods using monoclonal antireceptor antibodies.* Arch Pathol Lab Med, 1985. **109**(8): p. 716-21.
272. Taylor, C.R. and R.M. Levenson, *Quantification of immunohistochemistry--issues concerning methods, utility and semiquantitative assessment II.* Histopathology, 2006. **49**(4): p. 411-24.
273. Walker, R.A., *Quantification of immunohistochemistry--issues concerning methods, utility and semiquantitative assessment I.* Histopathology, 2006. **49**(4): p. 406-10.
274. McCabe, A., et al., *Automated quantitative analysis (AQUA) of in situ protein expression, antibody concentration, and prognosis.* J Natl Cancer Inst, 2005. **97**(24): p. 1808-15.
275. Meyer zum Buschenfelde, D., et al., *Molecular mechanisms involved in TFF3 peptide-mediated modulation of the E-cadherin/catenin cell adhesion complex.* Peptides, 2004. **25**(5): p. 873-83.
276. Ireton, R.C., et al., *A novel role for p120 catenin in E-cadherin function.* J Cell Biol, 2002. **159**(3): p. 465-76.
277. Wang, J., et al., *The transcription repressor, ZEB1, cooperates with CtBP2 and HDAC1 to suppress IL-2 gene activation in T cells.* Int Immunol, 2009. **21**(3): p. 227-35.
278. Adams, C.L., et al., *Mechanisms of epithelial cell-cell adhesion and cell compaction revealed by high-resolution tracking of E-cadherin-green fluorescent protein.* J Cell Biol, 1998. **142**(4): p. 1105-19.

279. Iino, R., I. Koyama, and A. Kusumi, *Single molecule imaging of green fluorescent proteins in living cells: E-cadherin forms oligomers on the free cell surface*. Biophys J, 2001. **80**(6): p. 2667-77.
280. Chen, C.C. and L.F. Lau, *Functions and mechanisms of action of CCN matricellular proteins.* Int J Biochem Cell Biol, 2009. **41**(4): p. 771-83.
281. Lau, L.F. and S.C. Lam, *The CCN family of angiogenic regulators: the integrin connection.* Exp Cell Res, 1999. **248**(1): p. 44-57.
282. Schmidt, A. and S. Jager, *Plakophilins--hard work in the desmosome, recreation in the nucleus?* Eur J Cell Biol, 2005. **84**(2-3): p. 189-204.
283. Wheelock, M.J. and K.R. Johnson, *Cadherin-mediated cellular signalling.* Curr Opin Cell Biol, 2003. **15**(5): p. 509-14.